

Affimer-based impedimetric biosensors: the new analytical platform for biorecognition applications

By

Pattanapong Thangsunan

Submitted in accordance with the requirements for the degree of
Doctor of Philosophy

The University of Leeds

School of Biomedical Sciences, Faculty of Biological Sciences

June 2018

The candidate confirms that the work submitted is his own and that appropriate credit has been given where reference has been made to the work of others.

This copy has been supplied on the understanding that it is copyright material and that no quotation from the thesis may be published without proper acknowledgement.

The right of Pattanapong Thangsunan to be identified as Author of this work has been asserted by him in accordance with the Copyright, Designs and Patents Act 1988.

Acknowledgements

Firstly, I would like to express my sincere gratitude to my supervisor, Prof. Paul Millner, for his continuous support that he has given me academically and also guidance for everyday life. I really appreciate his patience, motivation and kindness and I could not have come this far without him. I also would like to thank all the previous and current members in the Millner group, especially Ploy, Asif, Shazana, Jack and Kaniz, for the stimulating academic discussions and pleasant moments as we worked together in the lab. All of them made my times in Leeds unforgettable.

Additionally, I would like to thank my co-supervisors, Prof. Michael McPherson and Dr. Darren Tomlinson and the members of the BSTG, especially Anna, Christian and Tom, for their assistance regarding Affimers and important knowledge of molecular biology. I also thank Dr. Lars Jeuken, my assessor, for his guidance in electrochemistry and impedance spectroscopy. My deep appreciation also goes to Dr. James Robinson (at St James's University Hospital) for his assistance with surface plasmon resonance (SPR) and Dr. James Ault and his group for mass spectrometry facility.

I gratefully acknowledge the Royal Thai Government and the National Institute of Metrology (Thailand) for the financial support and the opportunity of PhD study. A million thanks go to my lovely friends at the University of Sheffield, particularly Sine and Tee, for being with me during our wonderful and memorable trips around UK and Europe. Special thanks also go to Piyanee for being my buddy when having meals, shopping and sharing our PhD experiences.

Last but not the least, for my family, I would like to thank my dad, my mom and my grandma for their immeasurable love and encouragement. Your support always boosts me up and makes me energetic to pursue my dreams. I also thank my

twin brother, Pan, for always believing in me and lifting my spirits during low points. Throughout my life, you have always been there for me as I will always be there for you as well. As this journey is coming to an end, I cannot wait to start a new journey of my life and hopefully it will be as an awesome experience as I have had here in the UK.

Pattanapong Thangsunan

June 2018

Abstract

Thanks to their high sensitivity and specificity, short-processing times, low cost of production, small size, and no requirement for professional users, biosensors have increasingly gained popularity. Electrochemical impedance biosensors have successfully been applied to detect a wide range of target analytes including whole cells, proteins, and small molecules. However, there are some limitations, for example reproducibility and non-specific binding, which still require further development. The main objective of this thesis is to develop impedimetric biosensors using Affimers, novel non-antibody binding proteins, as bioreceptors to detect a small molecule target, dichlorodiphenyltrichloroethane (DDT), and a protein biomarker, fibroblast growth factor receptor 3 (FGFR3).

Initial work in this thesis was the selection of Affimers using phage display technology. Affimers were selected from a phage library provided by the BioScreening Technology Group (BSTG) at the University of Leeds. The selected Affimer-encoding sequences were then subcloned into the pET expression vector and expressed in *E.coli* cells. Prior to using the selected Affimers for biosensor fabrication, specific interaction of the Affimers with their analytes was investigated using ELISA, surface plasmon resonance (SPR) and immunoprecipitation (pull-down) assay. Even though none of the Affimers against DDT succeeded in binding specifically to DDT, some of the Affimers against FGFR3 showed binding to it and were then utilised for biosensor fabrication.

Two sensor fabrication methods, the ELISHA “gluing” protocol and NeutrAvidin-biotin linkage, were tested and the latter one was selected for further study. By using the NeutrAvidin-biotin interaction method to functionalise the sensor surfaces, several parameters such as Affimer concentration, NeutrAvidin concentration and blocking agents to minimise non-specific binding were optimised. The fully fabricated Affimer-based biosensors were incubated with the analyte

(FGFR3) and electrochemical impedance spectroscopy (EIS) was employed to interrogate FGFR3 binding. The data showed that the Affimer-based sensors could detect FGFR3 protein to very low levels. However, further optimisation is still needed in order to minimise non-specific binding effects and make the sensors work consistently.

The work presented in this thesis is the first Affimer-based impedimetric biosensor for the detection of FGFR3, a promising biomarker for early diagnosis of bladder cancer. This sensor platform may not only provide an effective tool for bladder cancer surveillance, but also pave the way of designing a new analytical method for monitoring other protein biomarkers of disease.

Abbreviations

β 2M	Beta-2-microglobulin
BCA	Bicinchoninic acid
BLI	Bi-layer interferometry
BSA	Bovine serum albumin
BSTG	The BioScreening Technology Group
C_{dl}	Double-layer capacitance
CEA	Carcinoembryonic antigen
CPE	Constant phase element
CV	Cyclic voltammetry
DDT	Dichlorodiphenyltrichloroethane
DMSO	Dimethyl sulfoxide
DNA	Deoxyribonucleic acid
EDTA	Ethylenediaminetetraacetic acid
EIS	Electrochemical impedance spectroscopy
ELISA	Enzyme-linked immunosorbent assay
FGFR3	Fibroblast growth factor receptor 3
GFP	Green fluorescent protein
HRP	Horseradish peroxidase
HSA	Human serum albumin
Hz	Hertz
IgG	Immunoglobulin G
IPTG	Isopropyl β -D-1-thiogalactopyranoside
ITC	Isothermal titration calorimetry
K_D	Dissociation constant
k_{off}	Dissociation rate constant
k_{on}	Association rate constant

LC-MS	Liquid chromatography – mass spectrometry
PBS	Phosphate-buffered saline
PBST	Phosphate-buffered saline plus 0.05% (v/v) Tween-20
PCR	Polymerase chain reaction
PEG	Polyethylene glycol
PMDA	Pyromellitic dianhydride
R_{ct}	Charge transfer resistance
R_s	Solution resistance
SAM	Self-assembled monolayer
SDS-PAGE	Sodium dodecyl sulfate polyacrylamide gel electrophoresis
SEM	Standard error of the mean
SPR	Surface plasmon resonance
Sulfo-SMCC	Sulfosuccinimidyl 4-(<i>N</i> -maleimidomethyl)cyclohexane-1-carboxylate
TCEP	Tris(2-carboxyethyl)phosphine hydrochloride
TMB	3,3',5,5'-tetramethylbenzidine
W	Warburg impedance
Z'	Real component of impedance
$-Z''$	Imaginary component of impedance

Table of Contents

Acknowledgements	i
Abstract	iii
Abbreviations	v
Table of Contents	vii
List of Figures	xi
List of Tables	xvi
Chapter 1 Introduction	1
1.1 Overview	1
1.2 What is biosensor and how is it important?	2
1.3 Types of biosensors	5
1.3.1 Optical biosensors	5
1.3.2 Piezoelectric biosensors	7
1.3.3 Electrochemical biosensors	8
1.4 Electrochemical impedance spectroscopy (EIS)	12
1.4.1 The brief principle of electrochemical impedance spectroscopy	12
1.4.2 Fabrication of impedimetric biosensors	19
1.4.3 Applications of impedimetric biosensors	34
1.5 Classification of bioreceptors	37
1.5.1 Types of common bioreceptors used for fabricating electrochemical biosensors	37
1.5.2 Antibodies and their limitations	42
1.5.3 Antibody-derived fragments	51
1.5.4 Non-antibody binding proteins	54
1.5.5 Affimers	61
1.6 Dichlorodiphenyltrichloroethane (DDT)	65
1.7 Fibroblast Growth Factor Receptor 3 (FGFR3) as a promising biomarker for bladder cancer	67
1.7.1 Overview of bladder cancer	67
1.7.2 Standard methods of bladder cancer diagnosis	68
1.7.3 FGFR3 protein and its implication in bladder cancer	71
1.7.4 Available methods for FGFR3 detection	74
1.8 Project aims and potential applications	75

Chapter 2 Materials and Methods	77
2.1 Materials.....	77
2.1.1 Inorganic chemicals	77
2.1.2 Organic chemicals	77
2.1.3 Other reagents.....	77
2.1.4 Bacterial growth media ingredients	78
2.1.5 Antibodies and related reagents	78
2.1.6 Bacterial and viral strains.....	78
2.1.7 Enzymes.....	79
2.1.8 Solvents and buffers	79
2.1.9 Proteins	79
2.1.10 Kits and consumables.....	79
2.1.11 Electrodes.....	80
2.2 Methods	82
2.2.1 Phage display screening for DDT-binding Affimers	82
2.2.2 Phage ELISA	85
2.2.3 Subcloning of Affimer-encoding sequences into pET11a plasmids	86
2.2.4 Expression and purification of Affimers	90
2.2.5 Characterisation of Affimers against DDT using ELISA.....	92
2.2.6 Characterisation of Affimers against FGFR3 protein	94
2.2.7 Fabrication of impedimetric biosensors.....	101
Chapter 3 Affimer screening and production	109
3.1 Introduction.....	109
3.2 DDT Affimer screening	110
3.2.1 Preparation of biotinylated DDT as a target for phage display screening	110
3.2.2 Phage display screening.....	112
3.2.3 Phage ELISA	114
3.2.4 Affimer sequencing and sequence alignment.....	116
3.3 Subcloning of anti-DDT Affimer-encoding sequences into pET11a expression vector	119
3.3.1 Digestion of pET11a with <i>NotI/NheI</i> restriction enzymes..	119
3.3.2 Polymerase chain reaction (PCR) amplification of Affimer- encoding sequences	122
3.3.3 Digestion of PCR fragments using <i>NotI/NheI</i> and <i>DpnI</i> enzymes	124

3.3.4	Ligation and transformation.....	126
3.3.5	Colony PCR.....	130
3.3.6	Sequencing and alignment.....	132
3.4	Production of Affimers against DDT.....	135
3.4.1	Affimer expression.....	135
3.4.2	Affimer purification.....	136
3.5	Production of Affimers against FGFR3.....	138
3.5.1	Affimer screening from the phage display library.....	138
3.5.2	Anti-FGFR3 Affimer sequence and alignment.....	140
3.5.3	Anti-FGFR3 Affimer expression and purification.....	142
3.6	Discussion.....	144
Chapter 4	Affimer characterisation.....	146
4.1	Introduction.....	146
4.2	Characterisation of Affimers against DDT.....	147
4.2.1	ELISA to check the binding of Affimers to biotinylated DDT.....	147
4.2.2	Optimisation of Affimer concentration for competitive ELISA.....	149
4.2.3	Competitive ELISA to study the binding of Affimers to free DDT 151	
4.3	Characterisation of Affimers against FGFR3.....	155
4.3.1	Biotinylation of Affimers via biotin-maleimide.....	155
4.3.2	Double-sandwich ELISA to check the binding between Affimers and FGFR3.....	161
4.3.3	Binding kinetics study using surface plasmon resonance (SPR).....	163
4.3.4	Immunoprecipitation assay.....	168
4.3.5	ELISA to check the specificity of Affimers to FGFR3 protein.....	171
4.4	Discussion.....	174
4.4.1	Affimers against DDT.....	174
4.4.2	Affimers against FGFR3.....	175
Chapter 5	Biosensor fabrication.....	177
5.1	Introduction.....	177
5.2	Construction of impedimetric biosensors using ELISHA gluing method.....	178
5.3	Biosensor fabrication via NeutrAvidin-biotin linkage of the Affimers.....	182

5.3.1 Overview of sensor fabrication.....	182
5.3.2 Electrochemical impedance spectroscopy for detection of FGFR3.....	188
5.3.3 Optimisation of methods for biosensor fabrication.....	196
5.3.4 Modification of sensor construction protocol to minimise non- specific signal	222
5.4 Discussion	243
Chapter 6 General discussion.....	248
6.1 General discussion	248
6.2 The challenge of Affimer selection against small molecules	249
6.3 Production and characterisation of Affimers for FGFR3 detection.....	250
6.4 Optimising fundamental parameters affecting impedimetric biosensor performance	252
6.5 Effect of blocking agents on sensor response.....	255
6.6 Limitations in the field and possible opportunity of the sensors.	256
6.7 Future work	257
References	260

List of Figures

Figure 1.1 A schematic showing basic components of a biosensor system... 4	4
Figure 1.2 Schematic of a Nyquist plot alongside a Randles' equivalent circuit..... 15	15
Figure 1.3 Schematic showing possible impedance shifts resulting from binding of analytes and receptors on the sensor surface..... 17	17
Figure 1.4 Chemical structures of widely-used conducting polymers for construction of biosensors..... 22	22
Figure 1.5 Chemical structures of two non-conducting polymers used in biosensor applications..... 24	24
Figure 1.6 General methods to immobilise bioreceptors to transducer surface..... 25	25
Figure 1.7 Examples of covalent bonding reactions via the crosslinkers. 29	29
Figure 1.8 An immunoglobulin G (IgG) structure. 43	43
Figure 1.9 the structure of five classes of immunoglobulins..... 44	44
Figure 1.10 A schematic representation of basic phage display cycle. 48	48
Figure 1.11 Some examples of antibody-derived fragments..... 52	52
Figure 1.12 X-ray crystal structure of an Affimer scaffold (PDB ID no. 4N6T)..... 62	62
Figure 1.13 Chemical structure of DDT. 65	65
Figure 1.14 Overall structure of FGFR3 protein..... 72	72
Figure 2.1 A Dropsens gold screen-printed electrode chip.....81	81
Figure 2.2 The chemical structure of biotinylated DDT. 82	82
Figure 2.3 The schematic representation showing the brief protocol of phage display screening for DDT-specific Affimer selection. 83	83
Figure 3.1 A schematic representation of Affimer screening..... 111	111
Figure 3.2 ER2738 <i>E.coli</i> cells growing on LB-carbenicillin (carb) plates after the third competitive panning for DDT Affimer selection..... 113	113
Figure 3.3 Phage ELISA results showing 46 out of 48 clones of Affimers presenting on the coat of M13 phage bound specifically to biotinylated DDT. 115	115

Figure 3.4 Nucleotide and amino acid sequences of H25 Affimer.	117
Figure 3.5 Amino acid sequences of 16 selected Affimers against DDT...	118
Figure 3.6 The map of pET11a expression vector.....	120
Figure 3.7 The pET11a plasmid digested with <i>NotI</i> and <i>NheI</i> enzymes....	121
Figure 3.8 PCR products before the reactions were treated with <i>NotI/NheI</i> and <i>DpnI</i> enzymes.....	123
Figure 3.9 PCR products after the reactions were treated with <i>NotI/NheI</i> and <i>DpnI</i>	125
Figure 3.10 Digested pET11a vector and PCR products of genes encoding Affimers prepared for ligation.	127
Figure 3.11 A schematic representation of ligation and transformation of a pET11a expression vector containing an Affimer-encoding sequence.	128
Figure 3.12 XL1 Blue <i>E.coli</i> cells containing Affimer-encoding genes growing on LB carb plates.....	129
Figure 3.13 Colony PCR was performed in order to check the success of inserting Affimer-encoding sequences into pET11a vectors..	131
Figure 3.14 Sequence alignment of H25 Affimer obtained from pET11a vector and the H25 Affimer obtained from phagemid vector.	133
Figure 3.15 SDS-PAGE gels of purified anti-DDT Affimers.....	137
Figure 3.16 Amino acid sequences of 7 selected Affimers against FGFR3.....	139
Figure 3.17 Amino acid alignment of FGFR3 and GFP Affimers.....	141
Figure 3.18 SDS-PAGE gels of purified Affimers against FGFR3.....	143
Figure 4.1 Direct ELISA to examine the binding of Affimers to biotinylated DDT immobilised on a NeutrAvidin-coated plate.	148
Figure 4.2 Optimisation of Affimer concentration and incubation time point for competitive ELISA.....	150
Figure 4.3 Competitive ELISA to examine the binding between six Affimers to free DDT.	153
Figure 4.4 Hypothetical scheme showing the binding of the Affimer to the DDT moiety and spacer.....	154
Figure 4.5 Biotinylation of an Affimer via biotin-maleimide.....	156

Figure 4.6 ELISA to check the success of Affimer biotinylation.	157
Figure 4.7 LC-MS spectrum of a FGFR3-8 Affimer prior to biotinylation. ...	158
Figure 4.8 LC-MS spectrum of a FGFR3-8 Affimer after biotinylation.	159
Figure 4.9 Double-sandwich ELISA test to check the binding of Affimers and FGFR3 protein.	162
Figure 4.10 A typical SPR binding sensorgram showing association and dissociation phases.....	163
Figure 4.11 SPR sensorgrams showing the changes of refractive index in response units (RU).	165
Figure 4.12 The results of SPR data fitting with a one-site binding model available on Graphpad Prism 7 software.....	166
Figure 4.13 Immunoprecipitation assay showing the binding of the Affimers to FGFR3.	170
Figure 4.14 ELISA to confirm the specific binding of Affimers to FGFR3. .	173
Figure 5.1 Schematic representation of a sensor constructed following the ELISHA “gluing” method.....	179
Figure 5.2 A cyclic voltammogram of polyoctopamine and Affimer deposition onto a Dropsens gold screen-printed electrode.	179
Figure 5.3 Sensor response after cumulative addition of FGFR3 concentrations.....	181
Figure 5.4 Schematic illustration of a fully-constructed Affimer-based sensor.....	183
Figure 5.5 Cyclic voltammogram of polytyramine deposition.	184
Figure 5.6 Nyquist plot showing layer-by-layer construction of an FGFR3-21 Affimer-based biosensor.	185
Figure 5.7 Nyquist plot showing two fully constructed FGFR3-21 Affimer-based biosensors with the polytyramine layer prepared in different solvents.....	187
Figure 5.8 Impedance spectra showing the stability of baseline before a sensor was tested with a range of FGFR3 concentrations.....	188
Figure 5.9 Impedance spectra after cumulative addition of FGFR3 concentrations ranging from 10 ⁻¹⁴ M to 10 ⁻⁸ M to a fully constructed sensor.	190

Figure 5.10 The typical Cole-Cole plot showing complex capacitance of a FGFR3-21 Affimer biosensor before and after exposing to FGFR3 protein from 10^{-14} M to 10^{-8} M.....	192
Figure 5.11 The plot showing the relationship between phase shift and frequencies of a FGFR3-21 Affimer biosensor..	194
Figure 5.12 The plot showing the relationship between absolute values of impedance and frequencies of a FGFR3-21 Affimer biosensor..	195
Figure 5.13 Optimisation of Affimer concentration for impedimetric biosensors with data analysis based on the Rct values.	198
Figure 5.14 Optimisation of Affimer concentration for impedimetric biosensors with data analysis based on the capacitance values.	201
Figure 5.15 Optimisation of Affimer concentration for impedimetric biosensors with data analysis based on the phase shift..	203
Figure 5.16 Optimisation of Affimer concentration for impedimetric biosensors with data analysis based on the absolute values of impedance.	206
Figure 5.17 Optimisation of Neutravidin concentration for impedimetric biosensors with data analysis based on the Rct values.	211
Figure 5.18 Effect of blocking agents on biosensor performance with data analysis based on the Rct values.	215
Figure 5.19 Specificity of biosensors to the analytes with data analysis based on the Rct values.....	219
Figure 5.20 Schematic representation of Affimer sensor construction according to the modified protocol.....	223
Figure 5.21 Optimisation of Affimer concentration for impedimetric biosensors subject to the modified sensor construction protocol..	225
Figure 5.22 Effect of different clones of the FGFR3-specific Affimer on the sensor performance.	228
Figure 5.23 Effect of blocking agents on sensor performance subject to the modified protocol.....	230
Figure 5.24 Specificity of biosensors to the analytes with data analysis subject the modified construction protocol.....	233
Figure 5.25 Specificity of biosensors to the analytes with data analysis subject the modified construction protocol.....	236
Figure 5.26 Schematic representation of Affimer sensor construction. The sensor was blocked with polystyrene sulfonate after biotinylated Affimers were attached to the electrode.	239

Figure 5.27 Effect of polystyrene sulfonate as a blocking agent on sensor performance.....	241
---	------------

List of Tables

Table 1.1 Applications of impedimetric biosensors for the detection of different types of analytes	35
Table 1.2 Examples of some non-antibody binding protein scaffolds and their characteristics	55
Table 1.3 Comparison between cytology and other commercial biomarker tests for monitoring the occurrence of bladder cancer	71
Table 2.1 Lists of blocking reagents and working concentrations used in this experiment	106
Table 3.1 Amino acid sequences at variable peptide loops 1 and 2 of eight selected Affimers against DDT	134
Table 4.1 Comparison of molecular mass of the Affimers before and after biotinylation	160
Table 4.2 Fitting SPR data from a one-site binding model..	167

Chapter 1

Introduction

1.1 Overview

Recently, point-of-care (POC) diagnostics and environmental (“point of use”, POU) monitoring have gained popularity among scientific communities because they offer very rapid analyses without loss of process or use of expensive equipment. Biosensors are small devices developed to detect a variety of targets of interest, which can be small molecules, oligonucleotides, proteins, viruses and bacteria. Due to their capabilities of detecting a vast range of targets, biosensors are invaluable tools to track emergence of life-threatening diseases for POC diagnosis and for monitoring contamination by pollutants in the environments. Based on the methods of transduction, biosensors are in general categorised into three major types, namely optical, mechanical and electrochemical sensors.

Since the first glucose biosensor was launched in 1962 (Clark and Lyons, 1962), electrochemical biosensors have gained substantial attention from researchers because of their high sensitivity, ease of operation and possibility for miniaturisation. Impedimetric biosensors are a type of label-free electrochemical sensor, depending on the measurement of changes in capacitance and charge-transfer resistance. The benefit of using impedance rather than amperometry or potentiometry is that biorecognition elements are not limited to biomolecules involving enzymatic reactions, and for amperometric biosensors, oxidases and reductases. Mostly, antibodies have been used as bioreceptors for impedance biosensor fabrication during the past decade.

Although antibodies offer many advantages as bioreceptors, especially their antigen recognition specificity, they have disadvantages that can make them troublesome. It is not possible to produce antibodies such as IgG in microbial systems because post-translational modifications, e.g. glycosylation are required. Production of antibodies needs animal hosts, which leads to batch-to-batch variation. This can produce problems with repeatability of biosensor performance. Synthetic binding proteins have been developed in order to overcome the downside of antibodies and the Affimer is a recently developed non-antibody binding scaffold. In addition to properties such as specific recognition of the targets at high affinity, the ease of production and thermal stability are additional bonuses, making them an alternative to antibodies in biosensing applications.

In this thesis, the major focus is to develop a biosensor platform using the principle of electrochemical impedance spectroscopy (EIS), together with Affimers to detect specific targets, which can be a small molecule or a protein biomarker. This work includes Affimer screening, characterisation and the use of Affimers in impedance biosensor application.

1.2 What is biosensor and how is it important?

Recently, biosensors have gained increasing attention from the scientific communities since they offer a rapid and cost-effective measurement that can be applied to a wide range of research areas. Typically, for conventional laboratory-based methods, long-processing times, low sensitivity and specificity, cost, and specialised requirement for technicians and trained users are the disadvantages that prevent them from use in point-of-care (POC) diagnostics and for environmental monitoring. However, the advent of biosensors and miniaturisation technology, including microfluidics, make small lab-on-a-chip devices possible for self-monitoring and POC diagnosis (Rushworth et al., 2013, Ahmed et al., 2014).

A biosensor is an analytical device which detects the change in analyte concentration, which it then converts into a measurable signal that can be displayed by a detector (Rushworth et al., 2013, Conroy et al., 2009, Ronkainen et al., 2010). Basically, a biosensor is comprised of three components (Figure 1.1). The first part is a biorecognition element which binds to the target analytes such as small molecules, proteins, DNA, RNA, bacteria and viruses. The second component is a transducer e.g. electrochemical, optical and piezoelectric transducers that changes a biological event to a detectable signal. Finally, a measurable readout or signal processing display amplifies and interprets the signal and displays it (Rushworth et al., 2013).

In comparison with other conventional laboratory-based techniques, biosensors offer considerable advantages. Biosensors usually offer higher sensitivity and specificity. The processing time of target monitoring is short. As biosensors are created as smaller devices, they can be portable for field use. There is also minimal need for any specialist training before operation (Ahmed et al., 2014). Since the launch of the first glucose biosensor invented by (Clark and Lyons, 1962), there have been applications of biosensors to measure a wide range of analytes including bacteria, viruses, nucleic acids, small molecules and protein biomarkers of disease (Rushworth et al., 2013, Barton et al., 2009, Mejri et al., 2010, Ravalli et al., 2013).

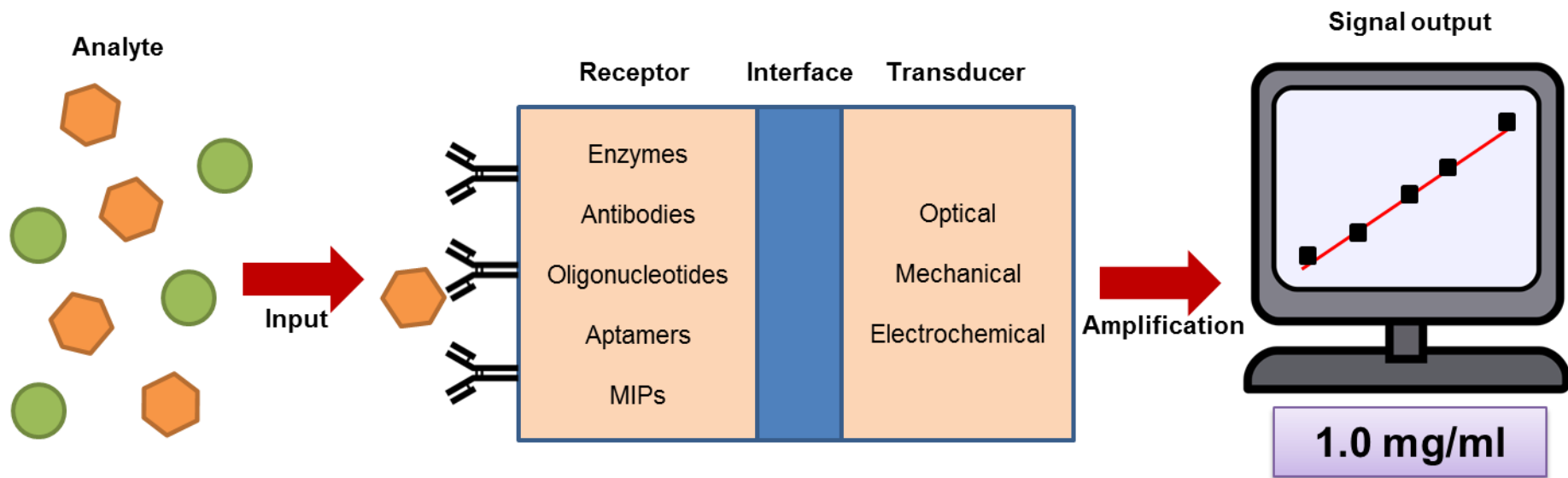


Figure 1.1 A schematic showing basic components of a biosensor system. A basic biosensor is comprised of three components, a biorecognition element, a transducer and a measurable readout.

1.3 Types of biosensors

1.3.1 Optical biosensors

Optical biosensors are sensors that work on the principle of measuring the changes in optical properties resulting from analyte-bioreceptor binding at the sensor surface (Ahmed et al., 2014). In general, based on different detection methods, optical biosensors are categorised into two types, label-based and label-free detections. In label-based platforms, either the target molecule or the biorecognition element is tagged with a chromophore or a fluorophore. In fluorescence-based biosensor platform, the fluorescent intensity detected indicates the concentration of the target molecules in the sample (Fan et al., 2008). Despite the fact that the fluorescence-based methods offer extreme sensitivity, possibly down to single molecule detection, the requirements for sample labelling and processing are the main disadvantages of this techniques (Ahmed et al., 2014, Fan et al., 2008). An example of fluorescence-based optical biosensors is fluorescence resonance energy transfer (FRET) biosensors. The FRET biosensor is non-radiative and works principally on the energy transfer from an excited donor fluorophore to an acceptor fluorophore via dipole-dipole interaction (Shi et al., 2015a, Shi et al., 2015b). The acceptor molecule is required to absorb energy at the emission wavelength of the donor (Chen et al., 2013). Despite its high sensitivity, the efficiency of a FRET sensor is limited by the nature of the dipole-dipole interaction with the distance ≤ 10 nm. In one study, the researchers applied a FRET biosensor to detect *mecA* gene of *Staphylococcus aureus* (Shi et al., 2015a). The oligonucleotide probes were immobilised onto graphene quantum dots (GQDs) whilst the reporter probes were captured on gold nanoparticles (AuNPs). In the presence of target oligonucleotides, the co-hybridisation of the target oligonucleotides, the capture probes and the reporter probes takes place, bringing GQDs and AuNPs into close proximity. This

leads to the decrease in fluorescence intensity or fluorescence quenching, which is measurable. The detection limit of the *S. aureus* gene was down to 1 nM. To date, label-free optical methods overcome these weak points of fluorescence-based techniques. Surface plasmon resonance (SPR) is one of the most widely-used label-free biosensors employed to detect a multitude of analytes (Owen, 1997). SPR system basically consists of plane-polarised light that passes through a glass prism. When the light propagates in the prism (higher refractive index medium) and hits the interface of a thin gold film and the solution (lower refractive index medium), total internal reflection (TIR) occurs. At the incident angles larger than the critical angle, evanescent waves, which decay exponentially with the distance away from the interface, are generated at the side of lower refractive index medium (solution). At a specific angle, the evanescent wave is able to excite delocalised electrons or plasmons of the gold film, leading to surface plasmon resonance phenomenon. This causes the immediate decrease of the intensity of reflected light. The incident angle with minimum reflectivity is called 'SPR angle'. The SPR angle can be shifted upon the change in refractive index of the solution of interest, which is subject to mass and/or density of materials deposited on the gold surface. In general, at the base of the prism, bioreceptors are functionalised onto gold surface. When the target analytes bind to the receptors, the refractive index in the transducer surface is altered, leading to a shift in the SPR angle. Optical biosensors based on SPR have been employed with various types of bioreceptors, for example, antibodies (Baccar et al., 2010, Wang et al., 2012), bacteriophage (Tawil et al., 2012, Tripathi et al., 2012), lectins (Gasparyan and Bazukyan, 2013, Wang et al., 2013), synthetic binding peptides (Michel et al., 2017, Hanenberg et al., 2014, Cheung et al., 2012) and oligonucleotides (Kambhampati et al., 2001, Teh et al., 2007).

1.3.2 Piezoelectric biosensors

A piezoelectric biosensor is an analytical device that measures the change in resonant frequency caused by the binding of an analyte to its bioreceptor (Rushworth et al., 2013, Borman, 1987, Janshoff et al., 2000). There are several examples of piezoelectric biosensors including the quartz crystal microbalance (QCM), atomic force microscopy (AFM), cantilever biosensors, surface acoustic wave (SAW) and others. QCM sensors measure the alteration in resonant frequency due to an increase of mass on the sensor surface. This technique has been applied in many fields (Xi et al., 2013). AFM is a very high-resolution scanning probe microscopy developed by (Binnig et al., 1986). For the basic principle, a cantilever with a sharp tip is employed to scan across the surface of the target to measure its surface morphology and show up a 3D image of the surface. In biosensor technology, the cantilever surface is modified with a layer of bioreceptors to increase detection of the analyte more selectively and specifically (Rushworth et al., 2013). Because of its highly sensitivity, AFM is a promising analytical method that has been used for pathogen detection, DNA analysis, and biomarker detection (Lavrik et al., 2004), although the equipment is complex and costly. Cantilever sensors work on the same principle of AFM. However, instead of using a sharp tip as in AFM, free-standing beams are used for bioreceptor immobilisation. The bottom of the beam is functionalised with bioreceptors whilst the top is coated with a protein resistive monolayer film in order to prevent the surface from non-specific binding of analyte and unwanted components (Fritz, 2008). In the presence of analyte, the binding of a bioreceptor and an analyte causes a compressive surface stress, leading to bending of the cantilever. This response change can be detected by optical beam deflection, which is translated into a change of the reflected laser spot position on a detector. Cantilever biosensors have been applied for detection of a number of targets such as bacteria (Campbell and Mutharasan, 2006, Tzen et al., 2011), parasite (Xu and Mutharasan, 2010), biomarker proteins (Arntz et al., 2003, Wu et al., 2001) and

oligonucleotides (Calleja et al., 2005, Johnson and Mutharasan, 2012). A SAW biosensor is a piezoelectric biosensor which relies on the use of surface acoustic waves to monitor biological phenomena such as binding of biomolecules. A basic SAW device contains a piezoelectric substrate such as quartz, GaAs, or LiNbO₃, an input interdigitated transducer, an output interdigitated transducer, and a space between two interdigitated transducers known as “the delay line”. The input interdigitated transducer converts an electrical signal into an acoustic wave, which travels across the surface of the delay line. At the output interdigitated transducer, this acoustic wave is converted back into an electrical signal by piezoelectric effect. For analyte detection, the delay line is functionalised with bioreceptors. When the bioreceptors bind their specific targets, changes in the mass or viscosity occurs (Durmuş et al., 2014). This leads to the change of acoustic wave velocity, which can be measured by the electrical signal. This type of biosensor has been used for monitoring many targets including pathogens (Rocha-Gaso et al., 2009, Howe and Harding, 2000, Bisoffi et al., 2008, Berkenpas et al., 2006), proteins (Krishnamoorthy et al., 2008, Lee et al., 2011) and odorant molecules (Di Pietrantonio et al., 2013).

1.3.3 Electrochemical biosensors

Electrochemical biosensors are one of the largest groups of biosensors and are widely used in many areas (Zelada-Guillen et al., 2013). Generally, electrochemical biosensors are divided into three different subtypes, amperometric, potentiometric, and impedimetric biosensors.

1.3.3.1 Amperometric biosensors

Amperometric biosensors are based on the direct monitoring of current produced by an electrochemical redox reaction in response to the interaction of analyte and bioreceptor while the potential applied between two electrodes remains at a constant value (Rushworth et al., 2013, Ahmed et al., 2014, Ronkainen et al., 2010). The relationship between current and time can be described using the Cottrell equation (equation 1.1) as follow.

$$I = nFAC_0\sqrt{\frac{D}{\pi t}} \dots\dots\dots(1.1)$$

Where :

I is current in amperes (A),

n is number of electrons,

F is Faraday constant (96,485 C mol⁻¹),

A is area of the electrode in cm²,

C₀ is initial concentration of analyte in bulk solution,

D is diffusion coefficient of species,

t is time in second (s).

In a flow or stirring system where mass-transfer limitation is eliminated, the current generated is directly proportional to the concentration of the target analytes in the samples (Hirst, 2014). In order for the sensors to measure the analyte-bioreceptor interaction, oxidoreductases and dehydrogenases are commonly used as biorecognition elements for constructing the sensors. A major example is glucose oxidase present in many medical glucose sensors (Wang, 2001). There are several advantages that amperometric biosensors can offer including a short response time when being used in point-of-care diagnostics. They are also sufficiently sensitive for detection, and can be miniaturised. However, because of the electrochemical

potential applied to the system, the specificity of the detection process can be low and other oxidisable species such as ascorbate and urate can interfere with the signal, leading to an error in the results (Higson, 2012). In modern amperometric biosensors, electron mediators such as Prussian Blue (PB) and ferrocene (Fc) or conducting polymers such as polypyrrole, polythiophene and polyaniline are introduced to sensor surface in order to facilitate electron transfer from substrate to transducer (Goode, 2015, Hirst et al., 2013, Dong et al., 1992, Qiu et al., 2009, Vidal et al., 2003). This enables amperometric biosensors to be operated at much lower applied potential and makes the sensors more specific to the analytes. More importantly, amperometric biosensors are limited to use for the detection of analytes in which an oxidoreductase is available (Rushworth et al., 2013, Ahmed et al., 2014) such as the pyrocatechol oxidation catalysed by the laccase enzyme (Kulys and Vidziunaite, 2003).

1.3.3.2 Potentiometric biosensors

In contrast to amperometric biosensors, potentiometric biosensors employ ion-selective electrodes to detect the change in potential that occurs in response to analyte-bioreceptor interaction while the current used in the system is kept constant at zero (Ahmed et al., 2014, Ronkainen et al., 2010, Hirst, 2014). In the sensor fabrication step, the chemical sensors are coated with a biorecognition element such as a hydrolase which catalyses and generates measurable ions such as H⁺ or NH₄⁺ (Ronkainen et al., 2010). The use of an ion-selective membrane defines the target ion measured (Korotcenkov, 2010). In potentiometry, the relationship between free ion concentration and potential is governed by the Nernst equation (equation 1.2).

$$E_{cell} = E_{cell}^0 - \frac{RT}{nF} \ln Q \dots\dots\dots(1.2)$$

Where :

E_{cell} is the observed cell potential at zero current and sometimes known as electromotive force (EMF),

E^0_{cell} is the constant potential contribution to the cell,

R is the universal gas constant ($8.314 \text{ J K}^{-1} \text{ mol}^{-1}$),

T is the absolute temperature in degree Kelvin,

n is the charge number of electrode reaction,

F is the Faraday constant,

Q is the ratio of ion concentration at the anode to cathode.

An example of these sensors is the penicillin sensor that uses a pH electrode coated with the enzyme penicillinase. This enzyme catalyses penicillin cleavage and production of H^+ which contributes to the change in pH that can be measured by the electrode (Papariel et al., 1973). The construction of potentiometric biosensors is inexpensive and the sensors are also easily portable. However, potentiometric biosensors are sensitive to pH-active components and interfering species such as urea, ammonia and creatine in the samples (Keusgen, 2002, Koncki, 2007). Therefore, the measurements of the sensors have to be performed in low buffer concentrations to avoid any interferences. However, in diluted buffer, the sensors are more sensitive to non-specific effects from pH and buffer capacity of samples (Koncki, 2007). In addition, they show a log response to the analyte concentration. Potentiometric biosensors are often used in food processing e.g. measurement of alcohol concentration in brewing (Rotariu et al., 2004), determination of urea in milk (Trivedi et al., 2009) and detection of bacteria in vegetables (Ercole et al., 2003).

1.3.3.3 Impedimetric biosensors

Impedimetric biosensing is based on the alteration in impedance, namely double-layer capacitance and charge transfer resistance, across the surface of

working electrodes resulting from the binding of an analyte to its bioreceptor (Ahmed et al., 2014, Rushworth et al., 2013). Typically, the change in impedance signal detected is proportional to the logarithmic scale of the concentration of analyte binding to the biorecognition element. However, as the concentration of analytes increases, the impedance might rise or fall down depending on the nature of the analyte (Rushworth et al., 2013). Impedimetric biosensors offer some advantages over other biosensors because they can be applied to a very wide range of target molecules since binding of the analyte and bioreceptor, rather than a specific substrate and enzyme, is required. However, there are currently limitations of using impedimetric biosensors owing to problems with reproducibility and nonspecific binding (Daniels and Pourmand, 2007, Berggren et al., 2001). Furthermore, no impedimetric biosensing device is commercially available in the market. In the work presented in this thesis, we focus on the use of impedimetric biosensors.

1.4 Electrochemical impedance spectroscopy (EIS)

Electrochemical impedance spectroscopy (EIS) has become one of the most promising and powerful tools employed in biosensor research, particularly for medical applications (Millner et al., 2012). The following are the general principle of EIS, and the fabrication and applications of impedimetric biosensors.

1.4.1 The brief principle of electrochemical impedance spectroscopy

As mentioned in Section 1.3.3.3, an impedimetric biosensor measures the change in capacitance and electron transfer resistance across the sensor surface of a working electrode when the biorecognition element captures the target molecule.

For faradaic impedance, an electron mediator solution which contains a redox pair such as $\text{Ru}(\text{NH}_3)_6^{3+/2+}$ (hexaammineruthenium III/II ions) or $\text{Fe}(\text{CN})_6^{3-/4-}$ (ferricyanide/ferrocyanide) is present (Chang and Park, 2010). The use of electron mediators is to ensure that the charge transfer within impedance is not limited by the supply of electrons. Without electron mediators, the monitoring of impedance can be achieved and it is known as non-faradaic impedance.

In EIS, a small amplitude sinusoidal voltage is applied to the system over a broad range of frequencies, typically 100 kHz to 1 mHz (Sekar and Ramasamy, 2013). The impedance value is calculated as the ratio between the voltage (V) applied to the system and the alteration of current (I) detected when V and I are plotted as an amplitude sine wave against time (t), or phase angle (θ). Both phase shift (θ) and the change in magnitude ($|Z|$) of the sine wave lead to the change in the impedance, that can be shown by the following equation (equation 1.3).

$$|Z| = \frac{V \sin \omega t}{I \sin(\omega t + \theta)} \dots\dots\dots(1.3)$$

Where :

$|Z|$ is impedance,

V is maximum voltage,

I is maximum current,

t is time (s),

ω is frequency of oscillating voltage (rad s^{-1}),

θ is phase angle (rad).

The data resulting from the EIS is often presented as a Nyquist plot (Figure 1.2A) and is modeled according to a Randles' equivalent circuit (Figure 1.2B). In general, a Nyquist plot is comprised of two components; the first is the real or resistive (Z') component of impedance whilst the other is the imaginary or capacitive ($-Z''$)

component. The shape of the Nyquist plot is semi-circular with a 45-degree rise of the Warburg impedance (W) line found at low frequencies due to mass transfer diffusion effects (Figure 1.2A). The semi-circle of the Nyquist plot indicates the different electrochemical phenomena on the sensor surface at a range of frequencies after the application of voltage. At high frequencies, $Z'/-Z''$ does not result from the binding between the analytes and receptors, but from the resistance in the solution itself. Under this condition, transfer of electrons can reach only the top of an electrode surface, but cannot go through it, since the oscillation in current happens too fast for electron transfer to take place between electron mediators in the solution and the sensor surface. This parameter is represented by the solution resistance (R_s), the x-axis intercept, which is actually constant. On the other hand, at low frequencies, there is adequate time for electrons to move from the mediators in the solution into electrode surface. Therefore the ratio of measured impedance is from both dielectric-layer capacitance (C_{dl}) and charge transfer resistance (R_{ct}). The Nyquist plot can also be translated into the Randles' equivalent circuit model which was first presented by (Randles, 1947).

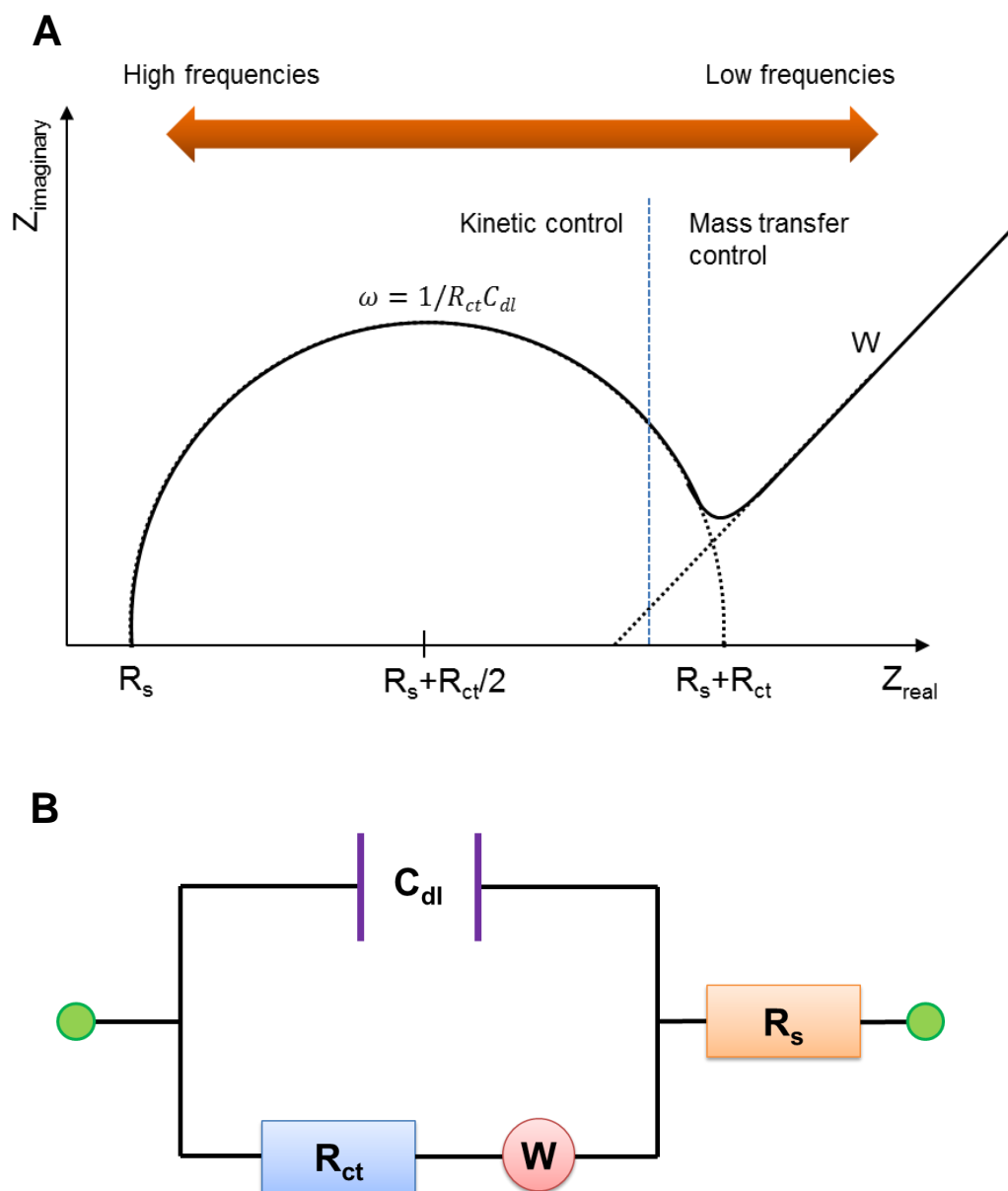


Figure 1.2 Schematic of a Nyquist plot alongside a Randles' equivalent circuit. (A) a Nyquist plot and (B) a Randles' equivalent circuit model. The values of R_{ct} and C_{dl} can be calculated from the Nyquist plot. (R_s = solution resistance; R_{ct} = charge transfer resistance; C_{dl} = dielectric-layer capacitance; W = Warburg impedance).

The signal intensity from impedimetric biosensors depends on the deposition of bulk materials on the sensor surface. In general, when the amount of material deposited on the electrode surface increases, a rise in impedance signal is seen (Figure 1.3A and 1.3B). There are two main reasons for this event. The first is that

the electrons from the mediator in the solution need to get through the multiple layers of bulk materials to reach the sensor surface, leading to an increase in charge transfer resistance. The other reason is that as the material over the electrode surface increases, there is an increase in charge storage capacity. An example of this is presented by the experimental data from myoglobin impedimetric sensors (Billah et al., 2010). It was observed that as the concentration of myoglobin increased, there was a rise in the R_{ct} values. However, this is not for all cases. In the presence of analytes that changes the nanostructure or chemical nature of the sensor surface (Rushworth et al., 2013), a fall in R_{ct} can be seen (Figure 1.3A and 1.3C). For example, in a previous study of a label-free electrical impedimetric biosensor for Alzheimer's amyloid-beta oligomers, it was found that the measured R_{ct} decreased with an increase of $A\beta O$ concentration, corresponding to increased capacitance and decreased resistance on the sensor surface (Rushworth et al., 2014). This is most likely due to the binding of $A\beta O$ to the biorecognition element, PrP₉₅₋₁₁₀, that can increase the conductivity of the electrode surface, leading to a decrease in impedance.

According to the Randles' equivalent circuit model (Figure 1.2), R_{ct} is the most frequently used parameter to evaluate the performance of impedimetric biosensors as the change of R_{ct} is proportional or inversely proportional to the amount or concentration of target analyte (Billah et al., 2010, Rushworth et al., 2014, Ahmed et al., 2013, Goode et al., 2016, Barton et al., 2008, Caygill et al., 2012). However, the change in capacitance has occasionally been employed for the same purpose. Double-layer capacitance (C_{dl}) is a parameter representing the storage of electrical energy occurred by the formation of electrical double layer at the interface between the electrode and the solution of electrolyte. This parameter is equivalent to a capacitor in the electrical circuit (Sekar and Ramasamy, 2013). The C_{dl} can be changed depending on a number of factors such as electrode polarisation, ionic concentration in bulk solution, temperature, type of ions and roughness of electrodes.

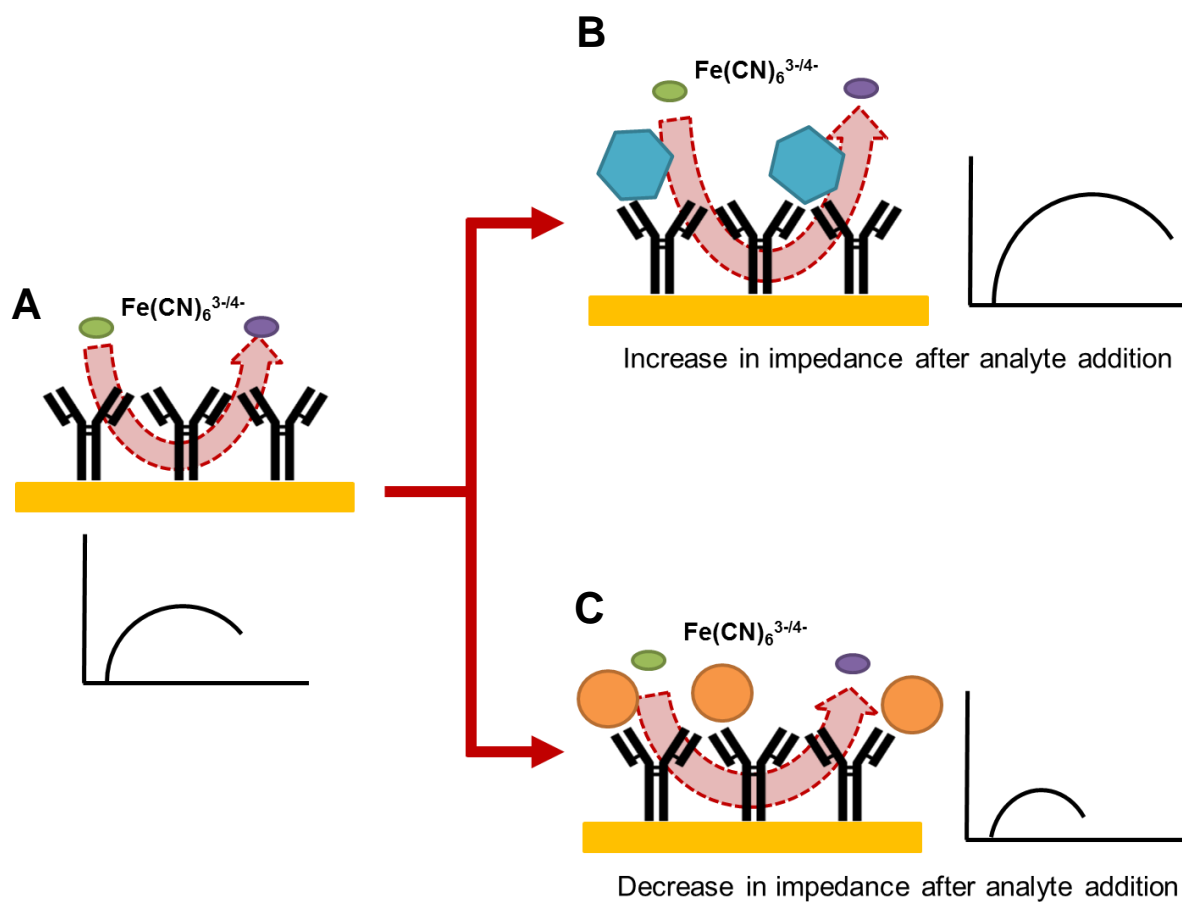


Figure 1.3 Schematic showing possible impedance shifts resulting from binding of analytes and receptors on the sensor surface. The $\text{Fe}(\text{CN})_6^{3-/4-}$ redox pair is widely used as electron mediator. In general, the impedance increases from (A), an electrode surface with attached bioreceptors to (B), an electrode surface with bioreceptors binding to target molecules. In some circumstances (C), a decrease in impedance can be found after bioreceptors bind to analytes.

In the case of a pure capacitor, the metal surface is perfectly smooth and undamaged, providing very high impedance with the phase shift at 90° . However, in impedimetric biosensors, the purely capacitive surface does not truly exist as there is contamination and roughness of the electrodes and the phase angles normally fall between 0° and 90° (Sekar and Ramasamy, 2013). As a result, the C_{dl} is replaced by constant phase element (CPE). As well as the R_{ct} , the CPE can be obtained from fitting with the Randles' equivalent circuit model. In impedimetric biosensors, the change in capacitance values has been used for a vast range of analytes of interest. In 2015, Jolly and co-workers developed an aptamer-based impedimetric biosensor to detect prostate specific antigen (PSA), a biomarker for prostate cancer (Jolly et al., 2015). The researchers used faradaic impedance measurement to investigate the binding of the aptamer and PSA. The impedance data were converted into complex capacitance and the changes in capacitance were then obtained. They found that the increase of capacitance was observed with increasing concentrations of PSA. Fernandes and his team reported the fabrication of impedimetric biosensors using antibodies to detect C-reactive protein (CRP) (Fernandes et al., 2014). The antigen-antibody interaction was detected via the change in capacitance. The decrease in capacitance was observed as the concentration of CRP increased. Kim and her colleagues also employed EIS to monitor bacterial adhesion and biofilm maturation using the change in capacitance values (Kim et al., 2011). The researchers observed that the decrease in capacitance was seen as the predetermined times indicating the growth of bacteria increased. Taken these examples together, the change in capacitance (increase or decrease) depends on the nature of target analytes and bioreceptors.

1.4.2 Fabrication of impedimetric biosensors

1.4.2.1 Electrodes

Screen-printed transducers are usually composed of three different types of electrodes, namely a working electrode, a reference electrode and a counter electrode. In some cases there can be more than one working electrode. The working electrodes are functionalised by attachment of biorecognition elements such as antibodies, enzymes, peptides and nucleic acid oligomers on their surface. The reference electrode has a role in measuring and controlling the working electrodes' potential when the current is applied to the surface of the working electrodes. Ultimately, the counter electrode supplies current to the system so that the balance of potential between the electrode and solution is still maintained.

To select suitable electrode materials, there are several key properties that are needed including high conductivity and biocompatibility (Rushworth et al., 2013). Regarding the limitations of each material, materials generally used for construction of biosensors are gold (Au), platinum (Pt) and various forms of carbon (Barton et al., 2009, Alizadeh and Akbari, 2013, Lee et al., 2008). However, in this review only gold is further mentioned in more detail. Gold is one of the most popular materials for the use as a working electrode material. This is because it can offer several advantages over other materials. For example, its high conductivity and potential surface flatness, which sometimes need to be modified for the reduction of roughness, can benefit functionalisation of the transducer surface. Moreover, for bioreceptors which possess external thiols, this makes it easy to attach the bioreceptors to the gold electrode surface via crosslinking between primary amine groups from the polymer and sulfhydryl groups from the bioreceptors (Millner et al., 2009). In principle, bioreceptors can be attached directly to gold via thiol-chemisorption, but this is usually inadvisable as it often causes inactivation of the bioreceptor. Gold has been

applied for use in a wide range of bioanalytical systems such as disease biomarker detection (Hu et al., 2013, Rushworth et al., 2014, Johari-Ahar et al., 2015) and small molecule measurement such as lysine, chloramphenicol and lead (Chauhan et al., 2013, Pilehvar et al., 2012, Cui et al., 2016).

1.4.2.2 Functionalisation of transducer surface

There are several techniques that are useful for functionalising transducer surfaces and the three most widely-used ones are self-assembled monolayers (SAMs), conducting polymers and non-conducting polymers.

1.4.2.2.1 Self-assembled monolayers (SAM)

SAM-based biosensors can be formed by chemisorption of organic molecules with functional groups such as thiols, disulphides, amines, acids and silanes, onto the surface of sensor electrodes (Arya et al., 2009). Typically, SAMs can be formed using long chain molecules consisting of a head group that can capture a target molecule, an alkyl chain that can make the assembly stable using van der Waals interactions and ω -functionality that is essential for the formation of a monolayer. Examples of long chain molecules are mercaptohexadecanoic acid (MHDA) (Billah et al., 2010, Rodgers et al., 2010) and other fatty acids (Lim et al., 2007, Litjebblad et al., 2014). In addition, small aromatic molecules including 4-aminothiophenol (4-ATP) (Conroy et al., 2010, Billah et al., 2010, Valerio et al., 2008) and many types of silane (Lessel et al., 2015, Herzer et al., 2010) can also be used for SAM formation. Because of its high stability, homogeneity of the surface structure and ease of generating different layers, SAMs can be a suitable choice for biosensor development. To employ SAMs for biosensing applications, modification of the SAM is needed. There are several methods that have been used to modify SAMs, for

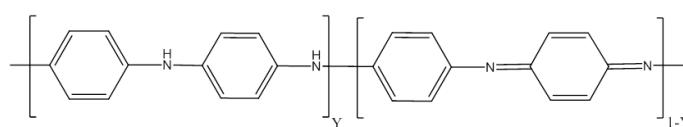
example, physical adsorption (Nam et al., 2004, de Groot et al., 2007), chemical activators (Dannenberger et al., 2000), chemical cross-linkers (Billah et al., 2010, Arya et al., 2007, Arya et al., 2006) and exchange processes (Satjapipat et al., 2001).

1.4.2.2.2 Conducting polymers

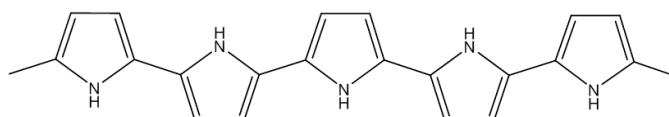
Recently, conducting polymers (CPs) have gained popularity for biosensor research thanks to their unique properties. Although some of their characteristics are similar to those of metals and semiconductors, many physical properties linked to their conventional counterpart such as flexibility and ease of synthesis, are still retained. It has been demonstrated that while interacting with biomolecules, CPs can still show good biocompatibility (Nambiar and Yeow, 2011). Therefore, CPs are promising candidates for biosensor development.

CPs can be categorised into three groups: intrinsically conducting polymers, redox polymers and ionically conducting polymers. Intrinsically conducting polymers including polyacetylene (PA), polypyrrole (PPy), polythiophene (PT) and polyaniline (PANI) (Figure 1.4) have been widely used as sensor base layers for biosensor construction. This is because intrinsically conducting polymers are more conductive than two other classes of CPs. The chemical structure of intrinsically conducting polymers is highly flexible due to their delocalised π -electrons, which makes them possess the desired electronic and mechanical properties after modification. In addition, because of their ability to transfer electrons generated by biochemical reactions, intrinsically conducting polymers have been widely used as a supporting layer between the bioreceptor and transducer surface in biosensors (Nambiar and Yeow, 2011). There are previous studies on a diverse range of conducting polymer based biosensors for measurement of viruses (Borole et al., 2006, Janata and Josowicz, 2003, Gerard et al., 2002). For impedimetric biosensors, CPs have

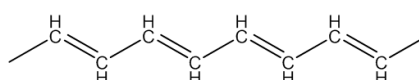
successfully been employed as a part of the sensor for detection of many different targets, for example, whole viruses (Caygill et al., 2012), foodborne pathogens (Arshak et al., 2009), small molecules such as Ochratoxin A (Khan and Dhayal, 2009), cardiac drugs e.g. digoxin (Barton et al., 2009) and oligonucleotides (Sosnowska et al., 2013, Peng et al., 2009).



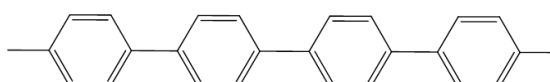
Polyaniline



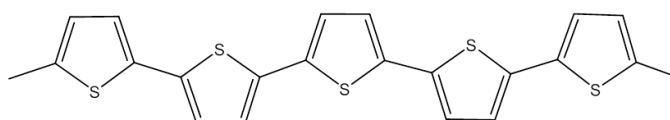
Polypyrrole



Polyacetylene



Polyphenylene



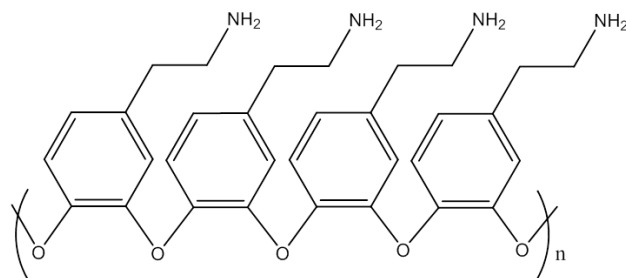
Polythiophene

Figure 1.4 Chemical structures of widely-used conducting polymers for construction of biosensors. The polymers are typically deposited onto sensor surfaces using electropolymerisation, which can be done by cyclic voltammetry.

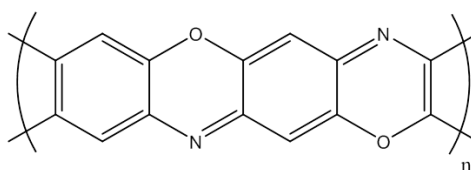
1.4.2.2.3 Non-conducting polymers

In the recent years, non-conducting polymers have gained more attention for their applications into biosensor fabrication. Apart from their similar properties to conducting polymers, non-conducting polymers offer resistivity and perm-selectivity, avoiding interference from oxidisable species such as ascorbate, urea, and acetaminophen (Miao et al., 2004). In addition, when electropolymerising this type of polymers on a solid surface, the formation of the film is often self-limiting. The thickness of non-conducting polymer layer is significantly thin and usually between 10-1000 nm. Often, charged species from aqueous solutions can easily travel through the polymer layer, making this type of polymer a suitable coating material for modifying transducer surface (Miao et al., 2004). Several non-conducting polymers have recently been applied for electropolymerisation in biosensors such as polytyramine, poly(1,3-diaminobenzene), poly(2-aminophenol), polyphenylenediamine and so on (Miao et al., 2004, Ahmed et al., 2013, Pournaras et al., 2008, Rushworth et al., 2014, Ekinci et al., 1996, Ekinci et al., 1998).

Polytyramine is one of the most non-conducting polymers extensively used for biosensor construction (Figure 1.5). A chain of polytyramine can be electrochemically formed from monomers known as tyramine or 4-(2-aminoethyl)phenol which is a derivative of tyrosine. As well as other non-conducting polymers, polytyramine has excellent properties that are effective when incorporated into biosensor fabrication. This polymer has one primary amine group per tyramine which is of benefit for immobilisation of biomolecules. With self-limiting growth when being electropolymerised on the surface of electrodes, a polytyramine film is very thin (1-100 nm) and fairly smooth, which enables charged molecules to diffuse rapidly. Therefore, the response of polytyramine-coated sensors can be highly sensitive (Miao et al., 2004, Ismail and Adeloju, 2010).



Polytyramine



Poly(2-aminophenol)

Figure 1.5 Chemical structures of two non-conducting polymers used in biosensor applications. The polymers are typically deposited onto sensor surfaces using electropolymerisation, which can be conducted by cyclic voltammetry.

1.4.2.3 Conjugation of bioreceptors to transducer surface

There are several techniques that can be used for tethering bioreceptors to electrode surfaces. Several of the most common methods are now described in more detail.

1.4.2.3.1 Adsorption

Adsorption is the simplest technique used for immobilising biomolecules onto sensor surfaces (Figure 1.6A). There are two types of adsorption, namely physical adsorption and ionic binding (Liebana and Drago, 2016). Physical adsorption requires the formations of hydrogen bonds, Van der Waals forces and hydrophobic interactions between amino acid side chains and the solid support surfaces, whereas

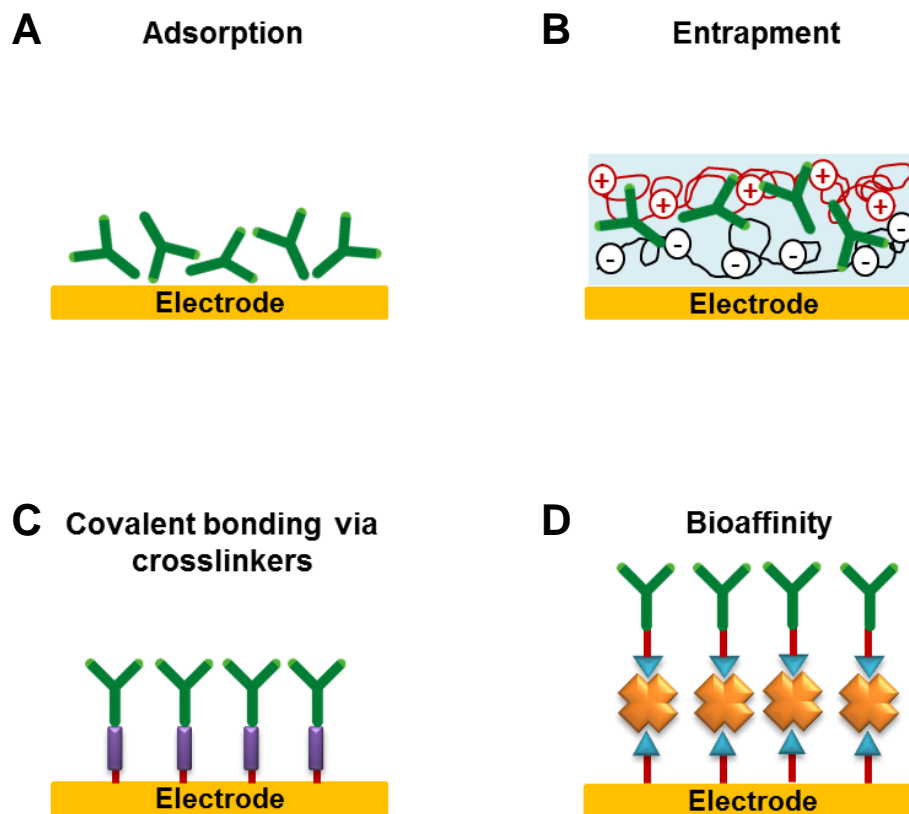


Figure 1.6 General methods to immobilise bioreceptors to transducer surface. (A) Adsorption, (B) Matrix entrapment, (C) Covalent bonding via crosslinkers and (D) Bioaffinity.

for ionic binding, positively charged and negatively charged components are needed when forming salt linkages (Mohamad et al., 2015). This method is simple, rapid and cost effective. However, because of weak interactions in the adsorption process, there are drawbacks such as reduced reproducibility and desorption of biomolecules following changes in the solvent including ionic strength and pH (Sassolas et al., 2012, Scouten et al., 1995, Liebana and Drago, 2016). Another downside is the random orientation of biomolecules attached to the surface that makes sensors less sensitive for detecting the analyte of interest.

1.4.2.3.2 Entrapment

Entrapment is a generally irreversible immobilisation technique (Figure 1.6B). Biomolecules, mostly enzymes, are entrapped in a polymeric support or fibre matrix, but do not bind or interact with the support (Liebana and Drago, 2016, Sassolas et al., 2012, Mohamad et al., 2015). The polymer layer allows substrates and products to pass through, whereas the enzymes are still trapped inside the matrix. Using this technique is advantageous since no enzyme modification is required and the enzymes still retain their function. As the enzymes are entrapped inside the polymer matrices, it can help improve mechanical stability and minimise the effects of environmental changes. However, entrapping the enzymes in thick layers of polymer can lead to mass transport limitations. In some cases, if the pore size of the matrix is too large, enzyme leakage can occur, leading to the loss of sensor sensitivity (Liebana and Drago, 2016, Sassolas et al., 2012, Scouten et al., 1995).

1.4.2.3.3 Covalent bonding via cross-linking of bioreceptors

Covalent bonding is another irreversible immobilisation method which is widely used for electrode surface modification in biosensor construction (Figure 1.6C). To immobilise biomolecules to sensor surfaces, the crosslinkers are used to facilitate the reactions (Liebana and Drago, 2016, Sassolas et al., 2012). Crosslinkers are molecules which often contain reactive groups at both ends of their structure and can interact with specific functional groups in amino acid side chains although some crosslinkers such as the EDC/NHS couple described in detail below catalyse the reaction of two side chains e.g. $-\text{NH}_2$ and $-\text{COOH}$ to form a peptide bond. Covalent cross-linking offers several advantages such as high stability and high binding strength. However, disadvantages can be found when using this type of immobilisation. For example, the reagents can be costly and diffusion limitation might occur, causing inactivation of the bioreceptor (Sassolas et al., 2012, Scouten et al., 1995, Liebana and Drago, 2016). The most common reactions used for covalent cross-linking are described as follows:

N-hydroxysuccinimide (NHS) ester reaction (Figure 1.7A): this reaction requires a crosslinker containing a NHS-carboxy ester and a primary amine ($-\text{NH}_2$) group typically found at the side chain of lysine (Hermanson, 2008). The reaction can be driven forward in pH 7-9 buffer and it should be noted that buffers containing primary amines cannot be used as they compete with the primary amine on biomolecules of interest. The examples of NHS ester crosslinkers are biotin N-hydroxysuccinimide ester (biotin-NHS) and sulfosuccinimidyl 4-(N-maleimidomethyl) cyclohexane-1-carboxylate (sulfo-SMCC).

EDC (carbodiimide) coupling reaction (Figure 1.7B): this reaction facilitates the conjugation of carboxylates ($-\text{COOH}$) to primary amine ($-\text{NH}_2$) (Hermanson, 2008). Carboxylic acid reactive groups can be found at C-terminus of proteins and side chains of aspartic acid and glutamic acid. In the reaction, EDC first reacts with a

carboxylic group on the protein and forms an active *O*-acylisourea intermediate. By nucleophilic attack, the primary amine present at the polymer surface reacts with the carboxylic group to form an amide bond, causing the release of EDC by-product as a urea derivative. The EDC cross-linking reaction can effectively be performed in acidic (pH 4.5) condition. However the reaction can still occur at neutral pH with excess amount of EDC. Frequently, NHS or sulfo-NHS (a more water-soluble analogue) is added to the reaction to improve the efficiency of the reaction and generate a dry-stable intermediate before the conjugation.

Maleimide reaction (Figure 1.7C): a thiol group from the side chain of cysteine can form a covalent bond with a maleimide reactive group via the maleimide reaction (Hermanson, 2008). Prior to bioconjugation, any disulfide bonds are usually broken using reducing agents such as dithiothreitol (DTT), 2-mercaptoethylamine (2MEA) and tris-(2-carboxyethyl)phosphine (TCEP), allowing free thiol groups to interact with maleimide reagents. In recent times, TCEP is favoured as DTT or 2MEA must be removed before conjugation or they would also react with the maleimide group. To form a thioether bond, the reaction is recommended to set at the near neutral (pH 6.5-7.5) conditions. An example of a maleimide-activated reagent is sulfo-SMCC.

Hydrazide reaction (Figure 1.7D): bioconjugation via the hydrazide reaction requires a carbonyl (aldehyde or ketone) group, which are present on oligosaccharides, as a target site for cross-linking (Hermanson, 2008). This reaction is especially useful for controlling the orientation of antibodies as there are polysaccharides located at the Fc region of IgG and other antibodies. Carbonyl groups can be created in polysaccharides by oxidising them with sodium meta-periodate. The activated moieties called oxidised sugars can now react with hydrazide reagents at pH 5-7 and create hydrazine bonds. An example of a hydrazine-containing reagent for bioconjugation is biotin-hydrazide.

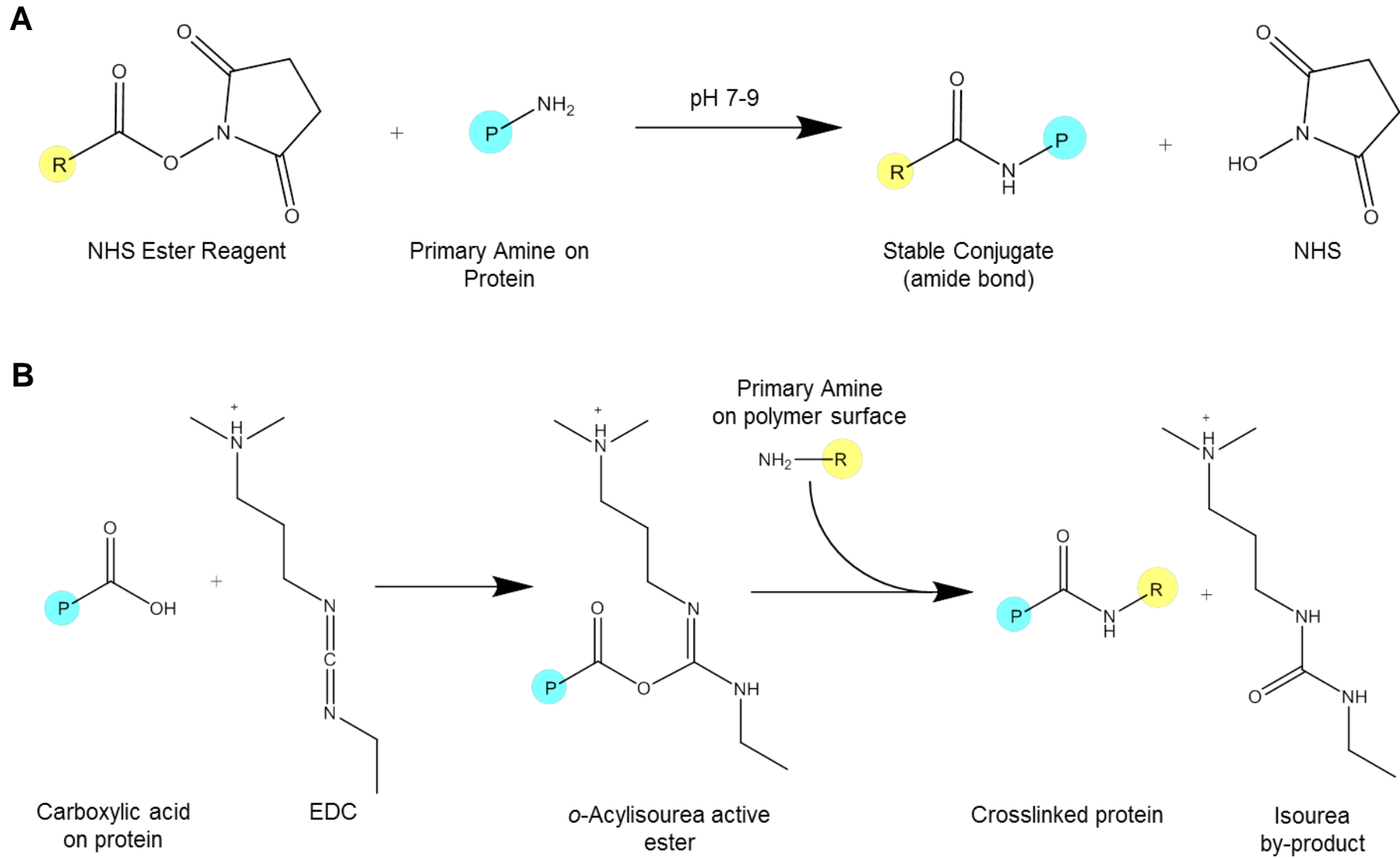


Figure 1.7 Examples of covalent bonding reactions via the crosslinkers. (A), NHS ester reaction; (B), EDC coupling reaction; (C), maleimide reaction and (D), hydrazide reaction. (R) represents a labelling reagent or a crosslinker molecule and (P) represents a protein.

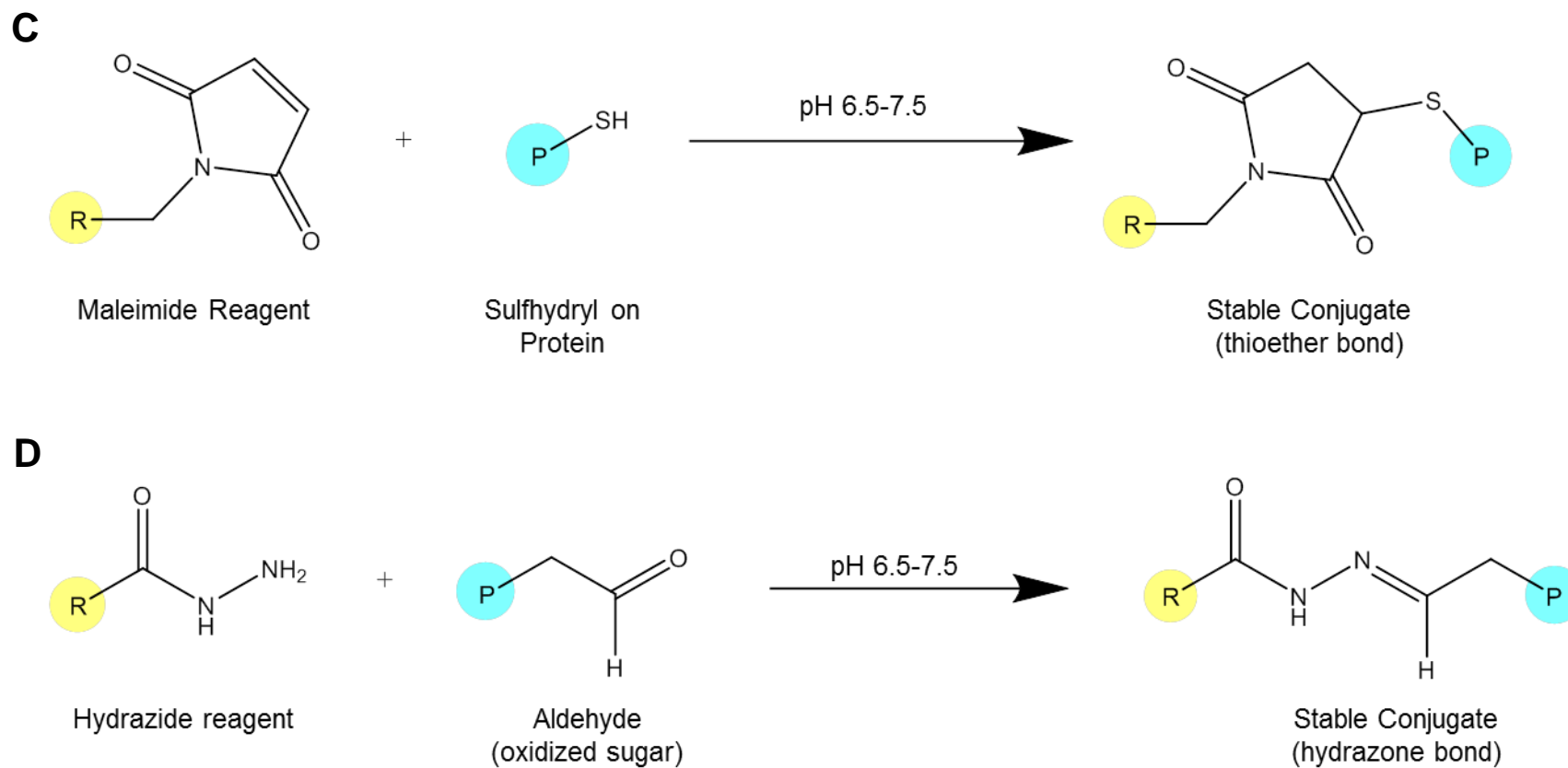


Figure 1.7 (continued) Examples of covalent bonding reactions via the crosslinkers. (A), NHS ester reaction; (B), EDC coupling reaction; (C) maleimide reaction and (D), hydrazide reaction. (R) represents a labelling reagent or a crosslinker molecule and (P) represents a protein.

1.4.2.3.4 Bioaffinity

Bioaffinity is a non-covalent immobilisation technique. The approach exploits the specific recognition between two molecules as a crosslinker (Figure 1.6D). Using this method, oriented and site specific immobilisation of bioreceptors can be effected, minimising the loss of function of bioreceptor because the binding site of the bioreceptor is placed in the correct orientation (Sassolas et al., 2012, Scouten et al., 1995, Liebana and Drago, 2016). Many specific interactions can be fairly easily reversed. This allows the electrode surface to be regenerated, reducing the cost of production. Examples of common bioaffinity couples that have been widely used in biosensors are avidin/biotin, polyhistidine tag/chelated metal ions, and antibodies/antigens.

Biotin-avidin interaction: one of the most commonly used techniques for bioreceptor immobilisation is via the biotin-avidin interaction. This method allows oriented bioreceptor immobilisation to take place conveniently. To use this method, both the biorecognition element and the polymer on the sensor surface need to be biotinylated prior to bioconjugation. During the conjugation step, avidin or one of its analogues such as streptavidin or NeutrAvidin, which are tetrameric biotin-binding proteins, are employed as a bridge connecting the biotinylated receptor molecule to the biotin-tagged polymer. Despite being a non-covalent bond, the biotin-avidin interaction has a dissociation constant (K_D) of approximately 10^{-15} M (Liebana and Drago, 2016, Sassolas et al., 2012) which makes it strong and stable enough to support the building of biosensors.

The avidins are tetrameric proteins, which are stable over a wide range of pH and temperature. Avidin protein itself is found in egg white. The molecular mass of this protein is about 67 kDa. Interaction with biotinylated molecules is barely affected by changes in pH, temperature, organic solvents, and denaturing agents. However, avidin is glycosylated and has an isoelectric point (pI) of 10, which can cause non-

specific binding. As an alternative, avidin's analogues, namely streptavidin (from *Streptomyces avidinii*) and Neutravidin (reengineered avidin) have minimal non-specific binding. Streptavidin is a 53 kDa protein and its isoelectric point is near neutral (6.8-7.5). Unlike avidin, there is no glycosylation site on streptavidin, which helps minimise non-specific binding to other molecules. However, with its RYD recognition sequence, Streptavidin tends to interact with fibronectin and other adhesion-related molecules (Alon et al., 1990). The other analogue of avidin is Neutravidin, which is a 60 kDa tetrametric protein. NeutrAvidin is a reengineered non-glycosylated version of avidin and has its isoelectric point of 6.3. Without carbohydrate modifications and RYD recognition sequences, Neutravidin should have even left non-specific binding. Currently, both streptavidin and Neutravidin are used as a linker in the fabrication of biosensors.

Biotin or vitamin H is naturally found in all living organisms. The structure of biotin contains two cyclic rings, a short spacer and a carboxyl functional group. This functional group can be modified to produce biotinylation reagents such as biotin-NHS, biotin-maleimide and biotin-hydrazide. As the biotin is small (MW = 244.309), the addition of biotin to proteins does not affect their conformation, size or functionality to any real extent (Rusmini et al., 2007).

Polyhistidine tag and metal ions: affinity tags enable interaction that can be used for biosensor applications. In general, 6-8 histidine residues are introduced to the N- or C-terminus of recombinant proteins as an affinity tag. The polyhistidine tag is placed far from the binding sites of proteins, allowing ligand binding to be unaffected (Rusmini et al., 2007). Histidine-rich regions in a protein are capable of interacting with divalent metal ions including Ni^{2+} , Cu^{2+} and Zn^{2+} . The solid support is initially coated with a chelating agent, typically nitrilotriacetic acid (NTA), prior to being loaded with divalent cations. Mostly Ni^{2+} is employed, but Cu^{2+} , Mn^{2+} and Fe^{2+} have all been used. Following this, recombinant proteins with polyhistidine tag attach to the surface via the Ni^{2+} -NTA group.

The dissociation constant for this interaction is in the low affinity range of 10 μM (Rusmini et al., 2007). The interaction can be interrupted by adding competitive ligands such as imidazole, histidine and ethylenediaminetetraacetic acid (EDTA). This is beneficial for a surface that requires regeneration. However, it is not suitable for sensors that need long-term storage.

Protein A/G, and antibodies: protein A and G are surface proteins found in some species of pathogenic bacteria. Protein A is expressed on the cell wall of *Staphylococcus aureus*, whereas protein G is obtained from *Streptococcus* species (Liebana and Drago, 2016, Liu and Yu, 2016). These two proteins bind to the Fc region of immunoglobulins, contributing to oriented immobilisation of IgGs. The specificities of protein A and G to the Fc regions of antibodies rely on the host species in which antibodies are produced. Protein A recognises antibodies from cats, humans, guinea pigs, rhesus monkeys, and rabbits (Liebana and Drago, 2016). In comparison, protein G however binds specifically to antibodies from rats, goats, sheep and cows. Despite the strong binding of protein A and G to Fc regions, they can also interact with the Fab regions of antibodies. Therefore, researchers who use this method for antibody attachment may need to take this into account. Protein G in its native form is also able to bind albumin (Sjobring et al., 1989), possibly causing a non-specific response when applying for biosensors. Nowadays, thanks to the advancement of genetic engineering techniques, protein A/G, a recombinant fusion version of protein A and G, can be generated (Eliasson et al., 1988). The recombinant protein A/G is very useful since the Fc binding properties of protein A and G are combined. Hence, a wider range of antibodies can be used with this protein.

1.4.3 Applications of impedimetric biosensors

Owing to the advantageous properties of impedimetric biosensors such as small device size, low sample volumes, label-free detection without sample preparation and low production cost, there have been a plethora of publications of impedimetric biosensors for detecting various kinds of analytes such as whole cells, proteins or peptides biomarkers for diseases and small molecules (Rushworth et al., 2013). Some of the analytes successfully detected by impedimetric protocols are indicated in Table 1.1.

According to the review of (Berggren et al., 2001), capacitive biosensors, based on the measurement of the electrical capacitance or impedance, were developed to be a tool for capturing a wide range of targets including antigens, antibodies, proteins, DNA fragments and heavy metal ions. Using interdigitated electrodes, the biosensor provided low detection limits down to 10^{-15} M for each kind of analytes. Impedimetric protocols were applied to detect different species of bacteria. Using a biotinylated polyclonal anti-*Escherichia coli* antibody and SAM based sensor with electrochemical impedance spectroscopy, *E.coli* cells were detected at a detection limit of 10 cfu/ml for whole cells compared to a concentration of 10^7 cfu/ml by the use of SPR (Maalouf et al., 2007). Another work was focused on the use of electrochemical impedance spectroscopy to detect *Escherichia coli* and *Salmonella typhimurium* (Laczka et al., 2008). The sensor was constructed by immobilising biotinylated polyclonal antibodies onto Neutravidin-coated chips and had a detection limit of around 10^4 - 10^5 cells/ml. Because of good selectivity and low cross-reactivity, an impedimetric biosensor was selected to detect *Streptococcus pyogenes*, a pathogenic bacterium that causes invasive and noninvasive infections in human (Ahmed et al., 2013). Regarding the protocol for this report, tyramine (Tyr) monomers were electropolymerised onto the sensor as a supporting layer and biotin-

Table 1.1 Applications of impedimetric biosensors for the detection of different types of analytes

Analyte	Electrode	Transducer surface	Bioreceptor	Reference
Bacteria				
<i>E.coli</i>	Gold	SAM	Antibody	(Maalouf et al., 2007)
<i>E.coli</i> and <i>S.typhimurium</i>	Gold	-	Antibody	(Laczka et al., 2008)
<i>S.pyogenes</i>	Gold	Polytyramine	Antibody	(Ahmed et al., 2013)
Viruses				
Dengue	Porous alumina membrane	Platinum	Antibody	(Peh and Li, 2013)
Adenovirus	Gold	Polyaniline and 2-aminobenzylamine	Half antibody	(Caygill et al., 2012)
Vaccinia virus	Gold	Thiol-modified primer	Aptamer	(Labib et al., 2012)
Proteins and peptides				
Ara-h-1	Gold	SAM	Antibody	(Huang et al., 2008)
Prostate specific antigen	Carbon	Polyaniline	Antibody	(Barton et al., 2008)
Amyloid-beta oligomer	Gold	Polytyramine/3-(4-hydroxyphenyl) propionic acid	Cellular prion protein (PrP ^C)	(Rushworth et al., 2014)
Myoglobin	Gold	4-aminothiophenol SAM	Half antibody	(Billah et al., 2010)
Human IgE	Gold	SAM	Aptamer	(Xu et al., 2005)
Anti-myc tag antibody	Gold	SAM	Affimer	(Raina et al., 2015)
C-reactive protein	Gold	SAM	Affimer	(Johnson et al., 2012)
Interleukin-8	Gold	SAM	Affimer	(Sharma et al., 2016)
Small molecules				
Ciprofloxacin	Carbon	Polyaniline	Antibody	(Tsekenis et al., 2008)
Uranyl ions	Gold	<i>L.sphaericus</i> JG-A12 S-layer protein	Uranyl binding protein	(Conroy et al., 2010)
Digoxin	Carbon	SAM/EDC/NHS	Antibody	(Barton et al., 2009)
Adenosine	Gold	SiO ₂	Aptamer/nucleic acid	(Zayats et al., 2006)
Ochratoxin A	Gold	4-carboxyphenyl monolayer	Antibody	(Radi et al., 2009)

Abbreviations: SAM, self-assembled monolayer; EDC, ethyl(dimethylaminopropyl) carbodiimide; NHS, *N*-hydroxysuccinimide

tagged whole antibodies against *S. pyogenes* were deposited on the polymer layer. The detection limits of this biosensor ranged from 10^4 - 10^7 cells/ml of bacteria.

Impedimetric biosensors have not only been used to detect bacteria, but also applied for detection and quantitation of viruses. For example, a novel impedimetric assay based on the use of reduced antibody fragments as biorecognition elements specific to a human Adenovirus 5 (Ad5) capsid protein was developed. The surface of the sensor chip was coated with a functionalised conducting co-polymer matrix consisting of polyaniline and 2-aminobenzylamine, followed by immobilisation of an anti-Ad5 half-antibody onto this layer. It was found that the limit of detection was 10^3 virus particles/ml (Caygill et al., 2012). Proteins are one of the most common targets for impedimetric biosensors. An impedance biosensor for peanut protein Ara-h-1, which is one of the allergenic proteins found in peanut was constructed successfully (Huang et al., 2008). A specific antibody against Ara-h-1 protein was immobilised onto a self-assembled monolayer (SAM). It was estimated that this reagentless biosensor provided a limit of detection of less than 0.3 nM and the K_D for the Ara-h-1 protein was around 0.52 nM. As well as the allergenic protein in peanuts, a labelless immunosensor assay based upon an ac impedance protocol used to detect prostate specific antigen (PSA) was also produced (Barton et al., 2008). Biotinylated antibodies for prostate specific antigen (APSA) were deposited onto screen-printed carbon electrodes by the classical avidin-biotin affinity technique. The limit of detection was down to a level of sub-pM PSA. Additionally, an immunoassay based on an AC impedance protocol was applied for the detection of fluoroquinolone antibiotics in milk. For this sensor, biotinylated antibodies against ciprofloxacin were immobilised onto a layer of polyaniline which was electropolymerised onto commercial screen-printed carbon electrodes. The assay could be employed to detect the analyte ciprofloxacin in the range of 0.3 – 300 nM (Tsekenis et al., 2008). A label-free and reagentless aptamer-based sensor was developed to detect the small molecule adenosine (Zayats et al., 2006). Aptamer/nucleic acid duplexes were

coated on the sensor surface as the bioreceptors. The device had a sensitivity limit of 5×10^{-5} M (Zayats et al., 2006). Also, a label-free impedimetric immunosensor for detection of ochratoxin A was constructed (Radi et al., 2009). The ochratoxin A antibody was immobilised onto the stable 3-carboxyphenyl (4-CP) monolayer which was deposited onto a gold electrode. The sensor had a detection limit of 1.2 nM.

1.5 Classification of bioreceptors

1.5.1 Types of common bioreceptors used for fabricating electrochemical biosensors

1.5.1.1 Enzymes

Enzymes act to accelerate chemical reactions in living organisms. As a part of the catalytic reaction, enzymes use a binding pocket, the active site to bind their substrates and convert them into products. Some enzymes require cofactors or coenzymes to work effectively. In biosensor applications, enzymes were the first biorecognition elements that were successfully used to detect a target in an electrochemical biosensor. This platform was developed in 1962 by Clark and Lyon (Clark and Lyons, 1962) who used glucose oxidase (GOx) as the bioreceptor to monitor glucose in blood. To date, enzymatic biosensors have been developed to be specific for a variety of targets including glucose, lactate, glutamate, urea and cholesterol (Ispas et al., 2012). Enzymes that have been widely employed in biosensor fabrication are oxidases and dehydrogenases (Rocchitta et al., 2016) since they can catalyse oxidation-reduction reactions, generating electroactive species that can be turned into a measurable signal. The catalytic activities of enzymes strongly rely on pH and temperature (Xu, 1997) and the extreme pH and temperature beyond the optimal conditions can cause enzymatic deactivation and denaturation.

1.5.1.2 Antibodies

Antibodies are one of the most widely used bioreceptors. In mammals, antibodies are proteins produced by B lymphocytes of the adaptive immune system in response to foreign antigens. Mostly, interactions between antibodies and their antigens are highly specific with dissociation constants (K_D) in the pM – nM range (Kim et al., 1990, Landry et al., 2015). The specific recognition of antibodies and their targets takes place at the complementarity determining regions (CDR) or hyper-variable regions. These regions show an extremely high diversity in their amino acid sequences as a result of gene rearrangements during B-cell development and somatic hypermutation (Conroy et al., 2009). The diversity of antibodies is necessary since different antigens require different antibodies with highly specific binding. Polyclonal antibodies can be produced by injecting antigens into animal hosts such as rabbits, goats or sheep (Byrne et al., 2009). These antibodies are a mixed population of antibodies from different B-cells and recognise different epitopes on antigens. If a recognition of a single epitope is needed, it is possible to isolate the particular clone responsible for that particular IgG. These antibodies, termed monoclonal, can be isolated using hybridoma technology (Byrne et al., 2009). Detail of monoclonal antibody production is described in Section 1.5.2.2.1.

1.5.1.3 Synthetic binding proteins

Synthetic binding proteins are recently developed bioreceptors as an alternative to antibodies. The core structure of synthetic binding proteins can be derived from different core scaffolds from a range of proteins (Nygren and Skerra, 2004, Skerra, 2007). The libraries comprising genes encoding non-antibody binding scaffolds with variable peptide regions are constructed in display systems such as phage display libraries (Conroy et al., 2009). Binders highly specific for a target of interest can be selected from these complex libraries using biopanning, which are

described in more detail in Section 1.5.2.2.2. Additionally, synthetic binding proteins offer properties that antibodies cannot. For example, synthetic binding proteins are typically highly stable, small in size and easy to immobilise onto a surface (Binz et al., 2005). Expression of synthetic binding proteins can be performed in *E.coli* and similar microbial systems. Up to this moment, a number of synthetic binding proteins have been released to the public including Affibodies (Lofblom et al., 2010), DARPins (Stumpp et al., 2008), Anticalins (Skerra, 2008) and Affimers (Ferrigno, 2016, Tiede et al., 2017).

1.5.1.4 Aptamers

Aptamers are RNAs or single-stranded DNAs that show specific interaction to their targets. As well as synthetic binding proteins, aptamers also provide an alternative to antibodies. Aptamers offer a structure which is usually stable at high temperature. The production of Aptamers is cost effective with great accuracy and reproducibility. As nucleic acids are typically not recognised by human immune system as foreign antigens, Aptamers are low-immunogenic to human bodies. These make Aptamers suitable for a variety of analytes (Song et al., 2012). The selection of the binders for the target of interest from a population of oligonucleotides can be achieved through Systematic Evolution of Ligands by Exponential enrichment (SELEX). In brief, a combinatorial oligonucleotide library is initially converted into single stranded nucleotides consisting random sequence regions. The target is then used to select Aptamers that bind to it before unbound Aptamers are removed. Polymerase chain reaction (PCR) is then used to amplify the selected oligonucleotides since the random region is flanked by defined primer sequence at each end. The steps above are repeated for a number of cycles to enrich the oligonucleotides that show strong binding to the target (Song et al., 2012, Darmostuk

et al., 2015). Aptamers have been applied for a plethora of targets, e.g. cells, bacteria, viruses, proteins, small molecules and ions (Wu and Kwon, 2016).

1.5.1.5 Whole cells

Whole cells have been used as bioreceptors to fabricate biosensors for detecting hazardous substances, contaminants and pollutants in the environments (Pancrazio et al., 1999, Ziegler, 2000, Lagarde and Jaffrezic-Renault, 2011, Banerjee and Bhunia, 2009). Both prokaryotic cells like bacteria and eukaryotic cells such as yeast and mammalian cells can be used since the cellular mechanisms of these organisms are affected or interrupted when exposed to pathogenic and toxic substances. In detection, receptors presenting on their cell membranes bind the analytes of interest. The receptors can be naturally present on the cell membranes or be engineered using recombinant DNA techniques (Pancrazio et al., 1999, Banerjee and Bhunia, 2009). The interactions between the cells and their targets cause changes in cell morphology and physiology, and cellular damage such as cell membrane leakage, pore formation, and apoptosis or cell death (Pancrazio et al., 1999, Banerjee and Bhunia, 2009). These events can be measured by a variety of techniques including enzymatic, fluorescent, and impedimetric techniques (Banerjee and Bhunia, 2009). Although the use of cell-based biosensors has been successful in some circumstances, they have some limitations such as low specificity, short-term stability, low robustness, and high production cost, especially when working with mammalian cells.

1.5.1.6 Molecularly imprinted polymers (MIPs)

MIPs are artificial biorecognition elements based on highly crosslinked polymers. MIPs can be made of organic or inorganic substances (Dickert, 2014).

MIPs have also been used as biosensing elements. In the polymerisation process, the reaction consists of a template (analyte of interest), functional monomers, cross-linking monomers, and a polymerisation initiator (Hussain et al., 2013). Briefly, to produce the MIPs, the target of interest is first imprinted in the polymer. The functional monomers are then polymerised to form polymer network with the target molecule. Prior to the removal of the target, cross-linking monomers are employed to form chemical bonds with functional polymer matrices and help them stay in the appropriate conformation (Algieri et al., 2014). As well as other bioreceptors, MIP based sensors can be utilised in combination with optical, piezoelectric, and electrochemical measurements in order to convert the binding of receptors and their target to a measurable signal. MIPs have gained attention in the area of biosensors because they not only offer the users the specificity to the target, repeated regeneration. Unlike most protein receptors, MIPs are more stable and resistant to extreme conditions such as high/low pH and temperature (Hussain et al., 2013). There have been applications using MIPs as receptors for detection of a number of analytes such as ions, neurotransmitters, proteins and whole cells (Peeters, 2015).

1.5.2 Antibodies and their limitations

1.5.2.1 An overview of antibodies

The immune system is a system that the human body uses to protect itself from bacterial and viral pathogens, and other toxins. In human beings, the immune system can be classified into two subtypes; the non-adaptive (innate) and adaptive (acquired) immune responses (Murphy, 2012). Non-adaptive immunity is always the first barrier to combat a variety of pathogens, but this protection is not long-lasting due to the lack of immunological memory and is non-specific. Cells that function in the non-adaptive system include phagocytes (macrophages, neutrophils, and dendritic cells), mast cells, eosinophils, basophils and natural killer cells. On the other hand, adaptive immunity is a specific immune response mediated by lymphocytes; T cells and B cells. While T cells normally involve cell-mediated immunity, B cells hold a key role in the humoral immune response by secreting specific antibodies against target antigens, and, in this review, only antibodies generated by B cells are focused on in more detail.

In general, an antibody or immunoglobulin molecule is comprised of two pairs of polypeptide chains which are different in size (Figure 1.8). Two of them are heavy chains of M_r about 50 kDa each whereas the other two are light chains of M_r around 25 kDa each. All four polypeptides are connected to one another by disulfide bonds. The heavy chains of antibodies usually contains a variable (V_H) domain, and three constant domains, the C_{H1} domain, C_{H2} domain and C_{H3} domain. In contrast, the light chains contain two domains, a V_L domain and a single C_L domain. Although antibody molecules share the same basic structure, they display remarkable variability in the areas that bind specifically to the antigen. To interact with target antigens, antibodies normally employ regions called the complementarity-determining regions (CDRs), which are present in both V_H and V_L domains and

located at the tips of the IgG “Y” structure. Immunoglobulins are categorised into five classes based on their heavy chain structure: IgA, IgG, IgM, IgD and IgE (Figure 1.9). The difference in structure is because during B cell development, B cells can switch from making one class of antibody to another, which is called class switching (Alberts et al., 2002). Gene recombination and somatic hypermutagenesis are two factors involving antibody diversity (Conroy et al., 2009). Combinatorial rearrangement of the V_H - D_H - J_H segments for heavy chains and the V_L - J_L segments for light chains during B cell development leads to production of a variety of antibodies with different affinities to antigens. Furthermore, somatic hypermutation, mainly base substitution, during B cell proliferation introduces a variety of nucleotide sequences into the coding regions, which is beneficial for producing antibodies specific for a vast range of analytes.

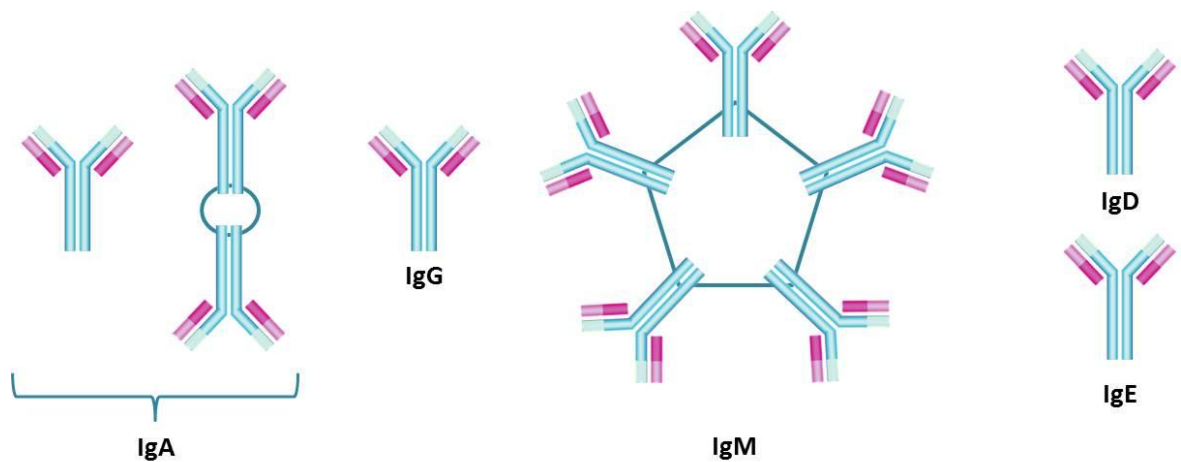


Figure 1.9 the structure of five classes of immunoglobulins. IgG, IgD and IgE presents as a monomer in the serum. Serum IgM exists as a pentamer whereas IgA can be found in both monomeric and dimeric forms. The blue lines connecting between IgA dimer and IgM pentamer indicate the joining (J) chains containing cysteine residues, resulting in the intracellular polymerisation of IgA and IgM monomers.

1.5.2.2 Production of antibodies

Polyclonal antibodies are widely applied in different areas of research including biological and medical applications because they can be made simply by immunising an experimental animal. However, batch-to-batch variability and cross-reactivity still limit their use in some applications that require an antibody specific to a single epitope, e.g., diagnostic manufacturing and therapeutic drug development. To overcome these limitations, several techniques have been developed to produce monoclonal antibodies to solve the problems.

1.5.2.2.1 Monoclonal antibody production

Hybridoma technology was first reported as a technique to be used for production of monoclonal antibodies in 1975 (Kohler and Milstein, 1975). Since then, this method has been employed for generating monoclonal antibodies against a wide range of antigens. Briefly, laboratory animals like mice are immunised by injection of a specific antigen. After several weeks, B cells are isolated from the spleen tissues known as splenocytes. Then, the extracted cells are immortalized by fusion with myeloma (B cancer cells) cells by electrofusion. The cell lines with desired binding specificity are isolated and then multiplied. Although hybridomas have gained an attention from researchers in biological and medical fields, antibodies obtained by this method are foreign proteins in humans. This can cause immunogenic symptoms to those exposed to the antibodies, initially leading to unsuccessful clinical applications (Carter, 2006). In order to minimise the effect of immunogenicity, humanised antibodies have been developed (Co and Queen, 1991, Tsurushita et al., 2005). To produce the first generation of humanised antibodies, genes encoding variable domains are isolated from the mRNA of B cell hybridoma using PCR. The V genes are constructed into an expression vector containing genes encoding constant domains from human IgGs. The recombinant IgGs are expressed in mammalian

cells. These IgGs are called “chimaeric mAbs”. However, variable domains which are originally from other animals can cause immunogenic response when antibodies are used in humans (Co and Queen, 1991). Therefore, in the second generation, only complementarity-determining regions (CDRs) from other animal species are transferred and embedded with human IgG frameworks. IgGs made by this approach are known as “CDR-grafted or humanised mAbs”. As a result, immunogenicity is reduced. In addition, because of Fc regions originally from human IgG, the half-life of antibodies in serum is extended and the effector function is still retained.

1.5.2.2.2 Phage display technology

Since the first publication on phage display technology in 1985 (Smith, 1985), there have been other research groups further developing this techniques in order to adjust it to suit their work (McCafferty et al., 1990, Barbas et al., 2001). Phage display is an extremely useful technique that is used to display single chain variable fragments (scFv) or antigen-binding fragments (Fab) since it can be manipulated *in vitro*. Additionally, this method can facilitate investigation of the human immune system mechanism via specific interaction of selected antibody-derived fragments and their targets (Hammers and Stanley, 2014). Principally, this approach starts with preparation of a gene library (Figure 1.10). mRNA of high quality is isolated from chosen cells, and then reverse transcribed to cDNA. Using sets of primers specific to antibody genes, the PCR products are obtained. The PCR products are then ligated into a phage display vector called a phagemid, resulting in the vector carrying an antibody gene fused to the pIII minor capsid protein gene of the M13 filamentous phage. Competent cells are transformed with a set of phage display vectors together with additional helper phage to allow complete phage production. To select antibodies specific to antigens, a technique called bio-panning is employed. This technique can allow users to enrich a small number of specifically bound phages from

a pool of phage with over 10^{10} clones (Schmitz et al., 2000). One cycle of panning consists of capture of phage by binding to the immobilised antigen, washing, elution, and then reamplification of the phage binders in *E. coli*. During several rounds of panning, the most highly specific binders are picked up from a large pool of phage. Then, the selected binders are once more tested by ELISA or western blotting. Phage from positive samples are re-amplified in *E. coli* for the production of monoclonal phage, which are then tested by phage ELISA to confirm the presence of specific clones binding to the target. Subsequently, the phage vectors, isolated from the positive clones, are sequenced, and compared to determine the variety of the genes selected. However, phage display still holds several limitations since it might not be possible to recover every antigen-specific antibody fragment using only one library. The scFv or Fab fragments obtained from this method may not imitate the immunoglobulins formed by *in vivo* production.

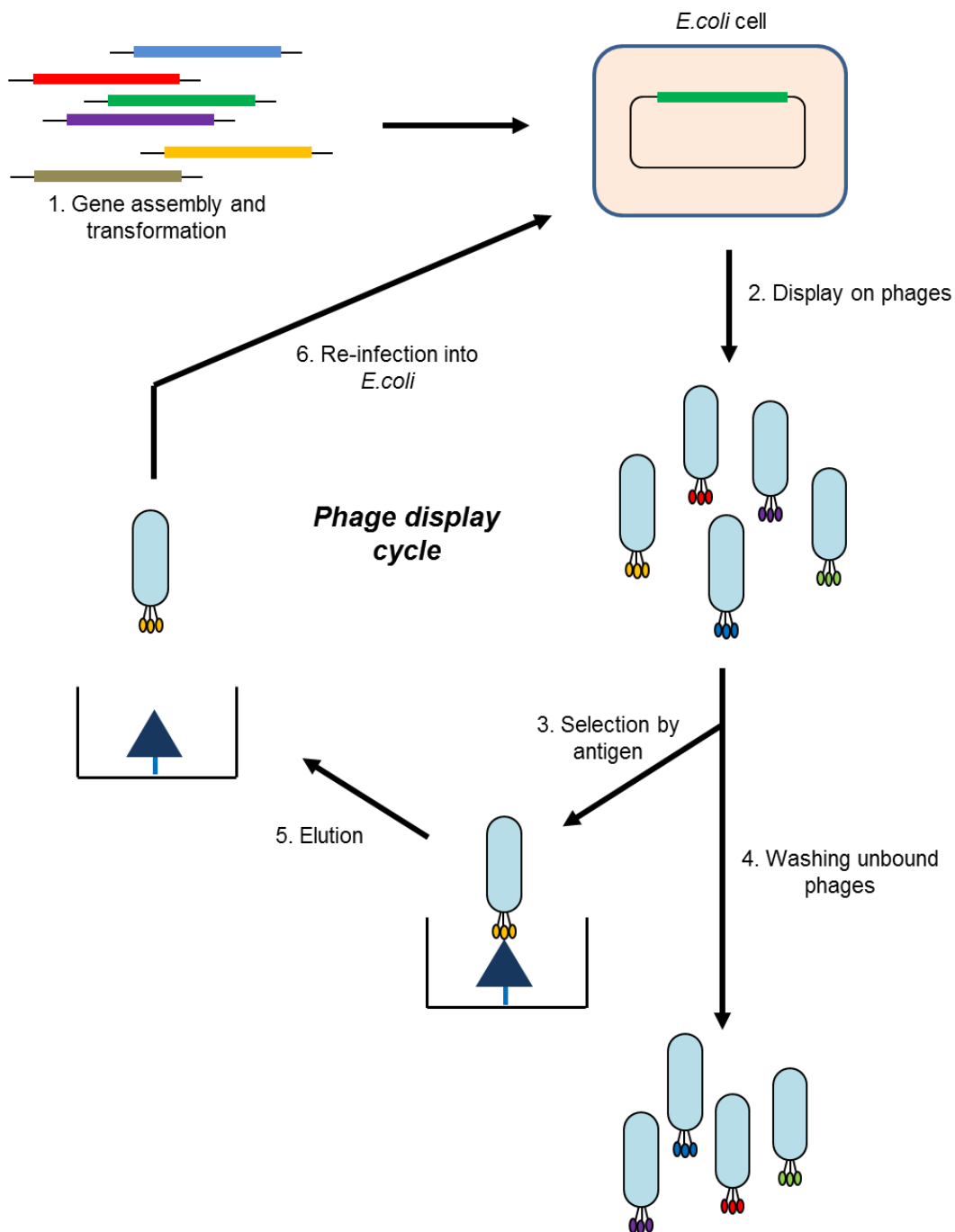


Figure 1.10 A schematic representation of basic phage display cycle. The diagram displays six key steps: (1), gene assembly and transformation; (2), protein scaffold display; (3), selection; (4), washing; (5), elution, and (6), re-infection into competent cells. The figure was modified from Mondon et al. (2008).

1.5.2.3 Applications of antibodies

Antibodies have been used in a variety of areas. For proteomic studies, in order to investigate the relative abundance of different specific proteins, antibodies are used as capturing reagents to construct antibody arrays. For example, for clinical diagnoses, antibody arrays directed towards more than 50 biomarker proteins of acute ischemic stroke have been applied for high-throughput screening of patients' plasma samples (Reynolds et al., 2003). Also antibody arrays have been used as an analytical platform for diagnosis of myocardial infarction (Wu et al., 2004, Mitchell et al., 2005) and screening of drugs of abuse (Buechler et al., 1992). Antibody arrays are a valuable tool to investigate clinical biomarker development in areas such as inflammatory bowel disease (Kader et al., 2005), lung and ovarian cancer (Gao et al., 2005, Mor et al., 2005).

In cancer therapy, tumour-specific antibodies can be conjugated to drugs. This method brings the benefits of selectively targeting cytotoxic drugs to tumours. Several antibodies are already approved by the Food and Drug Administration (FDA) of the USA to be used as therapeutic agents for cancer treatment. These include Trastuzumab (IgG1) against HER2/neu for metastatic breast cancer, Bevacizumab (IgG1) against vascular endothelial growth factor for metastatic chronic lymphocytic leukaemia, and Gemtuzumab (IgG4) against CD33 for acute myeloid leukaemia (Schrama et al., 2006). Antibodies can also take part in antibody-mediated liposome targeting for delivery systems. For instance, antibodies can be coated on the outer layer of liposomes via interactions e.g. the streptavidin-biotin interaction (Lee et al., 2005). The antibody-coated liposomes can be filled with drugs, genes or fluorescent dyes and then delivered to the specific tissues, leading to increased efficacy of disease treatment (Torchilin, 2005).

1.5.2.4 Limitations of antibodies

Although antibodies offer several benefits especially their specificity, some of their characteristics are disadvantageous. Cost of production for antibodies is typically high (Ruigrok et al., 2011, Hey et al., 2005, Stumpp et al., 2008, Haurum, 2006). This is because whole antibodies cannot be produced in microbial systems. The structure of antibodies comprises four polypeptide chains and post-translational glycosylation is required for structural stability. The complex structure of antibodies also requires disulfide linkages and other interactions to fold into native and functional domains. As a consequence, mammalian cell lines or animal hosts such as mice, rabbits, sheep and goats are needed as sources of antibody production. The production process is also time-consuming and typically small scale (Ruigrok et al., 2011). One of the major problems of using antibodies in many applications is batch-to-batch variation, in particular when polyclonal antibodies are employed (Haurum, 2006, Baker, 2015, Bradbury and Pluckthun, 2015). This can be explained by the fact that polyclonal antibodies are a mix of antibodies produced from different B cells in an immunised host. With different batches of antibodies, the ratios of different antibodies contained in the cocktail are not identical. This can be the major problem with reproducibility in experiments, including biosensor research. In this area, correct orientation of bioreceptors is necessary when immobilising them onto the surface. Antibodies consist of more than one cysteine and lysine, which makes it difficult to modify antibodies at a specific site to control the orientation. Because of all the above, researchers have attempted to find other ways to overcome the drawbacks of antibodies and the use of alternative binding proteins are one of those approaches.

1.5.3 Antibody-derived fragments

Because of the large size and complex structure, with four peptide chains, it is often difficult to develop antibodies for commercial applications. To overcome these limitations, the binding sites in the antibody structure have been applied to develop alternative antibody-derived structures (Hey et al., 2005, Ponsel et al., 2011, Richards et al., 2017, Chames et al., 2009). Over the past decades, there has been a broad spectrum of antibody fragments with desirable properties like smaller size and simpler structure.

Antibody-derived fragments are a group of proteins, where structures are derived from a part of an antibody. Antigen-binding sites on variable domains of heavy and/or light chain of antibodies are retained since they are capable of recognising the antigen. Fab, scFv, diabodies and nanobodies are all examples of antibody fragments mentioned in this chapter (Figure 1.11).

Antigen-binding fragment (Fab) is an antibody derivative. Its structure is comprised of one constant and one variable domains of each heavy and light chain. The Fc region of antibodies is excluded from the structure, which results in molecular mass of approximately 55 kDa (Holliger and Hudson, 2005). Fab can be generated through an enzymatic reaction using papain or conveniently screened from a phage display library (Crivianu-Gaita and Thompson, 2016). Even though the Fc region is removed, the capability of antigen recognition in Fab is still retained like its counterpart. Fab(s) have been screened via phage display technologies against such targets as *Staphylococcal* enterotoxin B (Urushibata et al., 2010), human p53 for monitoring colorectal cancer (Coomber et al., 1999) and B cell lymphoma (Shen et al., 2007). In clinical and preclinical settings, some Fab(s) have successfully been approved by the FDA as therapeutic agents for treatments of cardiovascular disease, rattlesnake bite, and overdose of digoxin (Holliger and Hudson, 2005).

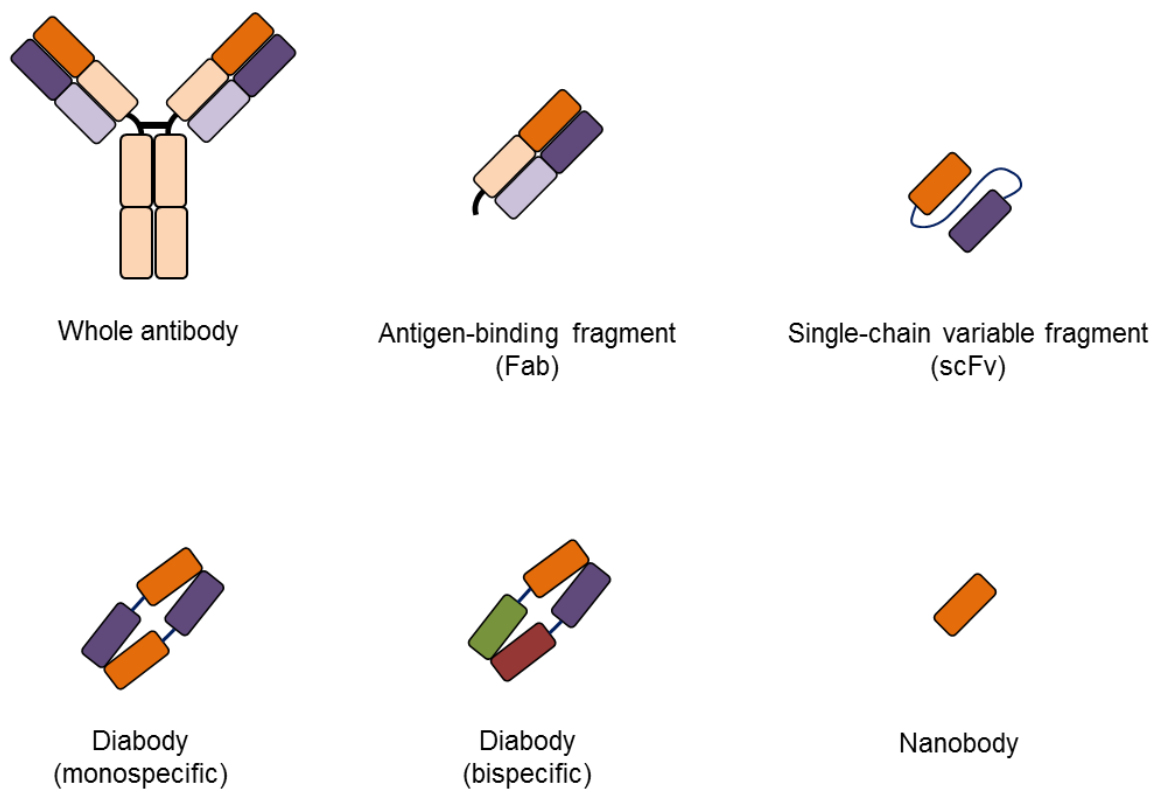


Figure 1.11 Some examples of antibody-derived fragments. All the fragments shown in the figure can be selected from recombinant libraries. The size of each fragment is significantly smaller than a whole antibody. More examples of IgG-derived fragments can be found in Herrington-Symes et al. (2013) and Little et al. (2000).

Single-chain variable fragment (scFv) is another antibody fragment, which can be obtained by the screening a phage display library (Mao et al., 1999, Crivianu-Gaita and Thompson, 2016). The basic structure of scFv consists of one variable region from the heavy chain and one variable region from the light chain. The two polypeptides are connected with a short peptide linker, which is between 10-30 amino acids (Crivianu-Gaita and Thompson, 2016). The linker is typically rich in small amino acids such as glycine, serine and threonine (Li et al., 2015). The average molecular size of scFv(s) is around 28 kDa (Holliger and Hudson, 2005). In therapeutic uses, scFv(s) are potential agents used as a part of radiation dosimetry for gastrointestinal malignancies (Shen et al., 2005) and drug targeting for breast cancer (Nellis et al., 2005).

Diabodies are small antibody fragments with two antigen-binding sites (Holliger and Hudson, 2005). Diabodies can be monospecific or bispecific depending on the scFv molecules that form the dimers. Dimerisation of two identical scFv domains results in monospecific diabodies whereas the formation of two scFv domains originating from different immunoglobulins provides bispecific diabodies (Kim et al., 2016). Two scFv domains are connected by a short peptide linker which contains three to five amino acids (Atwell et al., 1999, Hudson and Kortt, 1999). As a result, the average molecular size of diabodies is the combination of two scFv domains, which is roughly 50 kDa in total (Holliger and Hudson, 2005). Up until now, diabodies have widely been used for medical research. For example, diabodies showed great potential when employed as cross-linkers between *E. coli* β -galactosidase and three target antigens of interest; hen-egg lysozyme, carcinoembryonic antigen, and HIV gp120 in enzyme immunoassays (Kontermann et al., 1997). A bispecific diabody recognising both EPH receptor A10 on breast cancer cells and CD3 expressing in cytotoxic T cells was also generated (Kamada et al., 2015). The researchers proposed that this diabody could potentially be applied for breast cancer therapy.

A nanobody or single domain antibody is a single domain from the camelid immunoglobulin family developed by Ahlynx (Ghent, Belgium). The molecular weight of the nanobody is only 12-15 kDa which is much smaller than a full antibody (150-160 kDa) (Harmsen and De Haard, 2007). Nanobodies are obtained by screening via either phage display or ribosome display techniques (Ghahroudi et al., 1997). In preclinical diagnostics, nanobodies have shown potential use for the treatment of rheumatoid arthritis, inflammatory bowel disease and thrombosis (arterial stenosis). Additionally, it has been proposed to treat patients with psoriasis, solid tumours and Alzheimer's disease (Hey et al., 2005).

1.5.4 Non-antibody binding proteins

In addition to engineered antibody-derived fragments, there has been development of alternative binding proteins whose structures have no connection to that of IgG. Non-antibody binding proteins are a group whose original structures are based on a sequence or consensus sequence of proteins from various sources. The core structure is required to be rigid, stable, compact and monomeric. Mostly, introduction of randomised amino acid regions is necessary in order to generate new binding sites which imitate the recognition property of antibodies. Examples of non-antibody binding scaffolds worth describing here are monobodies, Anticalins, Kunitz domains, DARPins, Affilins and Affimers as follows (Table 1.2).

A monobody or Adnectin is a human fibronectin type III domain protein, which can be expressed in bacteria. Since 2007, this type of protein has been developed by Adnexus, a part of Bristol-Myers Squibb. The structure of the Adnectin is comprised of 94 amino acids with a molecular weight of 10 kDa. Three distinct loops in the structure link six antiparallel β -sheets to the same structure. The amino acids in these loops are diversified to mimic the CDR loops of antibodies, allowing Adnectins to bind a variety of analytes (Gill and Damle, 2006, Lipovsek, 2011). It is

Table 1.2 Examples of some non-antibody binding protein scaffolds and their characteristics

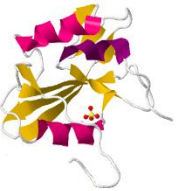
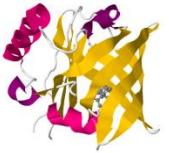
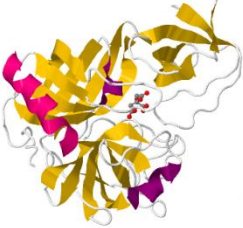
Scaffold name	Parent structure	Species origin	Randomisation	PDB code	Scaffold structure	Reference
Monobody/ Adnectin (1)	10 th domain of human fibronectin	Human	Residues in BC, DE, and FG loops (loop library)	3RZW		(Ramamurthy et al., 2012)
Monobody/ Adnectin (2)	10 th domain of human fibronectin	Human	Residues in C and D β -sheets, and DE and FG loops (side and loop library)	3UYO		(Koide et al., 2012)
Anticalin	Lipocalins	Human/insect	Four loops (up to 24 amino acids)	1LNM		(Korndorfer et al., 2003)
Kunitz domain	Protease inhibitor	Human	One to two loops	1KTH		(Arnoux et al., 2002)

Table 1.2 (continued)

Scaffold name	Parent structure	Species origin	Randomisation	PDB code	Scaffold structure	Reference
DARPin (1)	Ankyrin repeat proteins	Human	Six to seven residues in each n-repeat (original library)	2QYJ		(Merz et al., 2008)
DARPin (2)	Ankyrin repeat proteins	Human	Additional 13 residues in elongated loop (loop library)	4K5C		(Schilling et al., 2014)
Affilin (1)	γ -B-crystallin	Human	Eight residues	2JDG		(Ebersbach et al., 2007)
Affilin (2)	Ubiquitin	Human	Six residues in β -sheet	1UBI		(Hoffmann et al., 2012)

Table 1.2 (continued)

Scaffold name	Parent structure	Species origin	Randomisation	PDB code	Scaffold structure	Reference
Affimer (Adhiron)	Phytocystatin	Plant	Two variable peptide loops (18 amino acids)	4N6T		(Tiede et al., 2014)
Repebody	Leucine-rich repeat (LRR) modules	Jawless vertebrates artificial	Five residues in each LRR	4J4L		(Lee et al., 2012)
Fynomer	SH3 domain of Fyn tyrosine kinase	Human	Six residues in two loops	4AFQ		(Silacci et al., 2014)

expected that Adnectins will be effective in treating cancer, rheumatoid arthritis, psoriasis, and Crohn's disease (TNF α) (Hey et al., 2005). Additionally, CT-322, which is an Adnectin selected via mRNA display technology, showed great potential to be an anti-tumour agent for inhibiting vascular endothelial growth factor receptor 2 (VEGFR2) (Mamluk et al., 2010).

Anticalins are artificial proteins derived from *Pieris brassicae* lipocalin. The protein was first developed by a team of scientists from the Technical University of Munich, Germany (Beste et al., 1999). The basic structure of this peptide consists of eight antiparallel β -strands pairwise linked by loops and an α -helix. The four hypervariable loops at the open end of the structure form a cup shape, which is used as the binding site for both small compounds and large biomolecules (Skerra, 2008, Richter et al., 2014). To produce Anticalins in large amounts, microorganisms such as bacteria and yeasts are normally used (Hey et al., 2005, Skerra, 2008). There have been attempts to use anticalins for diagnostic and therapeutic applications. The applications of this protein have been focused on drug delivery (Schlehuber and Skerra, 2005). For example, as a carrier for drug delivery, the 'duocalin', an anticalin possessing binding activity for doxorubicin, has been developed (Schlehuber and Skerra, 2001). This is an excellent strategy for drug targeting since doxorubicin is a tumour drug that is poorly soluble (Constantinides et al., 2004) and has severe side effects (Perez, 2001).

Kunitz domains are active domains of protease inhibitors. The structure of the Kunitz domain consists of between 50 and 60 amino acids stabilised by three disulfide bonds, which results in a molecular weight of around 6 kDa. The Kunitz domains possess three loops that can be mutated without destabilising their structure and used as the binding site for targets of interest (Weidle et al., 2013, Hosse et al., 2006). They can be selected by the use of phage display technology (Lehmann, 2008). Kunitz domains have the potential to be used in the development of pharmaceutical drugs. For example, DX-88, a novel Kunitz domain, is an effective

and selective inhibitor of plasma kallikrein for the treatment of hereditary angioedema (HAE) (Williams and Baird, 2003).

*DARPin*s are genetically engineered binding proteins derived from natural ankyrin proteins. The structure of each *DARPin* is comprised of four or five repeat motifs, which are a β -turns followed by two antiparallel helices and a loop. Typically, the *DARPin*s have a molecular weight of 14-18 kDa. *DARPin*s are synthetic scaffolds that use their rigid secondary structure (α -helices) for recognition (Nygren and Skerra, 2004, Stumpp et al., 2008). Six randomised amino acids per repeat of the *DARPin*s play a role in interaction with their targets (Skerra, 2007). Resulting from their high affinity and specificity, there have been potential medical applications of *DARPin*s. For example, the designed ankyrin repeat protein, G3, was used as a specific binding molecule to reliably identify the amplification status of the epidermal growth factor receptor 2 (EGFR2) in breast cancer (Theurillat et al., 2010).

Affilins are engineered binding proteins derived from one of two human proteins, γ -B crystallin or ubiquitin. The structure of *Affilin* from the γ -crystallin consists of two identical domains, mainly β -sheets and a molecular weight of around 20 kDa, whereas the structure of *Affilin* from ubiquitin is comprised of 76 amino acid residues which are the building blocks of an α -helix and five β -sheet strands with a molecular weight of 10 kDa. The target binding regions of *Affilins* are located in β -sheet structure. Six (for γ -crystallin) or eight (for ubiquitin) amino acids in the binding sites are modified without losing structure stability (Weidle et al., 2013). Like the previous binding proteins, *Affilins* have been used as an alternative to antibodies in many applications, in particular medical research. For example, the E7 binder, an *Affilin* molecule selected against human Papillomavirus E7 protein, was used to inhibit the proliferation of target cells in cervical cancer (Mirecka et al., 2009).

Affimers are alternative binding proteins which their structure is derived from plant phytocystatins (Tiede et al., 2014). The core structure of *Affimers* is comprised

of a single- α -helix and four anti-parallel β -strands. Eighteen amino acid residues over two loops at one end of the structure are diversified in order to mimic the CDR regions of IgGs and use as recognition sites for the analytes. Typically, Affimers have molecular weight around 12-13 kDa. The selection of Affimers can be conveniently carried out using phage display technology (Tiede et al., 2017). Further detail of Affimers is provided in Section 1.5.5.

1.5.5 Affimers

The BioScreening Technology Group (BSTG) at University of Leeds has recently developed a scaffold protein, termed the Affimer (previously known as Adhiron), as an alternative affinity protein framework (Tiede et al., 2014). The structure of the Affimer II scaffold is based on the consensus sequence of plant-derived phytocystatins (Tiede et al., 2014) whilst the Affimer I library is derived from human stefin A (Stadler et al., 2011). All work in this thesis used the Affimer II construct and Affimer I will not be further discussed. X-ray diffraction of Affimer II showed a structure with a single α -helix and four anti-parallel β -strands (Figure 1.12). Using phage display, variants of Affimers, possessing different external loops, can be displayed on phage M13 as a fusion with coat protein pIII. The phage display Affimer II library shows a complexity of around 1.3×10^{10} individual clones, each of which displays 18 random residues split over two loops (2 x 9 residues). It has already been shown that Affimers offer an array of advantages including high thermal stability (some have a T_m up to 101°C), rapid production, and minimal cross-reactivity. The scaffolds can be expressed easily in *E. coli* cells. These features, especially the monoclonal nature of the Affimer II proteins, help users avoid the issue of batch-to-batch variation. Another key point is that Affimers lack cysteine residues and cysteines can be introduced at a specific site for modification. With such interesting properties, Affimers have become one of the more promising alternative binding proteins for a wide range of applications including molecular recognition.

To date, Affimers have been applied to a large range of research areas and the number of applications has been increasing from time to time (Tiede et al., 2017). In the field of biosensors, Affimers have been successfully used for the detection of several targets e.g. proteins and small molecules. In 2012, Johnson and coworkers reported the use of the Affimer as a receptor for impedimetric label-free assay to

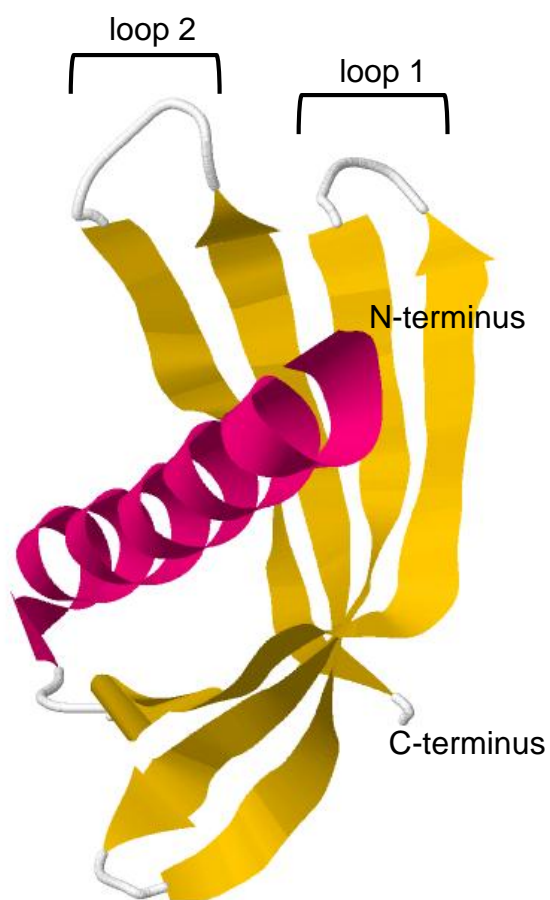


Figure 1.12 X-ray crystal structure of an Affimer scaffold (PDB ID no. 4N6T). The structure consists of a single α -helix and four anti-parallel β -strands. Two variable peptide sites are indicated by the brackets.

detect C-reactive protein (CRP) (Johnson et al., 2012). The researchers coated the electrodes with a SAM and used EDC/NHS to immobilise the Affimer onto the surface. Although the Affimer bound weakly to its target on the SPR assay with the K_D in μM range, by optimising conditions for sensor fabrication, the sensor detected CRP in the nM range. In 2015, the Affimer was used for the detection of anti-myc tag antibody (Raina et al., 2015). Using biolayer interferometry (BLI), the Affimer bound to its target with a K_D of 360 nM. To make the sensors, the Affimer was attached to the SAM-coated surface via EDC/NHS and impedance was used to determine the binding of the receptor and its protein target. The sensors showed a detection range of 6.7 – 330 pM. In 2016, Sharma and the colleagues published the use of Affimer impedimetric biosensors to detect human interleukin-8 (IL-8) in serum with higher sensitivity than conventional methods (Sharma et al., 2016). BLI showed that the Affimer bound to IL-8 with a K_D of 35 nM. The Affimer was then immobilised on the SAM-coated electrodes via EDC/NHS prior to impedance measurement. The biosensors showed a range of detection of 900 fg/ml – 900 ng/ml, which again is much more sensitive than conventional techniques. Affimers do not only detect protein targets on the biosensor platform, but they can also be used to detect small molecules with molecular weight less than 1 kDa. (Koutsoumpeli et al., 2017) used Affimers in association with quartz crystal microbalance (QCM) to detect methylene blue, a small compound. The researchers used QCM-D to determine the affinity of the Affimer to methylene blue and found that the K_D was 13.7 nM. To construct the sensors, the Affimer was directly immobilised onto the SAM layer, which was previously coated on the surface. Even though the fully constructed sensors showed a significant change in resonance frequency (F) and dissipation (D) when exposed to different concentrations of the targets, the optimisation to achieve a proper detection range is still under investigation. Zhurauski and his colleagues developed an Affimer-functionalised interdigitated electrode-based biosensor to detect human epidermal growth factor receptor 4 (Her4), a protein biomarker of gastrointestinal

stromal tumours (Zhurauski et al., 2018). The researchers used non-faradaic impedance and evaluated sensor performance by measuring the changes in capacitance. The sensors showed a dynamic range from 1 pM to 100 nM of Her4 with a limit of detection under 1 pM when the measurements were performed in both buffer and serum.

As well as applications for biosensors, Affimers have been used in other areas of research, for examples, as modulators to study protein-protein interactions, affinity histochemistry, pull-down assays, cell imaging, *in vivo* imaging, super resolution microscopy and formation of magnetic nanoparticles (Tiede et al., 2017). One example of studying protein-protein interaction is the use of the Affimer to inhibit the formation of HIF-1 α /p300 complex (Kyle et al., 2015). Using competitive fluorescence anisotropy assay, the Affimers showed the inhibition of this interaction with a low μ M IC_{50} . This IC_{50} was found to be better than the fragments of native HIF-1 α . The study is not only useful for dissecting signalling pathways, but also for the treatments of hypoxia. Affimers have also been utilised as a tool for nanoparticle synthesis. (Rawlings et al., 2015) screened Affimer binders that can interact with cubic nanoparticles. They also found that when mixing the Affimers with nanoparticle synthesis reaction, the shape of magnetic particles can be controlled towards a cubic shape. This idea is anticipated to pave the way of using alternative binding proteins for material synthesis.

1.6 Dichlorodiphenyltrichloroethane (DDT)

Dichlorodiphenyltrichloroethane (DDT) is a synthetic organochlorine insecticide. The chemical structure of DDT comprises two chlorobenzene rings attached to a tree of three chlorine atoms (Figure 1.13). DDT is highly hydrophobic, which makes it almost insoluble in water. The solubility of DDT in water is found to be 0.025 mg/L at 25 °C (Howard and Meylan, 1997). However, DDT is soluble in fats, oils and most organic solvents such as dimethyl sulfoxide (DMSO) and dimethylformamide (DMF).

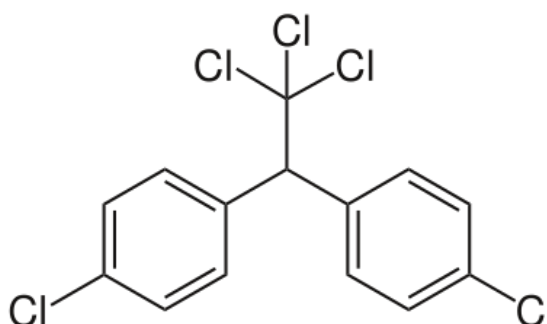


Figure 1.13 Chemical structure of DDT. The structure consists of two chlorobenzene rings linked to three chlorine atoms.

DDT has been used to control the spread of malaria caused by mosquitoes. It has an adverse effect on insects by targeting sodium ion channels in neurons (Davies et al., 2007, O'Reilly et al., 2006, Du et al., 2016). DDT acts as an agonist by binding to the sodium channels and stabilising them in the open state. As the depolarization of the membrane is prolonged, the neurons fire spontaneously. As a consequence, this leads to paralysis and death of the insects.

Despite its insecticidal property, DDT is now banned for use in many countries due to its long persistence in animal tissues and the environment. It has been calculated that DDT stored in adipose tissues normally takes 10 – 20 years to disappear from an individual (Turusov et al., 2002). As DDT is slowly degraded, it can be accumulated in the food chain and tissues of living organisms. The accumulation of DDT causes considerable thinning of the eggshell in avians (Turusov et al., 2002, Speich et al., 1992, Kolaja and Hinton, 1977). The effects of DDT and its metabolites on human health have also been studied. Even though further investigations are needed, some reports showed the association of abnormalities in people who had a long-term exposure background to DDT. For example, occupational exposure to DDT could adversely affect male fertility as it blocks the androgen receptor (Mehrpour et al., 2014, Whorton et al., 1977). In females, increasing concentrations of DDT in maternal serum caused decreasing probability of pregnancy (Rogan and Chen, 2005, Cohn et al., 2003). Exposure to DDT has also been associated with the occurrence of cancers including pancreatic and breast cancers, and neuropsychological dysfunction (Beard and Australian Rural Hlth Res, 2006, Rogan and Chen, 2005). For these reasons, DDT is a vital indicator for environmental monitoring and rapid-processing assays for DDT detection are required.

1.7 Fibroblast Growth Factor Receptor 3 (FGFR3) as a promising biomarker for bladder cancer

1.7.1 Overview of bladder cancer

Bladder cancer is a heterogeneous disease, in which the tissues in the bladder multiply abnormally and spread into neighbouring muscles. An early symptom of this cancer is blood detected in urine without pain or painless haematuria (Kaufman et al., 2009, Sexton et al., 2010, Letasiova et al., 2012). An additional symptom that can be found alongside with haematuria is frequent and urgent urination (Sexton et al., 2010). Bladder cancer can be categorised into two types based on the tissues invaded (Knowles and Hurst, 2015). The first type is non-muscle invasive bladder cancer which be found inside the lining of bladder. This type is the most common and is not generally fatal. The latter is muscle invasive bladder cancer, in which the cancer cells invade beyond the lining and into the muscles surrounding. It is more rarely found and is often the cause of death, especially if metastasis occurs. In general, 70% of diagnosed patients are found to have superficial or non-muscle invasive bladder cancer while the remaining 30% have muscle invasive bladder cancer (Kaufman et al., 2009, Sexton et al., 2010). In 2012, it was reported that bladder cancer was ranked the ninth most common cancer found worldwide (Antoni et al., 2017). GLOBOCAN estimated that about 430,000 cases were newly diagnosed bladder patients and roughly 165,000 deaths, which three quarters were males, were reported in 2012. The researchers also found that Europe showed the highest incidence rate of bladder cancer in the world whereas Africa showed the lowest rate (Antoni et al., 2017). There are several risk factors involving the occurrence of bladder cancer. Gender and age are the first two factors to be considered. The incidence rate of bladder cancer was evidently higher in men than in women and people with the ages between 50 and 70 showed higher probability of developing

bladder cancer compared other age groups (Kaufman et al., 2009). Occupational exposures to certain chemicals can cause bladder cancer. Workers who are exposed to aryl amines, cyclophosphamide and phenacetin-containing substances risk bladder cancer development (Vlaovic and Jewett, 1999, Sexton et al., 2010). The most important risk factor for developing bladder cancer is tobacco smoking (Kaufman et al., 2009, Sexton et al., 2010). A number of chemicals contained in the smoke of cigarettes including 2-naphthylamine, 4-aminobiphenyl and o-toluidine have been found to increase the risk of bladder cancer (Sexton et al., 2010, Letasiova et al., 2012). Being diagnosed at the early stage of cancer is necessary because this increases the survival rate of patients living with cancer cells since early treatment is enabled (Pepe et al., 2001, Budman et al., 2008, Reubsaet et al., 2009, Mazor et al., 2010). Therefore, an efficient point of care diagnosis capable of detecting the development of the cancer at the earliest stage will help reduce the mortality rate and help patients live longer.

1.7.2 Standard methods of bladder cancer diagnosis

Attempts have been made to establish efficient standard platforms to monitor the occurrence of bladder cancer in the early stages since this can affect the results of the treatments giving to patients. For an initial assessment, *cystoscopy* is known as the gold standard to be used for detecting bladder cancer (Kaufman et al., 2009, Sexton et al., 2010, Budman et al., 2008). The approach involves inserting a small thin camera into the bladder via the urethra, which allows the physicians to see abnormalities that are present. This method is invasive and makes the patients anxious during an operation (Budman et al., 2008). Moreover, if the malignant cells are flat such as carcinoma *in situ*, the doctors may fail to identify these abnormalities (Sexton et al., 2010, Budman et al., 2008). *Urinary cytology* is one of the widely used methods to detect bladder cancer cells. It is basically used in association with

cystoscopy. Voided urine samples are collected from patients and sent to the pathology laboratory to observe abnormal cells under the microscope. This approach is non-invasive and highly specific for bladder cancer detection (Budman et al., 2008). However, low sensitivity of the technique when detecting low-grade tumours is its major drawback.

Some urinary biomarkers have been researched in order to achieve detection of early-stage bladder cancer. Four widely used biomarker-based tests are briefly reviewed in this thesis. The first technique to be mentioned is *bladder tumour antigen test (BTA)* (Budman et al., 2008). The procedure is based on the use of antibodies for the detection of complement factor H-related protein (CFHrp) in voided urine (Proctor et al., 2010). This protein is secreted by tumour cells. Two commercial BTA kits are available in the markets. BTA stat (Polymedco) is a qualitative point-of-care assay using a lateral flow immunoassay to detect CFHrp whereas BTA Trak assay (Polymedco) is a quantitative techniques based on the ELISA. The second method is *nuclear matrix protein 22 (NMP22) test* (Budman et al., 2008). It has been found that the level of expressed NMP22 protein increases as an indicator of apoptosis in malignant urothelial cells compared to normal cells (Proctor et al., 2010). The detection procedure is based on the recognition of the target by antibodies. Two types of NMP22 test kits are available. NMP22 bladder cancer test (Alere) is an ELISA kit, which is a quantitative, sandwich immunoassay while the NMP22 Bladder Chek (Alere and Matritech) is a qualitative test strip based on lateral flow immunochromatography. Another widely used technique is *ImmunoCyt/uCyt+* (Budman et al., 2008). A mixture of three antibodies tagged with fluorescent dyes is utilised to detect specific antigens presented on exfoliated tumour cells (Greene et al., 2006). M344 and LDQ10 antibodies labelled with fluorescein can recognise a mucin-like antigen and 19A211 antibody is specific to the glycosylated version of carcinoembryonic antigen (CEA). The cells are fixed on a glass slide, stained with antibodies and detected under a fluorescent microscope. However, this technique is

not a stand-alone test and needs to be used with a cytology test (Budman et al., 2008, He et al., 2016). The last technique worth being mentioned is *UroVysion* (Budman et al., 2008). It is another fluorescent-based assay based on fluorescence *in situ* hybridisation (FISH) (Hammers and Stanley, 2014). The genetic alterations, namely aneuploidy for chromosome 3, 7, 17 and the loss of the 9p21 locus of chromosome 9, are detected using a set of oligonucleotide probes (Budman et al., 2008, Hammers and Stanley, 2014, Dimashkieh et al., 2013). All of the four methods mentioned have sensitivities that are better than urinary cytology. However, using all the four biomarkers is still less specific than urinary cytology since they suffer from more false positive results (Table 1.3). Therefore, up until the present, none of biomarker-based assays can be used as a replacement for cystoscopy and cytology, and there are obviously a number of opportunities for research on new biomarker-based techniques for bladder cancer monitoring.

Table 1.3 Comparison between cytology and other commercial biomarker tests for monitoring the occurrence of bladder cancer

Diagnostic test	Type of assay	Target	Sensitivity*	Specificity*
Cytology	Cell-based assay	Bladder tumour cells	12.1 - 84.6%	78.0 - 100%
BTA-stat	Qualitative, lateral flow immunochromatography	CFHrp	52.5 - 78.0%	69.0 - 87.1%
BTA-Trak	Quantitative, sandwich ELISA	CFHrp	51.0 - 100.0%	73.0 - 92.5%
NMP22 Test	Quantitative, sandwich ELISA	NMP22	34.6 - 100.0%	60.0 - 95.0%
MNP22 Bladder Chek	Qualitative, lateral flow immunochromatography	NMP22	49.5 - 65.0%	40.0 - 89.8%
ImmunoCyt/uCyt+	Fluorescent, cell-based assay	Mucin-like antigen and CEA	81.0 - 89.3%	62.0 - 77.7%
UroVysion	Fluorescence in situ hybridization (FISH)	Chromosome 3,7,9 and 17	68.6 - 100%	65.0 - 96%

*Data were obtained from (Budman et al., 2008).

1.7.3 FGFR3 protein and its implication in bladder cancer

Fibroblast growth factor receptor 3 (FGFR3) is a member of the FGFR protein family, playing an indispensable role in many biological processes, e.g. bone development and cell differentiation (Amizuka et al., 2004, Bolander et al., 2012). The structure of the protein comprises an extracellular domain (three immunoglobulin (Ig)-like domains), a hydrophobic transmembrane domain, and an intracellular tyrosine kinase domain (Figure 1.14). A previous study reported that among four FGFR proteins, FGFR3 showed the highest level of expression in normal urothelial cells, indicating that the FGFR3 could play a significant role in homeostasis of the urothelium (Tomlinson et al., 2005). In bladder cancer cells, both overexpression

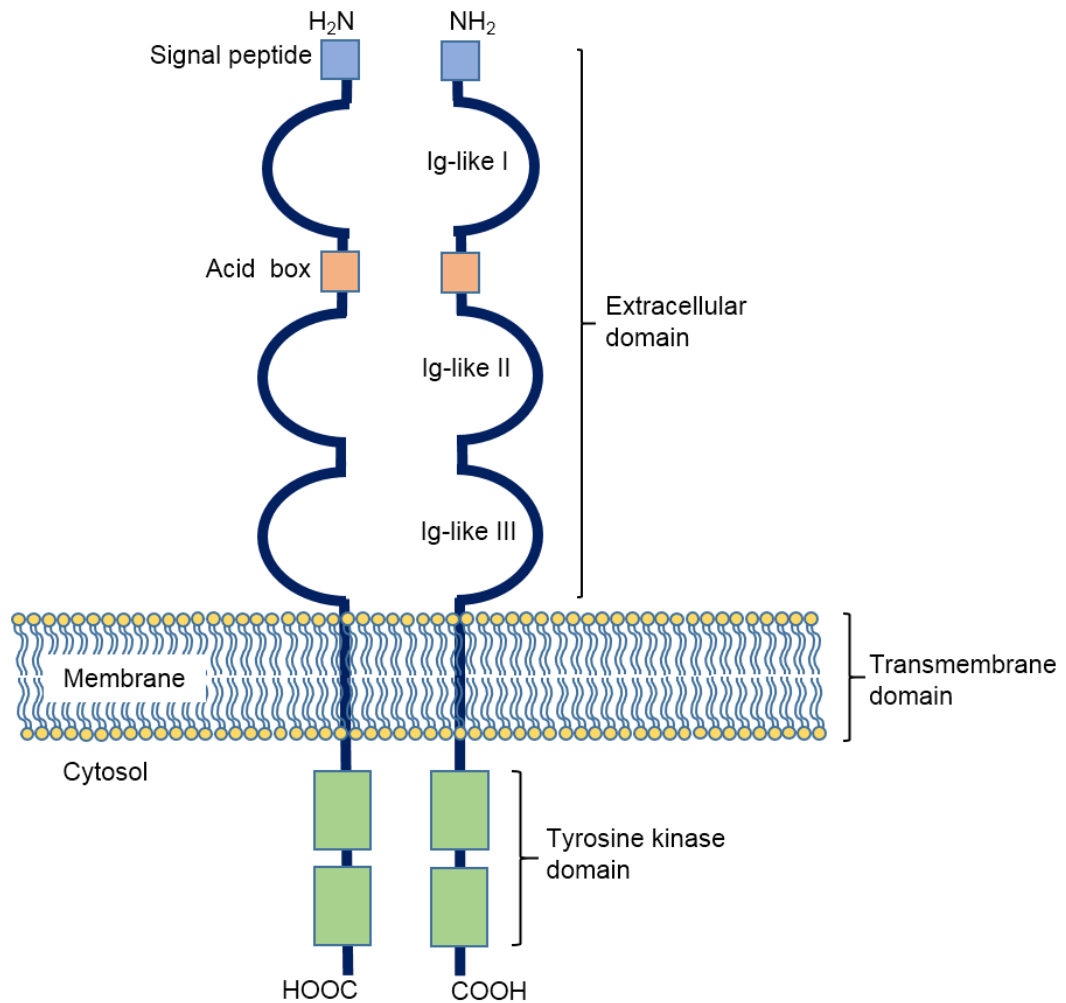


Figure 1.14 Overall structure of FGFR3 protein. The FGFR3 protein consists of three immunoglobulin-like domains, one transmembrane domain and one split tyrosine kinase domain. The binding of fibroblast growth factors (FGFs) to the receptors causes receptor dimerisation. Transphosphorylation on several tyrosines by kinase enzymes then occurs, leading the activation of downstream signalling pathways. This figure is modified from the previous publications (Turner and Grose, 2010, Wesche et al., 2011).

and mutation of FGFR3 have been found to have a relationship to the development of bladder tumours. The researchers utilised immunohistochemistry to reveal that there was an overexpression of FGFR3 in bladder cancer cells compared to normal urothelium (Tomlinson et al., 2007). An increasing expression level of FGFR3 was especially high at the superficial stages (pTa and pT1) and grades (1 and 2) of the cancer. As both overexpression and mutation of FGFR3 are common phenomena in bladder cancer, the relationship between mutational status and the expression level of FGFR3 has also been studied since gene mutations might result in the increasing level of FGFR3 proteins. It was found that approximately 85% of mutant tumours showed overexpression and the majority of them were classified into low grade or early stage cancers (Tomlinson et al., 2007). This finding was also supported by the research work from two different groups who also found that there was an increasing FGFR3 expression in bladder tumours during pTa and pT1 stages (Gomez-Roman et al., 2005, Mhawrech-Fauceglia et al., 2006). However, a contrary study reported that there was no relationship between the expression level and mutational status of FGFR3 at any stage or grade of bladder cancer cells (Matsumoto et al., 2004). Although the linkage between mutation and overexpression of the protein is still unclear, high expression level of FGFR3 is common in bladder cancer, especially at the superficial stages. There is also an evidence showing the detection of FGFR3 protein in urine samples. A previous study reported that using western blot analysis, the soluble form of FGFR3 could be detected in urine obtained from patients with non-invasive bladder cancer (Blanca et al., 2016). The researchers also found that the expression of FGFR3/Cyclin D3 proteins in urine could be a specific and sensitive approach for monitoring bladder cancer recurrence. There are two possible events that may explain the presence of soluble FGFR3 protein found in urine. The soluble form of FGFR3 can be generated by alternative mRNA splicing. A previous study reported that via mRNA splicing the secreted isoform, FGFR3 Δ 8-10, was detected (Tomlinson et al., 2005). The C-terminus of Ig-like domain III and

transmembrane domain were absent in this isoform, making it be secreted as a soluble form. The other process generating soluble FGFR3 is ectodomain shedding (Degnin et al., 2011). The researchers found that the proteolytic cleavage of extracellular domain of FGFR3 is carried out by cathepsins and γ -secretase, releasing the ectodomain of FGFR3 into extracellular fluids. This suggests that FGFR3 could become a potential biomarker for detecting early stage bladder cancer in urine.

1.7.4 Available methods for FGFR3 detection

In general, to detect the expression of FGFR3 in bladder cancer cells, immunohistochemical staining (IHC) is utilised in a clinical setting (Bodoor et al., 2010, Guancial et al., 2014, Sung et al., 2014, Tomlinson et al., 2007). Even though widely used in many laboratories and hospitals, there are several drawbacks of this technique, making it impractical in some circumstances. IHC is less sensitive in detecting its target, can be susceptible to photobleaching when using fluorescent tags, is time consuming and has a narrow dynamic range of detection. Because of these complications, the technique also needs trained users to perform it. Therefore, the resulting interpretation is subjective and this makes the technique not an ideal tool for point-of-care diagnostics.

ELISA is also one of the most widely used methods to detect protein biomarkers in biological fluids. At present, there are commercial ELISA kits capable of detecting FGFR3 in serum, plasma and biological samples for sale in the markets. The kits are claimed to have dynamic ranges from pM to nM (ab214027, Abcam, UK and LS-F6632-1, LifeSpan Biosciences, USA). However, it is known that ELISA is time-consuming, costly and needs a skilled user. Therefore, new techniques which can overcome the problems of IHC and ELISA are still required.

1.8 Project aims and potential applications

The major objective of this project was to develop an impedimetric biosensor platform using Affimers as bioreceptors to recognise targets of interest, which could be small molecules or protein biomarkers of diseases. Dichlorodiphenyltrichloroethane (DDT) was selected to represent a small molecule while fibroblast growth factor receptor 3 (FGFR3) is a protein biomarker of bladder cancer. To complete the tasks, the project was divided into three sections as follows.

The first part of the project was concerned with the screening and production of the Affimers to be used as biorecognition elements. DDT was used as a model analyte for the Affimer phage display screening. The Affimers were obtained by selecting from a phage display library within the Leeds BioScreening Technology Group. The selected Affimers were then subcloned and expressed prior to further use. Affimers directed against FGFR3 had already been selected and subcloned as part of another project.

The aim for the second part of the thesis was to characterise the specific interaction of chosen Affimers with their targets. Several approaches were employed to check the affinity of the Affimers and the targets. Enzyme-linked immunosorbent assay (ELISA) was picked to confirm the binding of Affimers against DDT. Further analysis was not done as the DDT Affimers proved non-specific. On the other hand, three techniques, ELISA, surface plasmon resonance (SPR) and pull-down assay (immunoprecipitation) were employed to investigate the binding of Affimers to FGFR3 protein. Affimers giving positive response to their target were then selected for biosensor fabrication.

The final section was focused on the fabrication of impedimetric biosensors using the Affimers selected from the first and second sections. Commercially screen-printed gold electrodes which had three electrodes (working, counter and reference) were used. Two different protocols, the ELISHA 'gluing method' and the NeutrAvidin-

biotin linkage-based protocol, were used to fabricate sensors to detect FGFR3. To establish the sensor construction protocol, the concentrations of Affimers and NeutrAvidin were optimised. Also, several blocking agents were investigated as an attempt to minimise non-specific binding background.

Although there have been biomarker-based tests commercially available in the markets at the present, none of these tests shows sufficient sensitivities to be used as a replacement for cystoscopy and urine cytology for bladder cancer detection. As a promising protein biomarker for bladder cancer, the development of an Affimer-based impedimetric biosensor to detect FGFR3 protein may become a useful analytical tool to be used as either a stand-alone test or in combination with other bladder cancer detection approaches for surveillance of early stage bladder tumours or the recurrence of cancer surgeries. If the platform is successfully established, it may not only be applied for bladder cancer detection, but also could be used to develop biosensors to monitor the emergence of other life-threatening diseases, in particular cancers, which affect a large number of people worldwide.

Chapter 2

Materials and Methods

2.1 Materials

2.1.1 Inorganic chemicals

$K_3Fe(CN)_6$ (99%), $K_4Fe(CN)_6 \cdot 3H_2O$ (98%), NaCl, and Tris were purchased from Fisher Scientific. NaOH and disodium tetraborate were supplied by BDH laboratory supplies. NaH_2PO_4 was purchased from Sigma-Aldrich.

2.1.2 Organic chemicals

D-Glucose, glycine and boric acid were purchased from BDH laboratory supplies. Isopropyl- β -D-thiogalactopyranoside (IPTG) was purchased from ThermoFisher Scientific. Imidazole, biotin-maleimide, tyramine, (+)-biotin N-hydroxysuccinimide ester (biotin-NHS) and pyromellitic dianhydride were purchased from Sigma-Aldrich. Glycerol was purchased from Fisher Scientific. 2-mercaptoethanol was purchased from Bio-rad. Poly(sodium-p-styrenesulfonate) was obtained from Acros Organics. mPEG-biotin (5K) was supplied by NEKTAR Transforming Therapeutics.

2.1.3 Other reagents

BugBuster protein extraction reagent was obtained from Novagen. Halt protease inhibitor cocktail, immobilised TCEP disulphide reducing gel and Pierce ECL western blotting substrate were purchased from ThermoFisher Scientific. Ni^{2+} - NTA slurry was purchased from IBA Solutions for Life Sciences. Laemmli sample

buffer was purchased from Bio-rad. Quick coomassie stain was obtained from Generon. Tween-20 was purchased from Fisher scientific. 3,3',5,5'-tetramethylbenzidine (TMB) substrate (SeramunBlau® fast TMB/substrate solution) was purchased from Seramun. 4% (w/v) copper (II) sulfate pentahydrate and bicinchoninic acid were purchased from Sigma-Aldrich. Streptavidin resin was obtained from Genscript.

2.1.4 Bacterial growth media ingredients

Tryptone, yeast extract and agar were purchased from Sigma-Aldrich. Carbenicillin was purchased from Alfa Aesar.

2.1.5 Antibodies and related reagents

Anti-His-tag antibodies HRP (ab1187) was purchased from Abcam. Anti-FGFR3 antibodies specific to extracellular domain (F3922) and anti-rabbit IgG antibodies – HRP (A0545) were purchased from Sigma-Aldrich. Pierce high sensitivity streptavidin-HRP was purchased from ThermoFisher Scientific.

2.1.6 Bacterial and viral strains

E.coli cells strain ER2738 and M13K07 helper phage were supplied by the BioScreening Technology Group (BSTG), University of Leeds. XL1-blue *E.coli* supercompetent cells and BL21 Gold (DE3) *E.coli* cells were purchased from Agilent technologies.

2.1.7 Enzymes

NheI-HF, *NotI*-HF, Antarctic phosphatase, DpnI and T4 DNA ligase were supplied by New England BioLabs (NEB). Phusion DNA polymerase was purchased from ThermoFisher Scientific. Benzonase nuclease was purchased from Novagen.

2.1.8 Solvents and buffers

Methanol was obtained from Fisher Scientific. 10x TGS (Tris/Glycine/SDS) buffer was purchased from Bio-rad. Dimethyl sulfoxide (DMSO), Phosphate buffered saline (PBS) tablets and 10x casein blocking buffer were purchased from Sigma-Aldrich. 10x PBS-P+ buffer was obtained from GE Healthcare Life Sciences.

2.1.9 Proteins

NeutrAvidin was purchased from Invitrogen. Bovine serum albumin (BSA), β -2-microglobulin, human serum albumin and sodium caseinate were purchased from Sigma-Aldrich. Purified recombinant FGFR3 protein was obtained from Genscript. Anti-digoxin IgG was provided by the Leeds Bionanotechnology Group.

2.1.10 Kits and consumables

NucleoSpin[®] gel and PCR clean-up kits were supplied by Macherey-Nigel. QIAprep Spin Miniprep kits were purchased from QIAGEN. Two-ml polystyrene columns, F96 Maxisorp Nunc-immuno plates and Zeba spin desalting columns (7K MWCO) were purchased from ThermoFisher Scientific. Mini-PROTEAN TGX gels (4-15%, 10 wells) were purchased from Bio-rad. Pur-A-Lyzer[™] Midi 6000 dialysis tubes were purchased from Sigma-Aldrich. Series S sensor chips SA and polyvinylidene difluoride (PVDF) membranes were obtained from GE Healthcare Life Sciences.

2.1.11 Electrodes

Gold-based screen-printed electrode chips (model CX223AT) were fabricated by and purchased from Dropsens (Spain). Each chip (Figure 2.1) offers a three electrode system. This makes its application more convenient since there is no requirement for additional reference and counter electrodes. Two working electrodes are circular whereas the counter electrode has a U shape. Working and counter electrodes were made of gold. A reference electrode was made of Ag/AgCl.

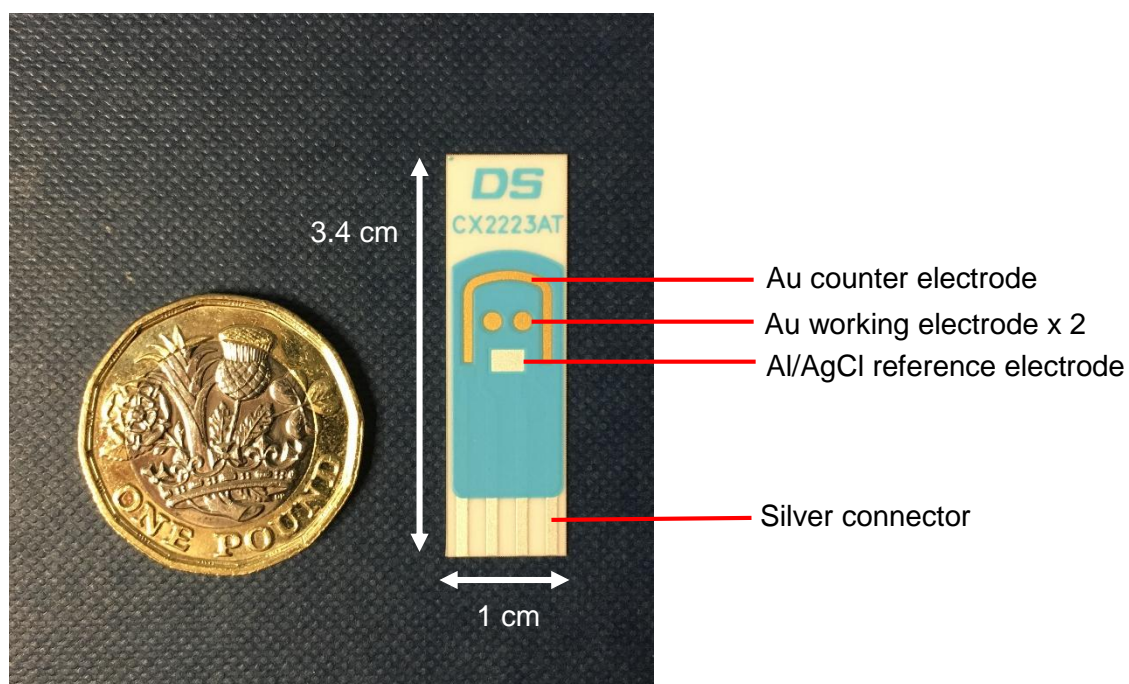


Figure 2.1 A Dropsens gold screen-printed electrode chip. Each chip has two working electrodes, one counter electrode and one reference electrode. Four silver connectors at the bottom are used to connect with a potentiostat via a Dropsens connector.

2.2 Methods

2.2.1 Phage display screening for DDT-binding Affimers

Biotinylated DDT (Hapten 2 – biotin) was synthesised and kindly provided by Dr. Hanafy Ismail from Liverpool School of Tropical Medicine, UK. The structure of biotinylated DDT is presented in Figure 2.2. Biotinylated DDT was dissolved in 80% (v/v) methanol at the concentration of 20 mg/ml. Prior to use for phage display screening, the stock of biotinylated DDT was diluted down to 1 mg/ml.

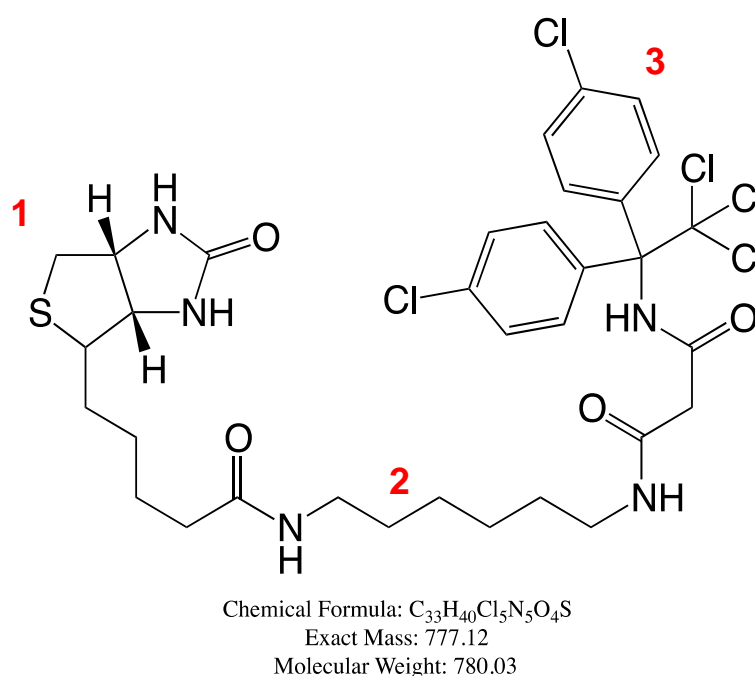


Figure 2.2 The chemical structure of biotinylated DDT. The structure contains (1) biotin, (2) hydrocarbon chain linker and (3) DDT moiety.

The Affimer phase display selection was performed as presented in Figure 2.3. In the first panning round, biotinylated DDT was immobilised onto a streptavidin-coated well (ThermoFisher Scientific) for 1 h and then 5 μ l of Affimer phage library was added and incubated on a vibrating shaker for 2 h at room temperature. The panning well was washed with PBST on a plate washer. Bound phage were then

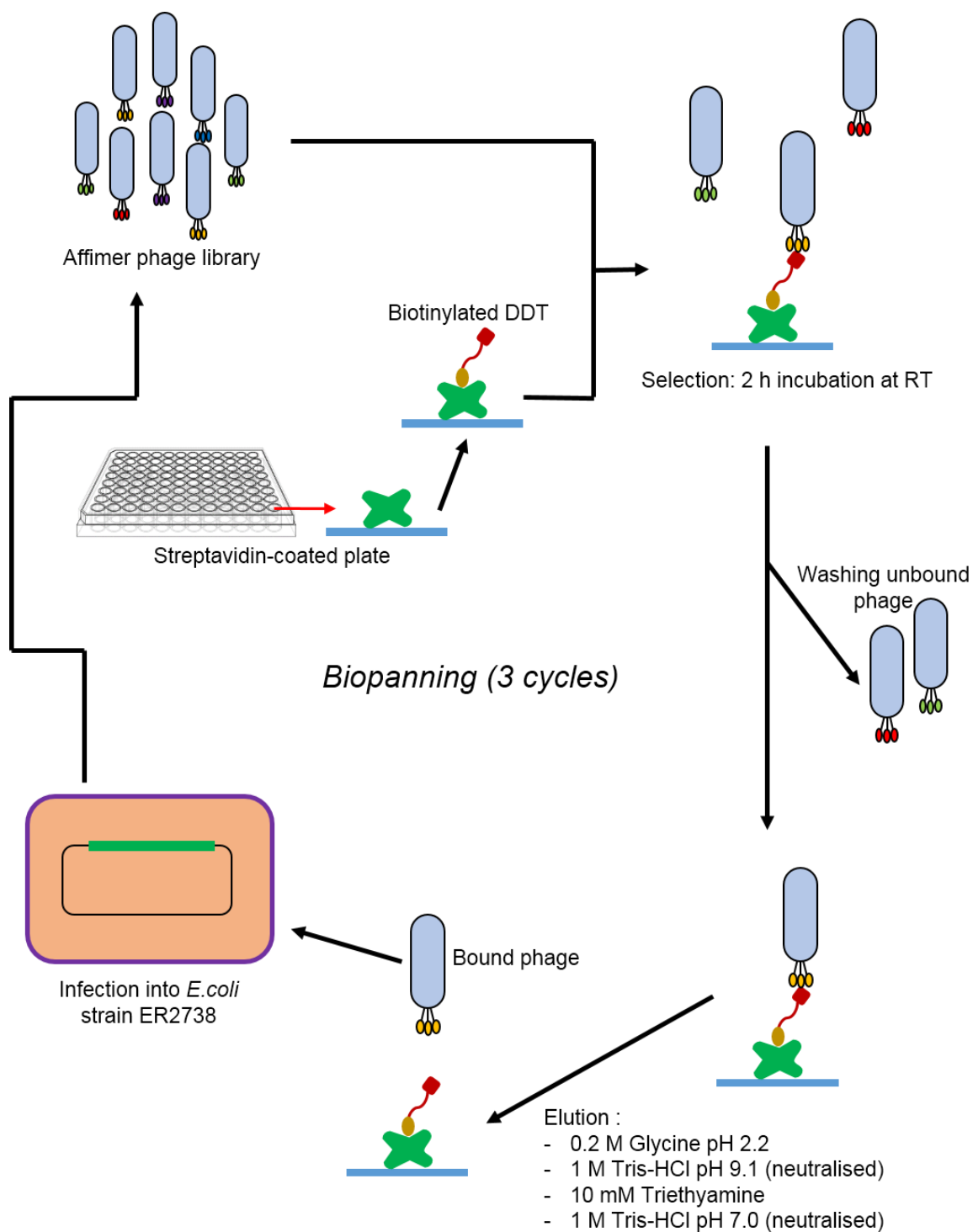


Figure 2.3 The schematic representation showing the brief protocol of phage display screening for DDT-specific Affimer selection. The procedure consisted of binding of the Affimer presented on phage to DDT, washing unbound phage, eluting bound phage and infecting *E. coli* cells with phage presenting the Affimer. In the second and third panning rounds, streptavidin-coated magnetic particles and a Neutraavidin-coated plate were used for the selection.

eluted from the target using 0.2 M glycine, pH 2.2 for 10 min, neutralised in 1 M Tris-HCl, pH 9.1, then eluted using 10 mM Triethylamine for 6 min, and neutralised in 1 M Tris-HCl, pH 7.0. Eluted phage were further employed for infecting *E.coli* strain ER2738 for 1 h at 37°C without shaking. The phage-infected *E.coli* cells were plated on LB agar plates with 100 µg/ml carbenicillin and incubated overnight at 37°C. Growing colonies were scraped into 5 ml of 2TY media with 100 µg/ml carbenicillin and infected with M13K07 helper phage (titre ca. 10^{14} /ml). After 30 min of incubation, 25 mg/ml kanamycin was added and the culture was left overnight with shaking at 25°C, 170 rpm. The phage were precipitated in polyethylene glycol-NaCl solution (4% (w/v) PEG 8000, 0.3 M NaCl) and the pellets were resuspended in TE buffer containing 10 mM Tris, pH 8.0, 1 mM EDTA.

In the second panning round, in order to pre-pan the phage, 125 µl of phage-containing supernatant from the first panning round was mixed with 25 µl of the streptavidin beads (Dynabeads® MyOne™ Streptavidin T1, 10 mg/ml, Invitrogen). The suspension was incubated on a rotator for 1 h at room temperature prior to centrifugation. The supernatant was transferred to a fresh tube and mixed with 25 µl of the streptavidin beads again, following by 1 h incubation and centrifugation. In the meantime, biotinylated DDT was coated on the streptavidin beads. Supernatant containing the pre-panned phage was mixed with the DDT-coated streptavidin beads. For competitive panning, non-biotinylated DDT was added into the suspension. The supernatant was allowed to incubate overnight on a rotator at room temperature. After competitive binding, the suspension containing the beads was washed using a KingFisher Flex robotic platform (ThermoFisher Scientific). Wash and elution protocols were identical to the first panning round. As soon as the run finished, the supernatant was incubated with ER2738 *E.coli* cells for 1 h at 37°C without shaking. After centrifugation, the bacterial cells were plated on LB agar plates with 100 µg/ml carbenicillin and left overnight at 37°C. The phage were precipitated in polyethylene

glycol-NaCl solution (4% (w/v) PEG 8000, 0.3 M NaCl) and the pellets were resuspended in TE buffer.

In the final panning round, a NeutrAvidin coated 8-well strip (ThermoFisher Scientific) was used to capture biotinylated DDT. 1 μ l of 1 mg/ml biotinylated DDT stock was added to the well and incubated for 1 h at room temperature. 100 μ l of supernatant containing phage from the second panning round was added to the DDT-coated well and incubated for 1 h at room temperature on a shaker. After washes, a solution containing 0.5 μ g/ μ l of non-biotinylated DDT was added into the DDT-coated well and left for incubation on a shaker overnight at room temperature. In the meantime, ER2738 *E.coli* cells were cultured in 2TY media plus 12 μ g/ml tetracycline and incubated overnight at 37°C, 230 rpm. The overnight ER2738 cell culture was diluted in 2TY media with a ratio of 1:15 and incubated for 1 h at 37°C, 230 rpm. After washes using a plate washer, the phage were eluted by 0.2 M glycine, pH 2.2 for 10 min, and neutralised in 1 M Tris-HCl, pH 9.1. The phage were immediately mixed with the ER2738 cells. Remaining phage in the panning wells were eluted using 10 mM triethylamine for 6 min, neutralised in 1 M Tris-HCl, pH 7.0 and transferred to the ER2738 cells. The mixture was left for incubation at 37°C for 1 h without shaking and then plated with a range of volumes (10-fold dilutions from 0.01 to 100 μ l) on LB agar plus 100 μ g/ml carbenicillin. The plates were incubated overnight at 37°C and were used for phage ELISA.

2.2.2 Phage ELISA

Preparation of phages: individual colonies of infected ER2738 *E.coli* cells from the final panning round were picked and grown in 200 μ l of 2TY media containing 100 μ g/ml carbenicillin in a 96-well V-bottom deep well plate for overnight at 37°C, with shaking at 1050 rpm. From each overnight culture, 25 μ l was then transferred to 200 μ l of fresh 2TY media containing 100 μ g/ml carbenicillin and

incubated for 1 h at 37°C with shaking. M13K07 helper phage (titre ca. 10^{14} /ml) were diluted in 2TY media with the ratio of 1:1000 and 10 μ l of the dilution was added to fresh bacterial cultures. The cultures were incubated for 30 min at room temperature at a shaking speed of 450 rpm. The phage-infected cultures were added to 10 μ l of 2TY media containing 1.25 mg/ml kanamycin and incubated overnight at room temperature and shaking speed of 750 rpm. The culture plate was centrifuged at 3,500 $\times g$ for 10 min. The supernatant was removed to check for binding to biotinylated DDT.

ELISA: to begin with, biotinylated DDT was immobilised on a streptavidin-coated 96-well plate. The plate was washed once in PBST prior to adding 10 μ l of 10x casein blocking buffer (Sigma-Aldrich) and 40 μ l of phage-containing supernatant. The plate was incubated for 1 hr at room temperature on a shaker. After washing once in PBST, 50 μ l of 1:1000 dilution of anti-Fd-Bacteriophage-HRP was added into the wells and incubated for 1 h at room temperature with shaking. The plate was washed 10 times in PBST before 50 μ l of TMB substrate (SeramunBlau® fast TMB/substrate solution, Seramun) was added. The absorbance at 620 nm was measured after 3 min incubation. The phagemid vectors from positive clones were then selected and extracted for sequencing.

2.2.3 Subcloning of Affimer-encoding sequences into pET11a plasmids

2.2.3.1 Digestion of pET11a with *NheI* and *NotI* enzymes

The 125 μ l reaction containing 5 μ g of pET11a plasmid, 1x CutSmart™ buffer, 100 units of *NheI* (NEB) and 100 units of *NotI* (NEB) was prepared and incubated overnight at 37°C. 14 μ l of 10x Antarctic phosphatase reaction buffer and 1 μ l of 5,000

units/ml of Antarctic phosphatase (NEB) were added to the overnight reaction and incubated for 15 min at 37°C. The reaction was then heated up to 65°C for 5 min in order to inactivate Antarctic phosphatase. The digested pET11a vector was examined using 0.7% (w/v) agarose gel electrophoresis. To extract the pET11a plasmid from the excised gel, a NucleoSpin® gel and PCR clean-up kit (Macherey-Nigel) was used according to the manufacturer's instructions. The absorbance at 620 nm was measured and the products were stored at -20°C for the further use.

2.2.3.2 PCR amplification of Affimer-encoding sequences

To amplify Affimer-encoding sequences from phagemid vectors, PCR reactions were set up. A 25 µl PCR reaction comprised of 1x Phusion HF Buffer (ThermoFisher Scientific), 200 µM dNTP mix, 3% (v/v) DMSO, 0.8 µM forward primer forward shorter (5' – ATGGCTAGCAACTCCCTGGAAATCGAAG - 3'), 0.8 µM reverse primer pDHIS-C-rev (5' – TTAATAATGCGGCCGCACAAGCGTCACCAACCGGTTTG – 3'), 0.02 units/µl of Phusion DNA polymerase (ThermoFisher Scientific) and 1 µl of phagemid DNA template. PCR was performed as follows. A cycle of initial denaturation was run at 98°C for 30 s, following by 30 cycles of denaturation at 98°C for 20 s, annealing at 54°C for 20 s and extension at 72°C for 20 s. Finally, a cycle of final extension was performed at 72°C for 10 min. PCR products were purified through a Macherey-Nagel Nucleospin® gel and PCR clean-up kit (Macherey-Nagel) according to the manufacturer's instructions prior to further use.

2.2.3.3 Digestion of PCR-amplified Affimer sequences using *NheI* and *NotI*

To digest PCR products, 60 µl reaction was prepared as follows: 1x CutSmart™ Buffer, 167 units/ml of *NheI*-HF™ (NEB), 167 units/ml of *NotI*-HF™ (NEB) and 50 µl of purified PCR products. The mixtures were incubated overnight at 37°C. After the incubation, 0.5 µl of DpnI enzyme (NEB) was added into the reactions in order to remove *dam* methylated phagemid DNA template. The reactions were then incubated for 1 h at 37°C prior to purifying with a Macherey-Nagel Nucleospin® gel and PCR clean-up kit (Macherey-Nagel) according to the manufacturer's instructions.

2.2.3.4 Ligation of digested Affimer-encoding sequence PCR fragments into the pET11a vector

In order to ligate Affimer-encoding sequences into the pET11a expression vector, 20 µl ligation reactions were prepared. Each reaction contained 1x T4 DNA ligase buffer (NEB), 75 ng of digested pET11a vector, 25 ng of digested Affimer sequence DNA fragment and 20,000 units/ml of T4 DNA ligase (NEB). The mixed reactions were incubated overnight at room temperature prior to transformation into *E.coli* cells.

2.2.3.5 Transformation of ligation products into competent cells

In transformation, XL1-Blue *E.coli* supercompetent cells (Agilent technologies) were selected for amplification of pET11a vectors carrying Affimer-encoding sequences. In brief, the competent cells were thawed on ice before 10 µl of the cells was gently mixed with 1 µl of the ligation mix. The mix was incubated on ice for 30 min, heated shock at 42°C for 45 s and incubated on ice again for 2 min. 190 µl of SOC medium was then added to the mix before incubating at 37°C for 1 hr

with shaking speed of 230 rpm. After the incubation, 100 μ l of the bacterial mixture was grown on LB agar with 100 μ g/ml carbenicillin overnight at 37°C. Single colonies growing on the media were randomly picked into LB media plus 100 μ g/ml carbenicillin and incubated overnight at 37°C. The subcloned plasmid DNA for each Affimer clone was extracted from transformed *E.coli* using a QIAprep Spin Miniprep kit (QIAGEN) according to the manufacturer's instructions. The plasmids were sequenced using a T7P primer (5' – TAATACGACTCACTATAGGG – 3'). The nucleotide sequences of Affimer were translated into amino acid sequences prior to alignment using Clustal Omega supplied by EMBL-EBI.

2.2.3.6 Colony PCR

5 μ l of sterile dH₂O was aliquoted into a fresh PCR tube. A single colony of transformed *E.coli* was picked and dipped in 5 μ l dH₂O as a template for colony PCR. A 12.5 μ l PCR reaction consisted of 1x Phusion HF Buffer (ThermoFisher Scientific), 200 μ M dNTP mix, 0.8 μ M forward primer forward shorter (5' – ATGGCTAGCAACTCCCTGGAAATCGAAG - 3'), 0.8 μ M reverse primer pDHIS-C-rev (5' – TTACTAATGCGGCCGCACAAGCGTCACCAACCGGTTTG – 3'), 0.02 units/ μ l of Phusion DNA polymerase (ThermoFisher Scientific). PCR cycling was performed as described previously in 2.2.3.2. The PCR products were examined using 1.4% (w/v) agarose gel electrophoresis in 1x TAE buffer and the gels were photographed under UV light using a Syngene G-BOX imager.

2.2.4 Expression and purification of Affimers

2.2.4.1 Transformation of pET11a – Affimer plasmids into BL21 Gold (DE3) *E.coli*

To express the Affimers, BL21 Gold (DE3) *E.coli* (Agilent technologies) was selected as a host for Affimer production. 1 μ l of plasmid DNA with an Affimer sequence was gently mixed with 10 μ l of the competent cells. The mix was then incubated on ice for 30 min, heated shock at 42°C for 45 s and moved back for incubation on ice for 2 min. SOC medium (180 μ l) was added into the transformed cells and incubated at 37°C for 1 h with shaking speed of 230 rpm. The bacterial mixture was then plated on LB agar plus 100 μ g/ml carbenicillin and incubated overnight at 37°C.

2.2.4.2 Affimer expression

Single colonies growing on LB agar were randomly picked and grown in 3 ml of 2TY media plus 100 μ g/ml carbenicillin and 1% (w/v) glucose overnight at 37°C and shaking speed of 230 rpm. In the meantime, 50 ml of LB was pre-warmed overnight at 37°C.

Into 50 ml pre-warmed LB media, 100 μ l of 50 mg/ml carbenicillin and 1 ml of the overnight culture were added. The culture was incubated at 37°C with shaking speed of 230 rpm until the OD₆₀₀ reached approximately 0.8, which typically took 2.5 h. The culture was then added with 25 μ l of 1M IPTG in order to induce Affimer production and incubated for another 6 h at 25°C with shaking speed of 150 rpm. The bacterial cells were harvested using centrifugation at 3,220 xg for 30 min. The supernatant was discarded and the cells were air-dried for 30 min prior to storage at -20°C until the extraction was ready.

2.2.4.3 Affimer purification

The harvested cells were lysed in 1 ml of lysis buffer containing 50 mM NaH_2PO_4 , 300 mM NaCl , 30 mM imidazole, 10% (v/v) glycerol, pH 7.4, plus 1x BugBuster Protein Extraction Reagent (Novagen), 10 units/ml Benzonase Nuclease (Novagen) and 1x Halt Protease Inhibitor Cocktail (ThermoFisher scientific). The mixtures were initially incubated at room temperature for 20 min on a Stuart SB2 fixed speed rotator. In order to eliminate contaminant proteins, the mixtures were heated up to 50°C for 20 min. The mixtures were then centrifuged at 16,000 $\times g$ for 20 min to separate cell debris and unwanted insoluble components from soluble proteins. Simultaneously, 300 μl Ni^{2+} -NTA slurry containing 150 μl (IBA Solutions for Life Sciences) was washed once in 1 ml of lysis buffer. The slurry was centrifuged at 1,000 $\times g$ for 1 min to sediment the resin and the buffer was then removed. After 20 min centrifugation, the supernatant containing soluble proteins was transferred into washed Ni^{2+} -NTA slurry and incubated on a fixed speed rotator for 2 h at room temperature. The mixtures were centrifuged at 1,000 $\times g$ for 1 min to sediment the resin. The supernatant containing unbound proteins was transferred to a fresh tube and stored at -20°C. The remaining resin was added with 1 ml wash buffer containing 50 mM NaH_2PO_4 , 500 mM NaCl , 30 mM imidazole, 10% (v/v) glycerol, pH 7.4. To remove non-Affimer proteins, the resin was washed through a disposable 2 ml polystyrene column (ThermoFisher Scientific) until the absorbance at 280 nm reached < 0.09. Finally, the Affimers were eluted from the columns using elution buffer containing 50 mM NaH_2PO_4 , 500 mM NaCl , 300 mM imidazole, 20% (v/v) glycerol, pH 7.4. SDS-PAGE was used to check the size and quantity of the Affimers.

2.2.4.4 Sodium dodecyl sulfate polyacrylamide gel electrophoresis (SDS-PAGE)

SDS-PAGE sample loading buffer was prepared by mixing 950 μl of 2x Laemmli sample buffer (Bio-rad) with 50 μl of 14.2 M 2-mercaptoethanol (Bio-rad). 10 μl of protein sample was mixed thoroughly with 10 μl of the sample loading buffer. The mix was incubated at 95°C for 10 min. Subsequently, 15 μl of heated mix was loaded into the well in a Mini-PROTEAN TGX gel (4-15%, 10 wells, Bio-rad). SDS-PAGE was performed in 1x TGS (Tris/Glycine/SDS) buffer (Bio-rad) with the applied potential of 100 V for 65 min. After the run, the gel was stained in Quick Coomassie Stain (Generon) for 30-40 min and de-stained in dH_2O for 1-2 h. The gel was photographed using a Syngene G-BOX imager.

2.2.4.5 Affimer dialysis

Prior to further use, purified Affimers were dialysed to eliminate imidazole. Pur-A-Lyzer™ Midi 6000 dialysis tubes (Sigma-Aldrich) were equilibrated in 1x PBS buffer for at least 5 min. Eluted Affimers (500-800 μl) were transferred to dialysis tubes and then dipped in 1x PBS buffer pH 7.4 (dialysis buffer) with magnetic stirring for 3 h at 4°C. The buffer was changed every hour. The supernatants containing Affimers were removed to fresh tubes and centrifuged at 13,000 $\times g$ for 5 min to eliminate aggregated components before storing at -20°C for further use.

2.2.5 Characterisation of Affimers against DDT using ELISA

2.2.5.1 Preparation of NeutrAvidin-coated 96-well plates

1 mg/ml stock of NeutrAvidin was prepared before diluting it into 5 $\mu\text{g}/\text{ml}$ in PBS. To immobilise NeutrAvidin on plates, 50 μl of 5 $\mu\text{g}/\text{ml}$ NeutrAvidin was aliquoted into each well of a F96 Maxisorp Nunc-Immuno plate (ThermoFisher Scientific) and

incubated overnight at 4°C. Prior to use, the plates were blocked with 2x casein blocking buffer (Sigma-Aldrich) overnight at 37°C.

2.2.5.2 ELISA to examine the binding of Affimers against biotinylated DDT

Biotinylated DDT was initially immobilised on a NeutrAvidin-coated plate. After 3 washes in PBST, 5 µg/ml of Affimers was added to the wells and incubated for 1 h with a shaking speed of 450 rpm. The plate was washed five times in PBST before anti-His-tag antibodies – HRP (1:1000 dilution, Abcam) were added and incubated for 1 h with shaking. After 5 final washes, TMB substrate was added and allowed to develop for 3 min. The absorbance at 620 nm was measured.

2.2.5.3 ELISA to optimise concentrations of Affimers and TMB incubation time for competitive assay

The assay was performed in the same way as described previously in Section 2.2.5.2. Concentrations of Affimers was prepared at 0, 0.04, 0.08, 0.16, 0.31, 0.63, 1.25 and 2.5 µg/ml by two-fold serial dilution. After TMB substrate addition, the absorbance at 620 nm was monitored at 10, 20, 30 and 60 min to investigate the optimal time point for competitive ELISA assay.

2.2.5.4 Competitive ELISA

Biotinylated DDT-coated plates were prepared as described previously. In the meantime, a range of DDT concentrations was prepared at 0, 0.07, 0.15, 0.31, 0.62, 1.25, 2.5, 5 and 10 µM by two-fold serial dilution. Affimers at the concentration of 0.3 µg/ml was mixed with different concentrations of DDT with 1:1 ratio and left for

incubation on a fixed speed rotator for 1 h at room temperature. After the plates were washed 3 times in PBST, the Affimer-DDT mixtures were added to the plates and incubated for 1 h with shaking. Anti-His-tag antibodies – HRP (1:1000 dilution) were added after 5 washes in PBST and the plates were incubated for 1 h with shaking. The plates were washed 5 times with PBST before TMB substrate was added. The absorbance at 620 nm was measured.

2.2.6 Characterisation of Affimers against FGFR3 protein

2.2.6.1 Biotinylation of FGFR3 and GFP Affimers

Prior to biotinylation, 150 μ l of each Affimer was mixed with 150 μ l of immobilised TCEP disulfide reducing gel (ThermoFisher Scientific) on a fixed speed rotator for 1 h at room temperature. The supernatants were then mixed with 6 μ l of 2 mM biotin-maleimide (Sigma-Aldrich) and incubated without agitation for 2 h at room temperature. The mixtures were desalted using Zeba Spin Desalting Columns, 7K MWCO (ThermoFisher Scientific) according to the manufacturer's instructions. The concentration of biotinylated Affimers was measured via BCA assay and the successful biotinylation was determined by ELISA and liquid chromatography-mass spectrometry (LC-MS).

2.2.6.2 Bicinchoninic acid (BCA) assay

BCA assay was used as a standard method to measure the concentration of the Affimers and protein samples used for the whole experiments. In the assay, BSA was employed to set a standard curve for protein concentration measurement. BSA at the concentrations ranging from 0 to 1 mg/ml was freshly prepared as well as the Affimers and protein samples. The BCA working reagent was prepared by mixing 1:50 ratio of 4% (w/v) copper (II) sulfate pentahydrate solution and bicinchoninic acid

together. Into a 96-well plate, 15 μ l of each protein sample including BSA was added to the wells, following by 120 μ l of the BCA working reagent. The reactions were incubated at 37°C for 30 min and were then measured the absorbance at 562 nm. The standard curve was generated using OriginPro 8.6 software.

2.2.6.3 Sandwich ELISA to investigate the binding of Affimers to FGFR3 protein

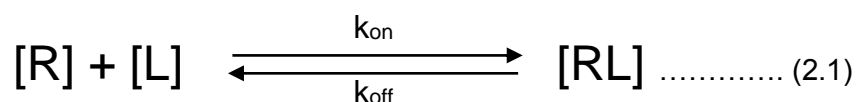
To perform the sandwich ELISA, a F96 Maxisorp Nunc-Immuno plate (ThermoFisher Scientific) was coated with 5 μ g/ml NeutrAvidin in 1x PBS buffer overnight at 4°C. The plate was then blocked with 2x casein blocking buffer (Sigma-Aldrich) overnight at 37°C. After 1x wash in PBST (PBS with 0.05% Tween-20), approximately 40 μ M of each biotinylated Affimer was added into the wells and incubated with the rotation speed of 450 rpm for 1 h at room temperature. The plate was washed twice in PBST before 45 μ M of purified FGFR3 (Genscript) was added into the wells and left for incubation for 1 h at room temperature. After washing steps as described previously, 2 μ g/ml of anti-FGFR3 antibodies specific to extracellular domain (F3922, Sigma-Aldrich) as primary antibodies was added to the plate, following by 2 μ g/ml of anti-rabbit IgG antibodies – HRP (A0545, Sigma-Aldrich) as secondary antibodies. The plate was washed 6 times with PBST before TMB substrate (SeramunBlau® fast, Seramun) was added. After 3 min of TMB addition, the absorbance at 620 was measured.

2.2.6.4 Surface Plasmon Resonance (SPR)

SPR was carried out using a Biacore T200 (GE Healthcare Life Sciences, USA) with a series S sensor chip SA with 1x PBS-P+ (GE Healthcare Life Sciences, USA) as a running buffer for the entire experiments. First, biotinylated Affimers were

immobilised to the sensor chip via streptavidin-biotin interaction on flow cell 2-4 whereas flow cell 1 was left empty as a reference surface. The Affimers at the concentration of 16.7 nM were injected into flow cells at a flow rate of 5 $\mu\text{l}/\text{min}$ until the surface density reached 200 response unit (RU). Kinetic binding data were collected by injecting purified FGFR3 at the concentrations between 0 and 1000 nM at a flow rate of 30 $\mu\text{l}/\text{min}$ and the temperature of 25°C. The contact time during the association phase was 300 s, following by 900 s of the dissociation phase with the running buffer. After each cycle of association and dissociation, the surfaces were regenerated using 10 mM glycine pH 2.5 for 120 s at a flow rate of 30 $\mu\text{l}/\text{min}$. To determine the dissociation constant (K_D) of each Affimer, the SPR data were analysed using GraphPad Prism 7 software.

In fact, an Affimer has only one binding site, which can bind specifically to an epitope on the analyte. Therefore, the most appropriate model to explain the mode of action when the Affimer binds to the target is a 1:1 binding model which can be expressed by equation 2.1.



Where :

[R] is the concentration of bioreceptor (M),

[L] is the concentration of ligand (M),

[RL] is the concentration of bioreceptor-ligand complex (M),

k_{on} is association rate constant in $\text{M}^{-1} \text{s}^{-1}$ unit,

k_{off} is dissociation rate constant in s^{-1} unit

At the start of the association phase, none of bioreceptor molecules attached to the chip surface is occupied. When ligand is injected into the flow cells, more and

more binding sites on the bioreceptors are occupied with ligands, resulting in a rapid increase of response of the sensor. As time passes the binding sites of bioreceptors become fully occupied and the sensor response becomes constant. At the steady state, the numbers of ligands binding to and dissociating from bioreceptors are equal. The association rate constant is governed by the concentration of free ligands and bioreceptors. The binding kinetics during the association period can be shown as equation 2.2.

$$\frac{d[RL]}{dt} = k_{on}[R][L] - k_{off}[RL] \dots\dots\dots (2.2)$$

Where :

$d[RL]/dt$ is change in receptor-ligand complex formation over time,

$[R]$ is bioreceptor concentration (M),

$[L]$ is ligand concentration (M),

$[RL]$ is bioreceptor-ligand complex concentration (M),

k_{on} is association rate constant in $M^{-1} s^{-1}$ unit,

k_{off} is dissociation rate constant in s^{-1} unit

A one-site specific model was used in order to calculate the association rate constant (k_{on}). The kinetic equation 2.2 is transformed to the format that can be resolved by computer programmes as shown in equation 2.3. The reference data and zero FGFR3 data were subtracted from the SPR data of each concentration of FGFR3. By fitting the SPR data from the association phase with this model, the k_{on} values for Affimers when binding to FGFR3 protein were obtained.

$$y = y_0 + A(1 - e^{k_{on}t}) \dots\dots\dots (2.3)$$

Where :

y is binding signal (response unit),

y₀ is minimum binding signal achieved (response unit),

A is the amount of ligand (M),

k_{on} is association rate constant (M⁻¹ s⁻¹),

t is time (s)

The dissociation phase occurs when the injection of ligand is stopped. The solution containing ligand of interest is replaced by running buffer. Therefore, the ligand concentration is zero. At this stage, bound ligands dissociates from the bioreceptors. The rate of dissociation is governed by time and the concentration of ligand-receptor complex and can be described by equation 2.4.

$$\frac{d[RL]}{dt} = -k_{off} \cdot [RL] \dots\dots\dots (2.4)$$

Where :

d[RL]/dt is change in receptor-ligand complex formation over time,

[RL] is bioreceptor-ligand complex concentration (M),

k_{off} is dissociation rate constant in s⁻¹ unit

In order to analyse the SPR data from the dissociation phase, a one phase decay model was used. The kinetic equation for dissociation is transformed to the rate equation presented in equation 2.5. By fitting the binding kinetic data with this model, the k_{off} values for the binding of Affimers to FGFR3 protein were obtained.

$$y = y_0 + A \cdot e^{-k_{off} \cdot t} \dots\dots\dots(2.5)$$

Where :

y is binding signal (response unit),

y₀ is minimum binding signals achieved (response unit),

A is the amount of ligand (M),

k_{off} is dissociation rate constant (s⁻¹),

t is time (s).

To determine the affinity of a bioreceptor for its target, the overall dissociation constant (K_D) is normally used. The dissociation constant (K_D) represents the concentration of ligand that saturates 50% of the binding sites of the bioreceptor. From this definition, the lower the K_D is, the stronger the interaction between bioreceptors and ligands is. The apparent K_D from the experiments can be calculated using equation 2.6.

$$K_D = \frac{k_{off}}{k_{on}} \dots\dots\dots (2.6)$$

Where :

K_D is dissociation constant (M),

k_{on} is association rate constant (M⁻¹ s⁻¹),

k_{off} is dissociation rate constant (s⁻¹)

2.2.6.5 Pull-down assay and western blot analysis

Prior to the pull-down assay, 60 µl of streptavidin resin (Genscript) was mixed with 60 µl of 4x casein blocking buffer (Sigma-Aldrich) and incubated for 1 h on a fixed speed rotator at room temperature in order to block unoccupied sites on the resin. The resin was washed once in 1x PBS before 20 µg of biotinylated Affimers

was added to the washed resin, following by 90 min incubation on a rotator at room temperature. After removing unbound Affimers and washing once in wash buffer, 15.75 μg of purified FGFR3 was added to the resin coated with Affimers. The mixtures were incubated overnight on a rotator at 4°C. The supernatant was removed and the resin was washed three times in wash buffer. The extra 30 μl of 1x PBS was added to suspend the resin.

For western blot analysis, the pull-down products as well as a biotinylated Affimer and purified FGFR3 as positive controls for the blots were prepared and separated using SDS-PAGE as mentioned in Section 2.2.4.4. It should be noted that two identical gels are required. To begin with, polyvinylidene difluoride (PVDF) membranes were pre-soaked in methanol for 1 min, following by equilibrating in transfer buffer containing 20% (v/v) methanol, 25 mM Tris, 190 mM glycine, pH 8.3 for at least 15 min. The gels containing protein samples were carefully packed into the cassettes in the following order: black side of blotting pad, 2 x filter paper, gel, PVDF membrane, 2 x filter paper, white side of blotting pad. The cassettes were moved to a tank filled with transfer buffer. An ice block was used to keep the temperature consistent during the transfer. The proteins in the gels were transferred to PVDF membranes using the applied potential of 115 V for 75 min. After transferring the proteins onto the membranes, the membranes were blocked in 5% (w/v) skim milk in PBST for 1 h on a rocker. The membranes were washed 3 times in PBST. In order to examine the existence of Affimers, one of the membranes was incubated in 1:1000 ratio of streptavidin-HRP (ThermoFisher Scientific) diluted in 2% (w/v) BSA in PBST for 1 h at room temperature. The membrane was washed 4 times in PBST and 3 times in 1x PBS. The results were revealed by Pierce ECL western blotting substrate (ThermoFisher Scientific). The membrane was then photographed using a Syngene G-BOX imager.

In the meantime, to examine the binding of Affimers to FGFR3 protein, the other membrane was incubated in 1:750 ratio of anti-FGFR3 antibodies (F3922,

Sigma-Aldrich) diluted in 2% (w/v) BSA in PBST overnight on a rocker at 4°C. The membrane was then washed 4 times in PBST before being incubated in 1:1000 ratio of anti-rabbit IgG antibodies – HRP (A0545, Sigma-Aldrich) diluted in 2% (w/v) BSA in PBST on a rocker for 1 h at room temperature. The membrane was washed 4 times in PBST, following by washing three times in 1x PBS. After 1 min addition of Pierce ECL western blotting substrate (ThermoFisher Scientific) solution, the membrane was photographed using a Syngene G-BOX imager.

2.2.6.6 ELISA to check the specific binding of Affimers to FGFR3 and other protein targets

10 µg/ml of each protein sample (FGFR3, β-2-microglobulin, antidigoxin IgG and human serum albumin) was added into the wells in a F96 Maxisorp Nunc-Immuno plate (Thermo Scientific) and left for immobilisation overnight at 4°C. The plate was washed 3 times in PBST, following by blocking with 10x casein blocking buffer (Sigma-Aldrich) for 3 h at 37°C. After washed three times in PBST, 5 µg/ml of biotinylated Affimers was added into the wells and left for incubation at room temperature for 1 h with the shaking speed of 450 rpm. The plate was then washed 6 times in PBST before 1:1000 ratio of streptavidin-HRP (ThermoFisher Scientific) was added to each well and incubated for 1 h as described previously. After 8 washes in PBST, TMB substrate was added and allowed to develop for 30 min. The absorbance at 620 nm was measured.

2.2.7 Fabrication of impedimetric biosensors

2.2.7.1 Biosensor construction using ELISHA gluing method

To begin with, 200 µg/ml of FGFR3-21 and GFP Affimers were prepared in 10 mM phosphate buffer pH 7.2. The Affimers were mixed with the linking reagent

supplied by ELISHA Ltd. with 1:1 ratio and incubated on a fixed speed rotator for 1 h at room temperature. The reagents were stored at 4°C until use.

In order to immobilise Affimers onto electrodes, cyclic voltammetry was used. FGFR3-21 Affimer was immobilised first onto working electrode 1 with the applied potential of 0-1.6 V, 2 cycles and a scan rate of 100 mV/s. After washes with 100 mM PBS pH 7.2, GFP Affimer was deposited to working electrode 2 with the identical approach. The Affimer-immobilised chips were soaked in 100 mM PBS pH 7.2 until EIS measurement. After the baseline impedance measurement, the sensors were tested with FGFR3 protein over the concentration range from 10^{-15} to 10^{-8} M with washing in PBS in between. The data obtained were analysed using Origin Pro v8.6 software.

2.2.7.2 Biosensor construction via NeutrAvidin-biotin linkage

- Electropolymerisation of polytyramine

Electropolymerisation of polytyramine was performed using NOVA 2.0.2 software on an AUTOLAB type III electrochemical workstation (Metrohm Autolab B.V.; Utrecht, Netherlands). To polymerise a layer of polytyramine, cyclic voltammetry was used. Three types of electrodes were covered with a solution of 25 mM tyramine (Sigma-Aldrich) dissolved in 0.3 M NaOH in Milli-Q water. The applied potential was cycled twice from 0 to 1.6 V and then back to 0 V at a scan rate of 200 mV/s. After polymer deposition, the electrodes were rinsed twice and incubated in 20 mM boric acid/disodium tetraborate buffer pH 9.0 for 20 min prior to bioconjugation.

- Immobilisation of Affimers

To immobilise Affimers, polytyramine-coated electrodes were rinsed twice in 20 mM boric acid/disodium tetraborate buffer pH 9.0 and dried gently with tissue paper. To tether biotinylated Affimers to the electrode surface, NeutrAvidin-biotin interaction was utilised. The electrodes were incubated with 10 μ l of 3 mM NHS-biotin (Sigma-Aldrich) for 30 min, following by 10 μ l of a selected concentration of NeutrAvidin for 45 min with washing in PBS in between. Finally, 2 μ l of a specific concentration of biotinylated Affimer was added onto a working electrode and left for 1 h at room temperature. After washing in PBS, the fully constructed electrodes were incubated in PBS for 1 h prior to EIS measurement.

2.2.7.3 Electrochemical impedance spectroscopy

To observe the binding of FGFR3 protein to Affimers on the electrode surface, electrochemical impedance spectroscopy (EIS) was performed using an AUTOLAB type III electrochemical workstation (Metrohm Autolab B.V.; Utrecht, Netherlands). The fully fabricated sensors were challenged by incubating sequentially with increasing concentrations of FGFR3 between 10^{-14} and 10^{-8} M for 15 min, following by washing in PBS in between. Impedance measurement was conducted in the presence of 10 mM $K_3[Fe(CN)_6]/K_4[Fe(CN)_6]$ (1:1 ratio) in 100 mM PBS, pH 7.2. The measurements were recorded at an applied potential of 0 V vs Ag/AgCl over a frequency range of 2.5 kHz to 250 mHz with a modulation voltage of 10 mV. All of the experiments were replicated ($n \geq 3$) with independent sensor chips.

To analyse the sensor responses, charge-transfer resistance (R_{ct}) obtained automatically from NOVA 2.0.2 software was employed. The R_{ct} of each FGFR3 concentration was normalised as percentage against the R_{ct} measured without analyte addition. The sensor response was revealed using equation 2.7. The resulting data were then analysed using Origin Pro v8.6 software.

$$\Delta Rct(\%) = \frac{Rct_{(\text{specific concentration of FGFR3})} - Rct_{(\text{no FGFR3})}}{Rct_{(\text{no FGFR3})}} \times 100 \dots\dots\dots(2.7)$$

Changes in capacitance, phase shift and absolute impedance were also considered as alternative approaches to measure sensor performance. To investigate effects on capacitance, impedance data were converted into complex capacitance using equation 2.8 obtained from Jolly et al. (2016).

$$C^* = -\frac{Z''}{\omega|Z|^2} - j\frac{Z'}{\omega|Z|^2} = C' + jC'' \dots\dots\dots(2.8)$$

Where:

C' = real part of capacitance (F)

C'' = imaginary part of capacitance (F)

Z' = real component of measured impedance (Ω)

Z'' = imaginary part of measured impedance (Ω)

$\omega = 2\pi f$, angular frequency of the measurement (rad/s)

The real and imaginary components of capacitance were plotted against each other, providing Cole-Cole plots, where the capacitance values (C') were obtained. The C' for each FGFR3 concentration was normalised as a percentage against the C' of the sensors without FGFR3. The calculation was done using equation 2.9.

$$\Delta C'(\%) = \frac{C'_{(\text{specific concentration of FGFR3})} - C'_{(\text{no FGFR3})}}{C'_{(\text{no FGFR3})}} \times 100 \dots\dots\dots(2.9)$$

To analyse phase shift data, phase shift values were plotted against frequencies and the data at the lowest frequency showing the maximum phase shift were chosen for further analysis. Here, phase shift at a frequency of 7.9 Hz was used to see the response of the sensors. The phase shift at 7.9 Hz of each FGFR3 concentration was normalised by subtracting the phase shift of the sensors without FGFR3 as presented in equation 2.10.

$$\Delta\text{Phase shift}_{7.9 \text{ Hz}}(^{\circ}) = \text{Phase shift}_{(\text{specific concentration of FGFR3})} - \text{Phase shift}_{(\text{no FGFR3})} \dots\dots(2.10)$$

To analyse absolute impedance data ($|Z|$), absolute impedance values were plotted against frequencies and the frequency showing the maximum change in absolute impedance was selected. Here, absolute impedance at 0.25 Hz was used for further analysis. The $|Z|$ at 0.25 Hz of each FGFR3 concentration was normalised as a percentage against the $|Z|$ of the sensors without FGFR3 as shown in equation 2.11.

$$\Delta|Z|_{0.25 \text{ Hz}}(\%) = \frac{|Z|_{(\text{specific concentration of FGFR3})} - |Z|_{(\text{no FGFR3})}}{|Z|_{(\text{no FGFR3})}} \times 100 \dots\dots\dots(2.11)$$

2.2.7.4 Optimising sensor fabrication

- Optimisation of Affimer concentration

In order to examine the optimal concentration of Affimers, 4 concentrations of Affimers, 0.05, 0.1, 0.3 and 1 μM , were tested. The concentrations of NHS-biotin and NeutrAvidin were kept constant at 3 and 0.1 μM , respectively. Sensors were fabricated according to the protocol in Section 2.2.7.2.

- Optimisation of NeutrAvidin concentration

The optimal concentration of NeutrAvidin for sensor fabrication was also investigated. The sensors were constructed following the protocols as described in Section 2.2.7.2. While the concentrations of NHS-biotin and Affimers were fixed at 3 and 0.3 μM , respectively, NeutrAvidin concentrations were varied at 0.033, 0.067 and 0.1 μM .

- Effects of blocking reagents on sensor performance

Several proteins and chemicals were introduced here in order to minimise the effect of non-specific binding of analytes to sensor surface. After fabricating sensors following the method in Section 2.2.7.2, the sensors were blocked with 10 μl of a specific concentration of blocking reagents (Table 2.1) for 30 min before 1 h incubation in PBS and EIS interrogation.

Table 2.1 Lists of blocking reagents and working concentrations used in this experiment

Blocking reagents	Concentration
Bovine serum albumin (BSA)	0.1 μM
Sodium caseinate	100 $\mu\text{g/ml}$
Pyromellitic dianhydride	10 mM
mPEG-biotin, 5K	0.1, 1 and 3 mM

2.2.7.5 Modification of sensor fabrication protocol and optimisation

Sensors were made using the protocol in Section 2.2.7.2. However, previous blocking procedures (Table 2.1) did not prove effective as presented in Chapter 5. The following, new blocking procedure, modified from (Esseghaier et al., 2008) was tested. Briefly, after polytyramine electrodeposition on electrode surface, 3 μM NHS-biotin and 0.067 μM NeutrAvidin were utilised to modify polytyramine-coated working electrodes. Prior to conjugating Affimers onto the working electrodes, three blocking reagents, 6.7 μM BSA, 2x casein blocking buffer (Sigma-Aldrich) and 0.2 mg/ml sodium caseinate, were tested for their capability to minimise non-specific binding effects by incubating with the sensors for 30 min. The concentration of Affimer used was fixed at 1 μM . After EIS measurements and data analysis, the sensor responses were compared to select the best blocking reagent. In this case, 6.7 μM BSA was selected for optimising Affimer concentration for sensor construction.

In order to optimise Affimer concentrations, the sensors were made layer-by-layer using 3 μM NHS-biotin, 0.067 μM NeutrAvidin and 6.7 μM BSA. Affimers at the concentrations of 0.3, 1 and 3 μM were tested. The responses of the sensors were determined after exposing them to the analyte.

2.2.7.6 Sensors tested with negative control analytes

Sensors were constructed using the protocols described previously in Section 2.2.7.5. The sensors were tested against β -2-microglobulin (Sigma-Aldrich), human serum albumin (Sigma-Aldrich) and antidigoxin IgG. A range of negative control analyte concentrations was freshly prepared from 10^{-14} to 10^{-8} M by 10-fold dilution in 100 mM PBS pH 7.2. EIS measurements were performed as described in Section 2.2.7.3.

2.2.7.7 Effect of poly(sodium-p-styrenesulfonate) on sensor performance

To construct sensors, the methods in Section 2.2.7.2 were followed. The concentrations of NHS-biotin, NeutrAvidin and Affimers were kept constant at 3 μM , 0.067 μM and 1 μM , respectively. After Affimer attachment, either 1, 5 or 10 μM of poly(sodium-p-styrenesulfonate) was used to block the sensor chips for 30 min. The sensors were tested with various concentrations of FGFR3 as described in Section 2.2.7.3.

Chapter 3

Affimer screening and production

3.1 Introduction

In biosensing applications, biorecognition elements play a significant role in the overall performance of the platforms. The major prerequisite for bioreceptors is the specificity with which they bind to their target although the affinity with which they bind their target governs the sensitivity of the device. During the past decades, antibodies have been widely used thanks to their specific recognition nature to the targets. However, large size and batch-to-batch variations make antibodies troublesome in many biosensor applications.

Non-antibody binding scaffolds have been considered as an alternative to antibodies as they offer some advantages. They include small size, high temperature stability and ease of production. The Affimer is a non-antibody binding protein developed for a number of applications (Tiede et al., 2017). Selection of Affimers is conveniently conducted via phage display screening, and with the library complexity of $> 10^{10}$ distinct clones (Tiede et al., 2014), Affimers are applicable to a wide range of targets, from small molecules to large proteins (Tiede et al., 2017).

This section is mainly focused on the screening and production of Affimers via the phage display library provided by the BioScreening Technology Group (BSTG). Dichlorodiphenyltrichloroethane (DDT) was initially selected as a model analyte for Affimer screening and represents a small molecule target and remains an important pesticide for malaria vector control. The protein target chosen was fibroblast growth factor receptor 3 (FGFR3) which is a promising biomarker for bladder cancer (Tomlinson et al., 2007). The chosen Affimer-encoding sequences were subcloned into a pET expression vector to allow the Affimers to be produced in

E.coli. In the production steps, DDT Affimers and FGFR3 Affimers were expressed and purified for further use.

3.2 DDT Affimer screening

The core structure of the Affimers is based on the consensus sequence of plant-derived phytocystatins (Tiede et al., 2014). To obtain Affimers recognising the targets of interest, the BioScreening Technology Group (BSTG) at University of Leeds screened the Affimer phage display library with the complexity of approximately 1.3×10^{10} distinct clones presenting two variable peptide regions with 18 random amino acid residues (Tiede et al., 2014).

3.2.1 Preparation of biotinylated DDT as a target for phage display screening

In this section, dichlorodiphenyltrichloroethane (DDT), a widely used insecticide for agriculture and malaria control, was chosen as the target of interest for Affimer screening. Basically, the targets of interest are required to be biotinylated first in order to allow immobilisation by streptavidin-biotin interaction prior to the screening steps.

Biotinylated DDT was synthesised and provided by Dr. Hanafy Ismail from the Liverpool School of Tropical Medicine. The original structure of DDT does not contain any functional groups that are useful for further modification and a carboxylic group was introduced into the structure of DDT. Then, a short spacer and biotin were linked to the DDT analogue. The resulting biotinylated DDT analogue was then attached to streptavidin-coated surfaces (Figure 3.1).

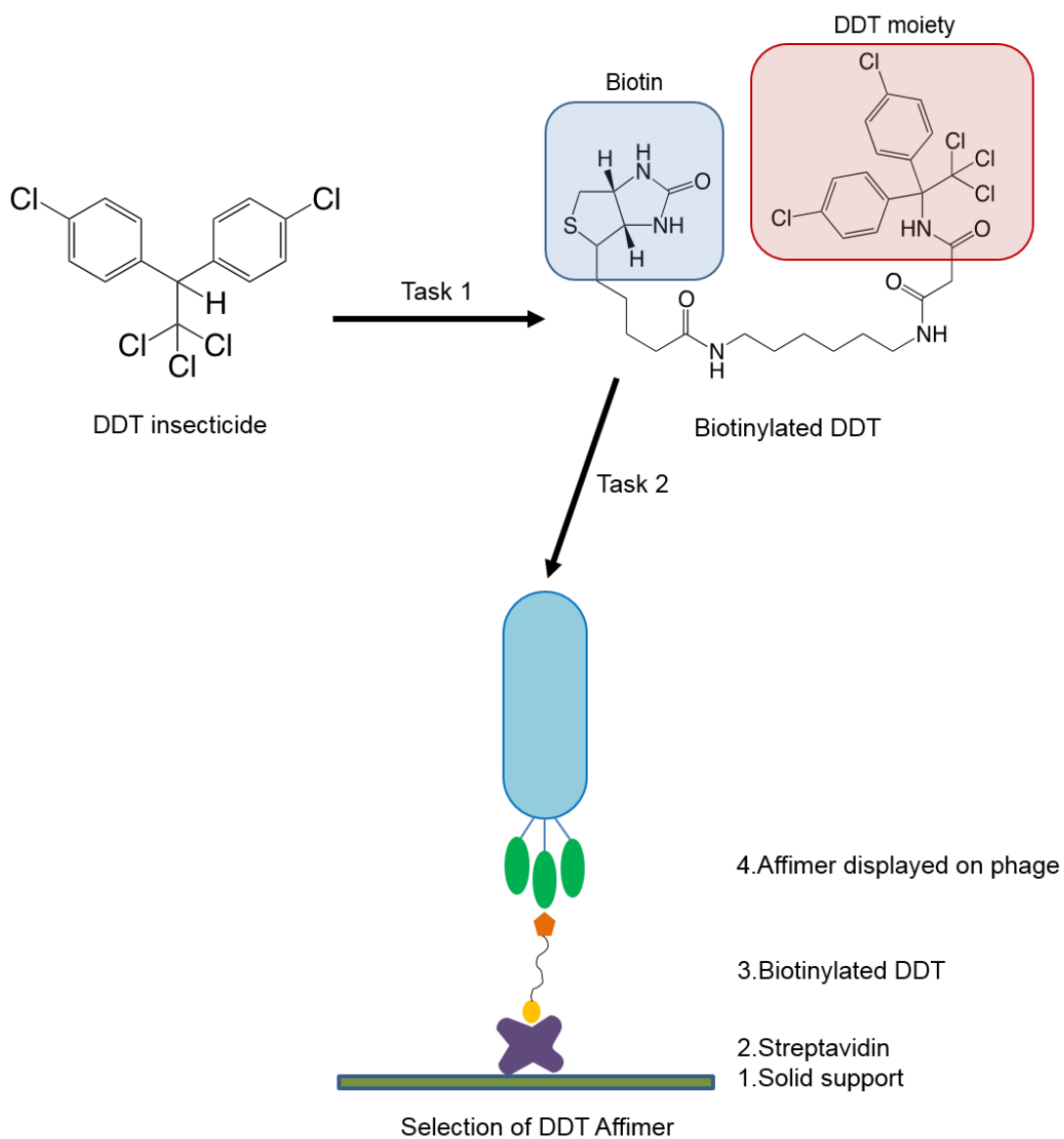


Figure 3.1 A schematic representation of Affimer screening. DDT is biotinylated prior to use for Affimer selection. The selection can be performed via phage display screening.

3.2.2 Phage display screening

DDT was selected as an analyte to screen for the Affimers in this study. Biotinylated DDT was immobilised onto a streptavidin-coated plate before phage presenting Affimers were added. After incubation for one hour, unbound phage were washed out and only phage with the Affimers binding to the DDT moiety still remained. Acid and alkaline buffers were then used to elute the remaining phage. In order to elute the remaining phage, it was suggested that the non-biotinylated form of analytes could be used, allowing Affimers binding specifically to the analytes to be selected. An example of this type of elution is using imidazole to elute His₆-tagged proteins from Ni²⁺-NTA coated resin as presented in Section 2.2.4. However, because of the fact that DDT is insoluble in water, it is impossible to prepare high concentration stock of DDT in water-based solvents such as PBS to be used as elution buffer. These phage were then used to infect *E.coli* strain ER2738, which allows the phagemid to amplify exponentially. The *E.coli* cells were then infected with M13K07 helper phage. This step is vital since the helper phage provides the necessary components for phage assembly and secretion. Three panning rounds were performed. However, during the second and final panning rounds, non-biotinylated DDT was added to perform competitive selection. The reason for the use of competitive selection is the strong binders with fast association and slow dissociation for the target of interest can be picked from a pool of other binders. After the final panning, 48 colonies of *E.coli* were randomly selected for the phage ELISA (Figure 3.2).

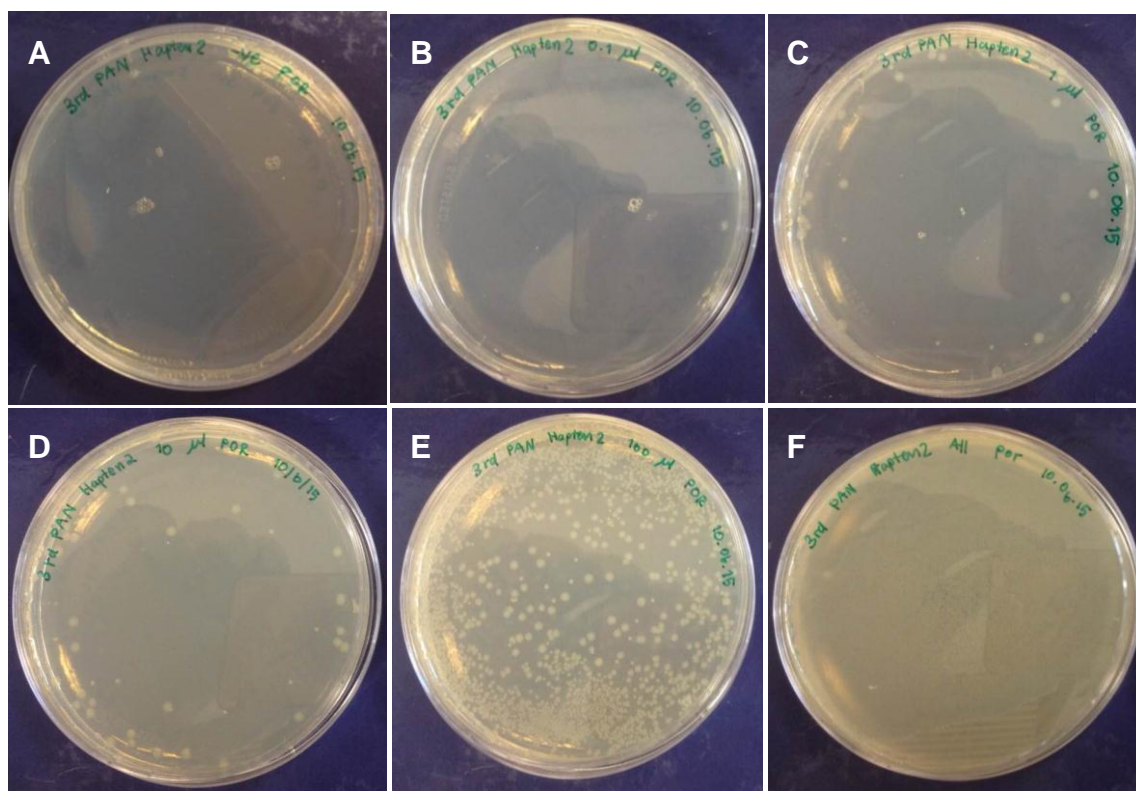


Figure 3.2 ER2738 *E.coli* cells growing on LB-carbenicillin (carb) plates after the third competitive panning for DDT Affimer selection. The LB carb plates were spread with (A) ER2738 cells without infection with phage, (B-F) ER2738 cells inoculated with 0.1, 1, 10, 100 μ l and remaining suspension of selected phage, respectively. Forty eight colonies from the plates in C, D and E were randomly picked and used in the phage ELISA step.

3.2.3 Phage ELISA

Forty eight single colonies of *E.coli* containing phagemid vectors were randomly picked and cultured. They were then infected with M13K07 helper phage to help form the phagemid presenting Affimers specific for DDT. To do phage ELISA, biotinylated DDT was captured on a streptavidin-coated plate, following by phage-containing suspension. The binding between biotinylated DDT and Affimers presented on the phage was examined using anti-Fd-bacteriophage-HRP. The results were revealed after adding a solution of 3,3',5,5'-tetramethylbenzidine, which is a substrate for HRP enzyme. Figure 2.5 shows the ELISA 96-well plate, where wells A1 to H6 with biotinylated DDT were immobilised and wells A7 to H12 were negative controls. The Affimer in well A1 had a negative control in well A7 and similarly for the other Affimers. Out of 48 selected clones, 46 clones showed specific binding to biotinylated DDT and none of the clones showed non-specific binding in the control wells (Figure 3.3). The clones showing positive results were selected and prepared for sequencing.

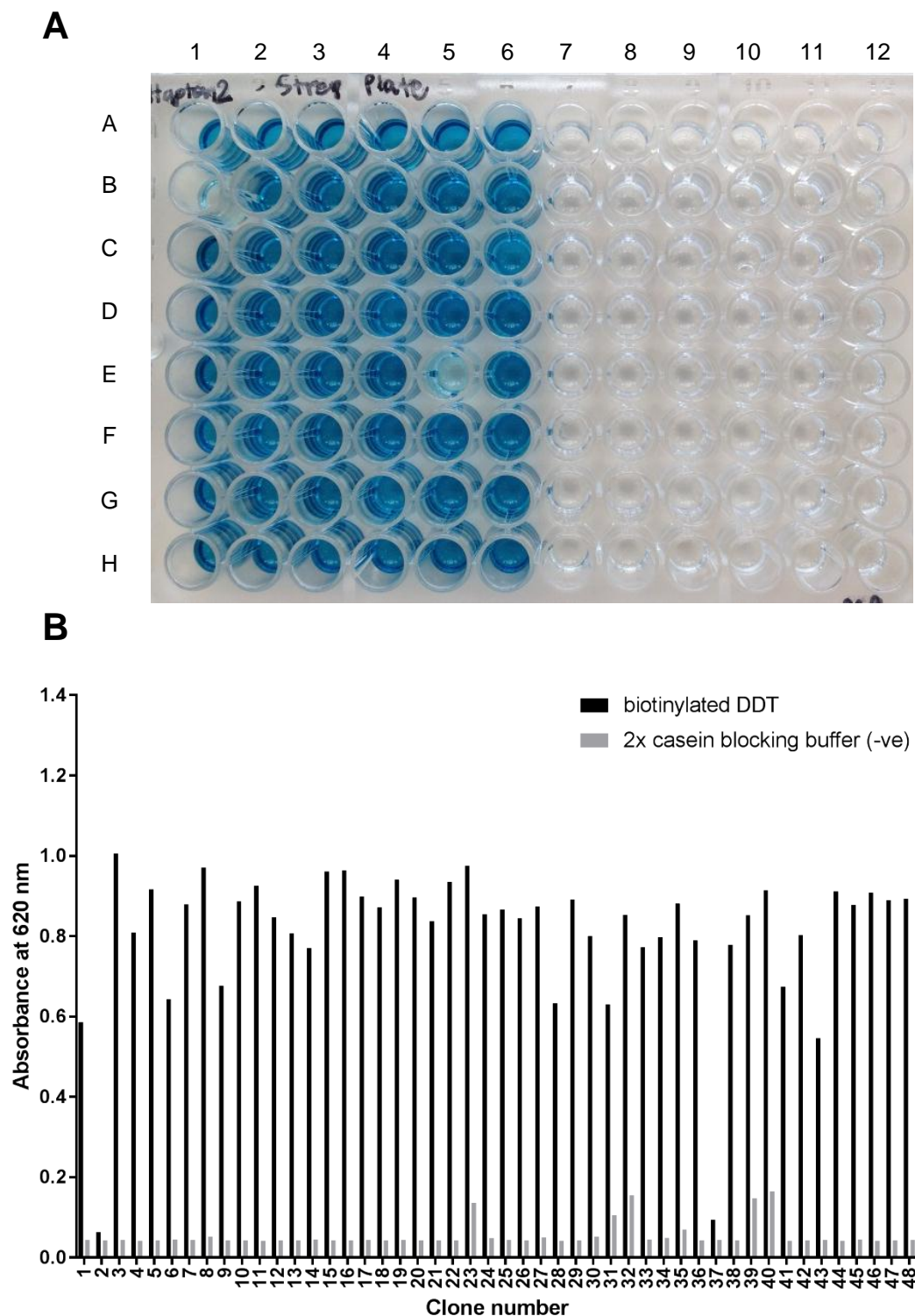


Figure 3.3 Phage ELISA results showing 46 out of 48 clones of Affimers presenting on the coat of M13 phage bound specifically to biotinylated DDT. (A) The ELISA 96-well plate after TMB substrate was added, the blue product was generated in the wells with phage presenting Affimers capable of binding to biotinylated DDT. (B) Absorbance at 620 nm showing the binding of 48 selected Affimers to biotinylated DDT.

3.2.4 Affimer sequencing and sequence alignment

The phagemid vectors of the 46 positive clones of DDT Affimers were prepared and sent for sequencing with the assistance of GENEWIZ Genomics, UK. The nucleotide sequences were obtained and translated to amino acid sequences using ExPASy translate tool (<https://web.expasy.org/translate/>). Amino acid sequences of each Affimer clone were aligned using Clustal Omega available on EMBL-EBI.

Out of 46 positive clones, 34 clones contained full-length functional sequences (the core structure and the variable peptide regions). The 34 functional clones showed 16 different patterns of amino acid sequence in the variable peptide loops. Interestingly, amongst the 16 unique patterns found, only clone H25 contained two variable peptide regions whereas the other Affimers showed only one inserted variable peptide loop (Figure 3.4 and 3.5). In order to produce the Affimers, eight clones, H8, H10, H18, H23, H25, H27, H38 and H39, were selected for further experiments. The clone selection was based on the variation in types of amino acids (non-polar/neutral, polar/neutral, acid/polar and basic/polar) found within the binding loop(s). For example, if two Affimers clones showed a similar pattern in the types of amino acid, one was arbitrarily selected as similar interactions of both Affimers with DDT could be expected. However, if two Affimers presented a different pattern of amino acid types in the binding loop(s), both of them were chosen for further investigation. By this means of selection, a workable number of eight Affimers was obtained.

```

1           _____M_K_K_I_W_L_A_L_____
1 TAGCTTGCTGCCAATTCTATTTTCAGGAGACAGTCATAATGAAAAAGATTTGGTTGGCTCT
9  _A_G_L_V_L_A_F_S_A_S_A_S_A_A_T_G_V_R_A_V_
61 GGCTGGTCTGGTTCTGGCGTTTTCTGCGTCTGCTAGCGCCGCTACCGGTGTTTCGTGCAGT
29  _P_G_N_E_N_S_L_E_I_E_E_L_A_R_F_A_V_D_E_H_
121 TCCGGGTAACGAAAACCTCCCTGGAAATCGAAGAACTGGCTCGTTTCGCTGTTGACGAACA
49  _N_K_K_E_N_A_L_L_E_F_V_R_V_V_K_A_K_E_Q_W_
181 CAACAAAAAAGAAAACGCTCTGCTGGAATTCGTTTCGTGTTGTTAAAGCGAAAGAACAGTG
69  T_E_Y_K_P_V_Y_A T_M_Y_Y_L_T_L_E_A_K_D_G_
241 GACTGAATACAAACCGGTTTACGCTACCATGTACTACCTGACCCTGGAAGCTAAAGACGG
89  _G_K_K_K_L_Y_E_A_K_V_W_V_K_ A_K_H_V_H_L_L
301 TGGTAAAAAGAAACTGTACGAAGCGAAAGTTTGGGTTAAGGCAAACATGTTTCATCTGCT
109 T_Q N_F_K_E_L_Q_E_F_K_P_V_G_D_A_A_A_A_H_
361 GACCCAGAACTTCAAAGAACTGCAGGAGTTCAAACCGGTTGGTGACGCTGCGGCCGCGCA
129  _H_H_H_H_H_*_____
421 TCACCATCATCACCCTAGGGTAACGGTGGTGGTAACGGTAACTCTGGTGGTGGTTCTGG

```

Figure 3.4 Nucleotide and amino acid sequences of H25 Affimer. H25 is selected as a representative to show the full-length Affimer sequence as it is the only selected Affimer presenting two variable peptide regions. The sequences highlighted in blue represent insertion region 1 and the ones highlighted in red show insertion region 2.

	Loop 1	Loop 2		Number of identical clones selected (clones)
H25	-----WTEYKPVYA-----	-----AKHVHLLTQ-----	120	1
H1	-----TDRILPPDI-----	-----KK-----	109	3
H7	-----SYARSMVVD-----	-----NF-----	109	1
H10	-----PDSRSDLYN-----	-----KF-----	109	3
H8	-----NIYMDYERN-----	-----YY-----	109	1
H40	-----RYMTPEEQN-----	-----KF-----	109	1
H27	-----YFVTNSETN-----	-----HY-----	109	6
H39	-----YFNSDVEQN-----	-----HW-----	109	2
H21	-----LKIRQEETN-----	-----HW-----	109	1
H14	-----EYEGFNEVN-----	-----EW-----	109	1
H23	-----AHPARYEKN-----	-----HW-----	109	2
H38	-----RYPLRSEKN-----	-----YW-----	109	2
H18	-----EFLDGPYST-----	-----QY-----	109	6
H2	-----NYEQEPYHN-----	-----LY-----	109	1
H24	-----IHFEGQYPM-----	-----KY-----	109	1
H29	-----QVAEGQYHN-----	-----LF-----	109	1

Figure 3.5 Amino acid sequences of 16 selected Affimers against DDT. The figure shows the amino acid sequences at two variable peptide regions. Only the H25 Affimer has two complete loops whereas the others have one loop. The number of identical clones for each Affimer is also presented.

3.3 Subcloning of anti-DDT Affimer-encoding sequences into pET11a expression vector

The phagemid vectors containing Affimer-encoding sequences cannot be used for protein expression in *E.coli*. The Affimer-encoding sequences needed to be subcloned into an expression vector such as pET11a in order to enable efficient expression of the Affimers in bacteria.

3.3.1 Digestion of pET11a with *NotI/NheI* restriction enzymes

The pET system is a powerful system developed for subcloning and expression of proteins of interest in *E.coli*. The pET11a vector used in this study contains the pBR322 origin of replication, which allows it to replicate in *E.coli* cells (Figure 3.6). It also has an ampicillin resistance gene, which can be used as a selectable marker for identifying the *E.coli* cells accepting the pET11a vectors. Finally, there is a T7 promoter site which is the recognition site for T7 RNA polymerase and a His₈ tag encoding region that allows purification of the Affimers conveniently, using Ni²⁺-NTA resin.

The pET11a vector was digested with two restriction enzymes, *NotI* and *NheI* before separating with 0.7% (w/v) agarose gel electrophoresis (Figure 3.7). In the lane of uncut pET11a, there were three bands of plasmid appearing on the gel. This is because the open circular or nicked form of plasmid migrates slowly. Therefore, it appeared on the top of the gel. The plasmid can also exist in supercoiled form. As the nature of supercoiled plasmids is compact, this makes them migrate faster than the open circular ones. Thus, the supercoiled forms (the lowest band in pET11a uncut lane) were visualised below the nicked circle form (the highest band in pET11a uncut lane). The middle band in pET11a uncut lane represents the plasmid in its linear form, which could be due to nuclease contamination or harsh treatment during the

purification process. In the *NheI/NotI* digested plasmid lane, two bands appeared. With excess plasmid before digestion, the restriction enzymes could not digest the plasmid completely. The digested plasmids are linear, which allows them to migrate more rapidly than the intact, circular form of the plasmids. The digested pET11a band was excised from the gel and purified to use for the further steps of subcloning.

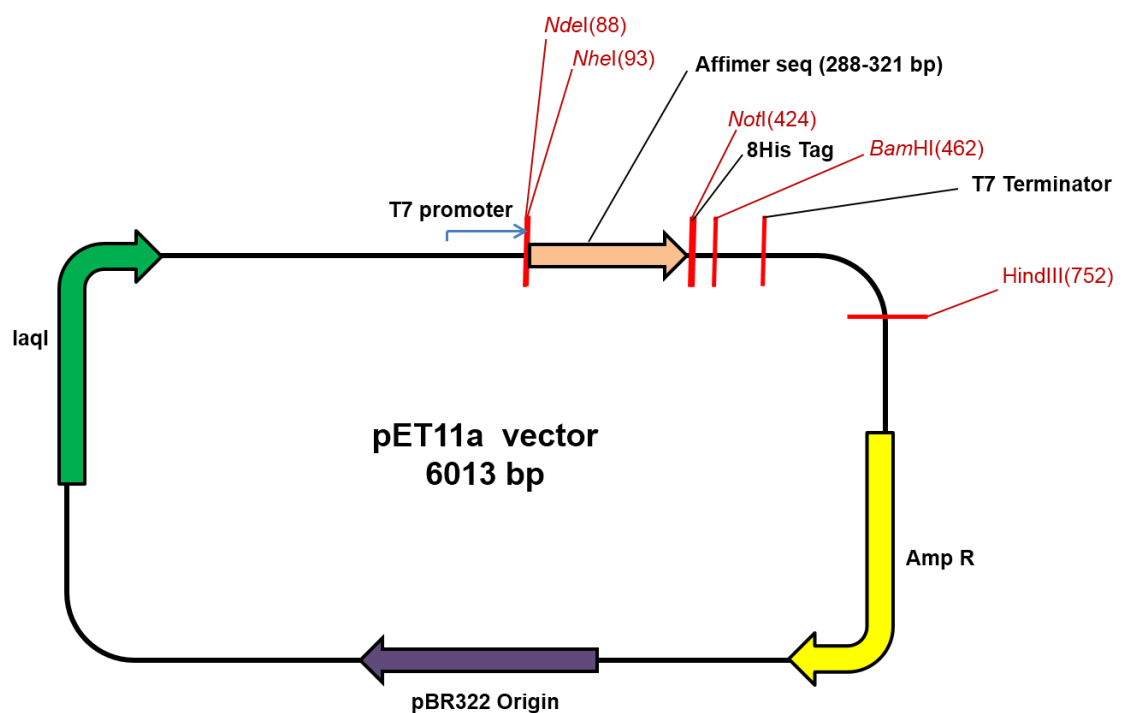


Figure 3.6 The map of pET11a expression vector. The vector contains *NotI* and *NheI* restriction sites, T7 promoter for T7 RNA polymerase, eight histidine residue region, and ampicillin resistance gene for selection and pBR322 origin of replication.

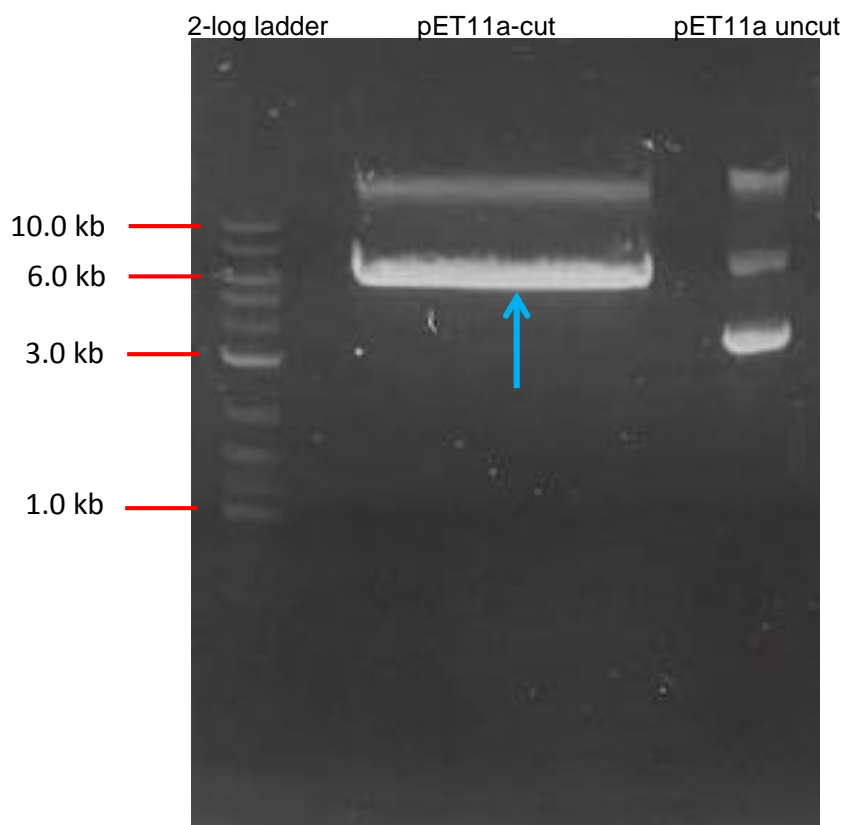


Figure 3.7 The pET11a plasmid digested with *NotI* and *NheI* enzymes. The digested products were separated using 0.7% (w/v) agarose gel electrophoresis in 1x TAE buffer system. The DNA marker in the first lane is 2-log ladder marker (NEB). The arrow (→) indicates the digested pET11a vector, which was cut out for the further use.

3.3.2 Polymerase chain reaction (PCR) amplification of Affimer-encoding sequences

PCR was used to multiply Affimer-encoding sequences selected previously from the phage display technique. In the PCR reaction, phagemid vectors for eight selected clones of Affimers against biotinylated DDT were used as DNA templates. The forward primer was designed using the nucleotide sequence located at the upstream region of the Affimer sequence including *NheI* restriction site on the phagemid vector whereas the reverse primer was positioned covering *NotI* restriction site. Additionally, the codon for cysteine was introduced into the reverse primer in order to introduce a specific site for chemical modifications.

The PCR products were examined using 0.7% (w/v) agarose gel electrophoresis as shown in Figure 3.8. The bands with the molecular size > 1000 bp represented the phagemid templates in both circular and supercoiled forms. The bands with the molecular sizes < 500 bp were PCR fragments of Affimer-encoding sequences, which were used in further experiments.

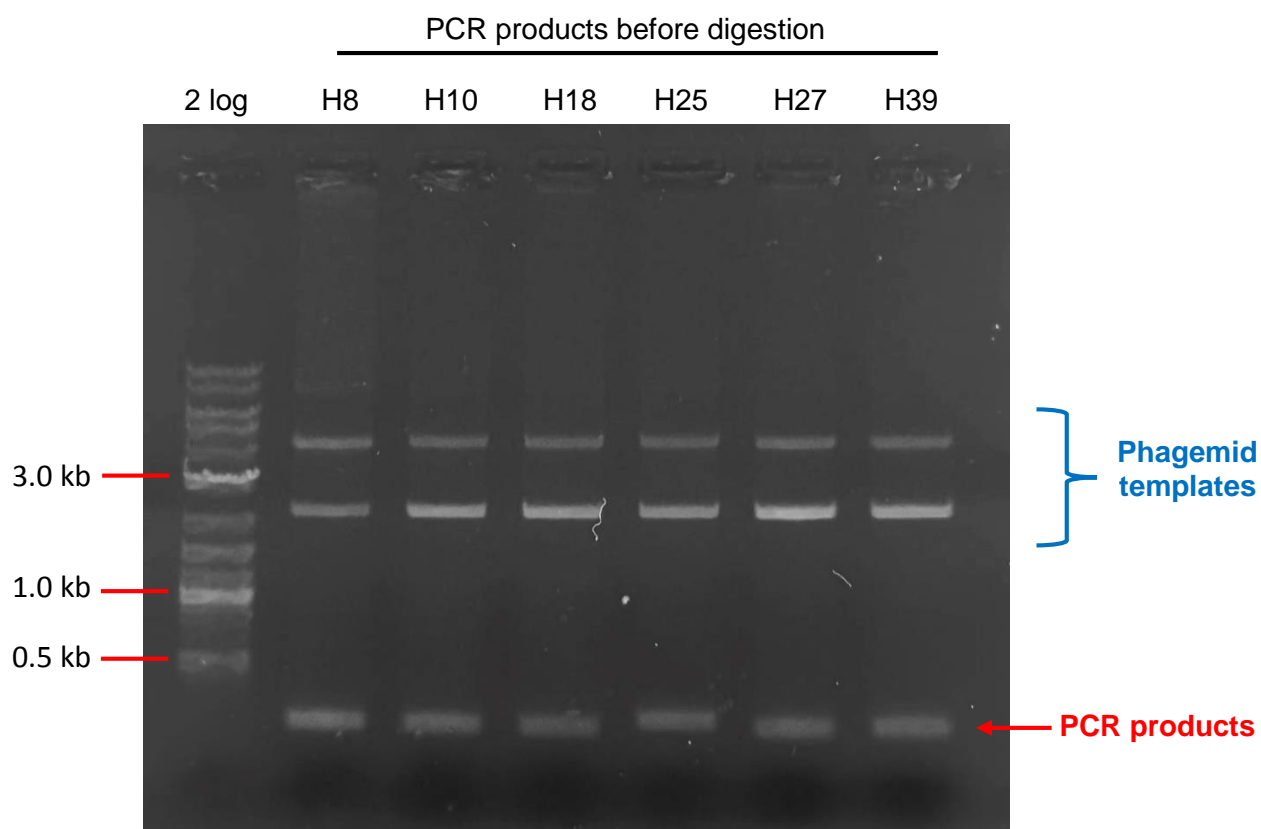


Figure 3.8 PCR products before the reactions were treated with *NotI/NheI* and *DpnI* enzymes. The products were separated using 0.7% (w/v) agarose gel electrophoresis in 1x TAE buffer system and stained with ethidium bromide. The DNA marker is 2-log ladder marker (NEB). The red arrow indicates Affimer-encoding sequence PCR fragments. The blue bracket indicates phagemid vector templates.

3.3.3 Digestion of PCR fragments using *NotI/NheI* and *DpnI* enzymes

Prior to ligation with the pET11a vector, the Affimer-encoding PCR fragments needed to be digested with the same restriction enzymes used to prepare the digested pET11a plasmid. PCR products were digested with *NotI* and *NheI* overnight to ensure that both ends of the PCR fragments were able to link with the sticky ends of the pET11a vector. After *NotI/NheI* digestion of PCR fragments, it was essential for the reactions to be treated with *DpnI* enzyme. This enzyme has the unique property of digesting *dam* methylated DNA templates. In this research, during the PCR amplification, the concentrated and diluted (1:30 ratio) phagemid vectors were studied as the appropriate templates for PCR. Figure 3.9 showed that when using the concentrated phagemid templates for PCR, *DpnI* was not able to digest all of the template and there was remaining template left in the reactions. However, when the phagemid template was diluted before PCR, the *DpnI* digestion was complete and none of the template was left. This is an important step since the remaining phagemid fragments could possibly compete with the Affimer sequence fragments during ligation, resulting in the expression vectors with unexpected sequences. Therefore, the digested PCR fragments amplified from the diluted template reactions were used for ligation.

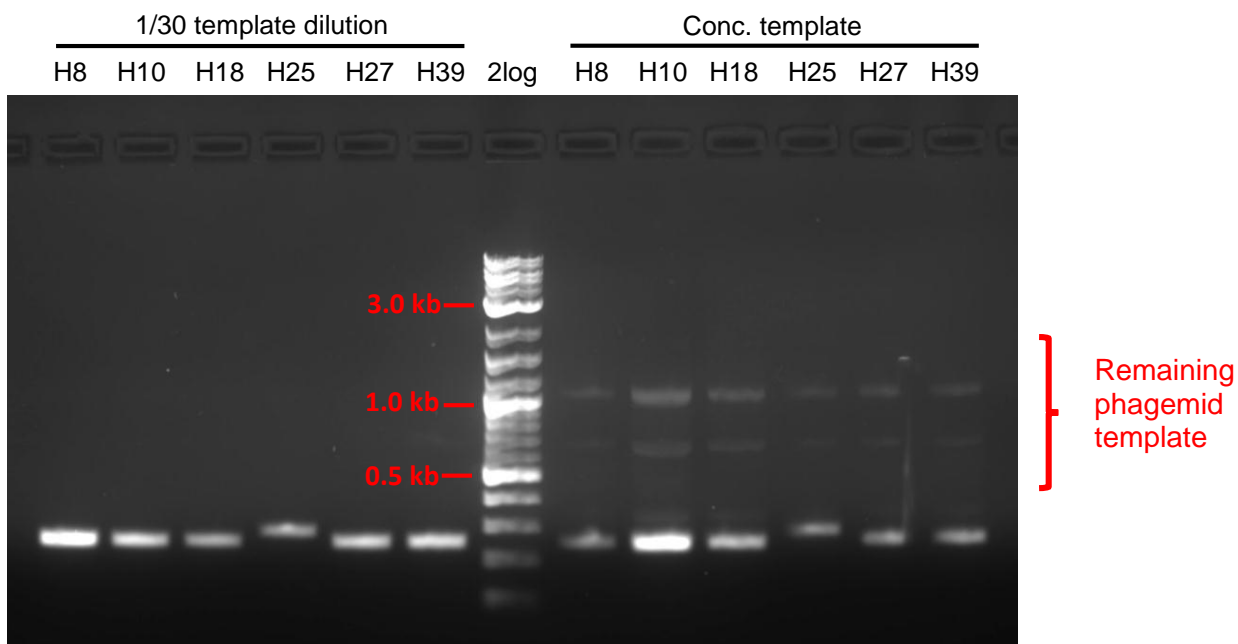


Figure 3.9 PCR products after the reactions were treated with *NotI/NheI* and DpnI. The phagemid templates were completely digested by DpnI when 1:30 dilution of the template was used. The products were separated using 1.4% (w/v) agarose gel electrophoresis in 1x TAE buffer system. The DNA marker is 2-log ladder marker (NEB). The red bracket indicates the remaining phagemid template after digestion.

3.3.4 Ligation and transformation

Ligation was performed in order to join a fragment of PCR product and a plasmid vector together. Prior to ligation, digested pET11a vector and PCR fragments of Affimer-encoding genes were run through a 1.4% (w/v) agarose gel to see if correct products were present (Figure 3.10). The band of 6000 bp on the second lane indicated the digested pET11a plasmid whereas the bands with molecular size around 300 bp in lanes 3-8 indicated the Affimer sequence fragments. In the ligation reaction, a PCR product and the pET11a vector were mixed with the ratio of 1:3 (w/w) (Figure 3.11). After the overnight ligation, the ligated pET11a vectors containing Affimer-encoding sequences were transformed into XL1 Blue *E.coli* competent cells using the heat-shock method. The transformed cells were grown overnight on LB agar media added with carbenicillin as an antibiotic for the selection. The colonies growing on the plates (Figure 3.12) were randomly selected for colony PCR and sequencing to check the successful ligation of expression vectors.

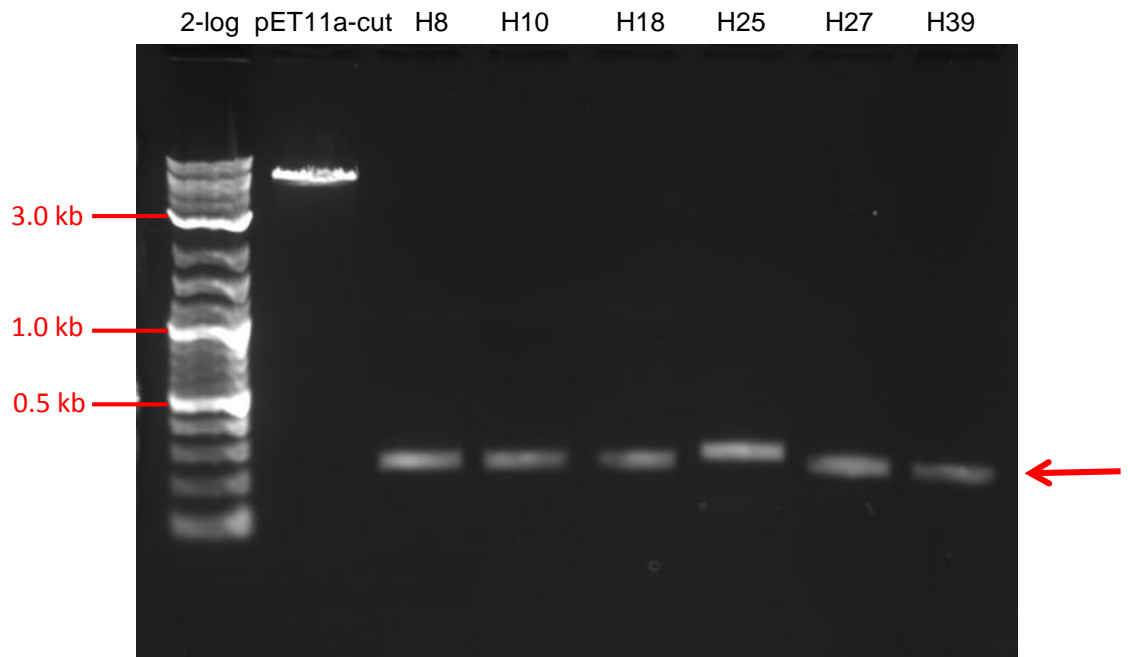


Figure 3.10 Digested pET11a vector and PCR products of genes encoding Affimers prepared for ligation. The products were separated using 1.4% (w/v) agarose gel electrophoresis in 1x TAE buffer system. The DNA marker is 2-log ladder marker (NEB). The arrow (→) indicates Affimer encoding fragments.

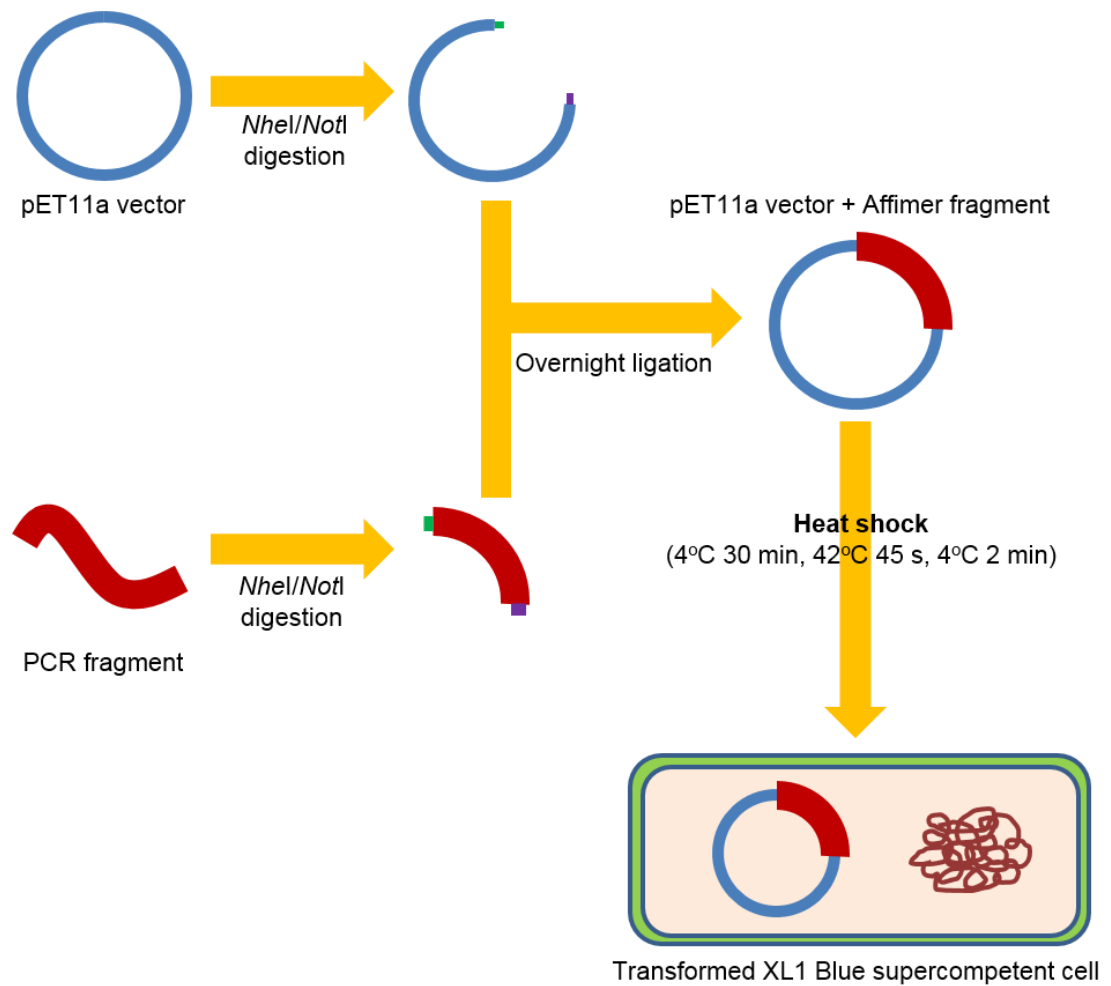


Figure 3.11 A schematic representation of ligation and transformation of a pET11a expression vector containing an Affimer-encoding sequence. Both pET11a vector and Affimer fragment are digested with *NheI* and *NotI* in order to allow the ligation between the vector and the PCR fragment. The resulting pET11a vector containing an Affimer sequence is transformed into an XL1 Blue *E.coli* cell using heat-shock method.

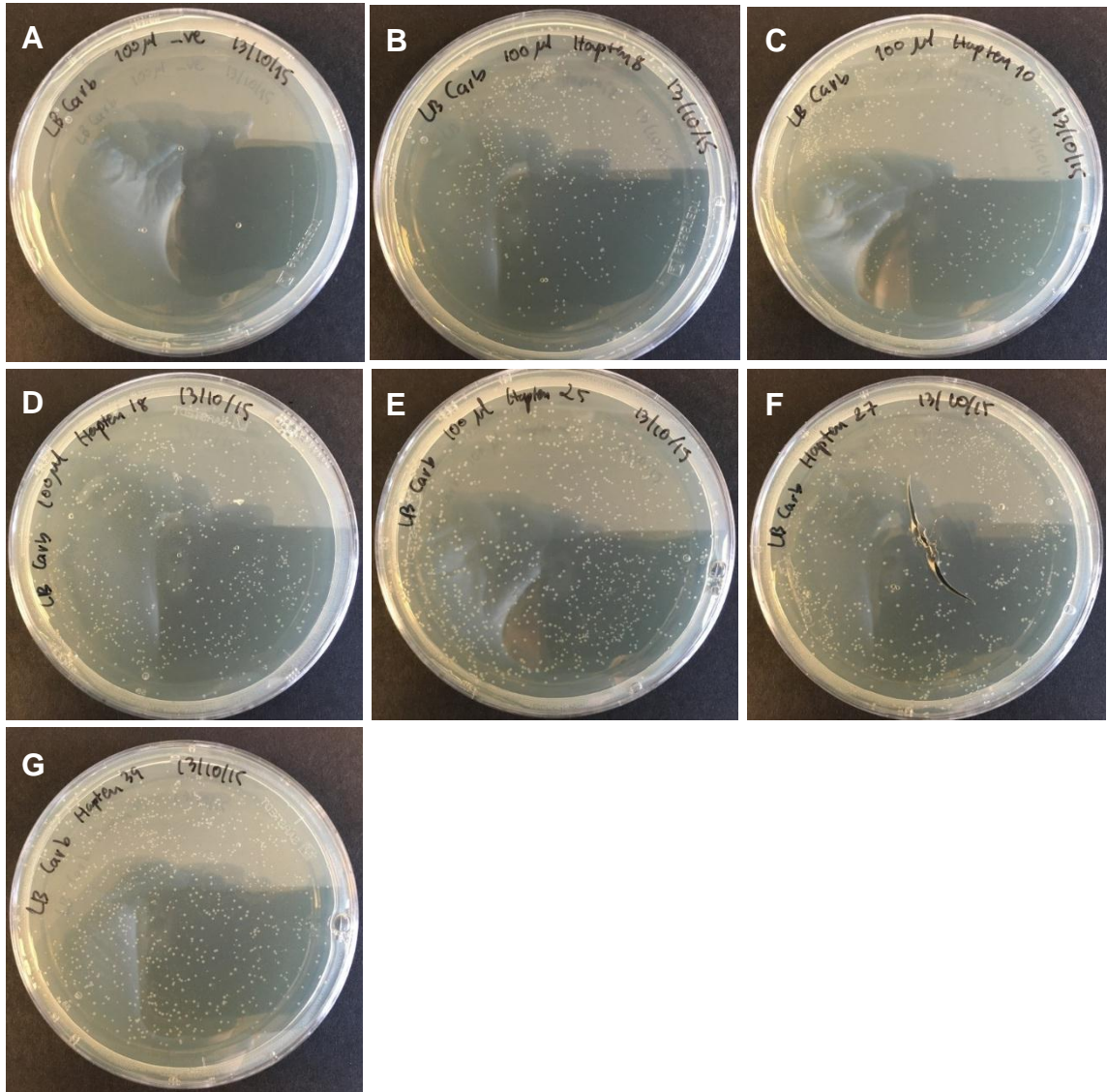


Figure 3.12 XL1 Blue *E.coli* cells containing Affimer-encoding genes growing on LB carb plates. The plates were spread with (A) *E.coli* without pET11a vector (negative control) and (B – G) *E.coli* transformed with pET11a vector containing the sequences of Affimer H8, H10, H18, H25, H27 and H39, respectively. Three colonies for each clone were randomly selected for colony PCR to check the success of insertion of Affimer-encoding gene fragments into pET11a vectors.

3.3.5 Colony PCR

To confirm the successful insertion of Affimer-encoding sequences into the pET11a expression vector, colony PCR was conducted. Five single colonies of transformed *E.coli* for each clone of Affimers were randomly picked as templates for PCR. The primers used for the PCR reaction were the same as in the subcloning step. The PCR products were separated using 1.4% (w/v) agarose gel electrophoresis and stained with ethidium bromide. Figure 3.13 revealed that out of all the bacterial colonies picked from the plates, some colonies had the pET11a vector containing Affimer sequences, in which 300-bp fragments were visualized. However, the other colonies did not show 300-bp bands, suggesting that there was no inserted Affimer sequence.

In order to confirm the correct Affimer sequences and the successful addition of a cysteine residue, sequencing was required. The bacterial cells showing positive detection on colony PCR were cultured in LB media containing carbenicillin and the plasmids were then extracted from the cells. The plasmids were sent for sequencing by GENEWIZ Genomics, UK.

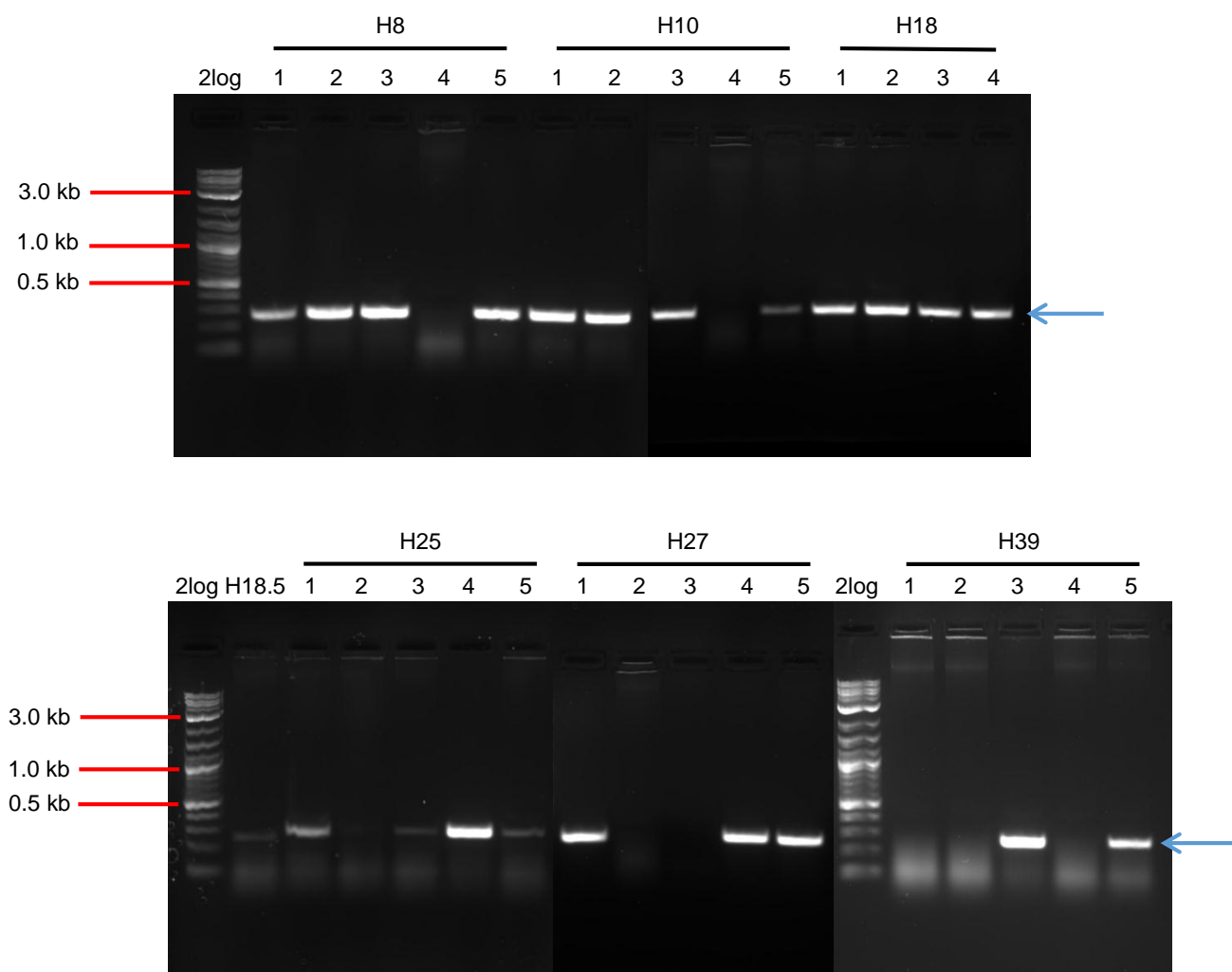


Figure 3.13 Colony PCR was performed in order to check the success of inserting Affimer-encoding sequences into pET11a vectors. The PCR products were separated using 1.4% (w/v) gel electrophoresis in 1x TAE buffer. The 300-bp PCR bands representing the Affimer-encoding genes are indicated by the arrows (\rightarrow). The positive colonies were selected for sequencing. The DNA marker is 2-log ladder marker (NEB).

3.3.6 Sequencing and alignment

Sequencing and alignment were the approaches used to confirm the correct nucleotide and amino acid sequences. The nucleotide sequences obtained from GENEWIZ Genomics, UK were translated to amino acid sequences using the Translate tool supplied by ExPASy. The amino acid sequences were then aligned with the same Affimer-encoding sequences from phagemid vectors using online Clustal Omega supplied by EMBL-EBI. Figure 3.14 shows the result of amino acid sequence alignment of H25 Affimer sequences from pET11a vector compared with the same Affimer from the phagemid vector. The core structure of the Affimer was almost identical except for the addition of a cysteine residue and the missing amino acids at N-terminus of the Affimer from the phagemid, which represents a part of the DsbAss signal sequence. The additional cysteine was useful because it provides a single –SH group for further modifications so that the orientation of the Affimers can be controlled.

To this point, the pET11a expression vectors carrying the nucleotide sequences for H8, H10, H18, H23, H25, H27, H38 and H39 Affimers were constructed. Affimer clone H25 contains two variable peptide regions whereas the others have only one inserted loop (Table 3.1). The expression vectors containing Affimer sequences were used for Affimer production which was described in the following sections.

```

H25_phagemid      MKKIWLALAGLVLAFSASASAATGVRVAVPGNENSLEIEELARFAVDEHNKKENALLEFVR  60
H25_1             -----MASNSLEIEELARFAVDEHNKKENALLEFVR  31
H25_4             -----MASNSLEIEELARFAVDEHNKKENALLEFVR  31
                  .*****

H25_phagemid      VVKAKEQWTEYKPVYATMYYLTLLEAKDGGKKKLYEAKVWVKAKHVHLLTQNFKELQEFKP  120
H25_1             VVKAKEQWTEYKPVYATMYYLTLLEAKDGGKKKLYEAKVWVKAKHVHLLTQNFKELQEFKP  91
H25_4             VVKAKEQWTEYKPVYATMYYLTLLEAKDGGKKKLYEAKVWVKAKHVHLLTQNFKELQEFKP  91
                  *****

H25_phagemid      VGDAAAHHHHHH---  133
H25_1             VGDACAAAHHHHHHHH  107
H25_4             VGDACAAAHHHHHHHH  107
                  ****. ** *****
                  ↑

```

Figure 3.14 Sequence alignment of H25 Affimer obtained from pET11a vector and the H25 Affimer obtained from phagemid vector. The red-highlighted region indicates the variable peptide loop 1 whereas the blue-highlighted region indicates the loop 2. The green arrow (→) shows the position of the introduced cysteine addition.

Table 3.1 Amino acid sequences at variable peptide loops 1 and 2 of eight selected Affimers against DDT. Only H25 contains two complete loops whereas the other clones have one inserted loop.

Clone number	Sequence of loop 1	Sequence of loop 2
H8	NIYMDYERN	-
H10	PDSRSDLYN	-
H18	EFLDGPYST	-
H23	AHPARYEKN	-
H25	WTEYKPVYA	AKHVHLLTQ
H27	YFVTNSETN	-
H38	RYPLRSEKN	-
H39	YFNSDVEQN	-

3.4 Production of Affimers against DDT

As well as other alternative binding protein scaffolds, one of the advantages of Affimers that make them an alternative to antibodies is that production can be carried out in bacterial system. By doing this, any batch-to-batch variation issues can be minimised. The results of anti-DDT Affimer production are described in the following section.

3.4.1 Affimer expression

Affimer expression was carried out using an established protocol developed by the BioScreening Technology Group (BSTG) at Leeds as described in Section 2.2.4. BL21-Gold (DE3) *E.coli* competent cells, a T7 promoter-driven expression system, were selected for Affimer production. pET11a plasmids carrying Affimer-encoding sequences were transformed into the *E.coli* cells. A single colony growing on a LB media plate containing carbenicillin was picked for making a start-up culture. The overnight culture containing bacteria was then transferred to 50 ml LB media containing carbenicillin to make a fresh culture of bacteria for induction. After 2.5 hours of incubation, the induction was started by adding 0.5 mM IPTG into the growing bacterial culture and incubation continued for 6 h. The *E.coli* cells containing Affimer were then harvested by centrifugation at 3,220 xg for 30 min and the Affimers were then extracted and purified.

3.4.2 Affimer purification

By following the procedure in Section 2.2.4.3, purification of the Affimer was conducted using Ni²⁺-NTA chromatography as the Affimers contain eight consecutive His residues at the C-terminus. The harvested bacterial cells were lysed in lysis buffer comprising 50 mM NaH₂PO₄, 300 mM NaCl, 30 mM imidazole, 10% (v/v) glycerol, pH 7.4, plus 1x BugBuster Protein Extraction Reagent, 10 units/ml Benzonase Nuclease and 1x Halt Protease Inhibitor Cocktail to allow protein release. The lysates were then centrifuged to remove cell debris and insoluble proteins. The supernatant containing Affimer was mixed with Ni²⁺-NTA resin. The resin mix was washed several times with wash buffer containing 50 mM NaH₂PO₄, 500 mM NaCl, 30 mM imidazole, 10% (v/v) glycerol, pH 7.4 to eliminate remaining unbound proteins using gravity flow. The Affimers were subsequently eluted from the resin using elution buffer containing 50 mM NaH₂PO₄, 500 mM NaCl, 300 mM imidazole, 20% (v/v) glycerol, pH 7.4.

In order to confirm the presence of Affimer after purification, SDS-PAGE was used (Figure 3.15). For each Affimer, five consecutive eluted fractions containing Affimers were run through a 4-15% (w/v) SDS-PAGE gel, alongside cell lysate and an unbound protein fraction. The data showed the migrated protein bands in lanes E1 to E5 with M_r between 10 – 15 kDa, indicating the correct Affimer size. Other proteins could not be detected in the lanes of Affimers, suggesting that the purity of the Affimer was sufficient for use in further experiments. The Affimer was then dialysed as recommended in Section 2.2.4.5 to eliminate imidazole before use.

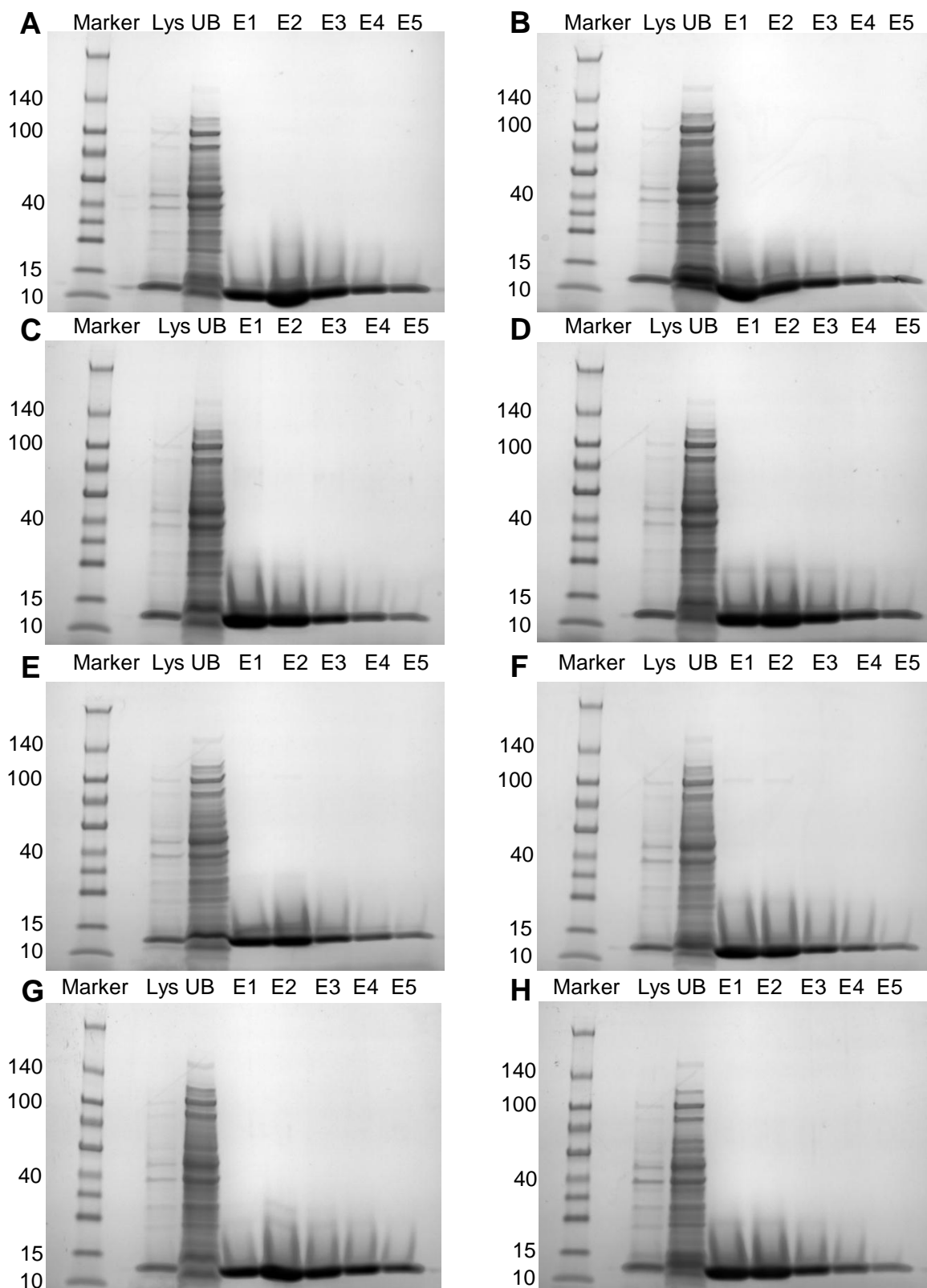


Figure 3.15 SDS-PAGE gels of purified anti-DDT Affimers. (A) – (H) the gels showing H8, H10, H18, H23, H25, H27, H38 and H39 Affimers, respectively. The protein markers are Spectra™ multicolour broad range protein ladder (ThermoFisher Scientific) in kDa unit. (Lys) is lysate fraction, (UB) is unbound protein fraction, (E1-E5) are purified Affimer fractions 1-5, respectively.

3.5 Production of Affimers against FGFR3

In addition to DDT Affimers, Affimers specific to FGFR3 were also produced. FGFR3 is a protein in fibroblast growth factor receptor (FGFR) family, whose overexpression appears to be correlated with bladder cancer occurrence. The production of Affimers specific to FGFR3 may be beneficial for the researchers who would like to study the potential of FGFR3 as a biomarker for detection bladder cancer at the early stages. The FGFR3 Affimers were previously selected and subcloned by Dr. Nidhi Lal as part of another project.

3.5.1 Affimer screening from the phage display library

The selection of Affimers from the phage library against FGFR3 protein was carried out by Ms. Anna Tang using the standard method established by the BSTG. Purified recombinant FGFR3 protein, which was the extracellular domain of the protein (Figure 1.14), was used for Affimer selection. FGFR3 was biotinylated before use in order for the target protein to use streptavidin-biotin interaction for Affimer selection. Initially, biotinylated FGFR3 was captured on a streptavidin-coated plate before phage-presenting Affimers were allowed to bind to the FGFR3 protein. Unbound phage were then removed during washing steps. Subsequently, bound phage were eluted using acid and alkaline buffers prior to infecting *E.coli* strain ER2738 for phagemid amplification. The *E.coli* cells were infected with M13K07 helper phage, contributing to phage-presenting Affimers production. Three biopannings were performed. The first panning round was the standard panning whereas the second and third rounds were the competitive panning. After the third panning, the *E.coli* colonies were randomly picked for phage ELISA and positive clones were sequenced. Out of all the clones sequenced, 7 different patterns of amino acid sequence were revealed (Figure 3.16).

	Loop 1	Loop 2	
FGFR3-7	-----LLWKTQIFS-----	-----TTAFGRSNM-----	95
FGFR3-8	-----MLWLTVEQS-----	-----RPLRISNMN-----	95
FGFR3-14	-----VKLIVTRWY-----	-----SKWQDDNAQ-----	95
FGFR3-15	-----KLMP-DNWS-----	-----HHTQVTRWK-----	94
FGFR3-16	-----PNKPYGYWA-----	-----EWMQNWEYT-----	95
FGFR3-21	-----VMWQNDYPA-----	-----VKW-----	85
FGFR3-27	-----VIWEHYYPV-----	-----HPFENEIIA-----	95

Figure 3.16 Amino acid sequences of 7 selected Affimers against FGFR3. The figure shows the amino acid sequences split over two variable peptide loops. Only FGFR3-21 Affimer possesses one inserted loop while the others have two inserted loops.

3.5.2 Anti-FGFR3 Affimer sequence and alignment

Seven anti-FGFR3 Affimer-encoding sequences from the phagemid vectors were subcloned into a pET11a expression vector by Dr. Nidhi Lal (School of Chemistry, University of Leeds). This was to allow the selected Affimers to be expressed in BL21 (DE3) *E.coli* cells. In accordance with the preliminary characterisation of the selected anti-FGFR3 Affimers, the experimental data from biolayer interferometry (Dr. Nidhi Lal) and immunofluorescence staining assay (Dr. Darren Tomlinson) suggested that out of 7 selected Affimers against FGFR3, clones FGFR3-8, FGFR3-14 and FGFR3-21 showed higher levels of binding to FGFR3 protein, compared to the other clones. Therefore, in this research, three anti-FGFR3 Affimers, FGFR3-8, FGFR3-14 and FGFR3-21, were studied alongside with a GFP Affimer as a negative control. pET11a vectors containing FGFR3 and GFP Affimer sequences were kindly provided by Dr. Nidhi Lal and Dr. Paul Beales (School of Chemistry, University of Leeds). Initially, the sequences of four Affimers were checked by sequencing via GENEWIZ Genomics, UK. The nucleotide sequences of the Affimers were translated before alignment using online Clustal Omega (EMBL-EBI). Figure 3.17 showed that all the four Affimers have the identical core structure and only vary in the sequences at the two peptide loop regions. Three Affimers, FGFR3-8, FGFR3-14 and GFP, contain two inserted loops whereas FGFR3-21 Affimer has only one variable peptide loop.

3.5.3 Anti-FGFR3 Affimer expression and purification

In order to produce the Affimers, the protocol established by the BSTG as described in Section 2.2.4 was followed. After the elution step, the purified Affimers were examined alongside with cell lysates and unbound protein fractions. Figure 3.18 shows the results of SDS-PAGE gels of purified Affimers FGFR3-8, FGFR3-14, FGFR3-21 and GFP. In elution fractions E1 to E5, protein bands with the M_r around 12.5 kDa, consistent with the size of an Affimer, were seen.

Although using this expression protocol resulted in expression yields of up to 3 mg/ml for FGFR3-21 and GFP Affimers, yields for FGFR3-8 and FGFR3-14 Affimers were under 1 mg/ml, causing difficulties for further experiments. Re-considering the original expression protocol from the BSTG, subsequently heating cell lysates at 50°C was avoided. Originally, heating the cell lysates is to remove non-specific (non-Affimer) proteins since Affimers are typically stable at higher temperatures. However, some Affimers tend to be degraded when the temperatures rise over 50°C. By excluding heating to 50°C, the expression yields of FGFR3-8 and FGFR3-14 Affimers increased to 2-3 mg/ml.

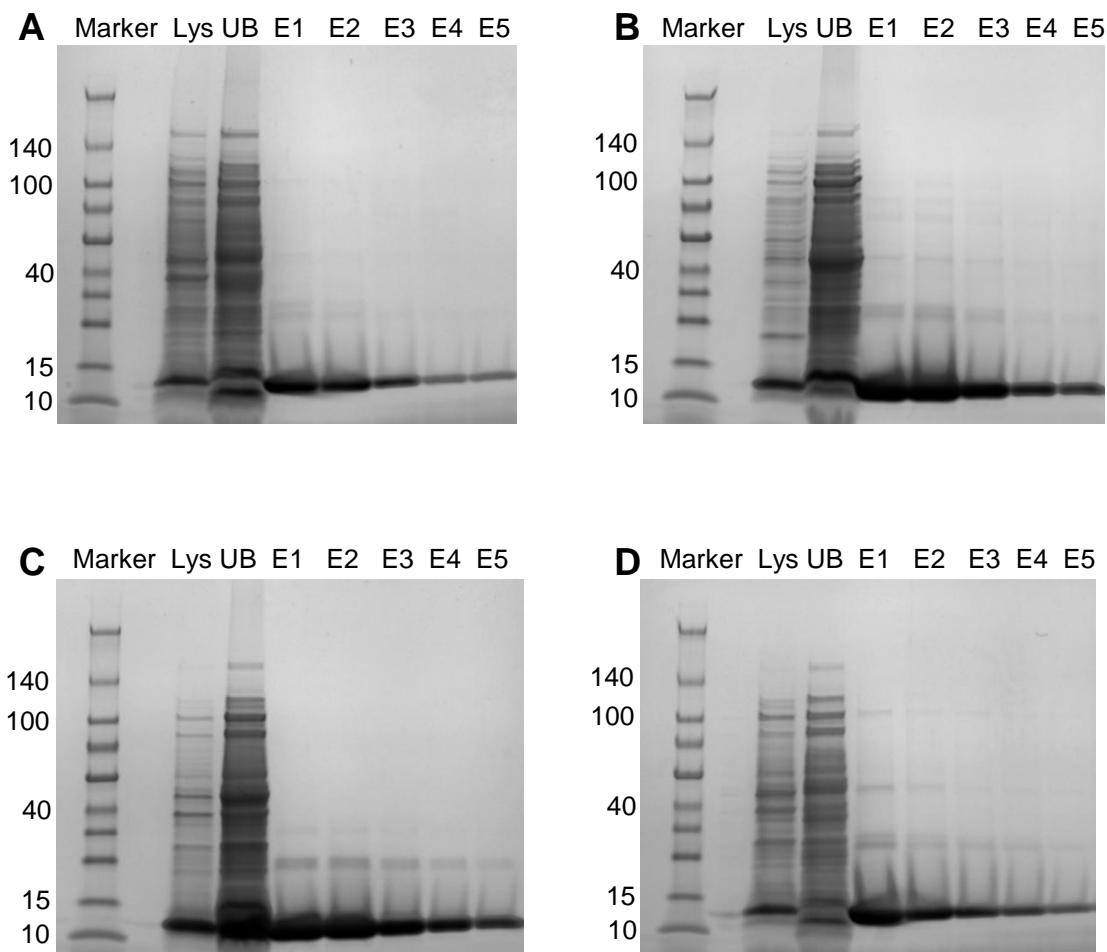


Figure 3.18 SDS-PAGE gels of purified Affimers against FGFR3. (A) – (D) the gels showing anti-FGFR3-8 FGFR3-14, FGFR3-21 and anti-GFP Affimers, respectively. The protein markers are Spectra™ multicolour broad range protein ladder (ThermoFisher Scientific) in kDa unit. (Lys), lysate fraction; (UB), unbound protein fraction; (E1-E5), purified Affimer fractions 1-5, respectively.

3.6 Discussion

The main focus of this chapter was to screen for, and produce, Affimers against DDT. The screening was successfully done using the Affimer-phage display library where 16 different clones of Affimers were obtained from the screening. The majority of the clones (15 out of 16 clones) possess one variable peptide loop whereas only the clone H25 has two variable peptide loops. The small size of the target, DDT, may only require a small number of amino acid residues for the interaction. Antigens such as proteins present multiple epitopes, which are large, so they can form a number of bonds with Affimer binding sites. Therefore, it is common that the Affimers selected against proteins e.g. yeast SUMO (Tiede et al., 2014) and anti-myc tag antibodies (Raina et al., 2015) possess two inserted peptide loops. On the other hand, when the targets are small organic compounds such as 2,4,6 – trinitrotoluene (TNT), some of the isolated Affimers possess one variable peptide loop (Tiede et al., 2017). This indicates selection of these Affimers from a minor population of the original phage display library.

After subcloning anti-DDT Affimer-encoding sequences into the pET expression vector system, Affimer production was carried out in *E.coli* cells alongside with the production of anti-FGFR3 Affimers. Mostly, the yield of purified Affimers was between 1 mg/ml and 4 mg/ml, which was acceptable. However, two FGFR3 Affimer clones, FGFR3-8 and FGFR3-14, provided the yields below 1 mg/ml when using the original purification protocol, making them impractical for the further work. Eliminating the cell lysate heating step to 50°C improved the yield of the two FGFR3 Affimers up to 2-3 mg/ml. Aggregation is a common problem that researchers working with Affimers may experience. The unique properties of the Affimer scaffold, plus the two loops which contribute to around 25% of the total mass, and the addition of cysteine residues can be causes of aggregation. It is recommended that to prevent Affimers

from precipitation, stabilising agents such as glycerol should be added in the storage buffer (Raina, 2013). However, users may need to take into account that the additional agents may interfere with the further assays or applications. In the next section, all the selected Affimers were checked for their specific binding to the targets prior to using them in biosensor applications.

Chapter 4

Affimer characterisation

4.1 Introduction

In an application requiring biorecognition, specific binding of the bioreceptor to its target dominates the successful outcome of the assay. When working with synthetic binding proteins, it is essential for users to confirm that the selected bioreceptor is specific to the target of interest. A number of approaches have been developed in order to determine the affinities between two or more biomolecules. Some techniques are suitable for equilibrium measurement or at a steady state such as enzyme-linked immunosorbent assay (ELISA), isothermal titration calorimetry (ITC), immunoprecipitation (pull-down) assay and fluorescence anisotropy. However, methods such as surface plasmon resonance (SPR) and biolayer interferometry (BLI) can be used to study the binding kinetics in real time and also provide steady state data. A combination of different methods can help scientists select the best bioreceptor for their assays.

In this chapter, the main focus is on characterisation of the selected Affimers from Chapter 3. Two model analytes, DDT (a small molecule) and FGFR3 (a macromolecular protein), were studied. The work in this chapter was divided into two parts. To study the binding of Affimers to DDT, ELISA was used as a tool to determine the affinities between the Affimers and DDT. On the other hand, specific interaction between the Affimers and FGFR3 protein are confirmed using several approaches including ELISA, SPR, and immunoprecipitation assay. At the end of the characterisation, none of Affimers against DDT showed binding to free DDT, whereas Affimers against FGFR3 performed well on specifically binding to the target and were selected for biosensor construction, as will be described in Chapter 5.

4.2 Characterisation of Affimers against DDT

Although phage ELISA showed the success of binding between the Affimers presented on the phage pIII and biotinylated DDT, it was necessary to confirm that binding ability of the selected Affimers could be retained whilst not displayed on phage. Direct and competitive ELISAs were employed to check the binding between selected Affimers and DDT itself.

4.2.1 ELISA to check the binding of Affimers to biotinylated DDT

The ELISA is a common immunoassay that is widely used to study interaction between bioreceptors (mostly antibodies) and targets of interest. In this section, a direct ELISA was used to evaluate the binding of eight Affimers to DDT. Biotinylated DDT was initially captured on a NeutrAvidin-coated Nunc-immuno plate via NeutrAvidin-biotin interaction. Each Affimer was used as the primary recognition element, following by anti-His₆ tag antibodies – HRP (at 1:1000 dilution) as the secondary detection agent (Figure 4.1A).

Out of eight Affimers previously selected, six binders, clones H10, H18, H23, H27, H38 and H39, showed strong binding to biotinylated DDT whereas clones numbered H8 and H25 did not bind to DDT captured on the plate (Figure 4.1B). Three replicates were included in each experiment and two independent experiments were repeated. The results from the two experiments were identical. An anti-GFP Affimer, which was used as a negative control, was unable to bind DDT, suggesting that the binding between the six positive Affimers and biotinylated DDT was specific. Therefore, the six Affimers which bound to biotinylated DDT were chosen for competitive ELISA, which is described in the following section.

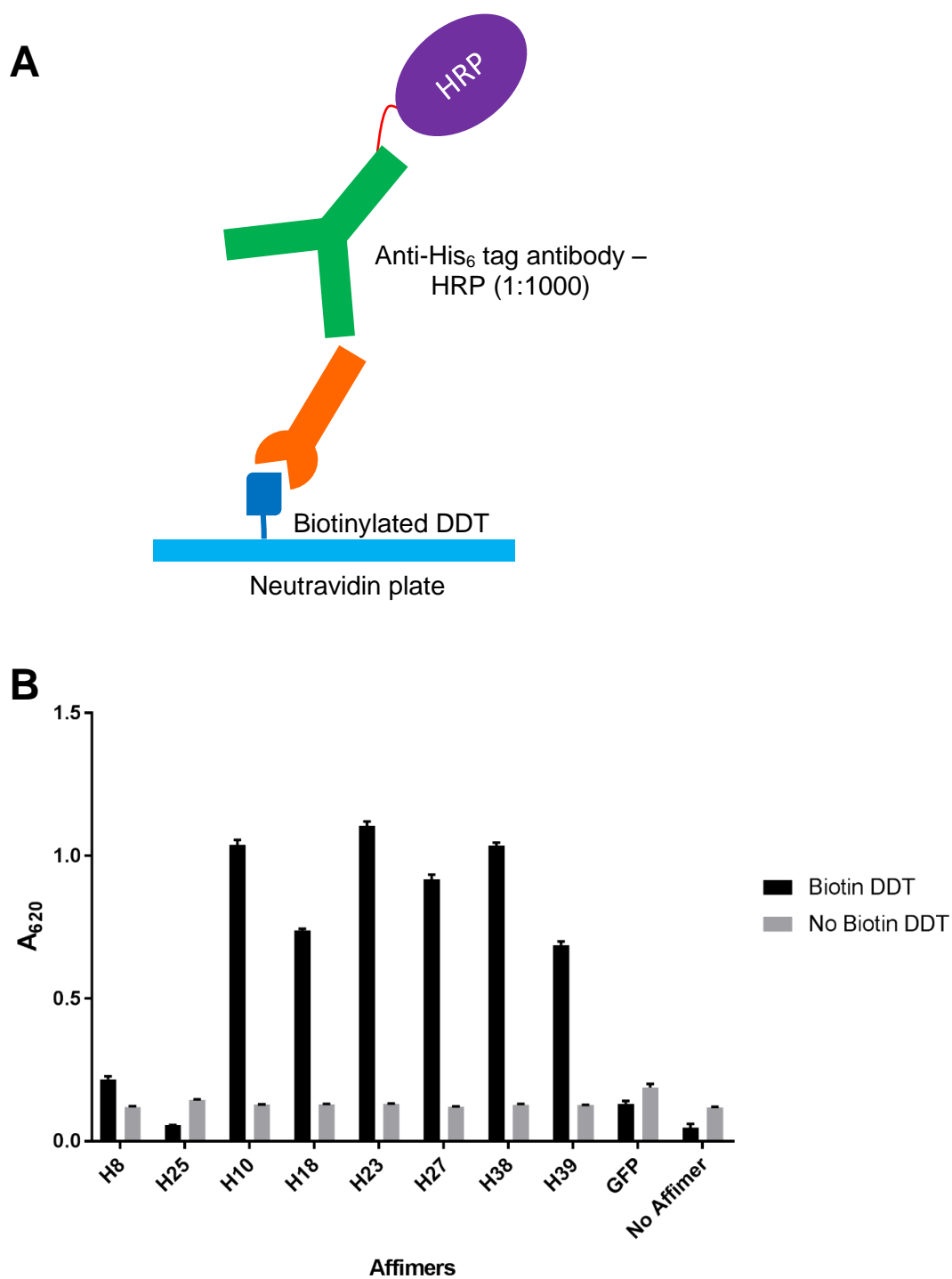


Figure 4.1 Direct ELISA to examine the binding of Affimers to biotinylated DDT immobilised on a NeutrAvidin-coated plate. (A) schematic showing ELISA platform and (B) the result of ELISA showing the binding between nine Affimers to biotinylated DDT. Six Affimers, H10 to H39, showed positive results on the assay. The error bars represent mean of $n = 3 \pm \text{SEM}$.

4.2.2 Optimisation of Affimer concentration for competitive

ELISA

The optimal concentration of the biorecognition elements is a key factor for success in competitive ELISA. In this section, a range of Affimer concentrations were studied to determine the optimal concentration used for further competitive ELISA. H10 and H23 Affimers were selected as representatives for this study. Initially, biotinylated DDT was immobilised to a NeutrAvidin-coated plate. Then the Affimers, which varied in concentration from 0 to 2.5 $\mu\text{g/ml}$, were added and allowed to bind to the biotinylated DDT. Anti-His₆ tag antibodies – HRP conjugate was used to develop the ELISA as described previously. For each experiment, three replicates were included. Two independent experiments were repeated in order to confirm the results. The optimal concentration of Affimer is the minimum concentration of Affimer where the generation of blue product after TMB substrate addition can still be visualised, compared to the Affimers absent (negative control). Figure 4.2A shows that an Affimer concentration (both H10 and H23) around 0.3 $\mu\text{g/ml}$ was the minimum point where the blue product could be defined while concentrations lower than this showed a lower response which was not sufficient for competitive ELISA.

In the meantime, the optimal incubation time for colour development and A₆₂₀ measurement was also investigated. After TMB addition, the absorbance at 620 nm was measured at different time points, from 10 min to 60 min. It was observed that after 30 min, the absorbance values changed slowly and was defined at 60 min (Figure 4.2B). Therefore, to conduct the competitive ELISA, an Affimer concentration of 0.3 $\mu\text{g/ml}$ and an incubation time of 30 min after TMB substrate addition were chosen.

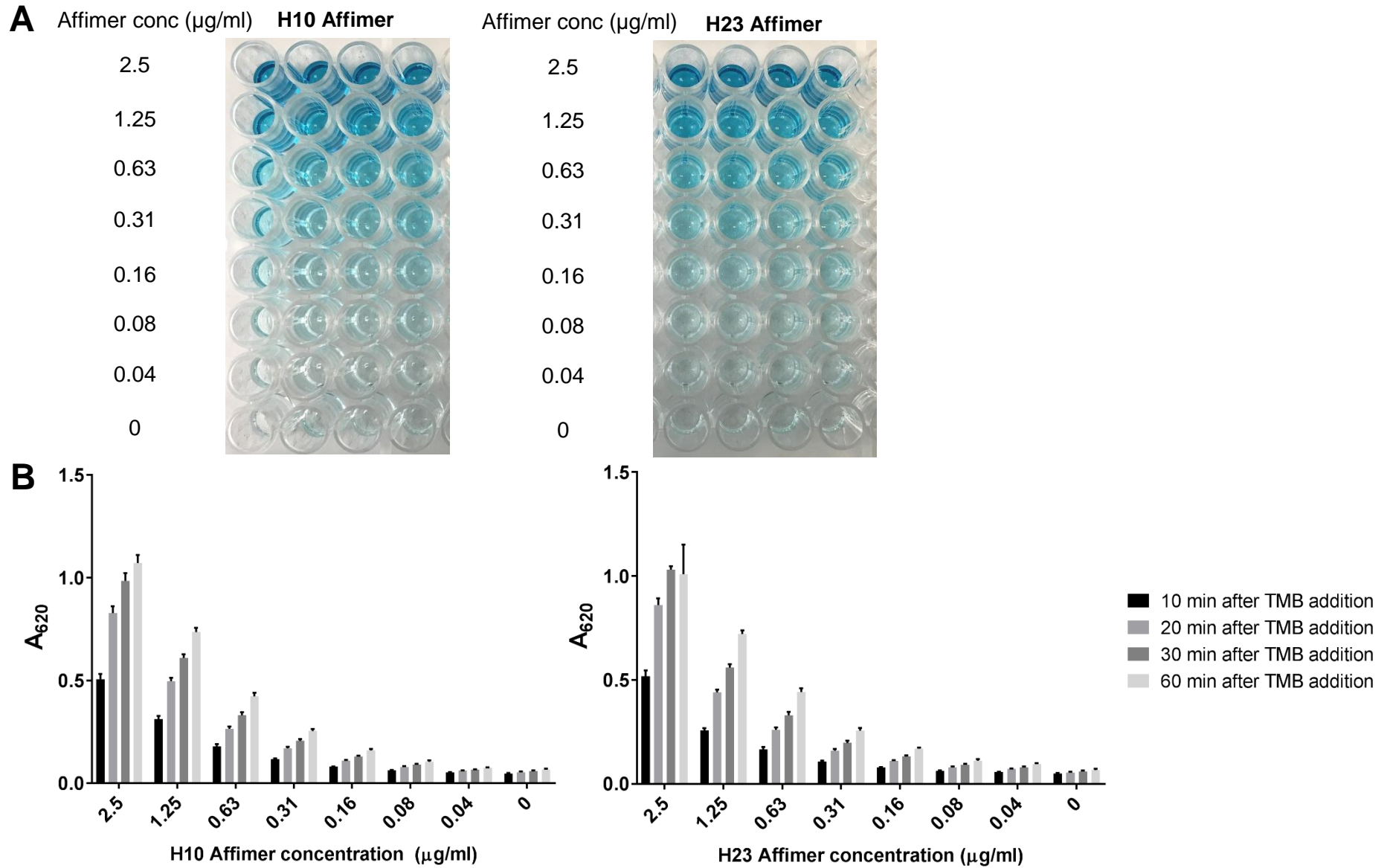


Figure 4.2 Optimisation of Affimer concentration and incubation time point for competitive ELISA. (A) 96-well plates showing the ELISA after 30 min of TMB addition. (B) Absorbance at 620 nm of ELISA upon the binding of H10 and H23 Affimers to biotinylated DDT. Affimer concentrations and incubation times were varied as shown. The error bars represent mean of $n = 3 \pm \text{SEM}$.

4.2.3 Competitive ELISA to study the binding of Affimers to free DDT

In the previous section, it was confirmed that some of the selected Affimers bound to biotinylated DDT. However, it was important to prove whether the Affimers were able to bind free DDT as well. Competitive ELISA is a standard and easy method to study the interaction between two molecules and was chosen to examine the interaction between the Affimers and free DDT. To set up the competitive assay, biotinylated DDT was immobilised onto a NeutrAvidin-coated plate. Six Affimers, H10, H18, H23, H27, H38 and H39, at 0.3 µg/ml were individually mixed with free DDT concentrations ranging from 0 to 10 µM. The mixture of Affimers and free DDT was then transferred to the biotinylated DDT coated plate to allow the free DDT to compete with biotinylated DDT for Affimer binding. The Affimers that have a strong interaction with free DDT should not be dissociated from free DDT whereas weaker binders should be more easily dissociated from the free DDT and bind to the biotinylated DDT instead. Bound Affimers were detected using anti-His₆ tag antibodies – HRP as described previously. For each experiment, three replicates were included. Two independent experiments were repeated so as to confirm the results.

The results from competitive ELISA showed that none of the six Affimers could bind to free DDT (Figure 4.3). All six Affimers were capable of binding to biotinylated DDT on the plate, which can be seen from the absorbance values from the wells containing Affimers, biotinylated DDT and free DDT, compared to the wells without Affimers or biotinylated DDT (negative controls). However, no increasing trend of A_{620} could be observed when allowing the Affimers to bind to different concentrations of free DDT, suggesting that the binding between the Affimers and free DDT did not occur with any appreciable affinity. During the phage display

screening, biotinylated DDT consisting of biotin, spacer and DDT moiety was used as a target for Affimer selection. It is assumed that as the biotin group was captured by NeutrAvidin on the plate, the Affimers may recognise the DDT moiety and a part of spacer (Figure 4.4). Without a short spacer on free DDT, the Affimers were unable to tightly bind DDT.

However, as seen in Figure 4.3B and 4.3F, the absorbance at 620 nm for Affimers H18 and H39 was lower compared to the other Affimers. As a result, the success of competitive binding of Affimers H18 and H39 to free DDT is still ambiguous. This may be because the optimal concentration of Affimer obtained from Section 4.2.2 is not suitable for all the Affimers tested. Therefore, optimisation of Affimer concentration for each Affimer clone should be a better approach to achieve a competitive ELISA.

Selecting Affimers against small molecule targets is a challenging task. Recently, an established method of Affimer screening for organic compounds from the BSTG has been released. The explosive 2,4,6-trinitrotoluene (TNT) was chosen as a target to screen for Affimers from the phage library (Tiede et al., 2017). Counter selection was performed and the TNT analogue, 2,4,6-trinitrobenzene sulphonic acid (TNBS) was conjugated to ovalbumin and IgG to act as an epitope for Affimer selection. The phage presenting Affimers were screened against TNBS-ovalbumin and TNBS-IgG conjugates as well as ovalbumin and IgG in order to select strong and specific binders. With this approach, four clones of Affimer specific to TNT were ultimately obtained. This method could be used as a model to select Affimers for other small molecules including DDT. Since TNT has three polar nitro groups, it may be a more amenable target than DDT which is much more hydrophobic.

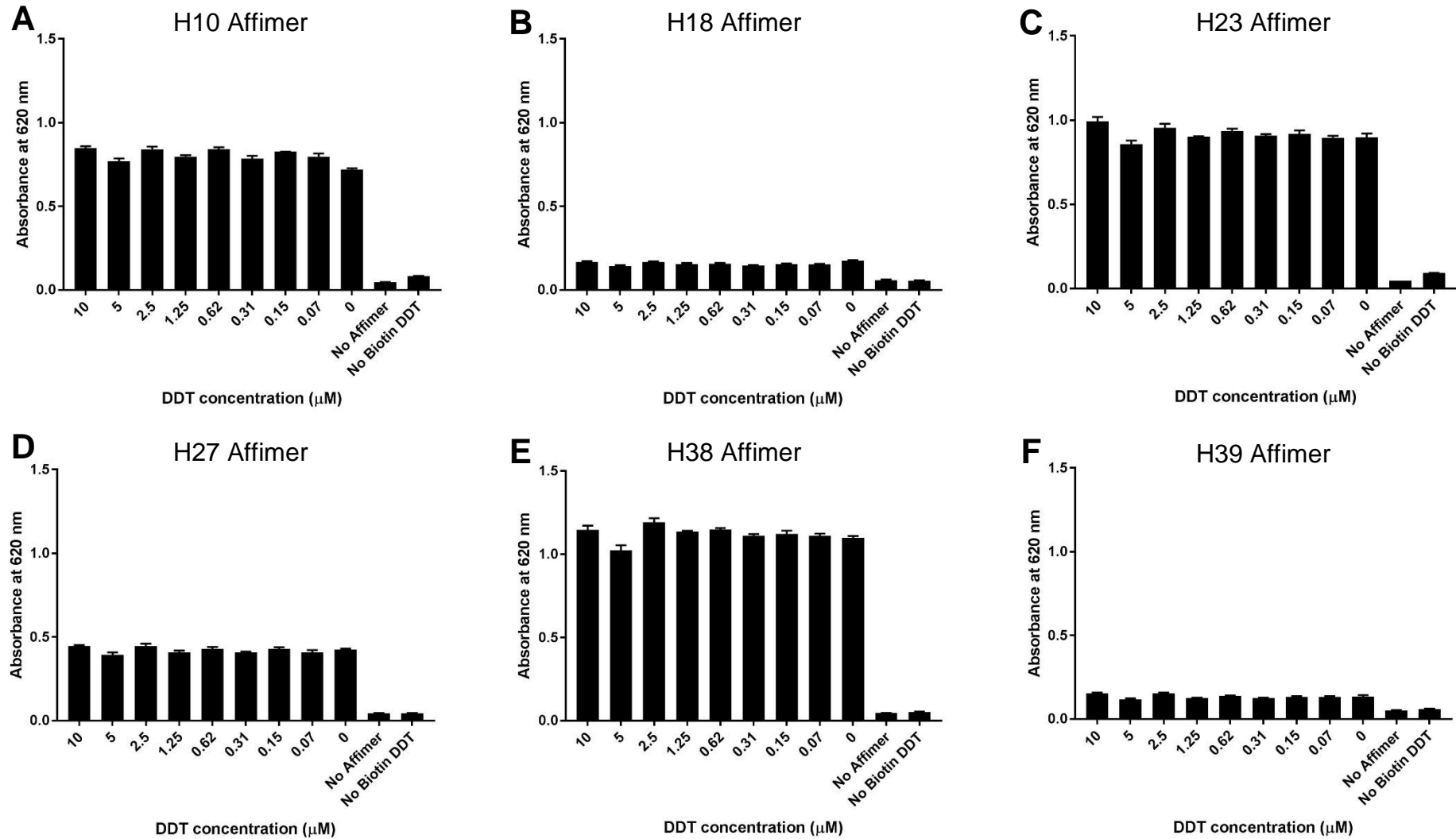


Figure 4.3 Competitive ELISA to examine the binding between six Affimers to free DDT. Panels A to F represent the binding between free DDT and (A) H10, (B) H18, (C) H23, (D) H27, (E) H38 and (F) H39, respectively. Free DDT was not able to compete at binding of the respective Affimers to the immobilised biotin-DDT. The error bars represent mean of $n = 3 \pm \text{SEM}$.

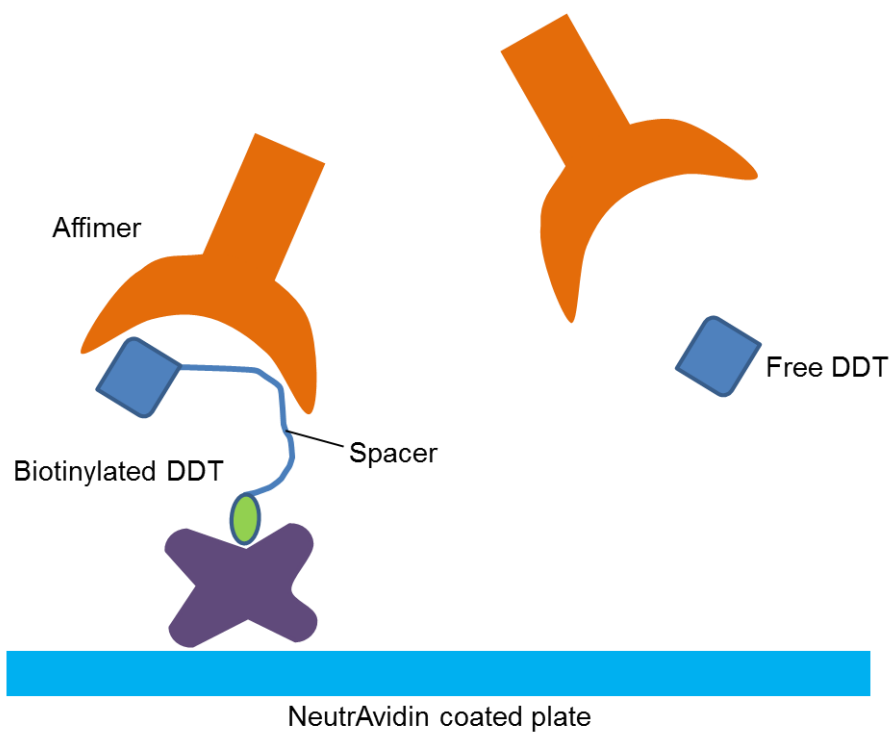


Figure 4.4 Hypothetical scheme showing the binding of the Affimer to the DDT moiety and spacer. It is hypothesised that the binding site of the Affimer may recognise DDT and part of spacer region in biotinylated DDT. Therefore the Affimer failed to bind free DDT molecule with high affinity.

4.3 Characterisation of Affimers against FGFR3

4.3.1 Biotinylation of Affimers via biotin-maleimide

One advantage of using Affimers is an additional cysteine can be introduced into the Affimer structure to provide a specific site for oriented modification as there are no cysteine residues in Affimers normally. The addition of a cysteine at the C-terminus of the Affimers was performed previously by PCR as described in Chapter 2. As the characterisation techniques to prove the binding of the selected Affimers and FGFR3 protein relied on avidin-biotin interaction, the Affimers were biotinylated before use. The benefit of using avidin-biotin linkage is correct orientation of the Affimers can be achieved on the solid surface, allowing the analyte to access the binding site of the Affimer.

Biotinylation of the Affimers can be carried out via maleimide chemistry. However, as a cysteine was added into the Affimer structure, during storage the Affimers dimerise via formation of a disulfide bond. Before biotinylation, Affimer dimers were cleaved using TCEP gel, providing a free thiol group to react with the maleimide group on biotin-maleimide (Figure 4.5). To confirm successful biotin labelling of the Affimers, ELISA and liquid chromatography – mass spectrometry (LC-MS) were employed. The ELISA data indicated successful biotinylation as shown in Figure 4.6. In addition, LC-MS was performed to compare the molecular size of the Affimers before and after biotinylation. The resulting LC-MS spectrum of the Affimer before biotinylation showed two distinct peaks (Figure 4.7). The peak representing the lower mass indicated the monomeric Affimers whereas the peak at twice the mass showed the Affimer dimers. After biotinylation of the Affimers, only one peak can be seen (Figure 4.8). This is because once modified with biotin-maleimide, the thiol group is unavailable to react and form a disulfide bond. The difference of the molecular mass between a monomer and a biotinylated version of each Affimer is

almost equal to the molecular mass of biotin-maleimide (MW = 451.54) (Table 4.1), indicating the success of the biotinylation process.

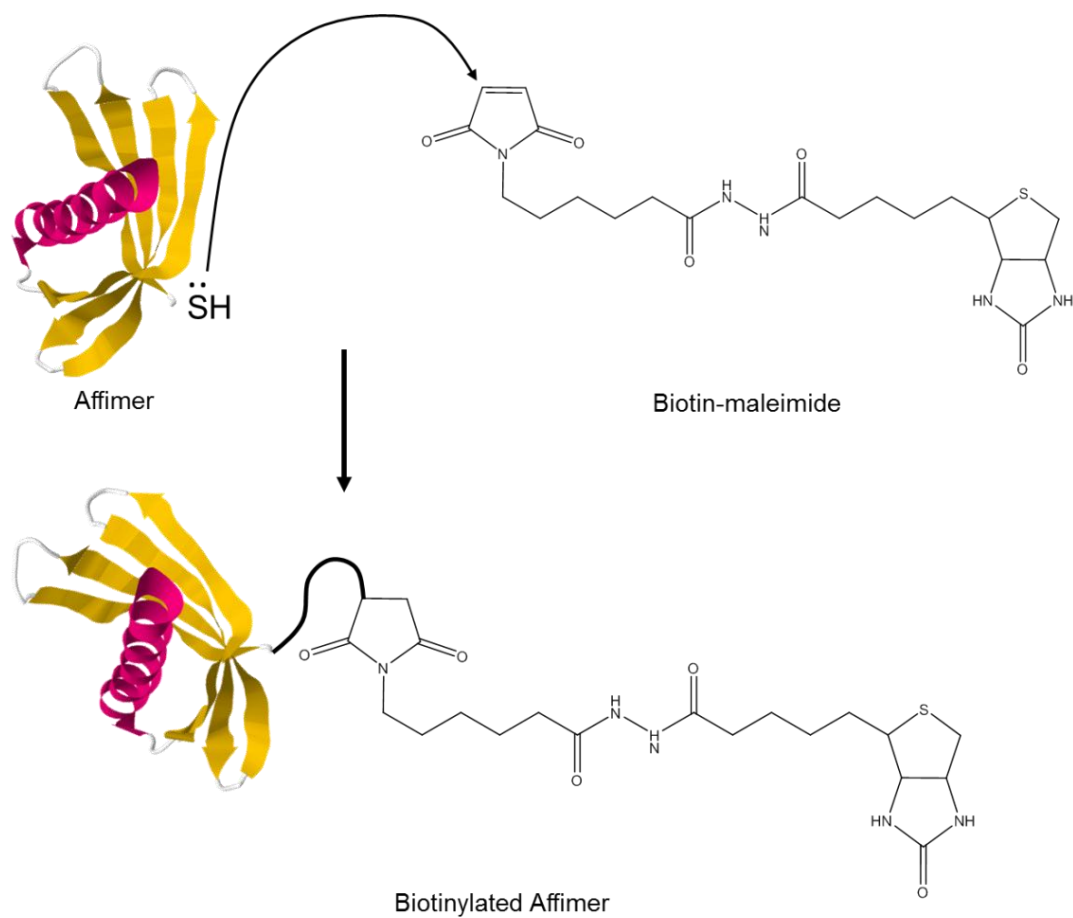


Figure 4.5 Biotinylation of an Affimer via biotin-maleimide. The process can be done using the maleimide reaction.

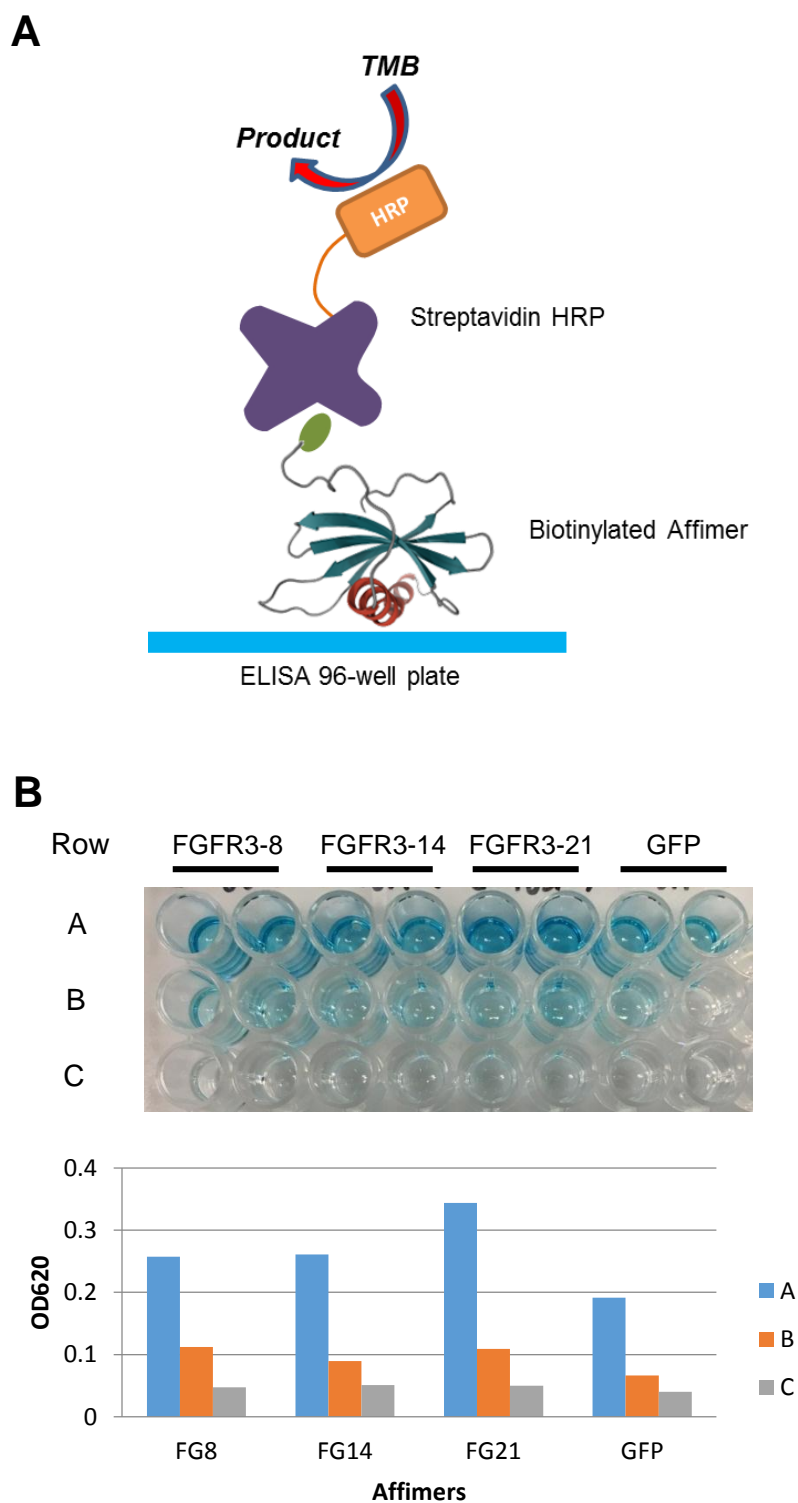


Figure 4.6 ELISA to check the success of Affimer biotinylation. (A) shows the ELISA setup. Biotinylated Affimer was coated on the plate and detected with streptavidin – HRP conjugate. (B) shows ELISA data. One μ l of biotin-tagged Affimer was placed in row A and serial 0.1x and 0.01x dilution into row B and C, respectively.

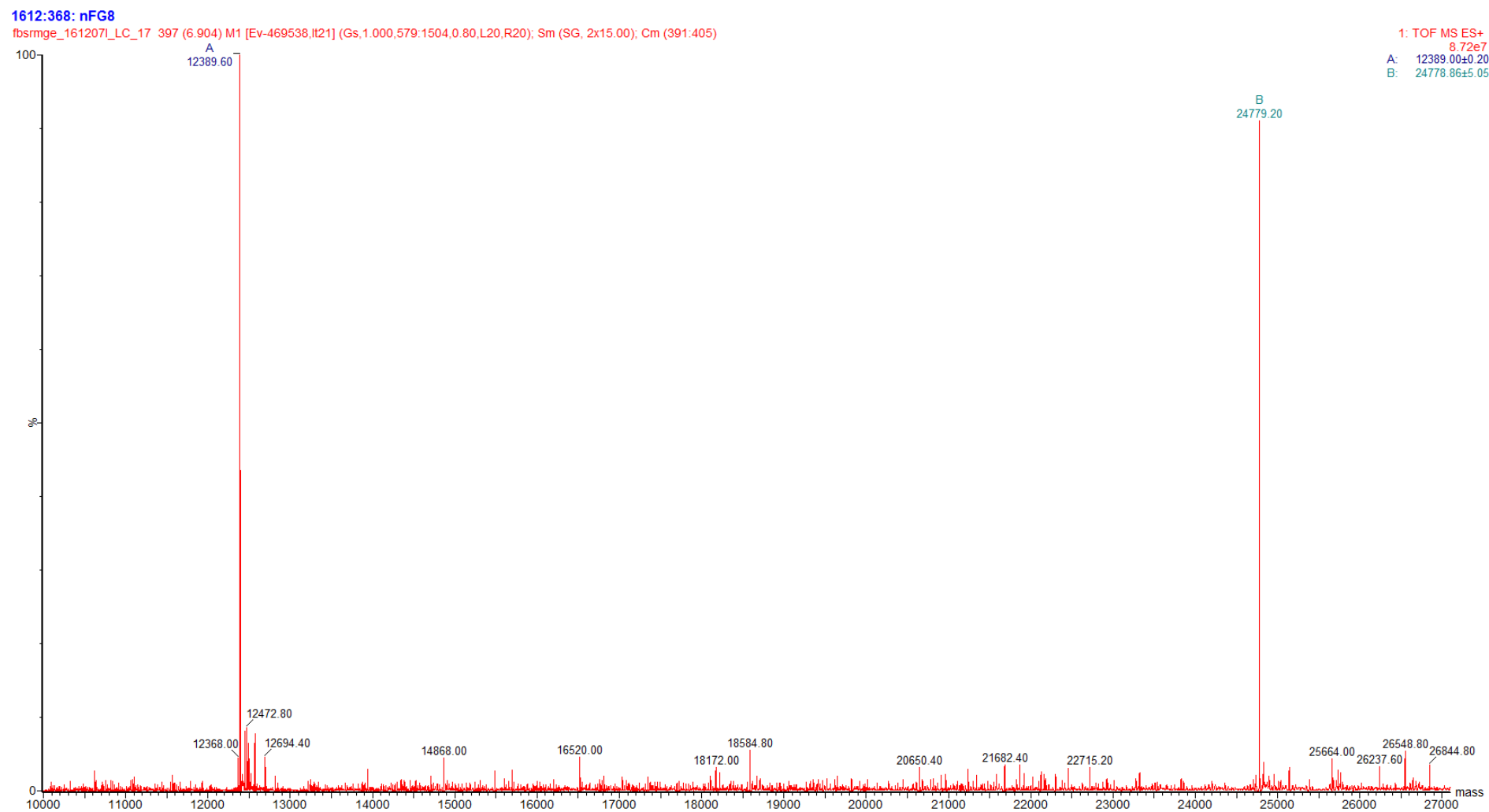


Figure 4.7 LC-MS spectrum of a FGFR3-8 Affimer prior to biotinylation. Two distinct peaks can be observed. Peak A represents the monomeric Affimer and peak B represents Affimer dimer, respectively.

1612-353: FG8

fbsrmge_161205X_LC_033 398 (6.921) M1 [Ev-156272.lt13] (Gs,0.400,911:1322,0.80,L80,R80); Sm (Mn, 2x20.00); Cm (394.402)



Figure 4.8 LC-MS spectrum of a FGFR3-8 Affimer after biotinylation. A, a distinct peak representing biotinylated Affimer monomer can be detected.

Table 4.1 Comparison of molecular mass of the Affimers before and after biotinylation

Affimers	Non-biotinylated form (Da)		Biotinylated form (Da)	Non-biotin monomer – Biotin form
	Monomer	Dimer		
FGFR3-8	12389.60	24779.20	12840.00	450.40
FGFR3-14	12449.60	24898.40	12902.40	452.80
FGFR3-21	11218.40	22436.80	11669.60	451.20
GFP	12590.40	25180.80	13040.80	450.40

4.3.2 Double-sandwich ELISA to check the binding between Affimers and FGFR3

To determine which selected Affimers have the highest affinity to FGFR3 protein, a double-sandwich ELISA was chosen as to confirm the binding between each Affimer and FGFR3. In brief, biotinylated Affimers were initially immobilised onto an ELISA 96-well plate via NeutrAvidin-biotin interaction (Figure 4.9A). Three Affimers, FGFR3-8, FGFR3-14 and FGFR3-21, previously screened against FGFR3, were tested whereas anti-GFP Affimer was used as a negative control. The captured Affimers on the ELISA plate were then challenged with purified FGFR3. To investigate successful binding, anti-FGFR3 antibodies were applied as primary antibodies, following by anti-rabbit IgG antibodies – HRP as secondary antibodies. Colourimetric detection using TMB substrate was finally utilised to report the binding of the Affimers to their FGFR3 target. For each experiment, three replicated were included. Two independent experiments were carried out and the results were identical. The result from the ELISA revealed that FGFR3-14 Affimer showed the highest binding ability to FGFR3 protein, following by FGFR3-21 Affimer. The binding between FGFR3-8 Affimer and FGFR3 protein could be detected but the level of the binding was not as strong as with FGFR3-14 and FGFR3-21 Affimers. As expected, the anti-GFP Affimer was unable to bind FGFR3 protein (Figure 4.9B).

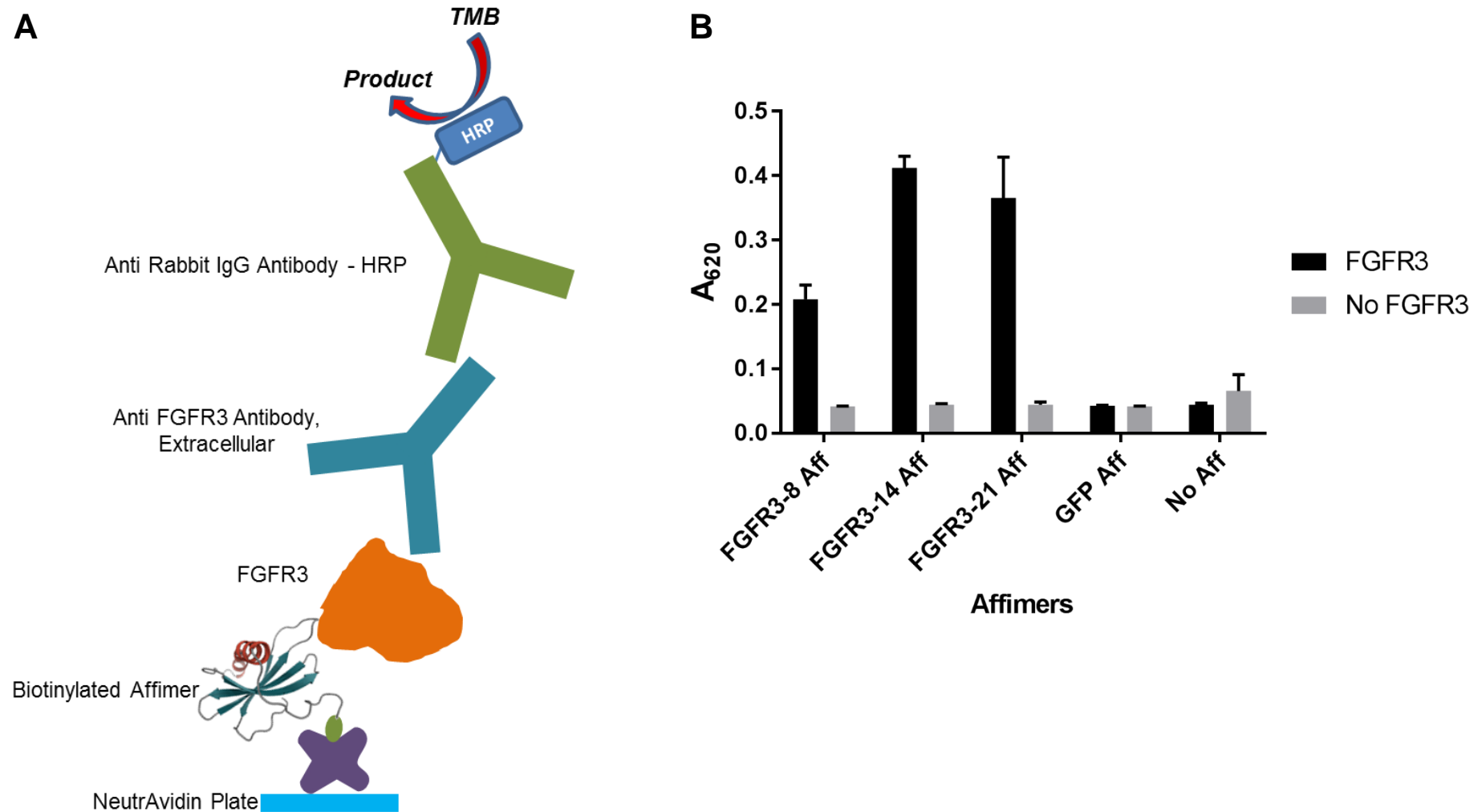


Figure 4.9 Double-sandwich ELISA test to check the binding of Affimers and FGFR3 protein. (A) A schematic of ELISA setup. (B) The result of the ELISA showing positive binding when the Affimers screened against FGFR3 were used. The absorbance was measured at 620 nm. The error bars represent mean of $n = 3 \pm \text{SEM}$.

4.3.3 Binding kinetics study using surface plasmon resonance (SPR)

As high sensitivity and specificity of biosensors are required and rely principally on the affinity between a bioreceptor and its target, the binding kinetics between the selected Affimers and FGFR3 were investigated using surface plasmon resonance (SPR). SPR is an optical biosensor where the basic principle of the measurement is based on a change in refractive index resulting from the binding between bioceptors and their target. The sensorgrams obtained provide useful information for studying protein-ligand interactions. A typical sensorgram offers real time binding data during association and dissociation phases that can be used to investigate binding parameters (Figure 4.10).

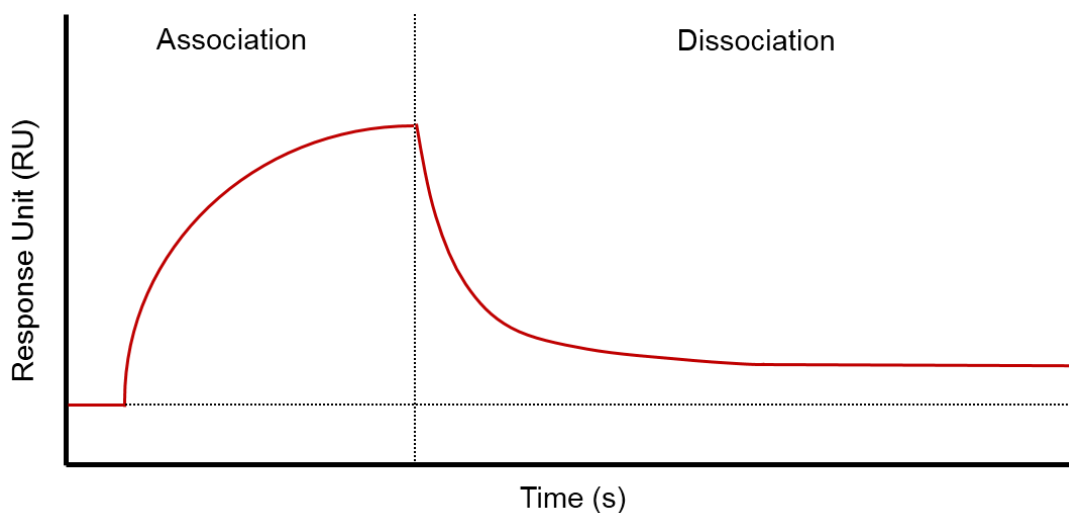


Figure 4.10 A typical SPR binding sensorgram showing association and dissociation phases. The association data are collected after the injection of the analyte. The dissociation data, on the other hand, are measured and recorded after stopping analyte injection and replacing by running buffer.

To set up the experiment, a streptavidin-coated SPR chip containing four flow cells was used. Biotinylated FGFR3-8, FGFR3-14 and FGFR3-21 Affimers were immobilised in flow cells 2 to 4, whereas flow cell 1 was left empty as a reference cell. The chip was then exposed to a series of FGFR3 concentrations ranging from 0 to 1000 nM. At each FGFR3 concentration, the cycle started with association phase for 300 sec, following by 900 sec of dissociation. As anticipated, the change in refractive index increased as the concentration of FGFR3 added to flow cells increased (Figure 4.11), indicating that the binding between Affimers and FGFR3 protein had occurred. The real time SPR data showed that FGFR3-14 and FGFR3-21 Affimers could bind to FGFR3 (Figure 4.11A and 4.11B) while FGFR3-8 Affimer failed to bind its target (Figure 4.11C). These data agreed with the double-sandwich ELISA which previously revealed that the binding of FGFR3-14 and FGFR3-21 to FGFR3 protein were somewhat higher than for FGFR3-8 (Figure 4.9B). However, the evidence from immunofluorescence staining experiments showed that FGFR3-8 was able to bind FGFR3 upon cell-based assays (Dr. Darren Tomlinson - personal communication). This suggested that immobilisation of FGFR3-8 Affimer onto a solid surface may negatively affect its binding ability to the target.

The SPR data showing the affinity between the selected Affimers and FGFR3 protein were analysed using the approach presented in Section 2.2.6.4. Due to the limited stock of purified FGFR3 protein, the SPR experiment could be conducted only once. The K_D for the interaction between the FGFR3-14 Affimer and FGFR3 protein was 327 pM while the K_D for the FGFR3-21 Affimer and FGFR3 was 18.5 pM (Table 4.2). Typically, the K_D values of antibody-antigen interaction range from pM to nM (Kim et al., 1990, Landry et al., 2015). It has earlier been reported that the K_D for a monoclonal anti-FGFR3 antibody is 16.2 pM (ab133644, Abcam, UK). This means that the affinity of the selected Affimers is comparable to anti-FGFR3 antibody and they could be promising reagents for biosensor fabrication.

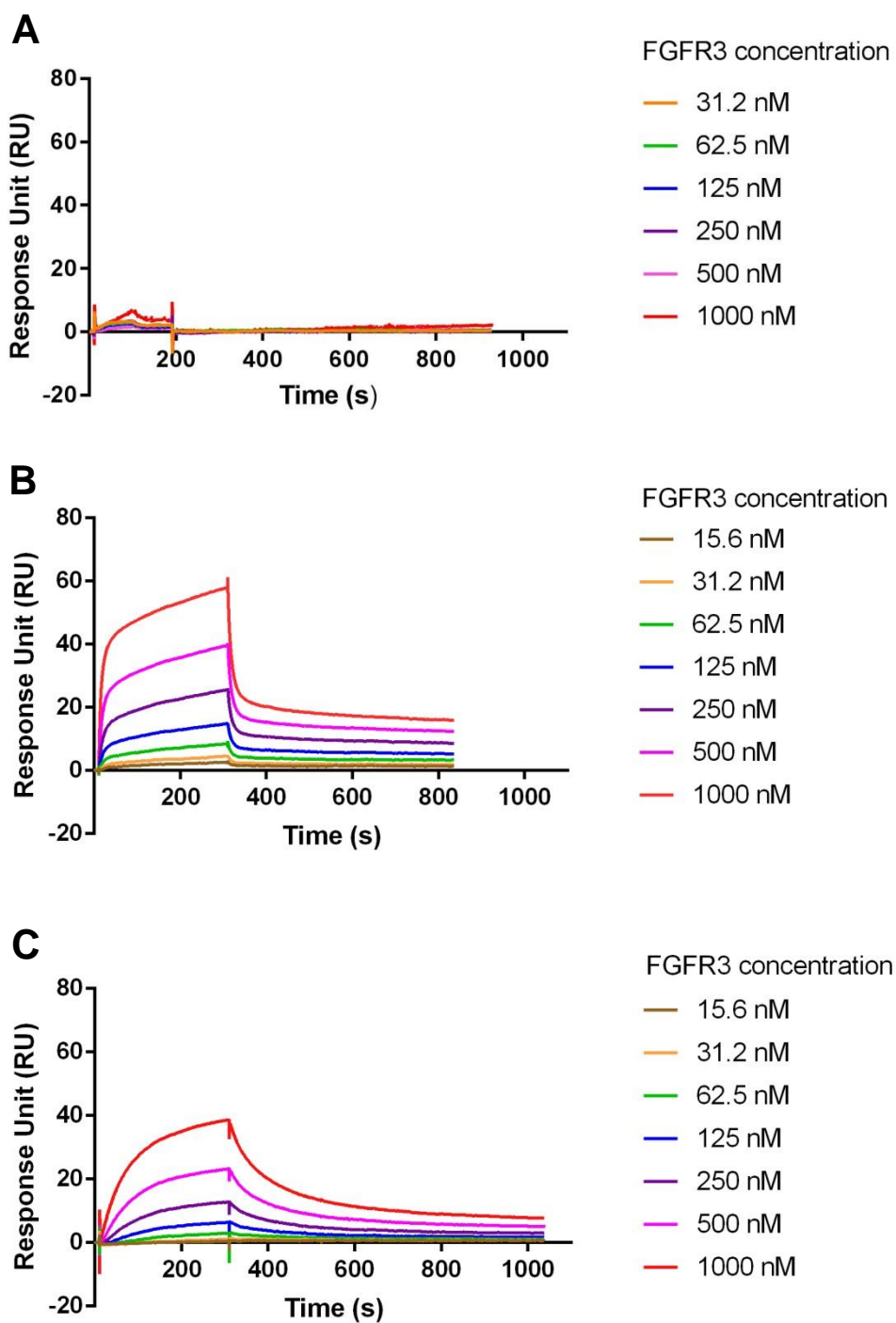


Figure 4.11 SPR sensorgrams showing the changes of refractive index in response units (RU). The sensors were immobilised with (A) FGFR3-8, (B) FGFR3-14 and (C) FGFR3-21 Affimers before challenged with FGFR3 protein concentration ranging from 0 to 1000 nM.

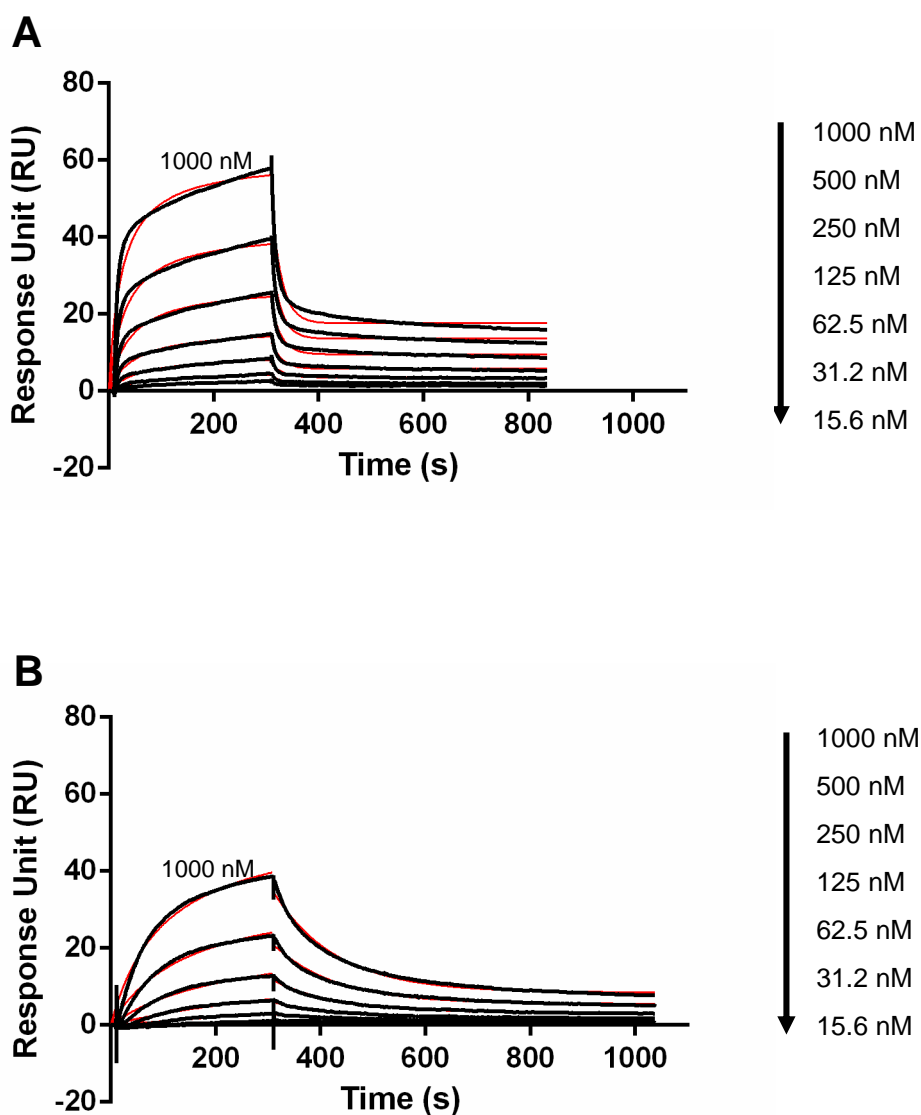


Figure 4.12 The results of SPR data fitting with a one-site binding model available on Graphpad Prism 7 software. (A) is the fitting for FGFR3-14 Affimer and (B) for FGFR3-21 Affimer. The black curves represent experimental data from SPR assays whereas the red curves represent the fitting results which are overlaid. The association phase was fitted with a one-site specific binding model while the dissociation phase was analysed using a one-phase decay exponential model.

Table 4.2 Fitting SPR data from a one-site binding model. The results showed the excellent fit as shown in Figure 4.12.

Affimer clones	FGFR3-14	FGFR3-21
k_{on} ($M^{-1} s^{-1}$)	1.60×10^8	4.49×10^8
k_{off} (s^{-1})	5.24×10^{-2}	8.31×10^{-3}
K_D (μM)	327	18.5
R^2	0.955	0.976
χ^2	1.610	1.071

4.3.4 Immunoprecipitation assay

Immunoprecipitation or pull-down assay is a well-known and widely used technique to isolate an analyte or protein of interest out of solution. The technique relies on the specific interaction between antibody and antigen. In this study, Affimers were used as an antibody replacement to bind FGFR3 in order to test their specificity. The experiment was set up as shown in Figure 4.13A. Biotinylated Affimers were immobilised to streptavidin-coated resin, and as the amount of the Affimers was excess, unbound Affimers were then removed using wash buffer. The Affimers coated onto the resin were incubated with FGFR3 protein overnight before unbound FGFR3 was removed by several washing steps. The pulled-down fractions were heated to 95°C for 5 min in order to release the Affimers and FGFR3 protein from the resin. SDS-PAGE was used to separate the Affimers and FGFR3. Two identical gels were prepared to check the presence of both Affimers and FGFR3 protein. Proteins on both gels were transferred to PVDF membrane in order to carry out western blotting. The first membrane was probed with streptavidin-HRP to detect biotin tagged Affimers. If biotinylated Affimers are successfully coated on streptavidin resin, they can be recognised by streptavidin-HRP. As seen in Figure 4.13B, all three Affimers, FGFR3-14, FGFR3-21 and GFP, used in this experiment were detected on the PVDF membrane, indicating successful immobilisation of Affimers onto streptavidin. The biotinylated Affimer used as a positive control was also detected in the first lane. In order to check whether the Affimers are able to bind FGFR3, the other membrane was probed with anti-FGFR3 antibodies (primary antibodies), following by anti-rabbit IgG antibodies – HRP (secondary antibodies). As presented in Figure 4.13C, pull-down products for FGFR3-14 and FGFR3-21 Affimers showed positive detection on the membrane, indicating the binding ability of FGFR3-14 and FGFR3-21 Affimers to FGFR3 protein. However, GFP Affimer, which was used as a negative control, did not bind to FGFR3 in this assay as pull-down product for GFP

Affimer did not show any detected signal. Purified FGFR3 protein, which was used as a positive control, also showed positive detection as expected. The result from the immunoprecipitation assay confirmed the results from double-sandwich ELISA and SPR that FGFR3-14 and FGFR3-21 Affimers were the two Affimers capable of binding to FGFR3 protein and could be used for biosensor fabrication.

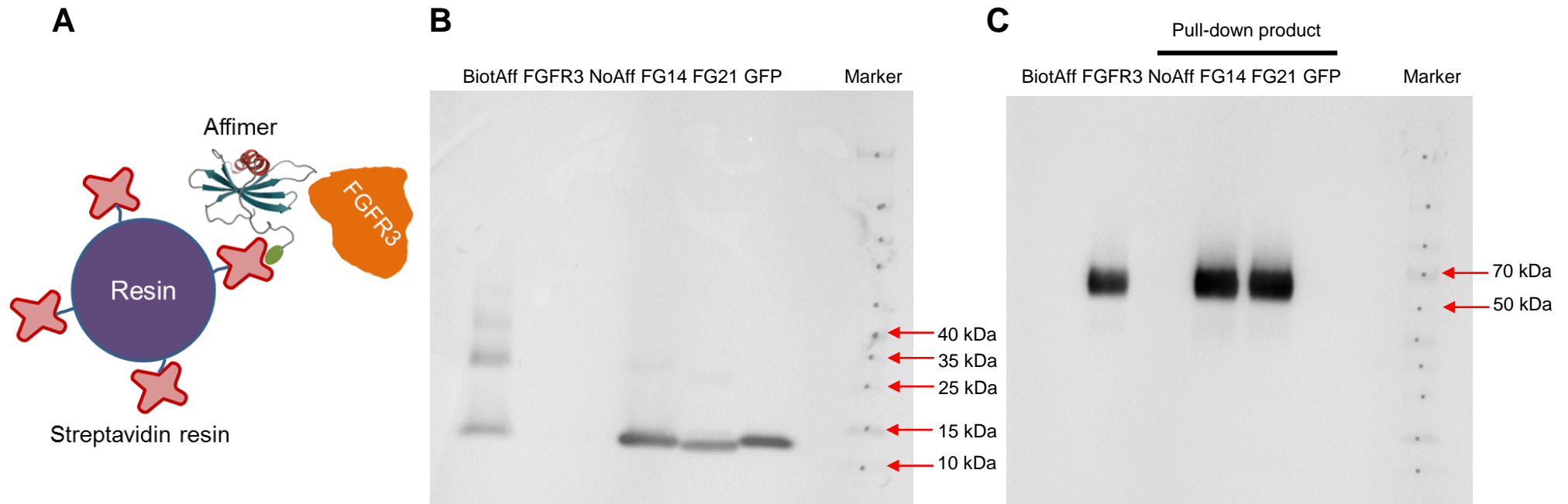


Figure 4.13 Immunoprecipitation assay showing the binding of the Affimers to FGFR3. (A) A schematic showing a pull-down platform. A molecule of Affimer is coated via avidin-biotin interaction before testing with FGFR3. (B) Western blotting showing the successful immobilisation of Affimers onto streptavidin resin after probing with streptavidin-HRP and (C) Western blotting showing the pull-down products of the Affimers after probing with anti-FGFR3 antibodies and anti-rabbit IgG antibodies – HRP. BiotAff = Biotinylated Affimer; FGFR3 = purified FGFR3 protein; No Aff = No Affimer; FG14 = FGFR3-14 Affimer; FG21 = FGFR3-21 Affimer; GFP = GFP. Affimer; Marker = Spectra™ multicolour broad range protein ladder (ThermoFisher Scientific).

4.3.5 ELISA to check the specificity of Affimers to FGFR3 protein

Non-specific binding is a common problem for immunoassays. There are a number of factors that may cause non-specific interaction between biomolecules, including interaction with scaffold of the bioreceptors. In order to prove whether the Affimers can bind specifically to FGFR3 protein, ELISA was utilised. In the assay, the selected Affimers against FGFR3 (FGFR3-14 and FGFR3-21) and GFP, were tested with different analytes including FGFR3, β -2-microglobulin, anti-digoxin IgG and human serum albumin. To set up the assay, each analyte was immobilised on an ELISA plate (Figure 4.14A) and then biotinylated Affimers were added and allowed to bind. After removing unbound Affimers, streptavidin-HRP was used to reveal whether binding had occurred. For each experiment, three replicates were included. Two independent experiments were repeated in order to confirm the results.

As presented in Figure 4.14B, FGFR3-21 Affimer had strong binding to FGFR3 protein but not to any of the other proteins. Affimer FGFR3-14 showed binding to FGFR3 but not as strongly as FGFR3-21. However, the results from double-sandwich ELISA, SPR and immunoprecipitation described previously showed that the strength of the binding between FGFR3-14 Affimer and FGFR3 protein was comparable as FGFR3-21 Affimer and FGFR3. It is assumed that the epitope on FGFR3 protein which was recognised by FGFR3-14 Affimer may form the interactions with the ELISA plate, preventing the Affimer from accessing the epitope. This may cause significantly lower level of detection of FGFR3 protein by this Affimer. As expected, the GFP Affimer, as a negative control showed no binding to FGFR3 protein.

The specificity of the selected Affimers to the FGFR3 protein is still unclear in this assay. The limitation of this experiment is that the assay could not distinguish between the wells with no protein and with non-FGFR3 proteins (β -2-microglobulin,

anti-digoxin IgG and human serum albumin). Although proteins can typically form hydrophobic interaction with polystyrene surfaces such as a 96-well plate it is still necessary for users to prove that the proteins are truly deposited on the surface. My recommendation is that antibodies specific to β -2-microglobulin, anti-digoxin IgG and human serum albumin can be used to detect their analytes, which are initially captured on the surface, via ELISA. By doing this, the specificity of the Affimers to only FGFR3 protein can be confirmed.

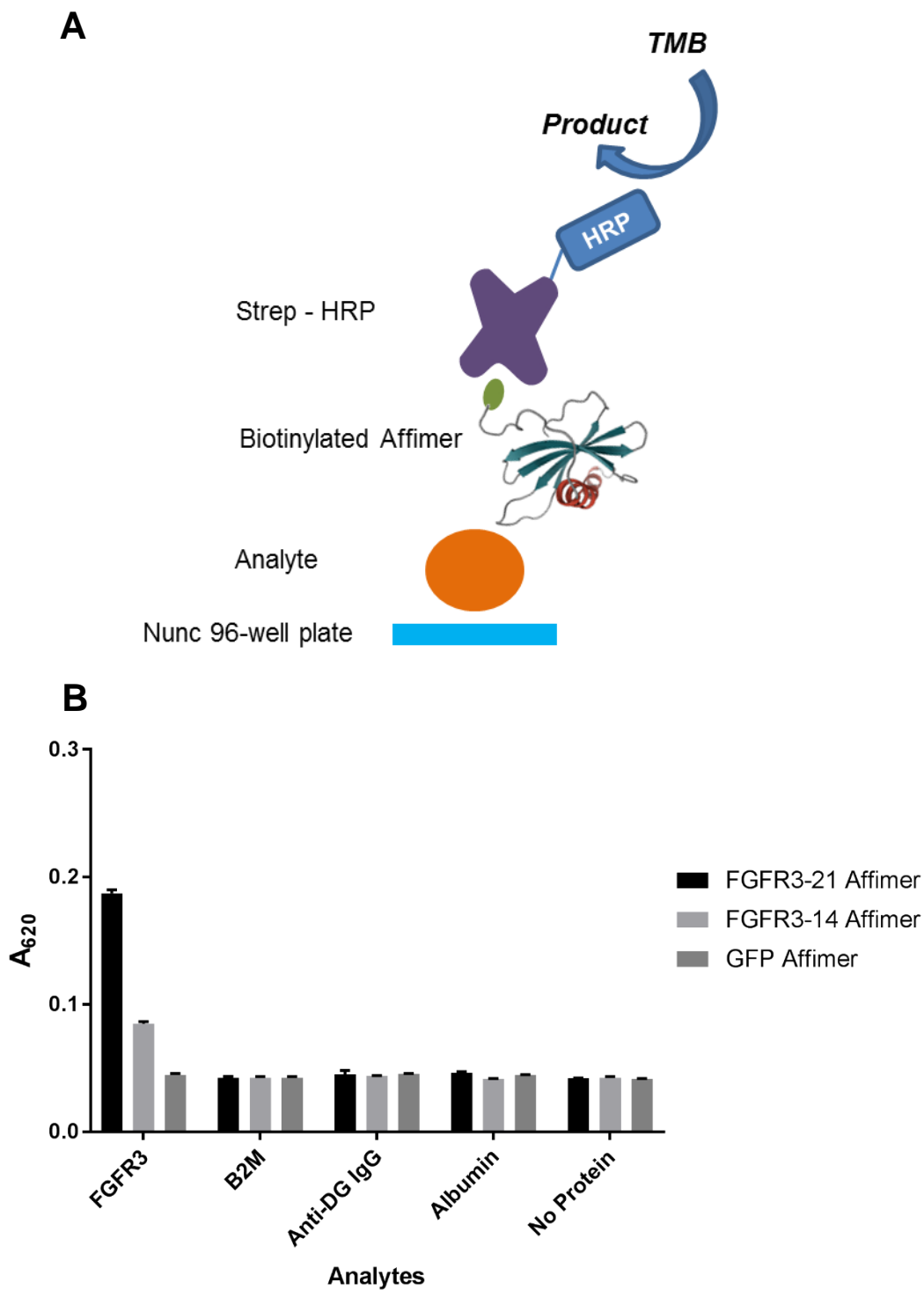


Figure 4.14 ELISA to confirm the specific binding of Affimers to FGFR3. (A) A schematic presenting the ELISA setup. (B) ELISA result upon the measurement of the absorbance at 620 nm showing anti-FGFR3-21 and FGFR3-14 Affimers bind to FGFR3 protein but do not bind to the other proteins tested. The error bars represent mean of $n = 3 \pm \text{SEM}$.

4.4 Discussion

The main focus of this chapter is to characterise the specific binding properties of Affimers selected from the phage display library against their targets, DDT and FGFR3. Several methods including ELISA, SPR and immunoprecipitation were employed to check the binding of the Affimers in soluble form to their analytes. As different analytes, a small molecule (DDT) and a protein (FGFR3), were used as the targets for the Affimers, the discussion will be split into two sections.

4.4.1 Affimers against DDT

ELISA was used to determine the binding between the selected Affimers and DDT. Even though the Affimers showed binding ability to biotinylated DDT attached onto a solid surface, they failed to bind DDT in its original form in a competitive ELISA. It was assumed that the Affimers recognised the DDT plus the spacer between DDT and biotin. Therefore the DDT moiety alone cannot interact strongly with the Affimers. One issue that we need to take into account is the methods used in phage display screening. Previously, the standard protocol for phage display screening recommended by BSTG required a biotinylated target and three panning rounds. However, this protocol may be suitable for larger analytes displaying multiple epitopes such as proteins, but not for small molecules like DDT. Recently, a protocol for Affimer screening against small molecules has been released (Tiede et al., 2017). In brief, counter selection was used to select Affimers against TNT. TNT was conjugated to two carrier proteins, ovalbumin and IgG. The competitive panning was performed using TNT-ovalbumin and TNT-IgG conjugates as well as ovalbumin and IgG. With this method, Affimers specific to TNT could be obtained. The protocol could be applied to select Affimers against DDT, but one issue to be considered is

the hydrophobic nature of DDT which makes it fairly insoluble in water. The conjugation of DDT to carrier proteins can be more difficult than for water-soluble small molecules.

4.4.2 Affimers against FGFR3

To characterise the binding of Affimers selected against FGFR3 protein, sandwich ELISA, immunoprecipitation (pull-down assay) and SPR were utilised. The sandwich ELISA and immunoprecipitation are both qualitative methods that are useful for studying protein-protein interactions. In the ELISA, anti-FGFR3-14 and FGFR3-21 Affimers showed strong binding to FGFR3 protein, which agreed with the performance of FGFR3-14 and FGFR3-21 Affimers in the pull-down assay. The FGFR3-8 Affimer showed the lowest level of binding to FGFR3 compared to the other two Affimers according to the result from the ELISA. It was assumed that the immobilisation of the FGFR3-8 Affimer may affect its binding ability since in the immunofluorescence staining assay (Dr. Darren Tomlinson - personal communication) showed a high binding level of FGFR3-8 Affimer to FGFR3 protein similar to that shown by FGFR3-14 and FGFR3-21 Affimers.

Surface plasmon resonance (SPR) is an optical sensing platform widely used to study binding kinetics parameters. SPR revealed that among the three selected Affimers, FGFR3-14 and FGFR3-21 were able to bind FGFR3 protein whilst FGFR3-8 failed to do so in this system. This supported the outcome of sandwich ELISA and immunoprecipitation methods. SPR provides a dissociation constant (K_D), which gives the strength of affinity between the receptor and ligand. The SPR data for both FGFR3-14 and FGFR3-21 Affimers were found to fit well to a one site binding model as expected because each Affimer contains one binding site and should have recognised one epitope on the protein. However, the K_D values obtained from the

fitting software were pM to nM (K_D for FGFR3-14 Affimer = 327 pM and K_D for FGFR3-21 Affimer = 18.5 pM), which seem to be overestimated as compared to the K_D of Affimers against other targets (Tiede et al., 2014, Raina et al., 2015, Sharma et al., 2016). At least three independent repeats for the SPR experiment should be performed in order to ensure the consistency of the measurement. Furthermore, K_D determination using other approaches such as radiolabelled ligand binding assay and fluorescence anisotropy should be performed in order to have confidence in the K_D values determined.

In this chapter, ELISA also used to examine the specificity of the Affimers to different types of analytes. In addition to FGFR3, Affimers were tested for their non-specific binding to β -2-microglobulin, anti-digoxin IgG and human serum albumin. It was found that anti-FGFR3-21 and FGFR3-14 Affimers showed binding to FGFR3 protein whereas the anti-GFP Affimer did not bind to FGFR3 protein. However, the evidence showing whether the Affimers bind to other proteins (β -2-microglobulin, anti-digoxin IgG and human serum albumin) is still needed to confirm the presence of the proteins on an ELISA plate. The data obtained from different characterisation methods suggested that either FGFR3-14 or FGFR3-21 Affimer could be used as the Affimer specific to FGFR3 protein for biosensor construction.

Chapter 5

Biosensor fabrication

5.1 Introduction

Impedimetric biosensors are known for their high sensitivity in detecting biological events. The technique is label-free, cost effective, easy to operate and applicable for different types of biorecognition elements such as enzymes, antibodies, synthetic peptides and oligonucleotides. During the past decades, an increasing number of impedimetric biosensors capable of monitoring a wide range of targets have been released. In general, multiple steps are involved in impedimetric biosensor fabrication. It is important that the sensor performance needs to be stable and reproducible. To achieve the highest efficiency of the sensors, strict and careful optimisation for the sensor construction protocol is required in order to minimise any variations that commonly occur during the construction processes.

The main focus of this chapter was to apply the Affimers obtained from Chapter 3 and Chapter 4 as bioreceptors for constructing impedimetric biosensors to detect FGFR3 protein. Two sensor construction protocols, the ELISHA “gluing method” and NeutrAvidin-biotin based procedure, were studied. As commonly known, a number of factors can govern the sensor performance and these affect the reproducibility of the sensors. We developed a NeutrAvidin-biotin interaction protocol where Affimer concentration, NeutrAvidin concentration, and effects of different blocking agents on sensor performance were investigated to establish an optimum protocol for biosensor fabrication.

5.2 Construction of impedimetric biosensors using ELISHA gluing method

The ELISHA “gluing method” is a protocol for fabricating impedimetric biosensors with Affimers. The protocol was developed by ELISHA Ltd. Selected Affimer binders were prepared using a mixture containing 5 mM octopamine and a bifunctional linker supplied by the company. This method allows control of the correct orientation of the Affimers when immobilised onto the sensor surface, thus allowing the optimum accessibility of the analyte (FGFR3) to the binding site on the Affimer.

In Figure 5.1, the construction overview of a sensor in accordance with ELISHA gluing method is presented. An anti-GFP Affimer was used as a negative control receptor and immobilised onto working electrode 1. Anti-FGFR3-21 Affimer was selected as the specific receptor to FGFR3 protein and immobilised onto working electrode 2. In order to immobilise both Affimers to a sensor chip, cyclic voltammetry was utilised as stated in Section 2.2.7.1. During the polymerisation of octopamine together with the Affimer-linker conjugates, a cyclic voltammogram was obtained (Figure 5.2). In the first cycle, there was a small peak representing the oxidation of octopamine at 0.65 V. However, the event could not be detected during the second CV scan. These data showed that octopamine has self-limiting growth property as with other non-conducting polymers e.g. tyramine (Ahmed et al., 2013, Losic et al., 2005). After the immobilisation, it was expected that the Affimers were tethered onto a layer of polyoctopamine via the bifunctional linker shown in Figure 5.1.

The fully constructed sensors were tested with FGFR3 protein in PBS buffer over the concentrations range from 10^{-15} to 10^{-8} M. The response of the sensors showed that the impedance signal represented by Nyquist plots decreased as

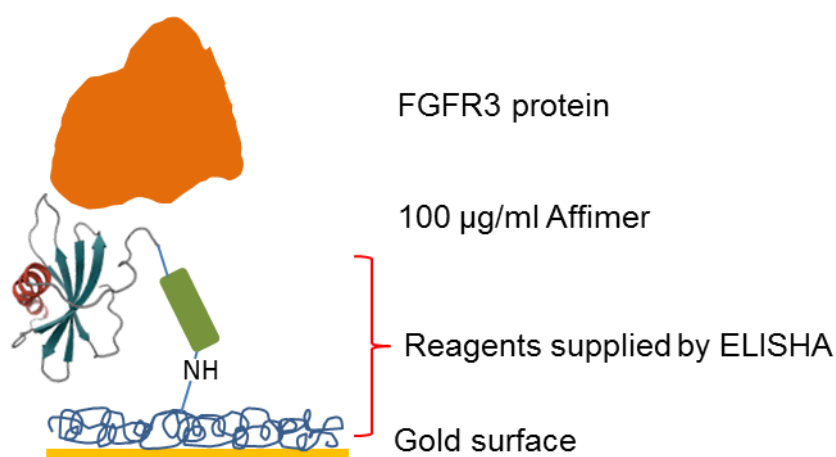


Figure 5.1 Schematic representation of a sensor constructed following the ELISHA “gluing” method. The Affimer was immobilised onto the polymer layer via a specific linker provided by ELISHA Ltd prior to FGFR3 addition.

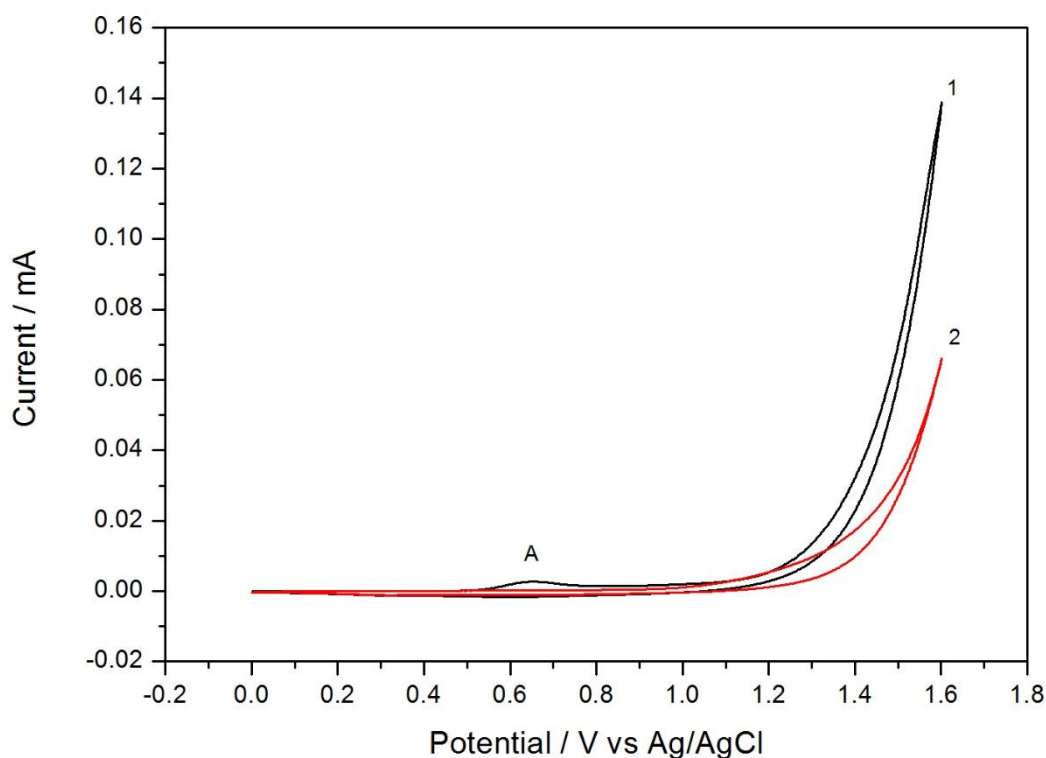


Figure 5.2 A cyclic voltammogram of polyoctopamine and Affimer deposition onto a Dropsens gold screen-printed electrode. The CV was performed for 2 cycles from 0-1.6 V at a scan rate of 100 mV/s. (A) is an oxidation peak at 0.65 V whereas (1) and (2) are CV scan cycles.

FGFR3 concentrations increased (Figure 5.3A). Sensor response was reported via the charge transfer resistance (R_{ct}) which was automatically calculated by NOVA software. Data were normalised by subtracting R_{ct} for each FGFR3 concentration with R_{ct} at the baseline (PBS buffer) and transformed to percent change in R_{ct} . The data showed that decrease in R_{ct} from 20% - 40% was found when exposing FGFR3-21 sensors to FGFR3 protein over the concentrations of 10^{-15} – 10^{-14} M, but beyond this range the R_{ct} value was almost constant (Figure 5.3B). In anti-GFP Affimer sensors which served as a negative control, a shift in impedance between -20% and -35% could be observed over the same FGFR3 range. This effect occurred because of non-specific binding of FGFR3 protein to the sensor surface, leading to a decrease in impedance on both FGFR3-21 and GFP Affimer sensors. It is plausible that the ELISHA gluing method was not suitable for making sensors to detect FGFR3 protein. However, the ELISHA gluing method has been successfully used to fabricate impedimetric biosensors to detect carcinoembryonic antigen (CEA) as a biomarker for colorectal cancer (Mrs. Shazana Shamsuddin - personal communication). Different target proteins have distinct properties thanks to their amino acid patterns and post-translational modifications. For example, CEA protein has over 60% glycosylation by mass, which may prevent non-specific binding to the modified surface on the electrode. Therefore, other sensor fabrication methods were considered in order to construct impedimetric biosensors for FGFR3 detection.

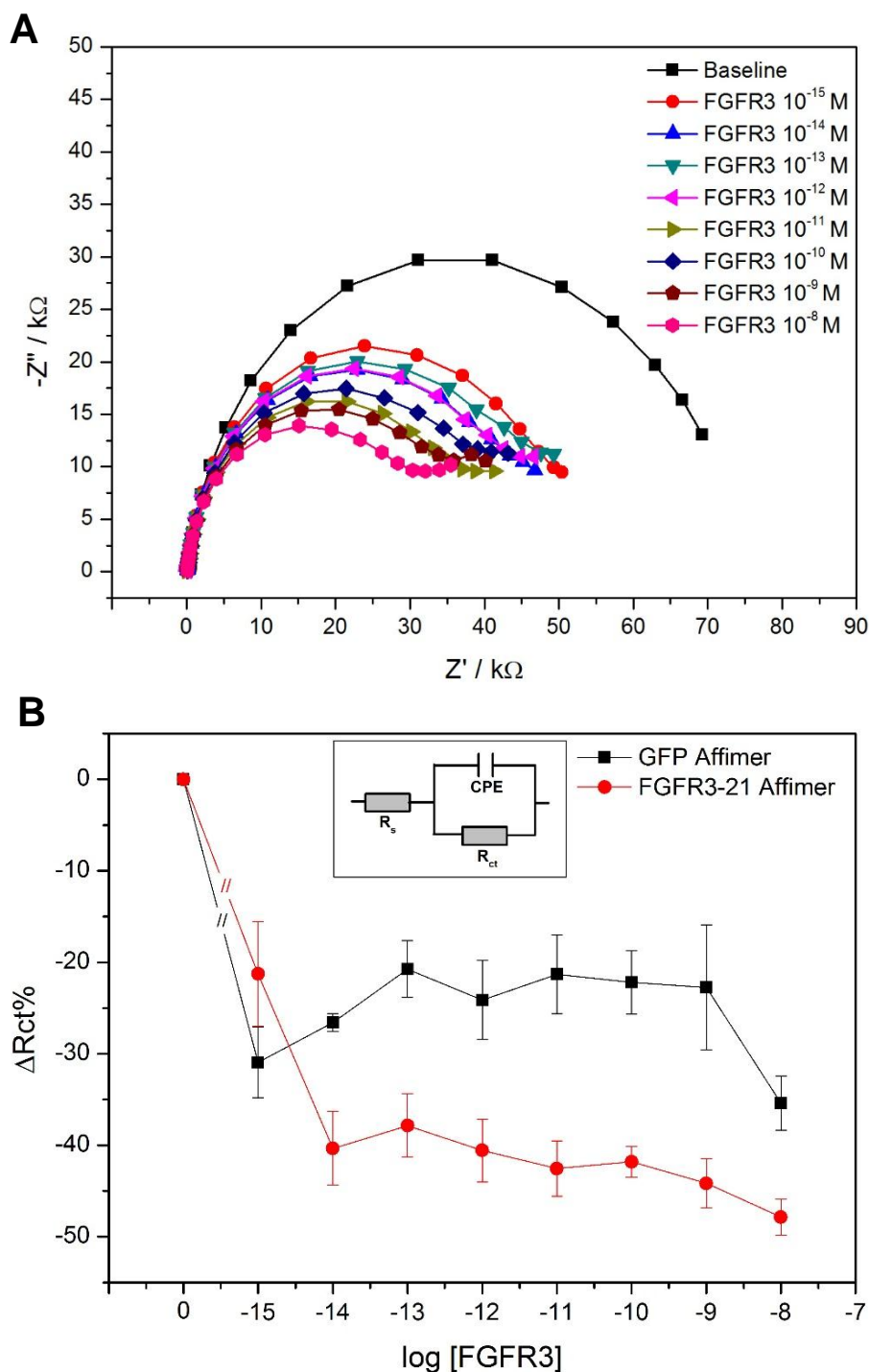


Figure 5.3 Sensor response after cumulative addition of FGFR3 concentrations. (A) Nyquist plots of impedance represent a PBS buffer baseline and a fully constructed FGFR3-21 Affimer-based sensor after exposing to 10^{-15} – 10^{-8} M FGFR3, respectively. (B) Calibration of the Affimer-based sensors for detecting FGFR3 protein ($n = 4 \pm \text{SEM}$). The response of the sensors was displayed in term of $\Delta R_{ct}\%$. Inset is the Randles' equivalent circuit model for this system where R_s is solution resistance, R_{ct} is charge transfer resistance and CPE is constant phase element.

5.3 Biosensor fabrication via NeutrAvidin-biotin linkage of the Affimers

5.3.1 Overview of sensor fabrication

The avidin-biotin interaction is known as the strongest non-covalent interaction used for bioconjugation with a dissociation constant (K_D) of approximately 10^{-15} M provided the bioreceptor is tethered by a specific residue. This type of interaction can offer specific orientation when attempting to tether a protein receptor onto the solid surface. In the work in this thesis, NeutrAvidin, a reengineered avidin which has no glycosylation, was used. Previously, avidin-biotin linkages were used to set up ELISA, SPR and immunoprecipitation assays in order to study specific binding between the Affimers and FGFR3 protein. A positive response resulting from Affimers-FGFR3 interaction was observed through all the three assays. Therefore, a NeutrAvidin-biotin interaction was also employed for impedimetric biosensor construction as well.

To fabricate a sensor chip for electrochemical impedance measurement, a layer-by-layer sensor construction protocol previously described (Ahmed et al., 2013, Rushworth et al., 2014) was modified. As presented in Figure 5.4, a molecule of biotinylated Affimer was immobilised onto polytyramine-coated gold surface via the NeutrAvidin-biotin interaction. At each step of immobilisation, polytyramine, NHS-biotin, NeutrAvidin and biotinylated Affimer were respectively deposited on working electrodes with washing in PBS in between as stated in Section 2.2.7.2.

The stability of the polymer layer is one of the most indispensable factors contributing to the sensitivities and specificities of biosensors. Polytyramine has been widely used in biosensor applications (Ahmed et al., 2013, Pournaras et al., 2008, Rushworth et al., 2014, Wu et al., 2005, Yang et al., 2012)

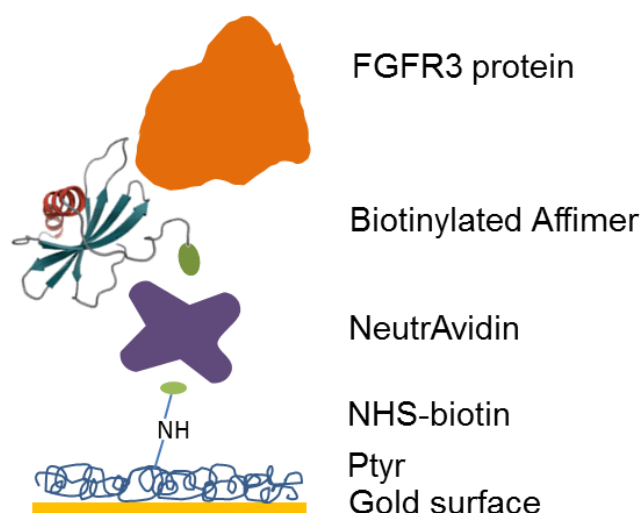


Figure 5.4 Schematic illustration of a fully-constructed Affimer-based sensor. The gold surface on an electrode chip was initially coated with polytyramine. Then a high affinity “NeutrAvidin-biotin linkage” allowed biotin-tagged Affimer to be tethered to the surface in an oriented fashion.

because it offers high stability, less or no conductivity and capabilities of self-controlling thickness and porosity (Ahmed et al., 2013, Losic et al., 2005). In this work, tyramine was prepared in 0.3 M NaOH in dH₂O prior to electropolymerisation. Typically there was a small peak evident at 0.5 V vs Ag/AgCl, indicating oxidation of the tyramine during the first cycle of CV while this event could not be seen in the second cycle (Figure 5.5). This confirmed polytyramine’s self-limiting property during polymerisation. The Nyquist plots showed that after electropolymerisation of polytyramine on the gold surface, the impedance increased, indicating successful polymer deposition (Figure 5.6). In the previous publications, tyramine was generally prepared in 0.3 M NaOH in absolute methanol (Ahmed et al., 2013, Pournaras et al., 2008, Rushworth et al., 2014). However, it was found here that using methanol as a solvent may cause an insufficient thickness of polytyramine layer coated as a base layer for Affimer-based sensors, leading to the inconsistency of the baseline

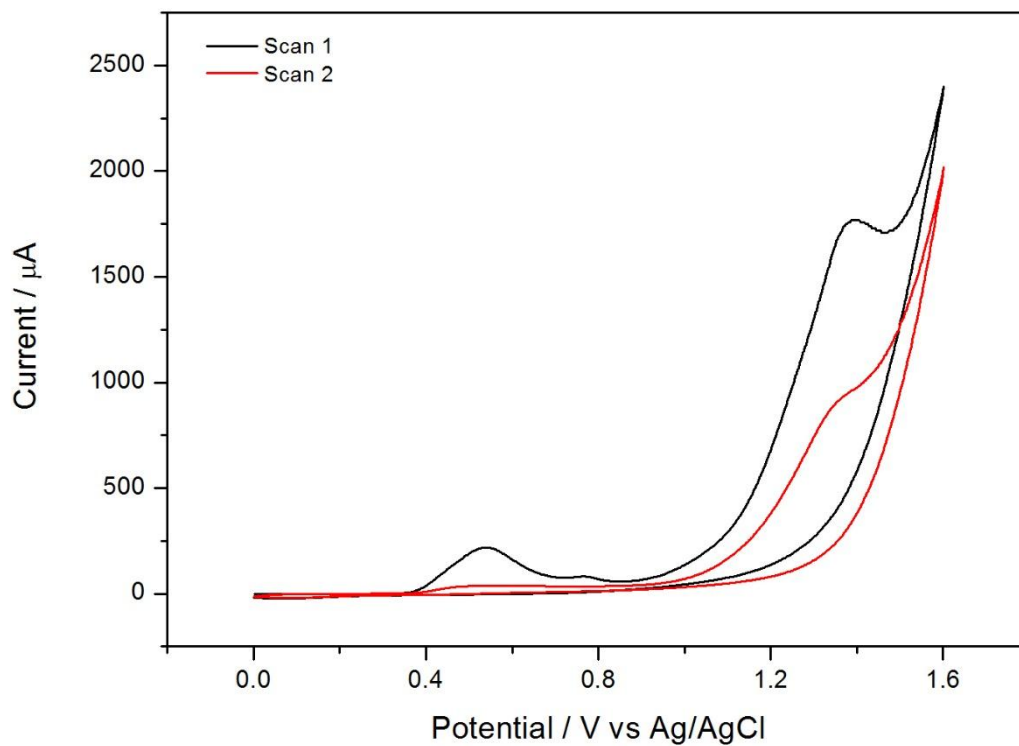


Figure 5.5 Cyclic voltammogram of polytyramine deposition. Cyclic voltammetry was performed in 25 mM tyramine in dH_2O with 0.3 M NaOH. The CV scan was run for two cycles from 0-1.6 V at a scan rate of 200 mV/s.

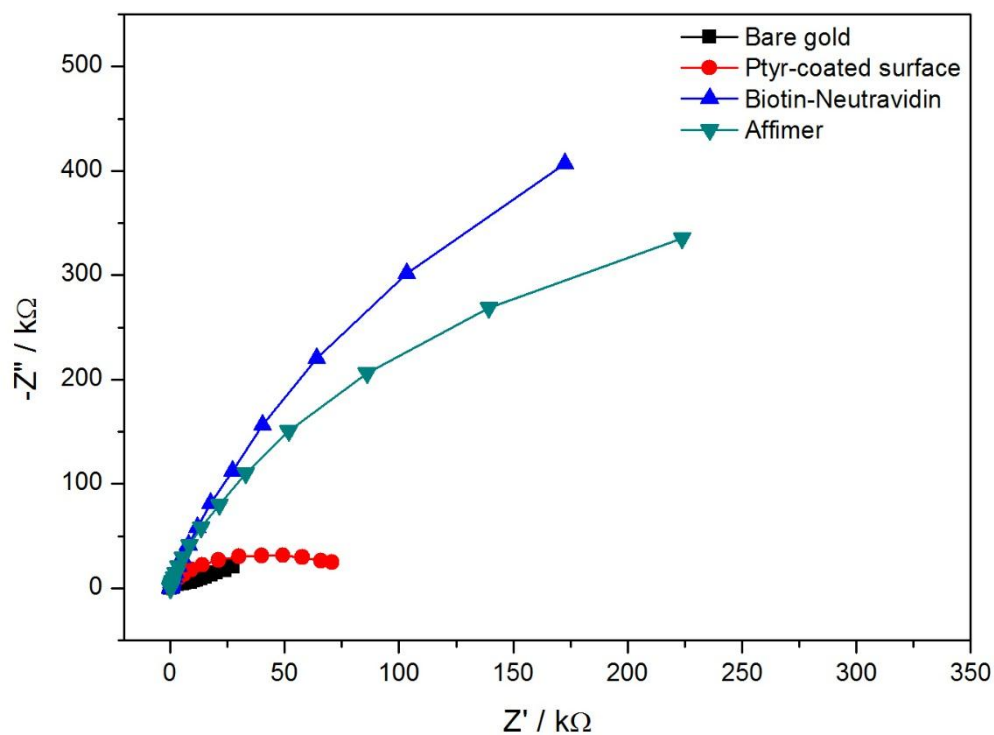


Figure 5.6 Nyquist plot showing layer-by-layer construction of an FGFR3-21 Affimer-based biosensor. The measurement was performed in a solution of 100 mM PBS pH 7.2 containing 10 mM $K_3Fe(CN)_6/K_4Fe(CN)_6$ over a range of frequencies from 2.5 kHz to 250 mHz. Nyquist plots were generated when using bare gold surface, polytyramine-coated surface, surface coated with biotin-NeutrAvidin and sensor with biotin-tagged FGFR3-21 Affimer immobilised.

and the responses when exposing sensors to the target. Changing the solvent to 0.3 M NaOH in dH₂O resulted in an increase of resistance and capacitance of the polymer layer (Figure 5.7), indicating increasing thickness of the polytyramine layer. As a result, the overall responses of the sensors were more consistent and reproducible.

After electropolymerisation of polytyramine, NHS-biotin and NeutrAvidin were introduced sequentially to the polytyramine-coated electrodes. NeutrAvidin was used as a bridge to tether biotinylated Affimers to the biotinylated transducer surface. As expected, there was a large shift in impedance after NHS-biotin and NeutrAvidin additions since deposition of large molecules can hinder the transfer of charge components to the transducer surface, resulting in an increase in resistance and decrease in capacitance (Figure 5.6). As each electrode chip contains two working electrodes, anti-GFP Affimer was immobilised on working electrode 1 as a negative control receptor whilst FGFR3-21 Affimer was captured on working electrode 2. However, the introduction of the Affimer to the functionalised surface resulted in decrease in impedance (Figure 5.6), implying that the binding of biotinylated Affimers to NeutrAvidin caused increased conductivity of the sensor surface.

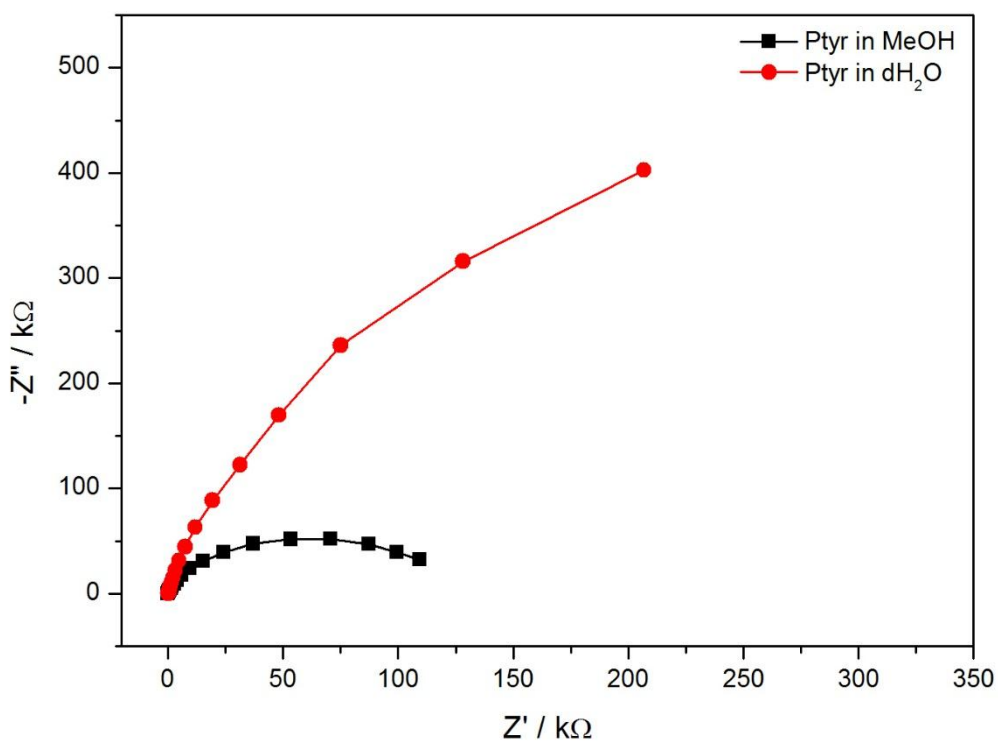


Figure 5.7 Nyquist plot showing two fully constructed FGFR3-21 Affimer-based biosensors with the polytyramine layer prepared in different solvents. The sensor deposited with polytyramine prepared in 0.3 M NaOH in MeOH and the sensor prepared using polytyramine dissolved in 0.3 M NaOH in dH₂O are compared. The measurement was performed in a solution of 100 mM PBS pH 7.2 containing 10 mM K₃Fe(CN)₆/K₄Fe(CN)₆ over a range of frequencies from 2.5 kHz to 250 mHz.

5.3.2 Electrochemical impedance spectroscopy for detection of FGFR3

In this study, prior to incubating the fully constructed biosensors with FGFR3 protein, four consecutive impedance measurements were performed to set the baseline (PBS buffer) for data normalisation. As presented in Figure 5.8, the impedance signal for the baseline was almost constant after the 4th measurement, indicating that the sensors were ready for testing with FGFR3 protein. The sensors were then incubated with increasing concentrations of FGFR3 protein in PBS buffer

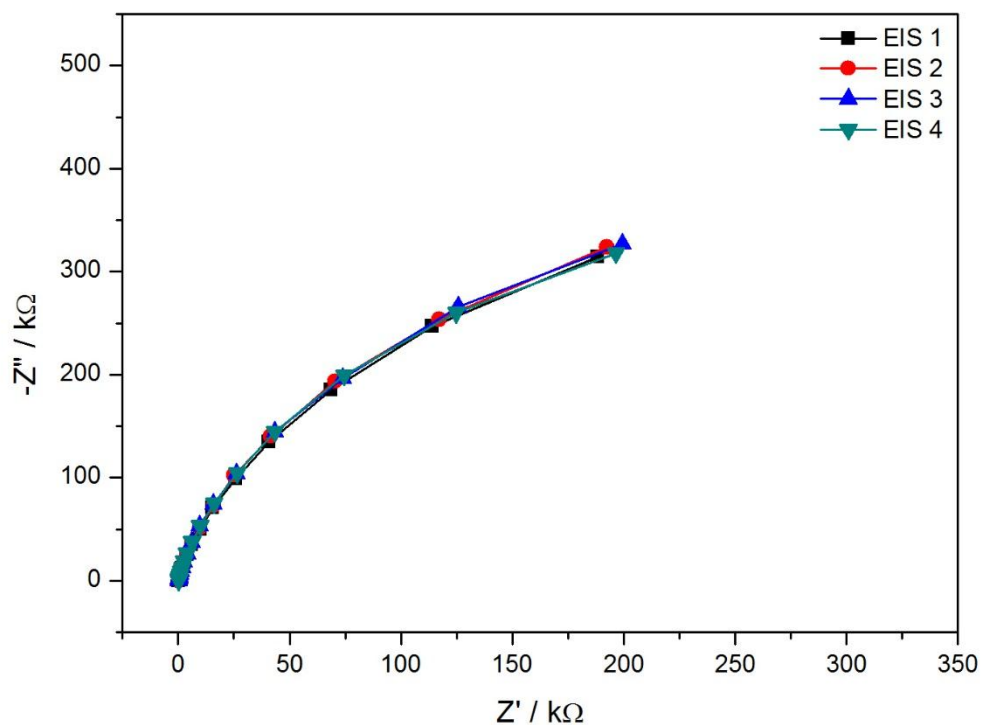


Figure 5.8 Impedance spectra showing the stability of baseline before a sensor was tested with a range of FGFR3 concentrations. Four consecutive impedance measurements were performed after a fully constructed sensor was incubated in PBS buffer for 1 h. The measurement was performed in a solution of 100 mM PBS pH 7.2 containing 10 mM $K_3Fe(CN)_6/K_4Fe(CN)_6$ over a range of frequencies from 2.5 kHz to 250 mHz.

varying from 10^{-14} M to 10^{-8} M with washes in between. The sensors were immersed in 10 mM $K_3Fe(CN)_6/K_4Fe(CN)_6$ redox mediator to perform EIS measurement. The EIS Nyquist plots from a representative sensor with FGFR3-21 Affimer immobilised are presented in Figure 5.9. It was observed that there was a decrease in impedance with the increasing FGFR3 concentrations. Mostly, in previous publications binding of analyte to its bioreceptor leads to an increase in impedance (Ahmed et al., 2013, Billah et al., 2010, Caygill et al., 2012, Millner et al., 2012). However, it has also been reported that the binding between synthetic proteins and their analytes sometimes causes a decrease in impedance (Goode et al., 2016, Rushworth et al., 2014). This observation can also be supported by the recent finding using Affimers to detect carcinoembryonic antigen (CEA), a glycoprotein biomarker for colorectal cancer where a decrease in impedance was found after exposing the Affimer sensors to CEA analyte (Mrs. Shazana Shamsuddin - personal communication). Nanobodies derived from camelid single chain antibodies in (Goode et al., 2016) are similar in size to the Affimers used in this study. Therefore, the decrease in impedance detected here could be explained by a similar mechanism. It has been suggested that the unexpected decrease in impedance happens owing to stresses in the polymer layer from the interaction of a large analyte with its small bioreceptor (Goode, 2015). The coated polymer on electrodes is semi-solid, making it quite mobile and flexible like a sponge (Bartlett and Cooper, 1993). When larger analytes bind to smaller bioreceptors tethered on the polymer layer, the immediate change of mass may cause a polymer shift on the surface, generating pinholes which let charged components pass through the polymer layer to contact with gold surface underneath. This process is known as the 'pinholing effect' and the reduction of the barriers to charge transfer process leads to the increasing conductivity across the sensor surface (Bharathi et al., 2001, Goode, 2015). This means that the resistance and

capacitance on the sensor interface are lowered, resulting in the decreasing impedance that was observed.

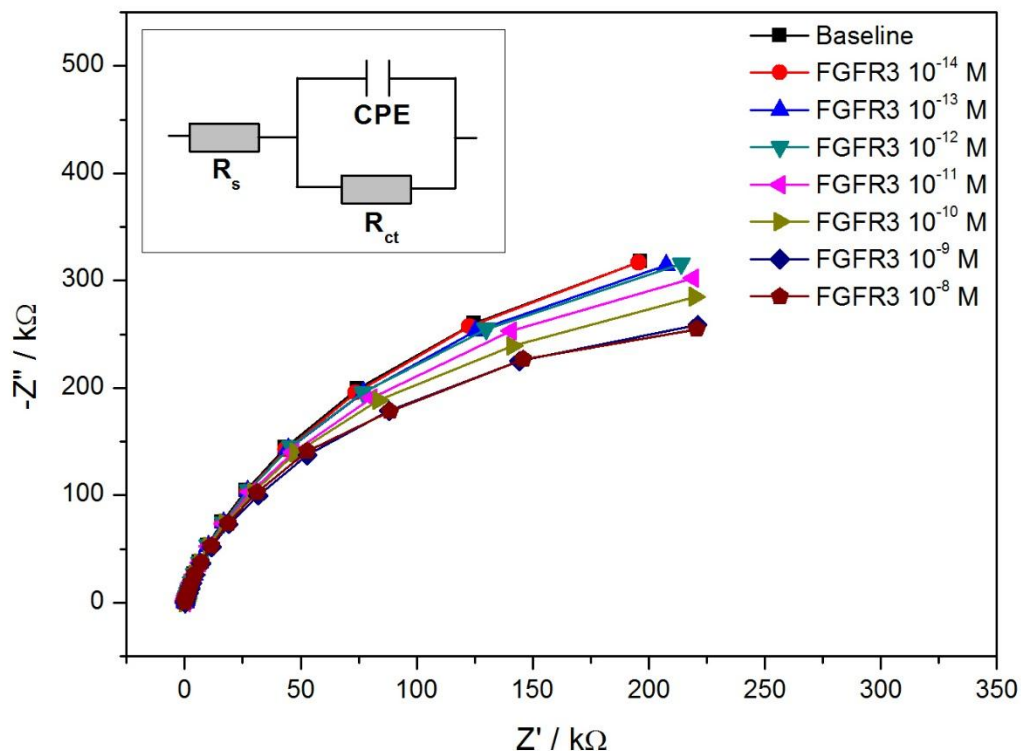


Figure 5.9 Impedance spectra after cumulative addition of FGFR3 concentrations ranging from 10^{-14} M to 10^{-8} M to a fully constructed sensor. Nyquist plots of impedance represent a baseline (PBS buffer) and a fully constructed FGFR3-21 Affimer sensor after exposing to 10^{-14} – 10^{-8} M FGFR3, respectively. The measurement was performed in a solution of 100 mM PBS pH 7.2 containing 10 mM $K_3Fe(CN)_6/K_4Fe(CN)_6$ over a range of frequencies from 2.5 kHz to 250 mHz. Inset is the Randles' equivalent circuit model for this system, where R_s = solution resistance, R_{ct} = charge-transfer resistance, and CPE = constant phase element.

In this thesis, R_{ct} values were initially used for monitoring the performance of fully fabricated sensors in response to FGFR3 protein as most faradaic impedance biosensors rely on the change in the R_{ct} as the analyte binds (Billah et al., 2010, Rushworth et al., 2014, Barton et al., 2008, Ahmed et al., 2013, Johnson et al., 2012). However, as seen in Figure 5.9, the limitation of using the R_{ct} is that approximately

half of semi-circular shape of a Nyquist plot was obtained from the impedance measurement, possibly resulting in inaccuracy in R_{ct} calculation when the data were fitted with the Randles' equivalent circuit model. Therefore, other alternatives were considered for presenting our sensor performance.

Change in capacitance is another way of showing the response of impedimetric biosensors. A shift in real part of capacitance was employed to monitor the binding of the targets to the modified surface (Jolly et al., 2015, Jolly et al., 2016, Weiss et al., 2005). However, it should be noted that their work relied on non-faradaic impedance measurement. To obtain the real component of capacitance, the impedance data were first converted into complex capacitance using Equation 2.8 as presented in Section 2.2.7.3. The real part of capacitance was plotted on the X-axis against the imaginary part of capacitance on the Y-axis, and this is called a Cole-Cole plot. Figure 5.10 shows the Cole-Cole plot of a representative of FGFR3-21 Affimer sensors after exposing to a range of FGFR3 concentrations. Only slight change in the real part of capacitance (C') could be seen here as the concentration of FGFR3 increased, indicating stable and thick layers on the electrode surface, which is unaffected by the biorecognition events. Significant changes, however, could be detected at the low frequencies of the impedance measurements. These are known as low frequency relaxations (Weiss et al., 2005). The sensors were highly resistive due to the thick layers of material deposited on them. The changes observed here indicated the binding of FGFR3 protein to the immobilised Affimers, which occurred beyond the thick layers on the electrode and did not affect the capacitance (Weiss et al., 2005). However, the small changes in capacitance were tried as the alternative to R_{ct} to monitor the sensor response in this work. To analyse the response of the sensor, the real part of capacitance at the far end of the semicircular curve was used and will be described in the next section.

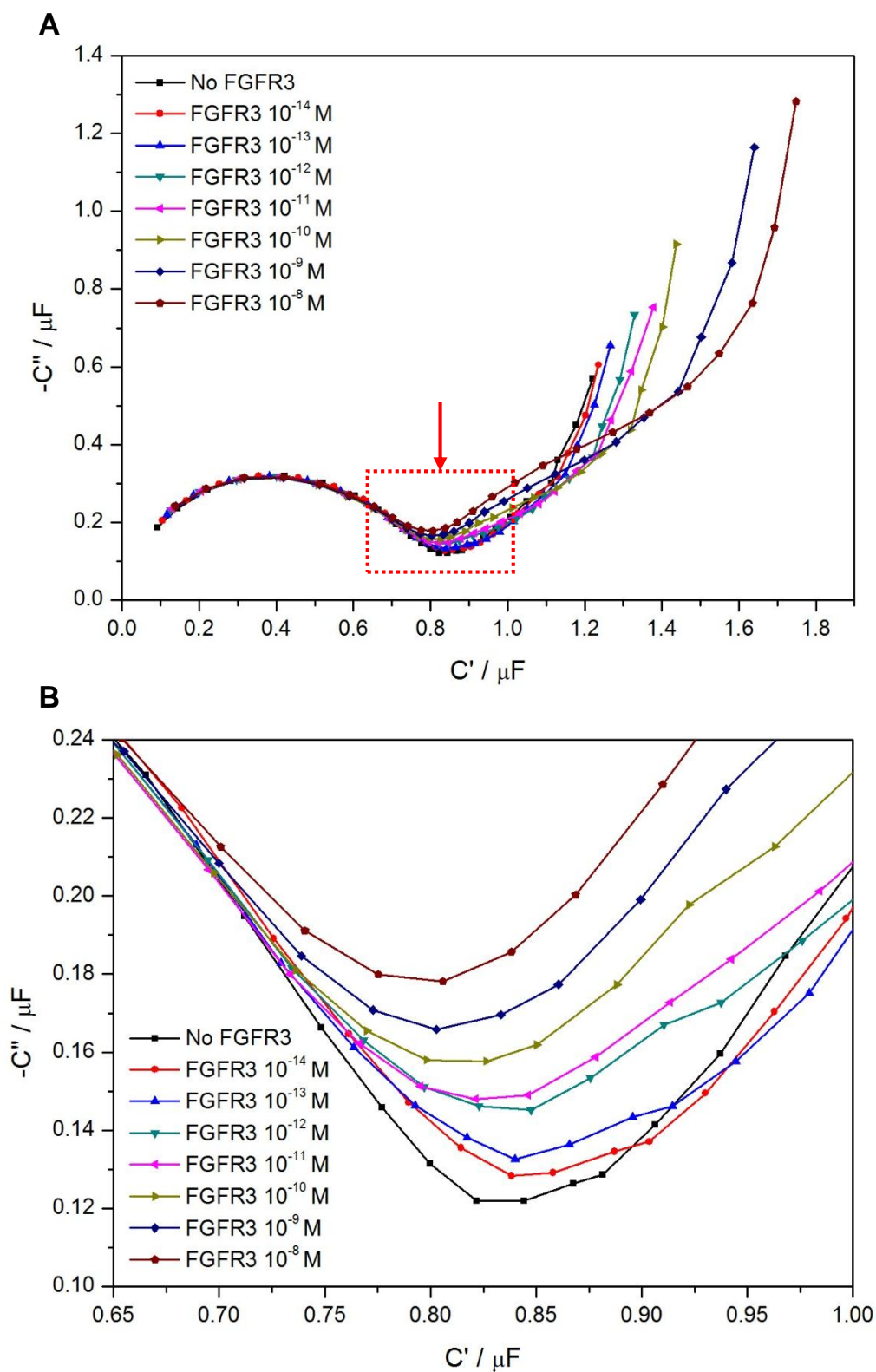


Figure 5.10 The typical Cole-Cole plot showing complex capacitance of a FGFR3-21 Affimer biosensor before and after exposing to FGFR3 protein from 10^{-14} M to 10^{-8} M (A) is the plot showing the full semicircular curves with low frequency relaxations whereas (B) is the zoomed-in area indicated by the red arrow (\rightarrow) in (A).

Phase shift is another approach that has been employed to evaluate the biorecognition events in impedance biosensor platforms. The phase shift is typically measured at a specific low frequency (0.1 Hz) to monitor the binding between the Affimers and the target analytes on the electrode surface (Sharma et al., 2016, Raina et al., 2015). However, again their sensor systems were non-faradaic. In this thesis, phase shift was plotted against a range of frequencies as shown in Figure 5.11. The lowest frequency presenting the maximum phase shift in this work was at 7.9 Hz. Therefore, the phase shift at this frequency was picked for further analysis and will be described in the next section.

The other method worth using to evaluate the response of biosensors is the change in absolute impedance ($|Z|$). The absolute impedance was used to present the impedance sensor response in the previous studies (Dapra et al., 2013, Park et al., 2018). The absolute values of impedance measured were plotted against a range of frequencies as shown in Figure 5.12. The data at 0.25 Hz were selected to be used for further analysis as the largest changes were observed at this point and will be described in the next section.

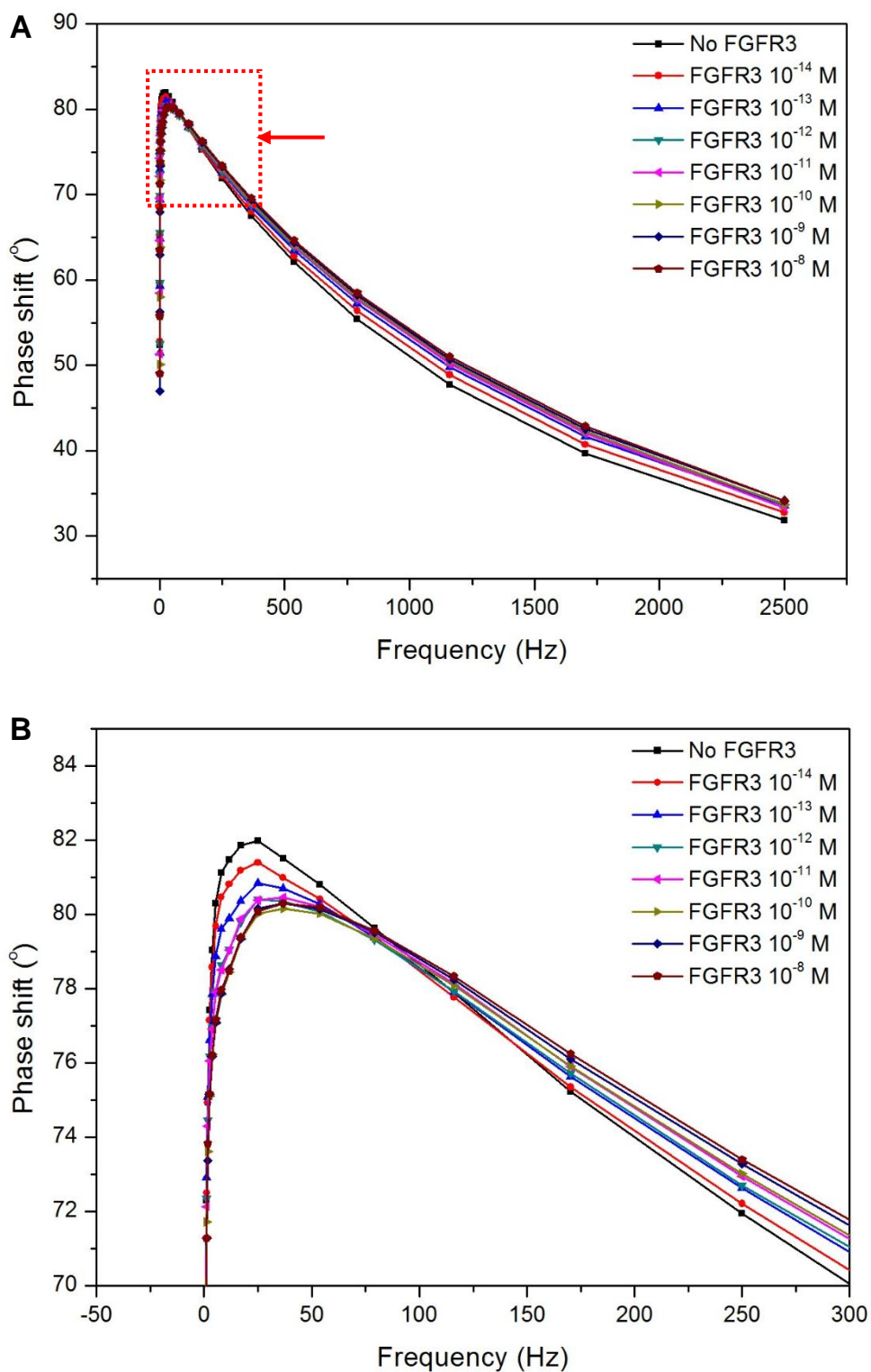


Figure 5.11 The plot showing the relationship between phase shift and frequencies of a FGFR3-21 Affimer biosensor. (A) shows the change in phase angle of the sensor before and after exposing to different concentration of FGFR3 and (B) is the close-up area as indicated by the red arrow (\rightarrow) in (A).

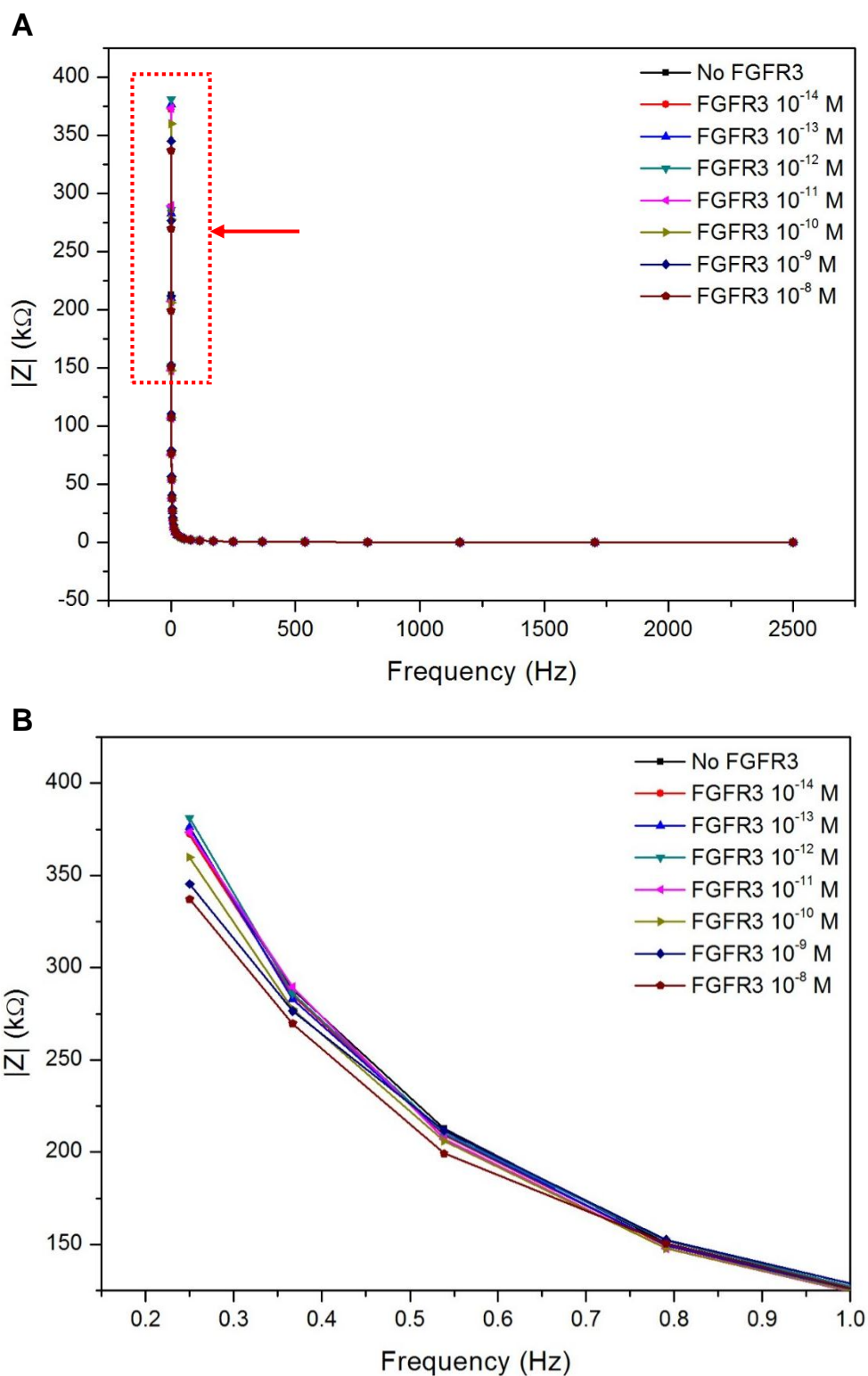


Figure 5.12 The plot showing the relationship between absolute values of impedance and frequencies of a FGFR3-21 Affimer biosensor. (A) shows the change in the absolute impedance of the sensor before and after exposing to different concentration of FGFR3 and (B) is the close-up area as indicated by the red arrow (\rightarrow) in (A).

5.3.3 Optimisation of methods for biosensor fabrication

Until now, there has been no electrochemical platform to detect FGFR3 protein in biological samples from human sources. The detection of FGFR3 in human fluids can be performed using an FGFR3 ELISA kit which is commercially available (ab214027, Abcam, UK). The reported dynamic range of detection is typically pM to nM, which has been used as a reference for developing impedimetric biosensors for FGFR3 detection because, as yet, there are no reports on the pathological levels of FGFR3 in biological samples, e.g. urine and serum. To achieve the construction of sensitive and specific biosensors to any analyte, a number of factors apart from the specificity of bioreceptors to the target are involved in sensor performance, reproducibility and stability. In this work, Affimer concentrations, NeutrAvidin concentrations and the effect of blocking agents were studied.

5.3.3.1 Optimising concentration of Affimers

One of the most critical factors to be taken into account is the optimum concentration of bioreceptors immobilised on the surface of the sensor electrode. This is because too high concentration of bioreceptors may lead to a high packing density of material on the surface, resulting in steric hindrance and the possibility of non-specific binding of unwanted components. In contrast, in the case of an insufficient amount of bioreceptors, the sensors may not generate sufficient response upon the binding of the analyte.

In this section, a range of Affimer concentration, from 0.05 to 1 μM , were examined while the concentrations of NHS-biotin and NeutrAvidin were fixed at 3 and 0.1 μM , respectively. Anti-GFP Affimer was used as a negative control on working electrode 1 whilst anti-FGFR3-21 Affimer was immobilised on working electrode 2. After consecutive 15 min incubations in the solution containing FGFR3 protein

ranging from 10^{-14} to 10^{-8} M, with washing in PBS in between, EIS measurements were performed in the presence of 10 mM $K_3Fe(CN)_6/K_4Fe(CN)_6$ redox mediator. To evaluate the performance of the sensor after testing with FGFR3 protein, four different approaches, namely changes in charge-transfer resistance, capacitance, phase shift and absolute values of impedance, were used to analyse the impedance data.

The first procedure used to analyse the sensor response is the changes in R_{ct} . At 0.05 μ M Affimer, it can be observed that although different responses on the negative control (GFP Affimer) and FGFR3-21 Affimer sensors can be seen, there was no significant change in R_{ct} upon increasing the FGFR3 concentrations (Figure 5.13A). When the concentration of Affimers was increased up to 0.1 μ M, a significant decrease of % R_{ct} was detected with an increase of FGFR3 concentrations on the specific sensors as the response on the negative control sensors remained constant with a slight drop at higher FGFR3 concentrations (Figure 5.13B). However non-specific binding was detected, causing a 5-20% change in R_{ct} on negative control sensors. At an Affimer concentration of 0.3 μ M, a steady decrease in % R_{ct} was observed on the FGFR3-21 Affimer sensor whilst no change in R_{ct} responses can be seen on control sensors (Figure 5.13C). Finally, at 1 μ M Affimers applied to the sensors, the decrease in R_{ct} can be seen on both FGFR3-21 and anti-GFP (negative control) sensors (Figure 5.13D). This may be due to the transducer surface being overcrowded at high concentration of bioreceptors, causing a steric hindrance effect. Conclusively, the optimal concentration of biotinylated Affimers used for the construction of biosensors here was 0.3 μ M.

Another method used to show the sensor performance is the changes in real part of capacitance (C'). At the Affimer concentration of 0.05 μ M, the capacitance increased 2% for FGFR3-21 Affimer sensors and 3% for GFP Affimer at 10^{-14} M before decreasing to -1% (FGFR3-21 Affimer) and 0% (GFP Affimer) at 10^{-8} M

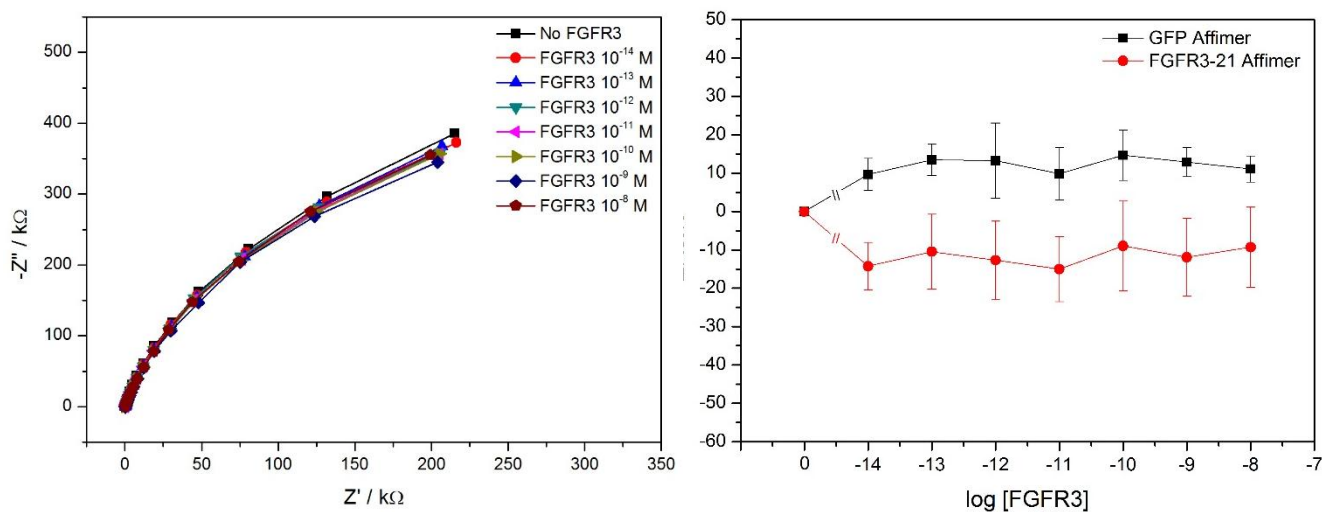
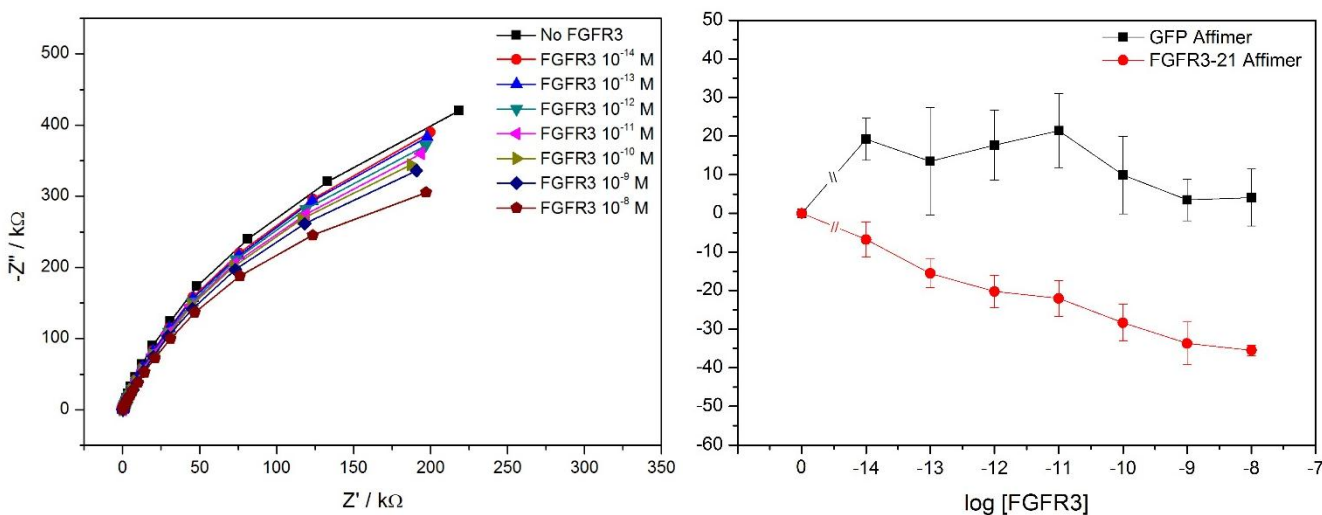
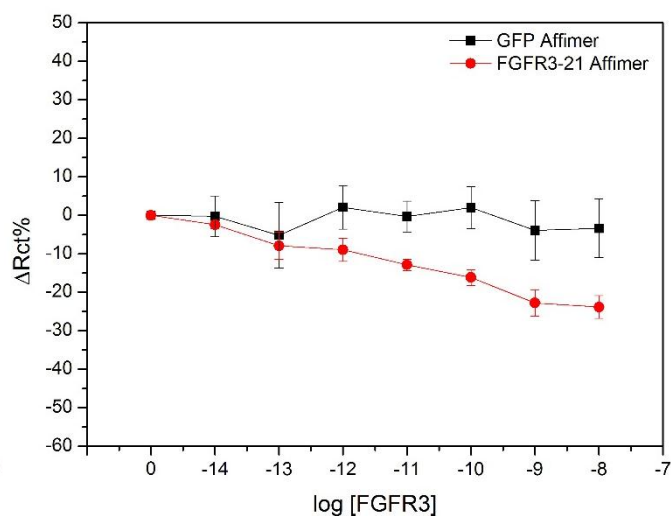
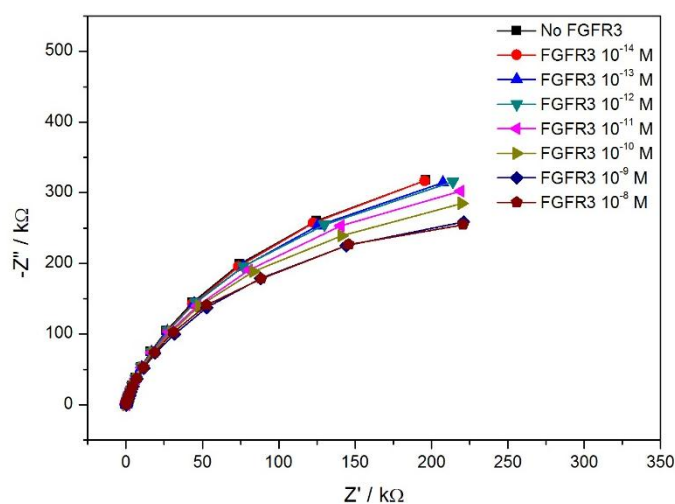
A 0.05 μM Affimer**B** 0.1 μM Affimer

Figure 5.13 Optimisation of Affimer concentration for impedimetric biosensors with data analysis based on the R_{ct} values. The figures on the left panel are Nyquist plot representatives of a FGFR3-21 Affimer sensor and the figures on the right panel are calibration curves of the biosensors for detecting FGFR3 in PBS buffer. Four different concentrations of Affimer, 0.05 μM , (A, $n = 4 \pm \text{SEM}$); 0.1 μM , (B, $n = 4 \pm \text{SEM}$); 0.3 μM , (C, $n = 3 \pm \text{SEM}$), and 1 μM , (D, $n = 3 \pm \text{SEM}$), were tested. The sensors were challenged with cumulative concentrations of FGFR3 ranging from 10^{-14} M to 10^{-8} M with PBS washes in between. The EIS measurements were performed in the presence of 10 mM $\text{K}_3\text{Fe}(\text{CN})_6/\text{K}_4\text{Fe}(\text{CN})_6$ redox mediator. The response of the sensors was displayed as $\Delta R_{ct}(\%)$.

C 0.3 μM Affimer



D 1 μM Affimer

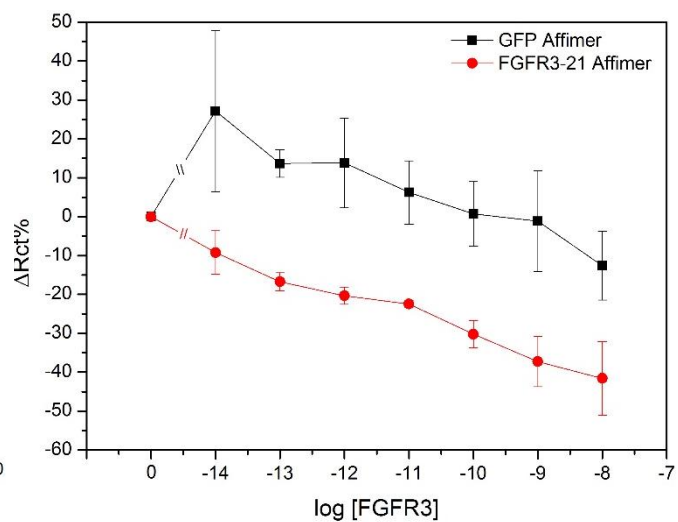
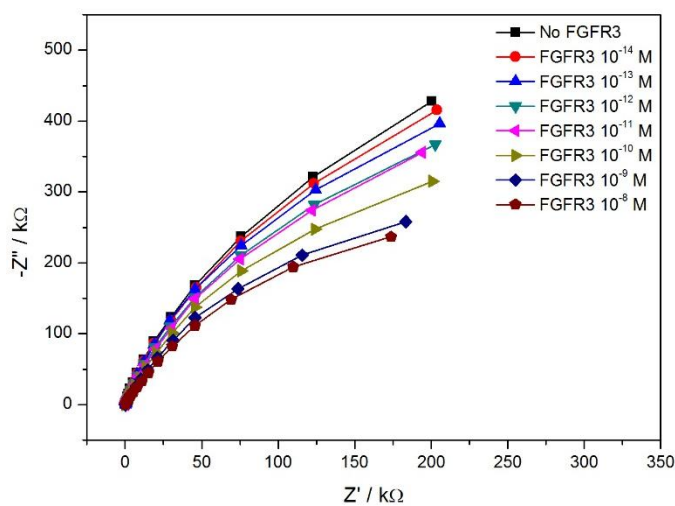


Figure 5.13 (continued) Optimisation of Affimer concentration for impedimetric biosensors with data analysis based on the R_{ct} values. Four different concentrations of Affimer, 0.05 μM , (A, $n = 4 \pm \text{SEM}$); 0.1 μM , (B, $n = 4 \pm \text{SEM}$); 0.3 μM , (C, $n = 3 \pm \text{SEM}$), and 1 μM , (D, $n = 3 \pm \text{SEM}$), were tested.

FGFR3. There was no significant difference between the response on the FGFR3-21 Affimer and control sensors (Figure 5.14A). The concentration of Affimers was then increased to 0.1 μM . At this concentration, the $\Delta C'$ values were increased to 2% (FGFR3-21 Affimer) and 3.5% (GFP Affimer) at 10^{-14} M FGFR3 and decreased to around -2% (both Affimers) at 10^{-8} M FGFR3. Again, the sensors could not distinguish between specific and non-specific response (Figure 5.14B). At 0.3 μM Affimer, the $\Delta C'$ for FGFR3-Affimer sensors increased about 2% at 10^{-14} M FGFR3 but remained stable at 0% for GFP Affimer sensors. The decrease in $\Delta C'$ was seen for both Affimer sensors until reaching 10^{-8} M FGFR3 with the $\Delta C'$ of -4% (Figure 5.14C). The sensors failed to show the signal from specific interaction of FGFR3 and the Affimer. At an Affimer concentration of 1 μM , the increase in $\Delta C'$ to 2% for both FGFR3-21 and GFP Affimer sensors was seen when challenging the sensors with 10^{-14} – 10^{-13} M FGFR3 before the decrease in $\Delta C'$ at higher concentrations of FGFR3 (Figure 5.14D). At 10^{-8} M FGFR3, the $\Delta C'$ dropped to -2% for FGFR3-21 Affimer sensors and -3% for control sensors. As the trends for FGFR3-21 and GFP Affimer sensor performance were similar, specific response could not be seen. From the above results, using the changes in capacitance proved ineffective for use to show the response of our fabricated Affimer-based impedimetric biosensors. Hence, other approaches will be considered here.

The changes of phase angle is another method used to monitor the binding of the Affimers and FGFR3 protein on biosensors in this thesis. At an Affimer concentration of 0.05 μM , the phase angles were almost unchanged for both specific Affimer and control sensors with phase shift between 0° to -1° as the concentration of FGFR3 increased (Figure 5.15A). The response from specific interaction of FGFR3 and the Affimer could not be seen at this Affimer concentration. As the concentration of Affimers was changed to 0.1 μM , a decrease of phase angles was observed on both specific Affimer and control sensors with the a between 0° and -5° as the

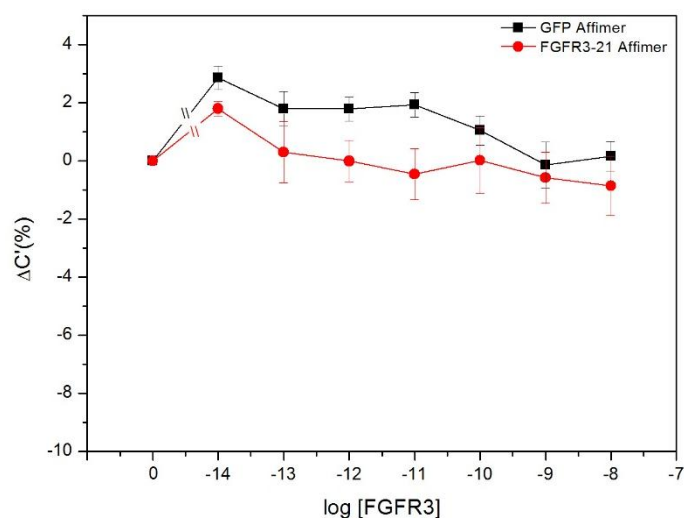
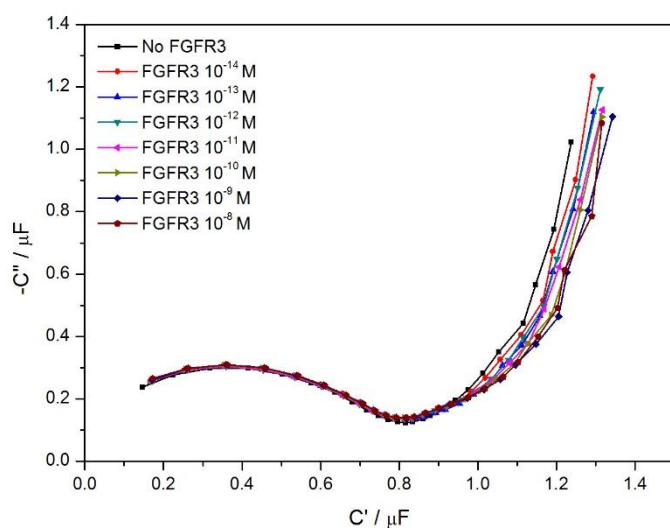
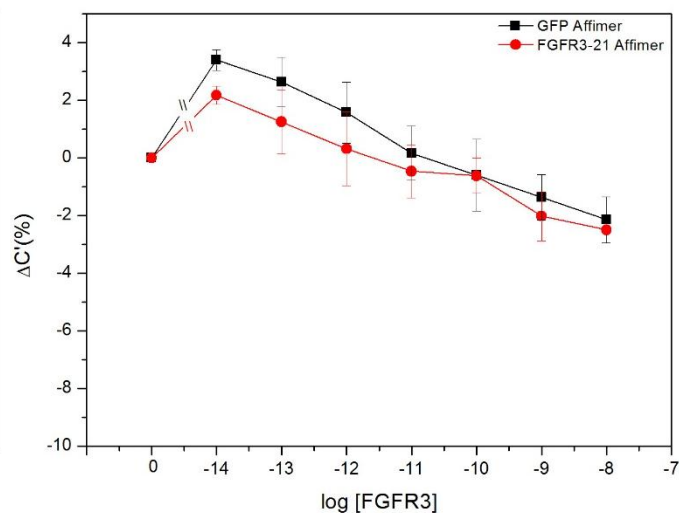
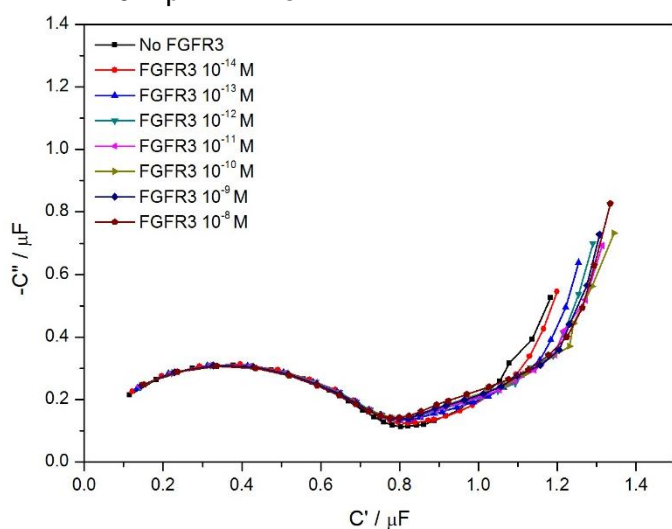
A 0.05 μM Affimer**B** 0.1 μM Affimer

Figure 5.14 Optimisation of Affimer concentration for impedimetric biosensors with data analysis based on the capacitance values. The figures on the left panel are Cole-Cole plots of a FGFR3-21 Affimer sensor and the figures on the right panel are calibration curves of the biosensors for detecting FGFR3 in PBS buffer. Four different concentrations of Affimer, 0.05 μM , (A, $n = 4 \pm \text{SEM}$); 0.1 μM , (B, $n = 4 \pm \text{SEM}$); 0.3 μM , (C, $n = 3 \pm \text{SEM}$), and 1 μM , (D, $n = 3 \pm \text{SEM}$), were tested. The sensors were challenged with cumulative concentrations of FGFR3 ranging from 10^{-14} M to 10^{-8} M with PBS washes in between. The EIS measurements were performed in the presence of 10 mM $\text{K}_3\text{Fe}(\text{CN})_6/\text{K}_4\text{Fe}(\text{CN})_6$ redox mediator. The response of the sensors was displayed as $\Delta C' (\%)$.

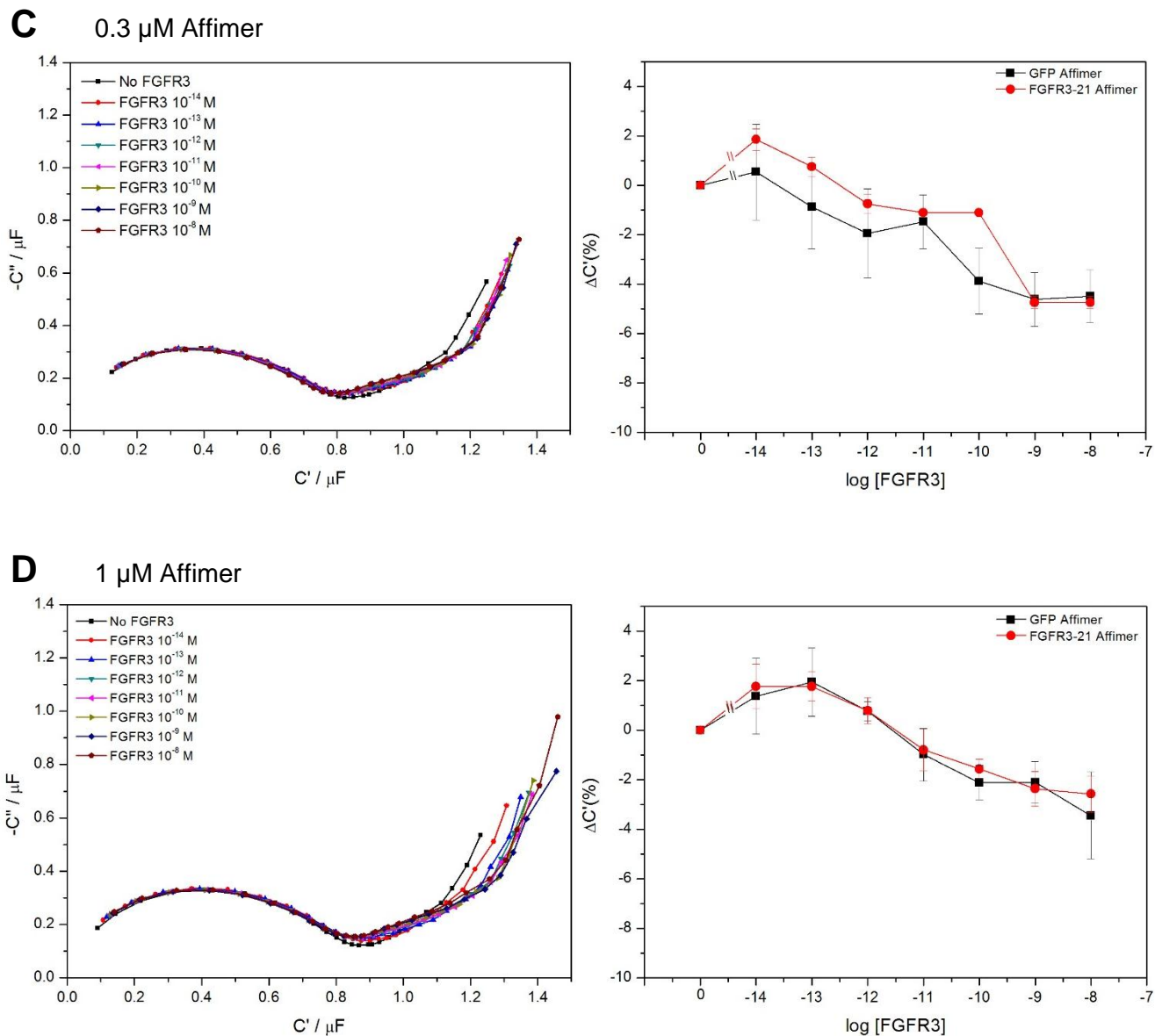


Figure 5.14 (continued) Optimisation of Affimer concentration for impedimetric biosensors with data analysis based on the capacitance values. Four different concentrations of Affimer, 0.05 μM , (A, $n = 4 \pm \text{SEM}$); 0.1 μM , (B, $n = 4 \pm \text{SEM}$); 0.3 μM , (C, $n = 3 \pm \text{SEM}$), and 1 μM , (D, $n = 3 \pm \text{SEM}$), were tested.

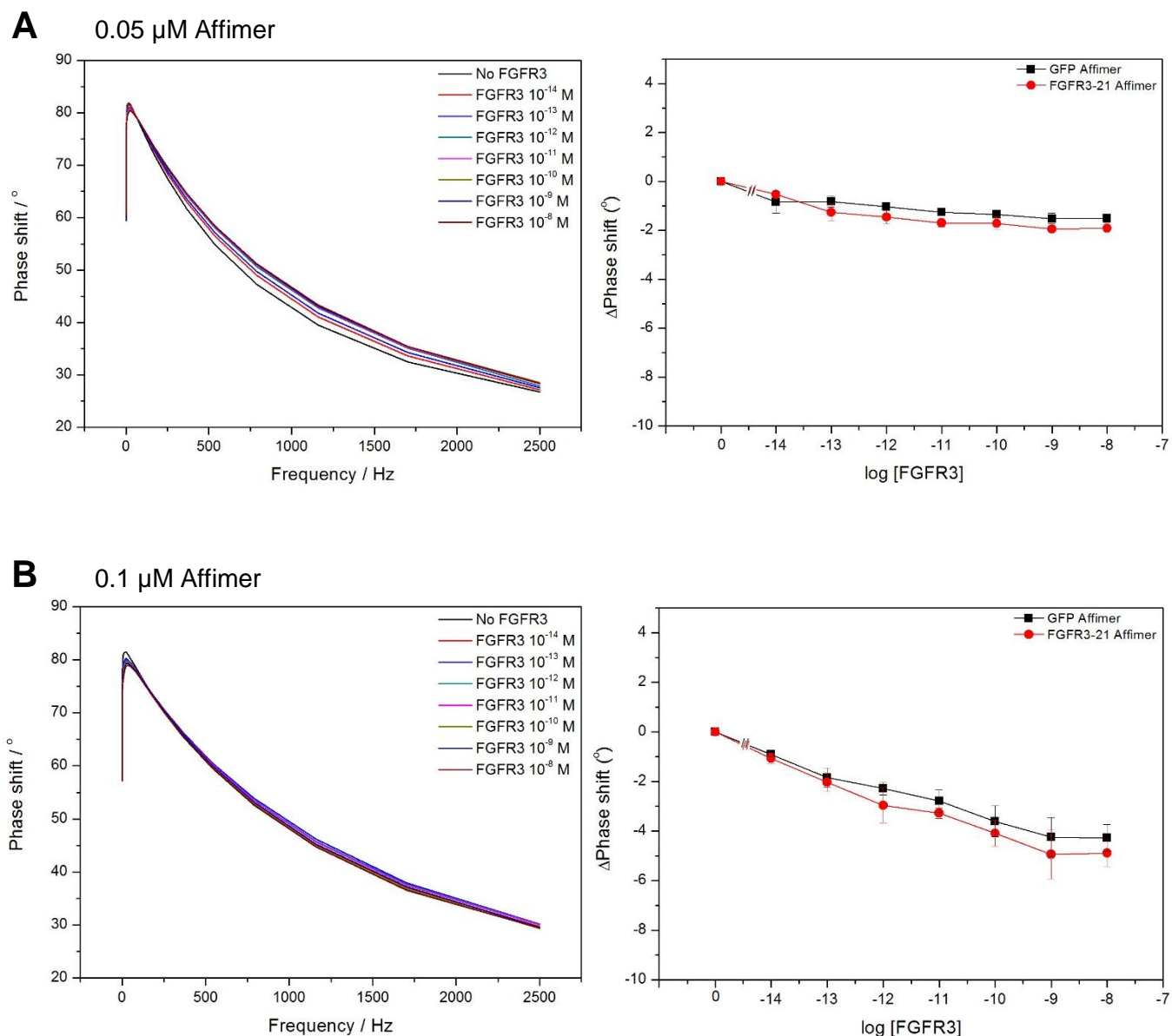


Figure 5.15 Optimisation of Affimer concentration for impedimetric biosensors with data analysis based on the phase shift. The figures on the left panel are phase shift-frequency plots of a FGFR3-21 Affimer sensor and the figures on the right panel are calibration curves of the biosensors for detecting FGFR3 in PBS buffer. Four different concentrations of Affimer, 0.05 μM , (A, $n = 4 \pm \text{SEM}$); 0.1 μM , (B, $n = 4 \pm \text{SEM}$); 0.3 μM , (C, $n = 3 \pm \text{SEM}$), and 1 μM , (D, $n = 3 \pm \text{SEM}$), were tested. The sensors were challenged with cumulative concentrations of FGFR3 ranging from 10^{-14} M to 10^{-8} M with PBS washes in between. The EIS measurements were performed in the presence of 10 mM $\text{K}_3\text{Fe}(\text{CN})_6/\text{K}_4\text{Fe}(\text{CN})_6$ redox mediator. The response of the sensors was displayed as phase shift ($^\circ$).

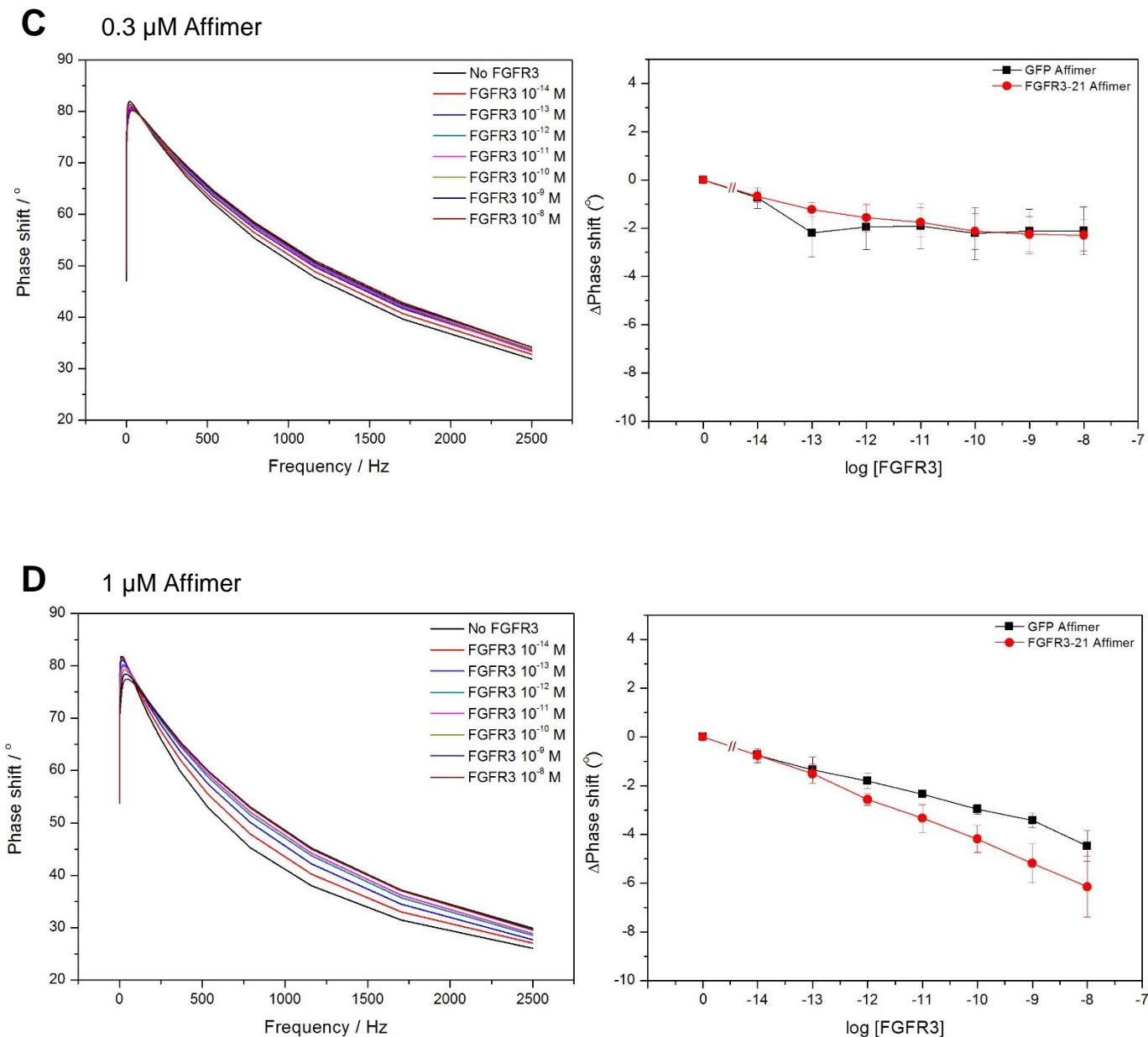


Figure 5.15 (continued) Optimisation of Affimer concentration for impedimetric biosensors with data analysis based on the phase shift. Four different concentrations of Affimer, 0.05 μM , (A, $n = 4 \pm \text{SEM}$); 0.1 μM , (B, $n = 4 \pm \text{SEM}$); 0.3 μM , (C, $n = 3 \pm \text{SEM}$), and 1 μM , (D, $n = 3 \pm \text{SEM}$), were tested.

concentration of FGFR3 increased (Figure 5.15B). However, the sensors could not distinguish specific from non-specific response. As the concentration of Affimer was increased to 0.3 μM , the phase shift was detected between 0° and -2° over an increasing range of FGFR3 concentrations (Figure 5.15C). The sensors still could not be used to show the signal from specific binding of FGFR3 to the Affimer. At 1 μM Affimers, the decrease of phase shift was seen on both FGFR3-21 and GFP Affimer sensors. The phase angle decreased to -1.5° for both Affimer sensors at 10^{-13} M FGFR3, but the response of phase shift for these two Affimer sensors showed differences at higher concentrations of FGFR3 (Figure 5.15D). At FGFR3 of 10^{-8} M, the phase shift for FGFR3-21 Affimer sensors was about -6° whilst that for control sensors was -4° . However, these changes were still not sufficient to distinguish specific from non-specific response. This suggested that the phase shift is not suitable to use as a method to see the sensor performance in our work.

The last approach for monitoring the binding of FGFR3 to Affimers in our work is the change in absolute values of impedance ($|Z|$). At an Affimer concentration of 0.05 μM , as the concentration of FGFR3 increased, the $\Delta|Z|$ for control sensors was almost stable with a shift between 0% and -2% whilst the $\Delta|Z|$ for FGFR3-21 Affimer sensors remained in the range of -5% to -10% (Figure 5.16A). At 0.1 μM Affimer concentration, a decrease in $\Delta|Z|$ was detected on both FGFR3-21 Affimer and control sensors. The decrease of $\Delta|Z|$ from 0% to -10% was seen on the control sensors whereas the $\Delta|Z|$ for the FGFR3-21 Affimer sensors dropped continually to -20% (Figure 5.16B). Although the difference of specific and non-specific response could be seen, the change was insufficient for further use, especially in the case of biological sample tests with high background noise. Finally, as the concentration of Affimers was increased to 0.3 μM , the $\Delta|Z|$ for control sensors was almost stable between 0% and -4% whereas the $\Delta|Z|$ for FGFR3-21 Affimer sensors decreased from 0% to -8% when the concentration of FGFR3 was increased (Figure 5.16C).

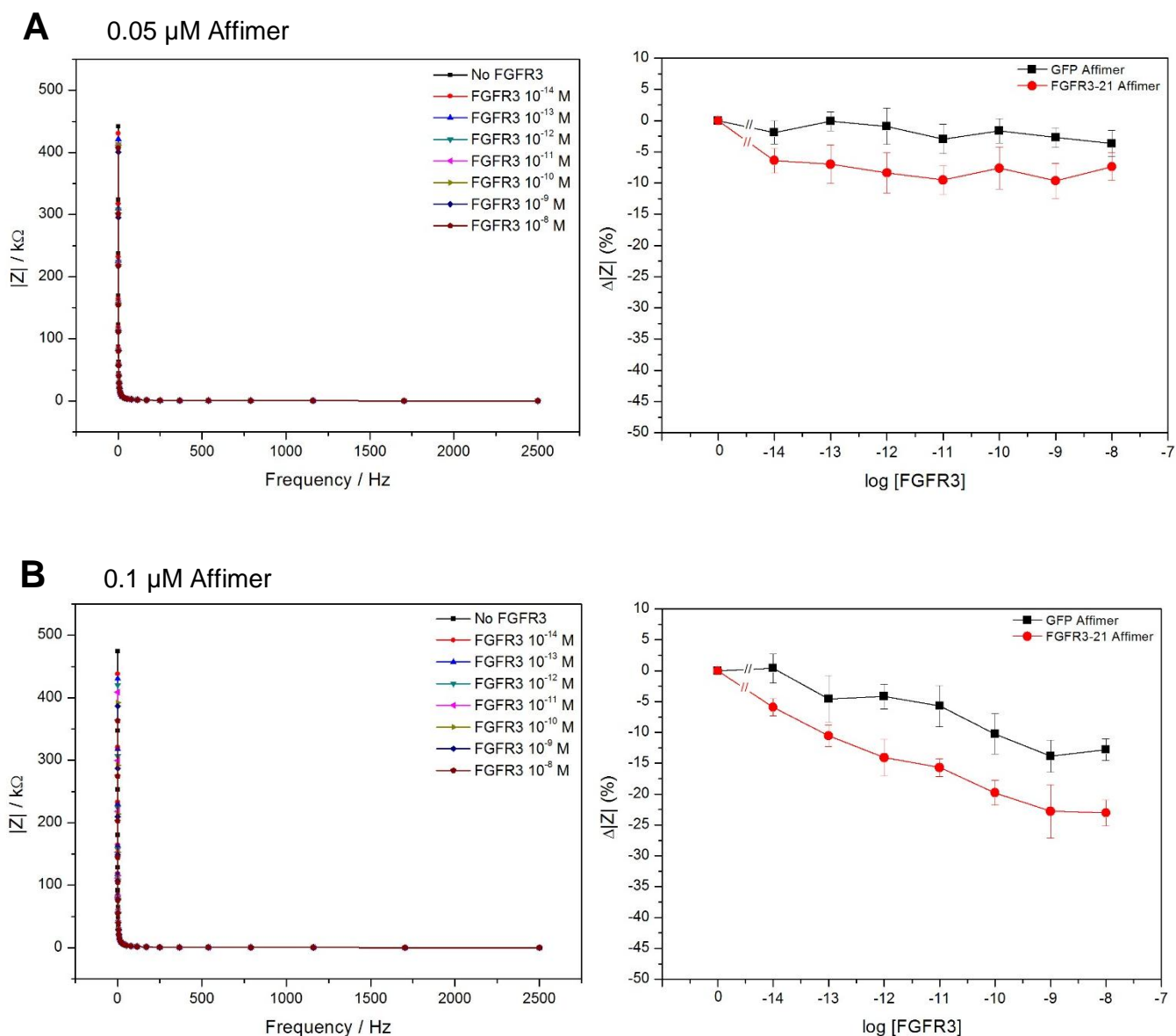


Figure 5.16 Optimisation of Affimer concentration for impedimetric biosensors with data analysis based on the absolute values of impedance. The figures on the left panel are absolute impedance-frequency plots of a FGFR3-21 Affimer sensor and the figures on the right panel are calibration curves of the biosensors for detecting FGFR3 in PBS buffer. Four different concentrations of Affimer, 0.05 μM , (A, $n = 4 \pm \text{SEM}$); 0.1 μM , (B, $n = 4 \pm \text{SEM}$); 0.3 μM , (C, $n = 3 \pm \text{SEM}$), and 1 μM , (D, $n = 3 \pm \text{SEM}$), were tested. The sensors were challenged with cumulative concentrations of FGFR3 ranging from 10^{-14} M to 10^{-8} M with PBS washes in between. The EIS measurements were performed in the presence of 10 mM $\text{K}_3\text{Fe}(\text{CN})_6/\text{K}_4\text{Fe}(\text{CN})_6$ redox mediator. The response of the sensors was displayed as $\Delta|Z|$ (%).

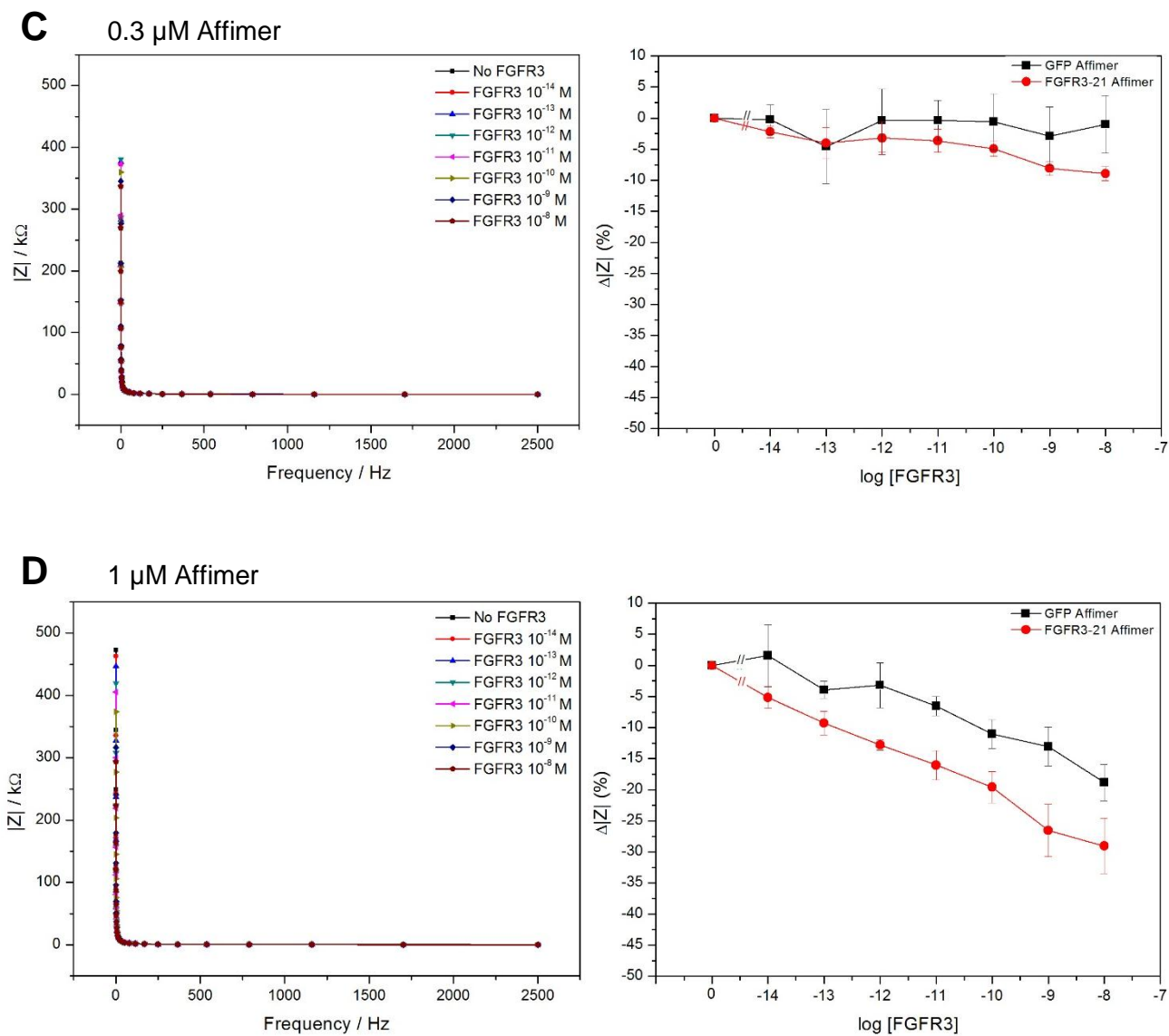


Figure 5.16 (continued) Optimisation of Affimer concentration for impedimetric biosensors with data analysis based on the absolute values of impedance. Four different concentrations of Affimer, 0.05 μM , (A, $n = 4 \pm \text{SEM}$); 0.1 μM , (B, $n = 4 \pm \text{SEM}$); 0.3 μM , (C, $n = 3 \pm \text{SEM}$), and 1 μM , (D, $n = 3 \pm \text{SEM}$), were tested.

The signal obtained was not large enough to distinguish specific from non-specific binding response. At 1 μM Affimer, the $\Delta|Z|$ for GFP Affimer sensors decreased from 0% to -17% as increasing FGFR3 whilst the $\Delta|Z|$ for FGFR3-21 Affimer sensors decrease to almost -30% (Figure 5.16D). Although the shifts for the FGFR3-21 Affimer and the sensors were different, the effect of non-specific binding on the control sensors was very large. Comparing the sensor response trend for the $\Delta|Z|$ to that for the changes in R_{ct} (Figure 5.13), even though similar patterns of the sensor response could be observed, using R_{ct} provided larger changes than using $|Z|$, assisting in data analysis.

Amongst the four techniques used to analyse the impedance data, the change in R_{ct} was proven to be the best alternative for monitoring the binding of the Affimers to FGFR3 protein in our biosensor platform. Although 0.3 μM seemed to be the optimal concentration for the making of biosensors, the change in R_{ct} on FGFR3-21 Affimer sensors, corresponding to the overall performance of the sensors, is modest, with a 23% change at the highest concentration of FGFR3 (Figure 5.13C). As presented in Figure 5.6, after functionalising the polytyramine-coated surface with biotin-NeutrAvidin, there was a massive shift of impedance, indicating that there was a large barrier deposited on the polymer layer. This could potentially interfere with the charge transfer process, making the binding between the Affimers and the target analyte less detectable. Thus it was decided that the concentration of NeutrAvidin as a linkage between the polytyramine-coated surface and biotin-tagged Affimers was needed to be optimised. This will be presented in the next section.

5.3.3.2 Optimising the concentration of NeutrAvidin

Even though NeutrAvidin was utilised as a linker between the biotinylated transducer surface and biotinylated Affimers, the fairly large size of NeutrAvidin can potentially interfere with the transfer of charged components to the transducer surface, resulting in the loss of impedance signal. In this section, the optimal concentration of NeutrAvidin was investigated. Sensors were constructed as described in Section 5.3.1. During the construction, the concentrations of NHS-biotin and Affimers were kept constant at 3 and 0.3 μM . Three concentrations of NeutrAvidin, 0.1, 0.067 and 0.033 μM , were tested. After fabrication, the sensors were challenged with FGFR3 concentrations from 10^{-14} M to 10^{-8} M as with previous optimisation studies.

The results for optimisation of NeutrAvidin concentration are shown in Figure 5.17. At a NeutrAvidin concentration of 0.1 μM , although the decrease of R_{ct} over the increase of FGFR3 concentrations can be observed on the FGFR3-21 based Affimer sensors, the shift in R_{ct} values with the increasing FGFR3 was detected on the control sensors (Figure 5.17A). These data were surprising because the condition for fabricating the sensors was identical to the sensors in Figure 5.17C. The only different issue was the electrodes used came from different batches. It was assumed that even though the manufacturer uses the same procedure to produce electrode chips, there is still variation in the manufacturing processes causing batch to batch variation. This can result in decreased reproducibility when electrodes are used for functionalisation and impedance measurement. When the concentration of NeutrAvidin was reduced to 0.067 μM , the decrease in impedance with the increasing concentrations of FGFR3 on the FGFR3-21 Affimer sensors can still be seen. However, on the control sensors, a -30% shift in R_{ct} response was detected at 10^{-14} M FGFR3 and this response remained consistent until 10^{-8} M FGFR3 (Figure 5.17B). It was assumed that the impedance shift detected here may be due to non-specific

interaction of the analyte with the surface. At the lowest NeutrAvidin concentration of 0.033 μM , although non-specific response showing by the shift of impedance on the control sensors was decreased, the R_{ct} response on the FGFR3-21 Affimer sensors also dropped (Figure 5.17C). Therefore, amongst the three concentrations of NeutrAvidin tested, 0.067 μM seemed to be the most suitable choice for constructing the sensors. However, non-specific binding resulting in impedance shift on the control sensors was still problematic. In the next section, the effect of some blocking agents was investigated in order to minimise non-specific interactions and improve the efficiency of the sensors.

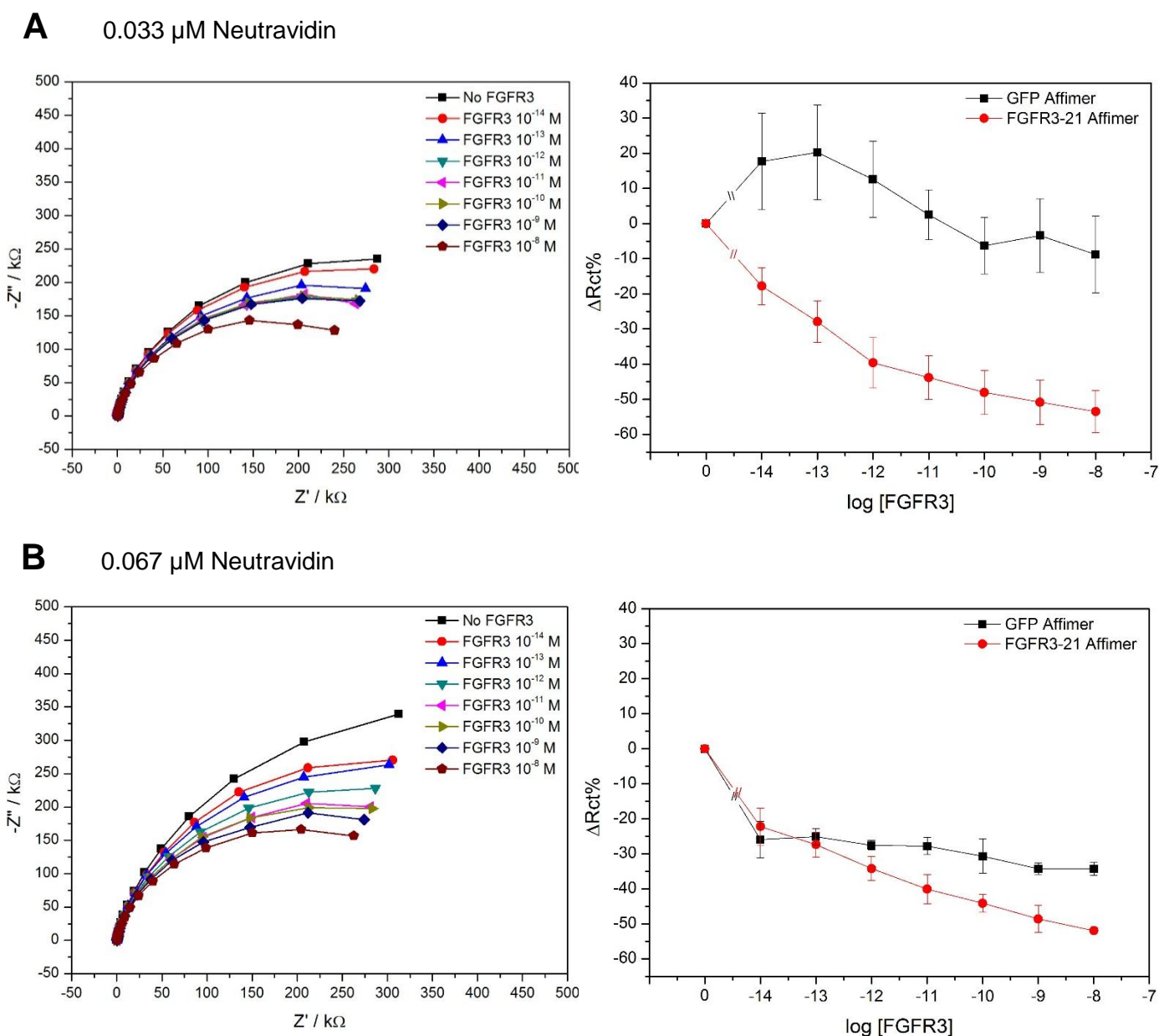


Figure 5.17 Optimisation of Neutravidin concentration for impedimetric biosensors with data analysis based on the Rct values. The figures on the left panel are Nyquist plots of a FGFR3-21 Affimer sensor and the figures on the right panel are calibration curves of the biosensors for detecting FGFR3 in PBS buffer. Three different concentrations of NeutrAvidin, 0.1 μM , (A, $n = 3 \pm \text{SEM}$); 0.067 μM , (B, $n = 3 \pm \text{SEM}$), and 0.033 μM , (C, $n = 4 \pm \text{SEM}$), were examined. The sensors were challenged with cumulative concentrations of FGFR3 ranging from 10^{-14} M to 10^{-8} M with PBS washes in between. The EIS measurements were performed in the presence of 10 mM $\text{K}_3\text{Fe}(\text{CN})_6/\text{K}_4\text{Fe}(\text{CN})_6$ redox mediator. The response of the sensors was displayed as $\Delta\text{Rct}(\%)$.

C 0.1 μM Neutravidin

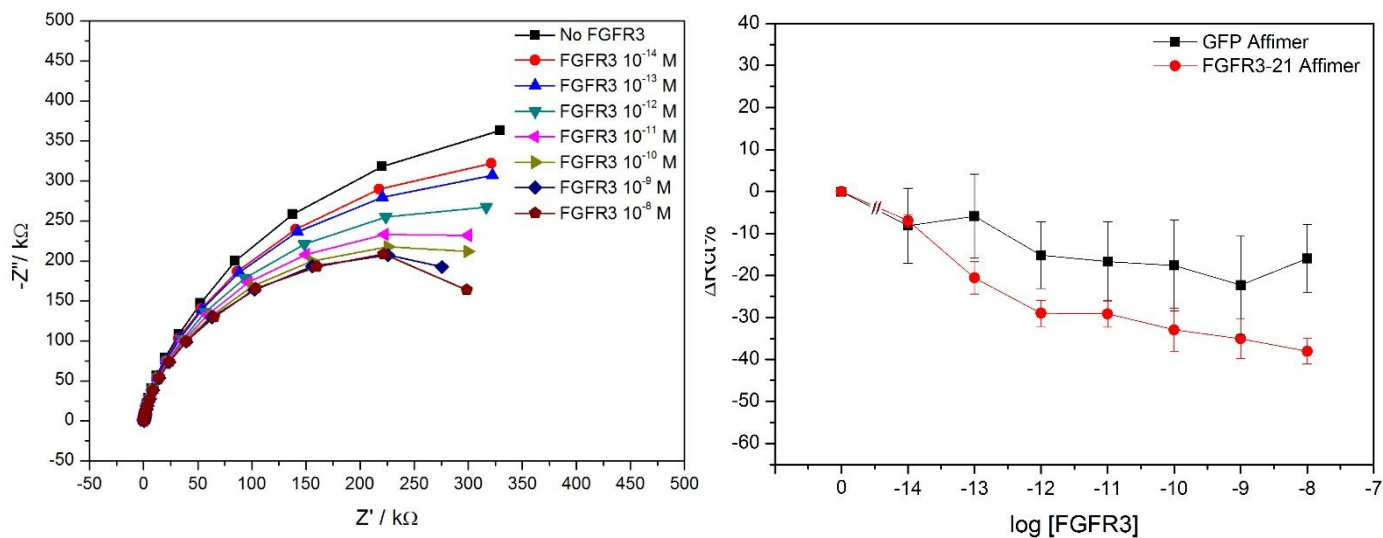


Figure 5.17 (Continued) Optimisation of Neutravidin concentration for impedimetric biosensors with data analysis based on the R_{ct} values. Three different concentrations of NeutrAvidin, 0.1 μM , (A, $n = 3 \pm \text{SEM}$); 0.067 μM , (B, $n = 3 \pm \text{SEM}$), and 0.033 μM , (C, $n = 4 \pm \text{SEM}$), were examined.

5.3.3.3 Effect of blocking agents on sensor performance

Mostly, in immunoassays, blocking agents are used in order to minimise non-specific background, allowing the specific interaction to be monitored. In the previous experiments, non-specific binding was problematic as detected by the shift of impedance on control sensors. Attempts in this section were to discover the methods of reducing or eliminating non-specific background. Several agents that might have surface blocking properties were tested. Those were 0.1 μM bovine serum albumin (BSA), 10 mM pyromellitic dianhydride (PMDA), 100 $\mu\text{g/ml}$ sodium caseinate, 0.1, 1 and 3 mM of mPEG-biotin. The sensors were fabricated using the method previously described in Section 5.3.1. During the construction, NHS-biotin, NeutrAvidin and biotin-tagged Affimers were fixed at 3, 0.067 and 0.3 μM , respectively. In the last step, blocking agent was applied to the sensors prior to cumulative additions of FGFR3 protein.

Comparing with the performance of the sensors without any blocking agent (Figure 5.18A), when using BSA, PMDA and sodium caseinate to block the sensor surface, non-specific binding can still be detected, as shown in Figure 5.18B, C and D. Moreover, reproducibility of the sensor performance was problematic since the SEM values representing the variation among different chips were very large. This indicated that BSA, PMDA and sodium caseinate were not suitable to be used as blocking agents. mPEG-biotin was another choice of blocking agents used to minimise non-specific binding in this study. It was assumed that mPEG-biotin can bind to unoccupied binding sites on NeutrAvidin that were left after adding biotinylated Affimers. It was found that mPEG-biotin at a concentration of 1 μM , a decrease in R_{ct} response over the increasing concentration of FGFR3 on FGFR3-21 Affimer sensors can be observed whereas the response on control sensors was around at 0% irrespective of the concentration of FGFR3 (Figure 5.18F). However, when the concentration of mPEG-biotin was decreased to 0.1 mM (Figure

5.18E) or increased to 3 mM (Figure 5.18G), suppression of non-specific binding was much less effective. This indicated that the optimal concentration of mPEG-biotin as a blocking is 1 mM as it is best in eliminating non-specific binding effect. Accordingly, it was included as the last step of sensor fabrication.

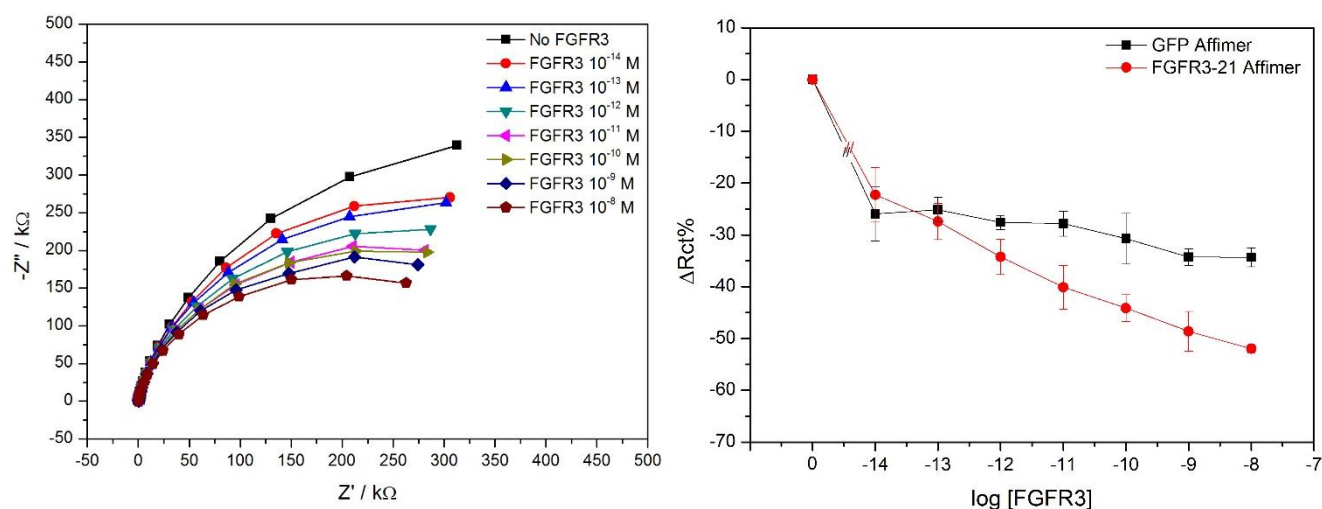
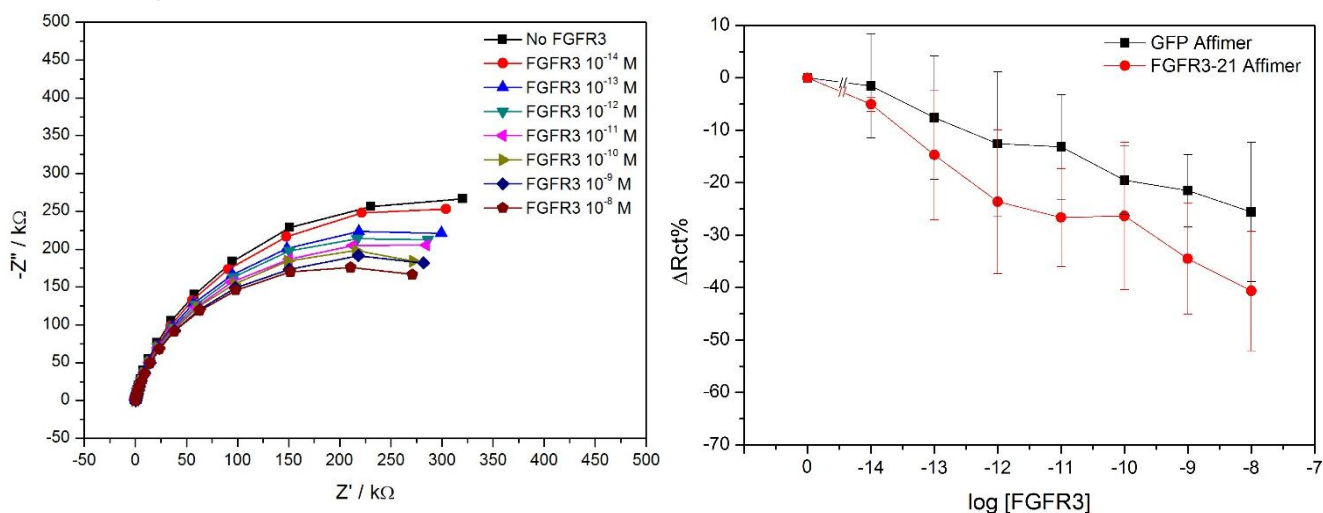
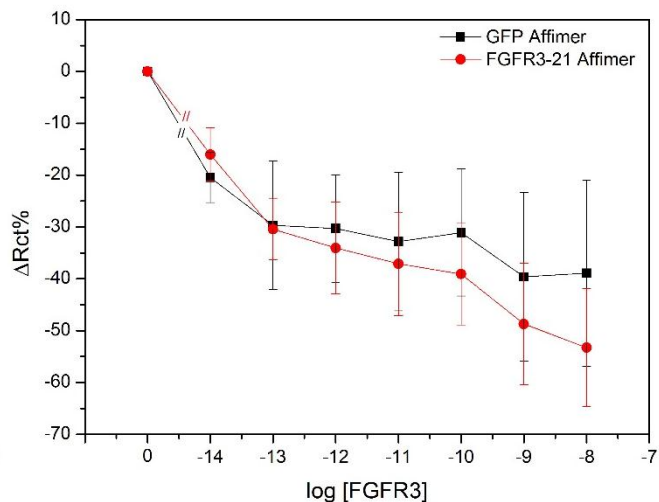
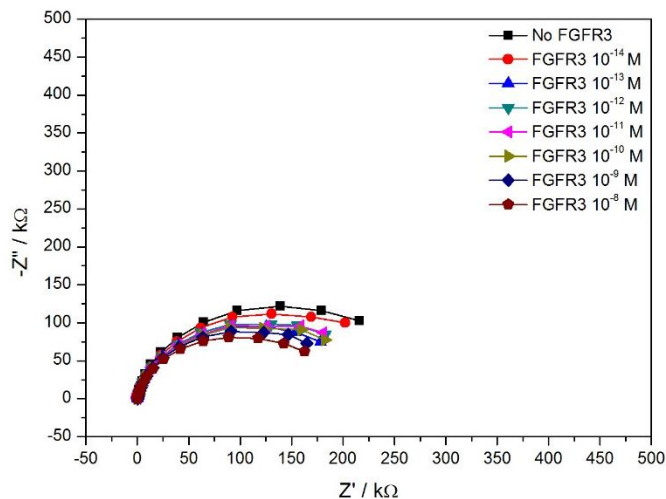
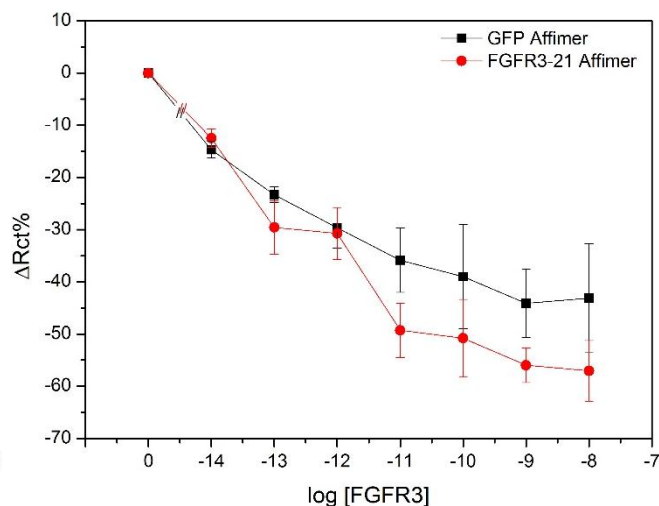
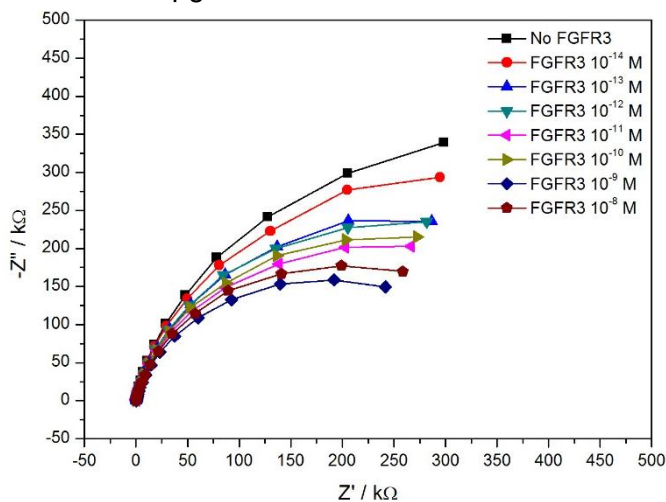
A No blocking**B** 0.1 μ M BSA

Figure 5.18 Effect of blocking agents on biosensor performance with data analysis based on the Rct values. The figures on the left panel are Nyquist plots of a FGFR3-21 Affimer sensor and the figures on the right panel are calibration curves of the biosensors for detecting FGFR3 in PBS buffer. Prior to testing with FGFR3 protein, the sensors were blocked with different blocking agents. Sensors without blocking agent was used as a control, (A, $n = 3 \pm \text{SEM}$), following by sensors blocked with 0.1 μ M BSA, (B, $n = 3 \pm \text{SEM}$); 10 mM pyromellitic dianhydride, (C, $n = 3 \pm \text{SEM}$); 100 μ g/ml sodium caseinate, (D, $n = 3 \pm \text{SEM}$); 0.1 mM mPEG-biotin, (E, $n = 3 \pm \text{SEM}$); 1 mM mPEG-biotin, (F, $n = 3 \pm \text{SEM}$), and 3 mM, mPEG-biotin (G, $n = 3 \pm \text{SEM}$). The sensors were challenged with cumulative concentrations of FGFR3 ranging from 10^{-14} M to 10^{-8} M with PBS washes in between. The EIS measurements were performed in the presence of 10 mM $K_3Fe(CN)_6/K_4Fe(CN)_6$ redox mediator. The response of the sensors was displayed as $\Delta R_{ct}(\%)$.

C 10 mM pyromellitic dianhydride



D 100 μg/ml sodium caseinate



E 0.1 mM mPEG-biotin

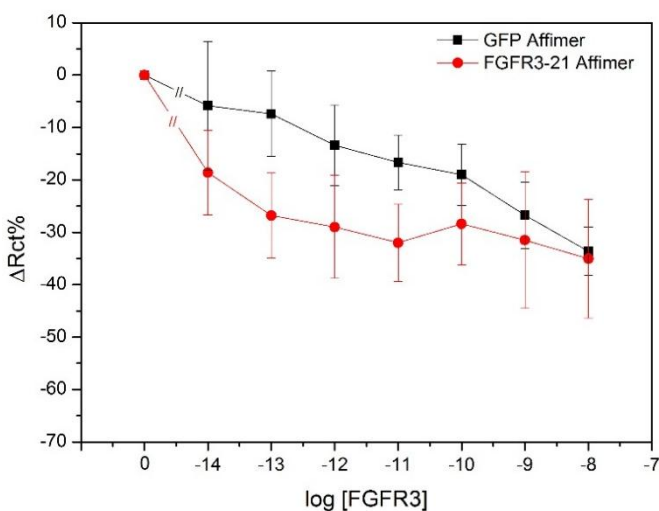
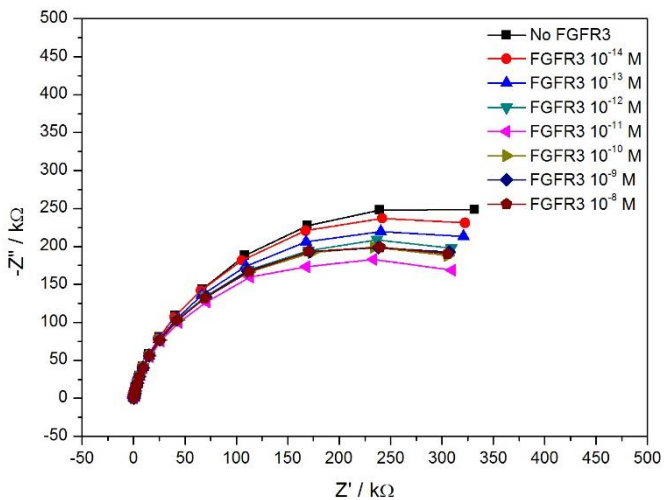


Figure 5.18 (continued) Effect of blocking agents on biosensor performance with data analysis based on the Rct values. Prior to testing with FGFR3 protein, the sensors were blocked with different blocking agents.

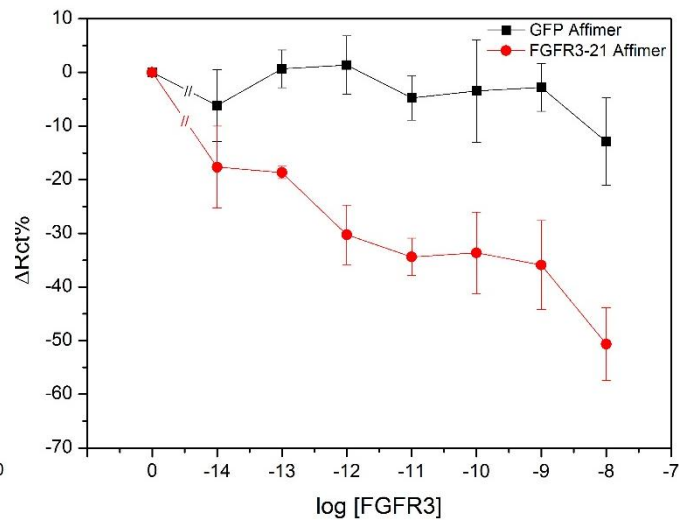
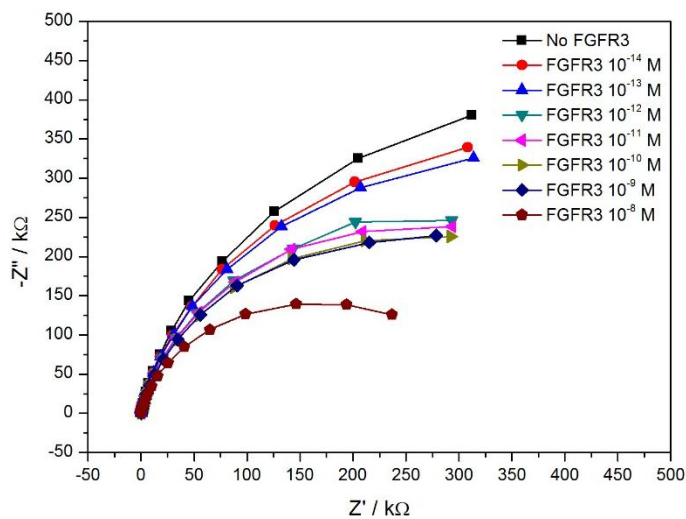
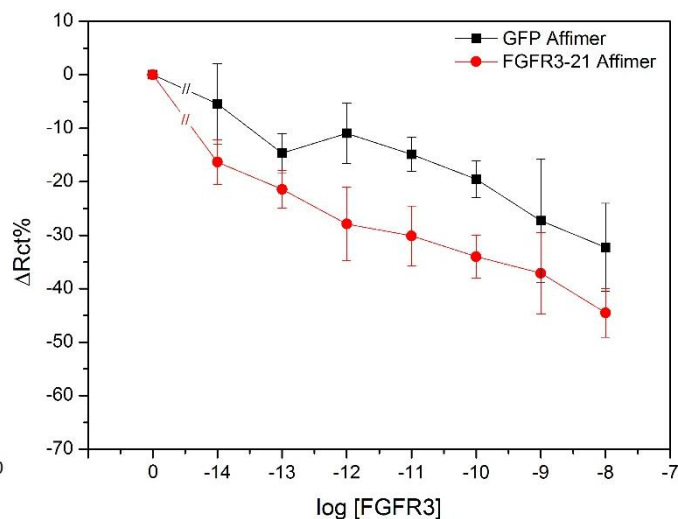
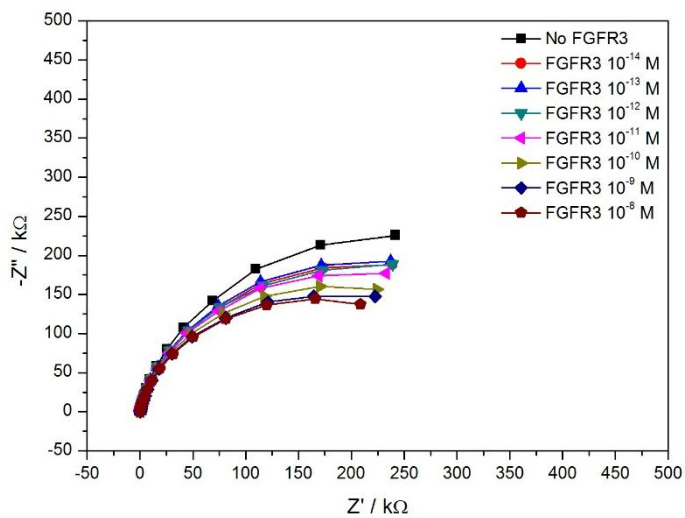
F 1 mM mPEG-biotin**G** 3 mM mPEG-biotin

Figure 5.18 (continued) Effect of blocking agents on biosensor performance with data analysis based on the R_{ct} values. Prior to testing with FGFR3 protein, the sensors were blocked with different blocking agents.

5.3.3.4 Specificity of the sensors for the analytes

One of the requirements for any sensor is the specificity to the target of interest. Even though the sensors immobilised with FGFR3-specific Affimers showed binding of FGFR3 protein, it was necessary to test them with other non-related proteins to confirm the specificity. The sensors were fabricated using the same method as described in Section 5.3.1 and then blocked with 1 μ M mPEG-biotin to minimise non-specific background. In addition to FGFR3 protein, β -2-microglobulin (β 2M) and human serum albumin (HSA) were selected as non-related analytes to test. This is because β 2M is used as a predictive biomarker for acute kidney injury (Vaidya et al., 2008). β 2M is basically filtered by the glomerulus and almost totally reabsorbed and demolished by the proximal tubular cells (Vaidya et al., 2008, Miyata et al., 1998). Dysfunction of the proximal tubular cells can cause elevated levels of intact β 2M in urine, indicating renal failure. HSA, on the other hand, is the most abundant protein in plasma which plays a role in controlling oncotic pressure in plasma and carrying other components such as fatty acids in bloodstream (Fanali et al., 2012). In the case of kidney dysfunction, HSA is one of the first proteins released into urine. As the presence of β 2M and HSA in urine may interfere with the binding of anti-FGFR3 Affimers and FGFR3 on sensors, both of them were selected to test for sensor specificity to the target.

The results of specificity test for the fully constructed Affimer sensors are presented in Figure 5.19. When the sensors were tested with FGFR3 protein, a continuous decrease of R_{ct} over a range of FGFR3 concentrations was seen on FGFR3-21 Affimer sensors whereas the response with control sensors was almost constant with the change between 0 and -10% (Figure 5.19A). However, when the sensors were exposed to β -2-microglobulin (Figure 5.19B) or human serum albumin (Figure 5.19C), non-specific binding to the sensors can be observed.

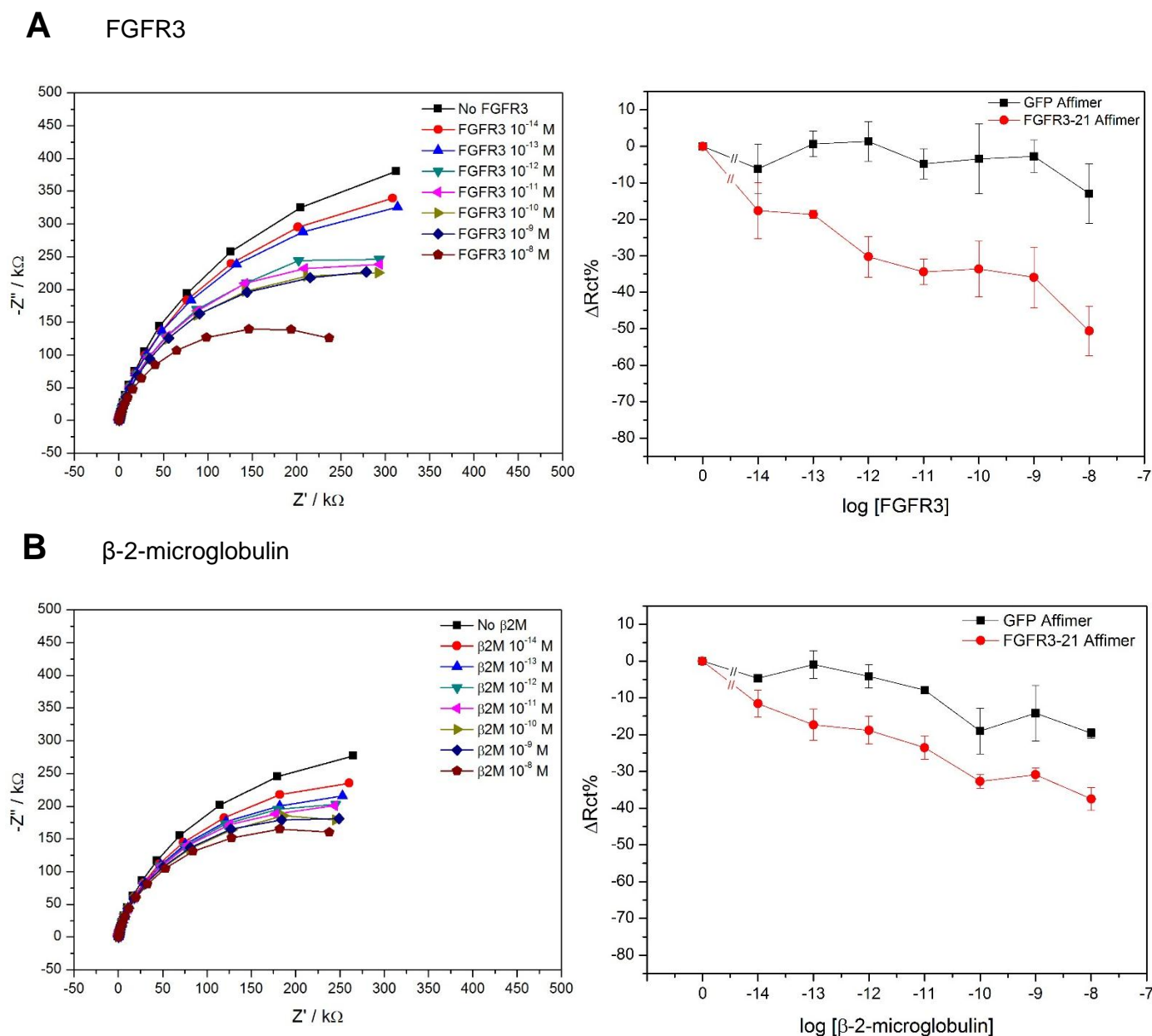


Figure 5.19 Specificity of biosensors to the analytes with data analysis based on the Rct values. The figures on the left panel are Nyquist plots of a FGFR3-21 Affimer sensor and the figures on the right panel are calibration curves of the biosensors for detecting FGFR3 in PBS buffer. The sensors were blocked with 1 μ M mPEG-biotin prior to exposing to analytes. The sensors were challenged with cumulative concentrations of analytes ranging from 10^{-14} M to 10^{-8} M with PBS washes in between. The analytes tested were FGFR3, (A, $n = 3 \pm \text{SEM}$); β -2-microglobulin, (B, $n = 3 \pm \text{SEM}$), and human serum albumin, (C, $n = 3 \pm \text{SEM}$). The EIS measurements were performed in the presence of 10 mM $\text{K}_3\text{Fe}(\text{CN})_6/\text{K}_4\text{Fe}(\text{CN})_6$ redox mediator. The response of the sensors was displayed as $\Delta\text{Rct}(\%)$.

C Human serum albumin

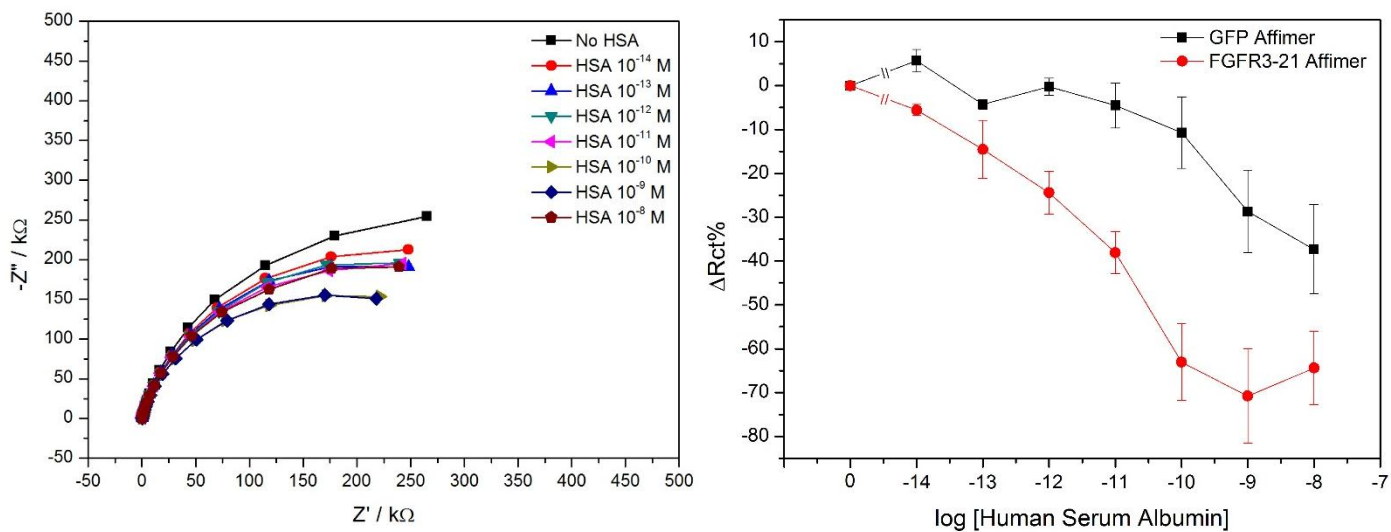


Figure 5.19 (continued) Specificity of biosensors to the analytes with data analysis based on the R_{ct} values. The analytes tested were FGFR3, (A, $n = 3 \pm \text{SEM}$); β -2-microglobulin, (B, $n = 3 \pm \text{SEM}$), and human serum albumin, (C, $n = 3 \pm \text{SEM}$).

The decrease of R_{ct} was seen on both the sensors functionalised with FGFR3-21 Affimer and anti-GFP Affimer. The effect of non-specific binding of the non-related analytes on FGFR3-21 Affimer sensors was higher than that with anti-GFP Affimer.

As previously mentioned in 4.3.5, the ELISA showed that only the Affimers screened against FGFR3 bound FGFR3 protein. None of the tested Affimers showed binding to β -2-microglobulin and human serum albumin (Figure 4.14). Non-specific binding detected when challenging the sensors with different types of analyte could be from the interaction between the analyte and the functionalised surface. In this experiment (Figure 5.19), mPEG-biotin had been used as a blocking agent in order to minimise the effect of non-specific binding. The antifouling properties of polyethylene glycol (PEG) to resist the adsorption of proteins to the surface are well recognised (Liu et al., 2013, Ostuni et al., 2001, Furuya et al., 2006). However, the ability of PEG to bind to proteins has been reported as well. In a previous study by (Ogi et al., 2009), PEG was found to interact non-specifically with human immunoglobulin G (IgG) although it was used as a blocking agent for the system. These data were also supported by a finding by (Riquelme et al., 2016). These researchers found that PEG can enhance the attachment of *Staphylococcus intermedius* to a PEG-functionalised gold surface. The binding between PEG and BSA protein has also been studied (Rawat et al., 2010). The researchers suggested that the binding of PEG and BSA occurs through a strong physical adsorption of PEG to the hydrophobic region of BSA, leading to the stabilisation of the protein structure. Different proteins have unique properties, resulting from amino acid patterns. Therefore the interaction of different proteins to an antifouling agent can be various and unpredictable. PEG could be used to minimise non-specific binding of FGFR3 but not for some proteins. In the next section, attempts were made to find more suitable agents other than mPEG-biotin to reduce non-specific background.

5.3.4 Modification of sensor construction protocol to minimise non-specific signal

In immunoassays including ELISA, western blotting and even biosensors, bovine serum albumin (BSA) has been commonly used as a blocking agent. In this work, BSA was previously used to block the sensor surface in section 5.3.3.3. However, blocking the sensor surface with 0.1 μM BSA after Affimer immobilisation did not minimise non-specific binding from FGFR3 on control sensors (Figure 5.12B). It was proposed that the choice of blocking agents should be based on the molecular size of biorecognition elements (Riquelme et al., 2016). If a small bioreceptor is utilised, using BSA or large molecule as an antifouling agent may interfere with specific recognition events between the bioreceptor and the target (Riquelme et al., 2016). This could explain the inability of BSA to eliminate non-specific binding when applied after Affimer attachment.

In 2008, Esseghaier and co-workers revealed a method of making impedimetric biosensors using NeutrAvidin-biotin interaction as a linkage between the gold surface and a recognition element (Esseghaier et al., 2008). The researchers trapped NeutrAvidin molecules into a polypyrrole (PPy) layer using cyclic voltammetry. Prior to immobilising biotinylated anti-triazine Fab fragments, PPy/NeutrAvidin-modified electrodes were blocked with BSA. Interestingly, the concentration of BSA used was much higher than that of NeutrAvidin. With this fabrication protocol, specific responses of the sensors could be observed. In this section, the protocol for fabricating the sensors described in Section 5.3.3 was modified as presented in Figure 5.20. Sensors were constructed step-by-step by starting with polytyramine deposition. The sensors were then functionalised with NHS-biotin, following by NeutrAvidin as usual. However, prior to immobilising biotinylated Affimers, the sensors were blocked with BSA. The concentration of BSA

used in this study was $6.7 \mu\text{M}$, which was 100 times higher than the concentration of NeutrAvidin ($0.067 \mu\text{M}$). After Affimer immobilisation completed, the sensors were ready to test with FGFR3 protein.

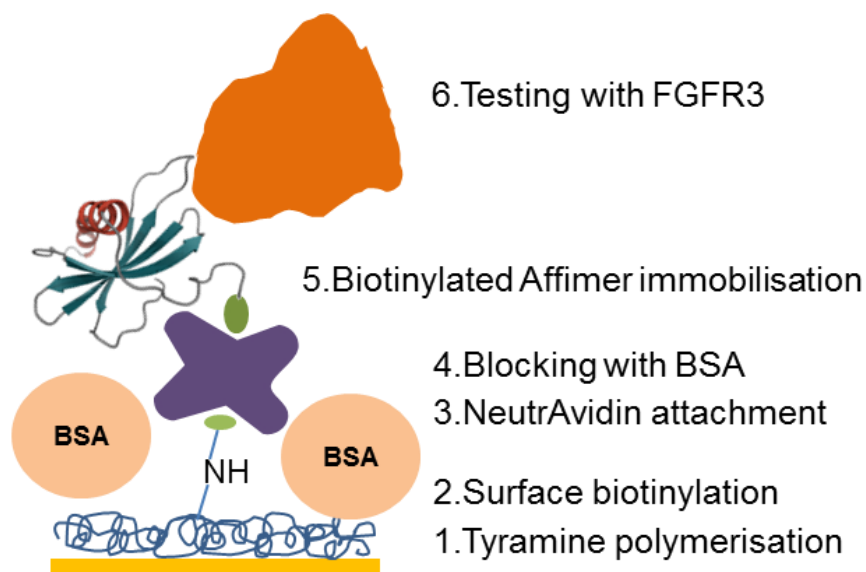


Figure 5.20 Schematic representation of Affimer sensor construction according to the modified protocol. The modification was suggested by the report of Esseghaier et al. (2008). After NeutrAvidin attachment, the sensor was blocked with BSA before biotinylated Affimers were attached to the electrode.

5.3.4.1 Optimisation of Affimer concentration in sensors blocked with BSA at high concentration

As the sensor construction protocol has been modified, in order for the sensors to achieve the highest level of their performance, the optimal concentration of biorecognition elements is required. Blocking NeutrAvidin-coated surfaces with BSA before immobilising Affimers may reduce the possibility of biotinylated Affimers to interact with NeutrAvidin because BSA could block the binding sites of NeutrAvidin or cause a steric hindrance effect, resulting in interference with NeutrAvidin-biotinylated Affimer interactions. Optimal concentration of Affimers may help the Affimers access the NeutrAvidin binding sites, improving a number of Affimers successfully immobilised on the sensor surface.

In this section, three concentrations of Affimers were tested. The sensors were fabricated following the modified version of the protocol as mentioned in 5.3.4. Polytyramine-modified electrodes were functionalised with 3 μM NHS-biotin and 0.067 μM NeutrAvidin. Then, 6.7 μM BSA was employed to minimise non-specific binding events prior to immobilising different concentrations of Affimers. Anti-GFP Affimer was used as a control receptor. As shown in Figure 5.21, three concentrations of the Affimers showed similar patterns of sensor performance. However, on sensors with 1 μM of Affimer, non-specific background on negative control (GFP Affimer) sensors was the lowest (between 0% and -12%) whereas the response of R_{ct} on FGFR3-21 Affimer sensors was found to decrease continually as the concentration of FGFR3 increased (Figure 5.21B). At the Affimer concentration of 0.3 μM (Figure 5.21A) and 3 μM (Figure 5.21C), even though the decrease in R_{ct} over the increasing concentration of FGFR3 was detected, approximately -20% shift of impedance indicating non-specific binding effect can be seen. Taken the data together, an Affimer concentration of 1 μM was selected as the optimal concentration for the

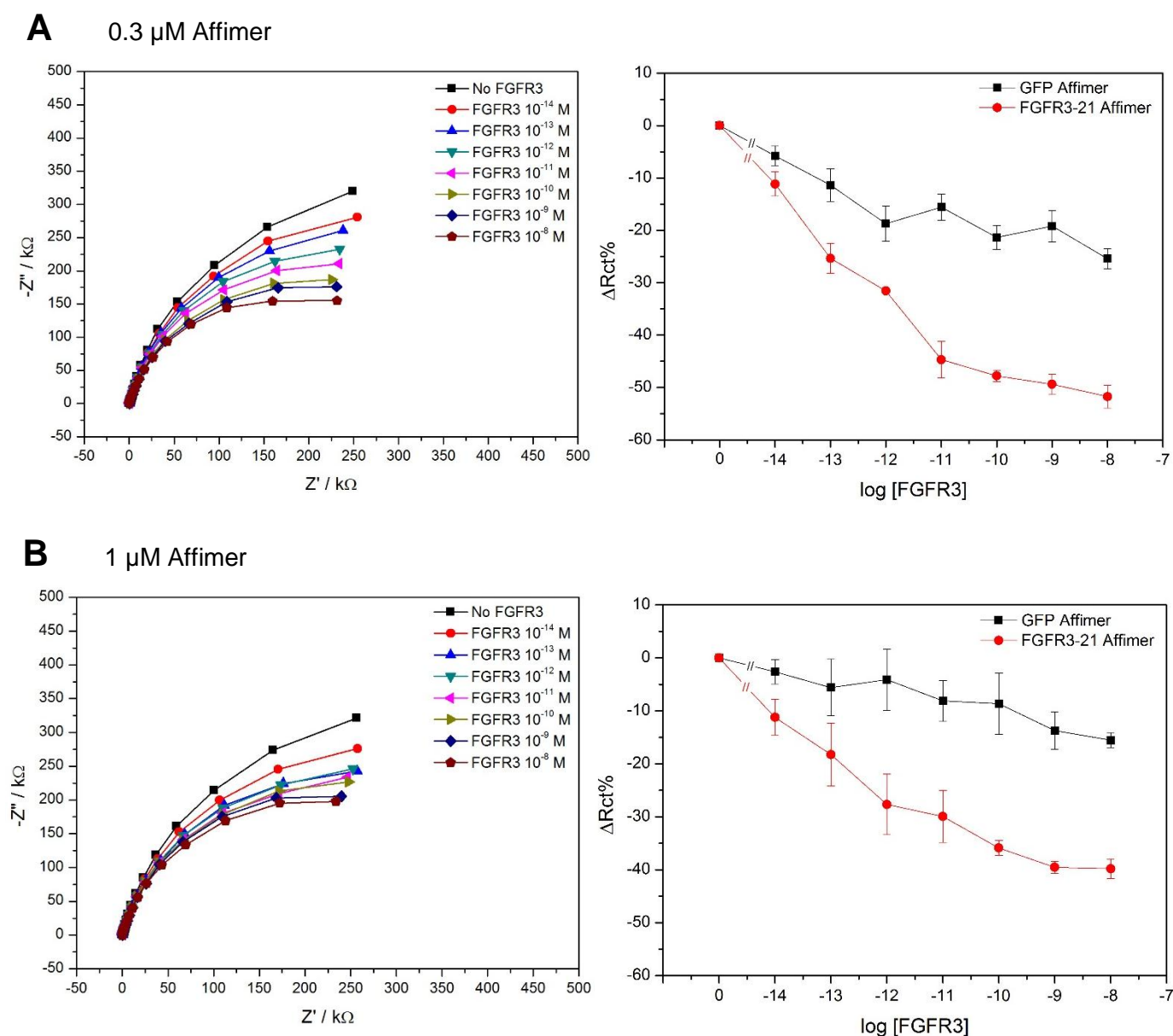


Figure 5.21 Optimisation of Affimer concentration for impedimetric biosensors subject to the modified sensor construction protocol. The figures on the left panel are Nyquist plots of a FGFR3-21 Affimer sensor and the figures on the right panel are calibration curves of the biosensors for detecting FGFR3 in PBS buffer. The sensors were blocked with $6.7 \mu\text{M}$ BSA prior to Affimer immobilisation. Three concentrations of Affimers, $0.3 \mu\text{M}$, (A, $n = 3 \pm \text{SEM}$); $1 \mu\text{M}$, (B, $n = 3 \pm \text{SEM}$), and $3 \mu\text{M}$, (C, $n = 4 \pm \text{SEM}$), were tested. The sensors were exposed to FGFR3 concentrations from 10^{-14} to 10^{-8} M. The EIS measurements were performed in the presence of 10 mM $\text{K}_3\text{Fe}(\text{CN})_6/\text{K}_4\text{Fe}(\text{CN})_6$ redox mediator. The response of the sensors was displayed as $\Delta\text{Rct}(\%)$.

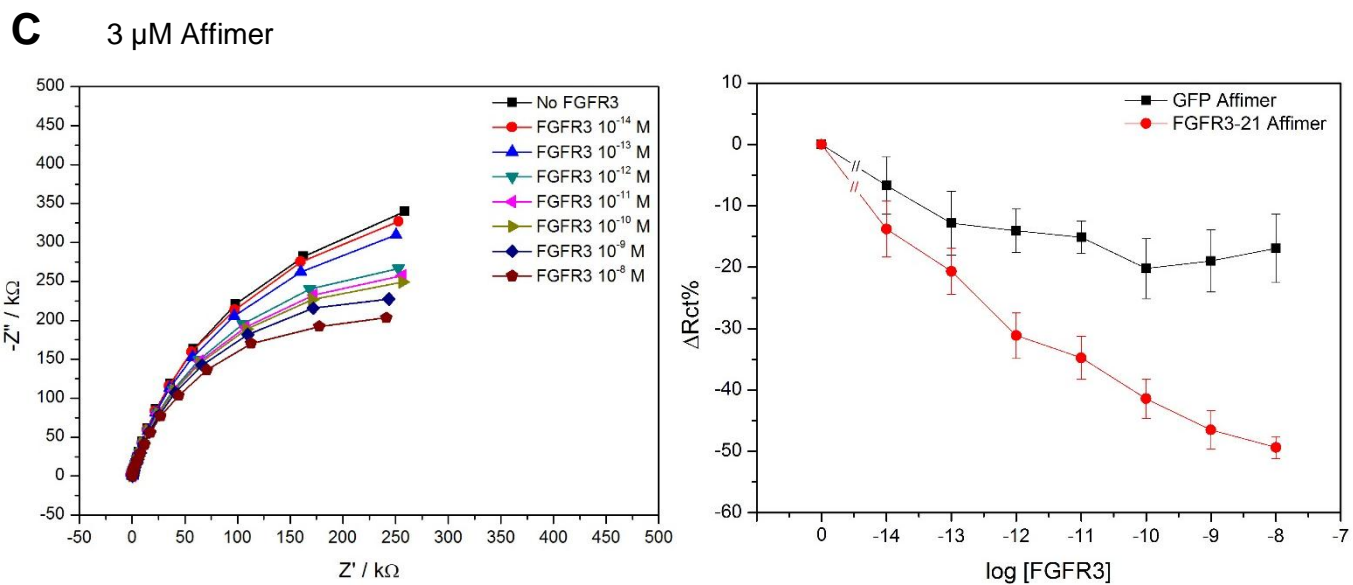
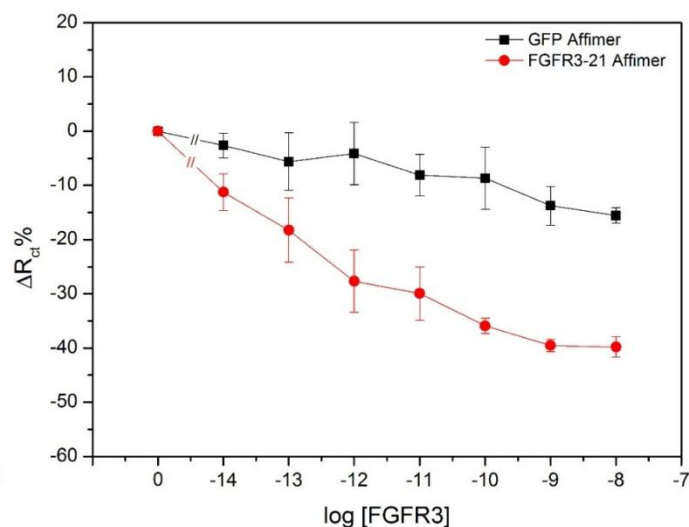
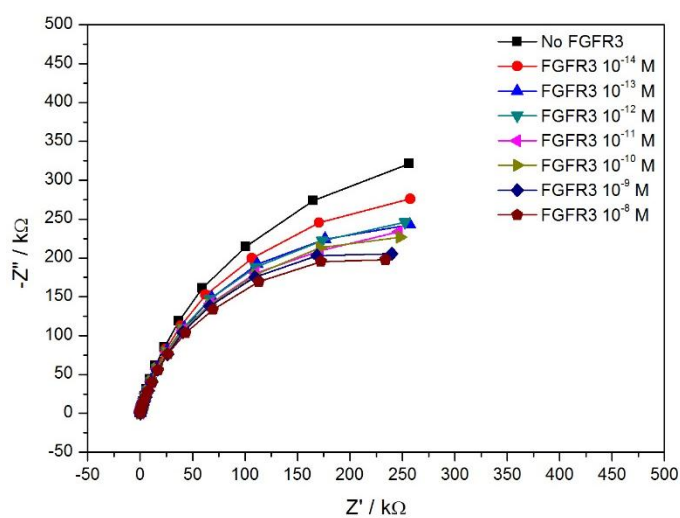


Figure 5.21 (continued) Optimisation of Affimer concentration for impedimetric biosensors subject to the modified sensor construction protocol. Three concentrations of Affimers, 0.3 μM , (A, $n = 3 \pm \text{SEM}$); 1 μM , (B, $n = 3 \pm \text{SEM}$), and 3 μM , (C, $n = 4 \pm \text{SEM}$), were tested.

modified version of the sensor fabrication protocol.

In order to confirm that the positive response on FGFR3-21 Affimer sensors was from binding of the Affimers to FGFR3 protein, another Affimer clone selected against FGFR3 protein, the FGFR3-14 Affimer, was used instead of FGFR3-21 Affimer. The sensors were constructed as before. The concentrations of NHS-biotin, NeutrAvidin, BSA and Affimers were kept constant at 3, 0.067, 6.7 and 1 μM , respectively. Anti-GFP Affimer was used as a control on working electrode 1 and FGFR3-14 Affimer was immobilised on working electrode 2. Comparison of the sensors using FGFR3-21 and FGFR3-14 Affimers is shown in Figure 4.15. Compared to GFP/FGFR3-21 Affimer sensors (Figure 5.22A), GFP/FGFR3-14 Affimer sensors showed similar responses. The R_{ct} shift on control anti-GFP Affimer sensors was found to fall between 0% to -10% whereas a continuous decrease in R_{ct} was detected on FGFR3-14 Affimer sensors increasing FGFR3 (Figure 5.22B). These data confirmed that the Affimers can be used to sense the presence of FGFR3 protein in PBS buffer when being used in corporation with an electrochemical sensor platform.

A GFP/FGFR3-21 Affimers



B GFP/FGFR3-14 Affimers

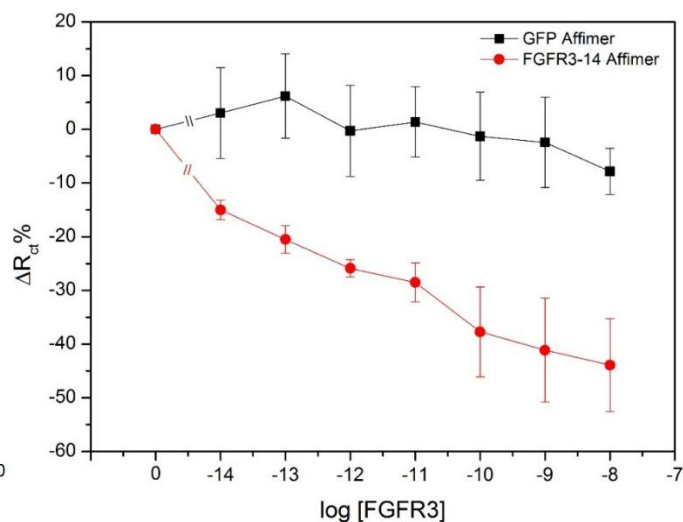
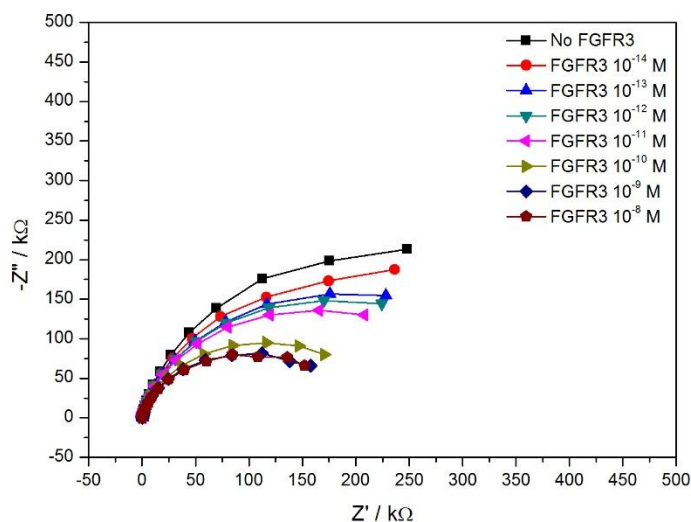


Figure 5.22 Effect of different clones of the FGFR3-specific Affimer on the sensor performance. The figures on the left panel are Nyquist plots of a FGFR3-specific Affimer sensor and the figures on the right panel are calibration curves of the biosensors for detecting FGFR3 in PBS buffer. The sensors were blocked with 6.7 μM BSA prior to Affimer immobilisation. The sensors were immobilised with 1 μM of GFP and FGFR3-21 Affimers, (A, $n = 3 \pm \text{SEM}$) and, GFP and FGFR3-14 Affimers, (B, $n = 3 \pm \text{SEM}$). The sensors were exposed to FGFR3 concentrations from 10^{-14} to 10^{-8} M. The EIS measurements were performed in the presence of 10 mM $\text{K}_3\text{Fe}(\text{CN})_6/\text{K}_4\text{Fe}(\text{CN})_6$ redox mediator. The response of the sensors was displayed as $\Delta R_{ct}(\%)$.

5.3.4.2 Effect of BSA and casein at high concentrations as blocking agents on sensor performance

Although BSA showed the best effect on blocking non-specific binding of FGFR3 to the sensor surface, there are other blocking agents such as casein that are commonly used in bioimmunoassay applications. In addition to BSA, two forms of casein were tried for their ability to minimise non-specific background and compared with BSA. The electrodes were modified with polytyramine, NHS-biotin and NeutrAvidin, respectively. Different blocking agents, 6.7 μM BSA, 2x casein blocking buffer (Sigma-Aldrich) and 0.2 mg/ml sodium caseinate, were used to block the functionalised surface before biotin-tagged Affimers were added. In this experiment, anti-GFP Affimer was used as the control receptor with FGFR3-21 Affimer as the specific receptor.

As shown in Figure 5.17, using BSA as a blocking agent minimised non-specific binding on negative control sensors with little shift of R_{ct} (approximately -12% at the highest FGFR3 concentration tested) whilst the decrease in impedance on FGFR3-21 Affimer sensors was still retained (Figure 5.17A). However, when using either 2x casein blocking buffer (Figure 5.17B) or sodium caseinate (Figure 5.17C) as a blocking solution, non-specific interactions of FGFR3 protein to the sensor surface can still be seen on control sensors. The data presented here showed that BSA was the best alternative to be used as an antifouling agent to minimise non-specific binding for this sensor platform.

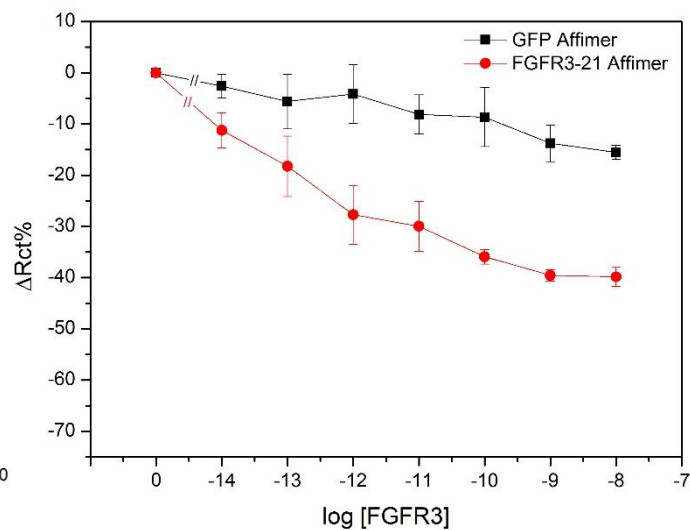
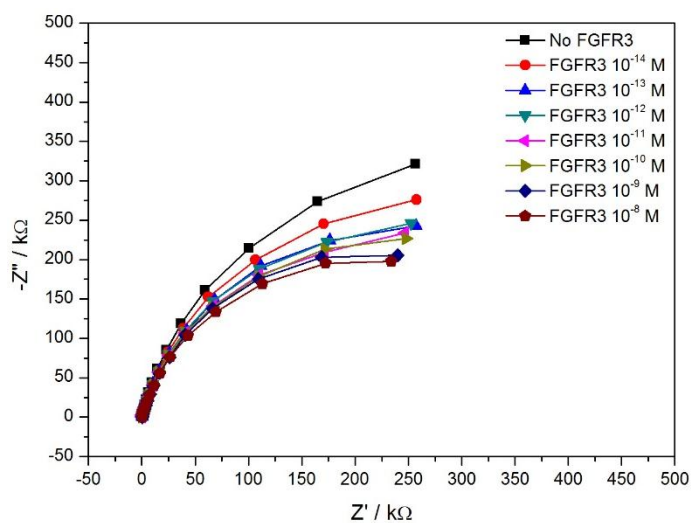
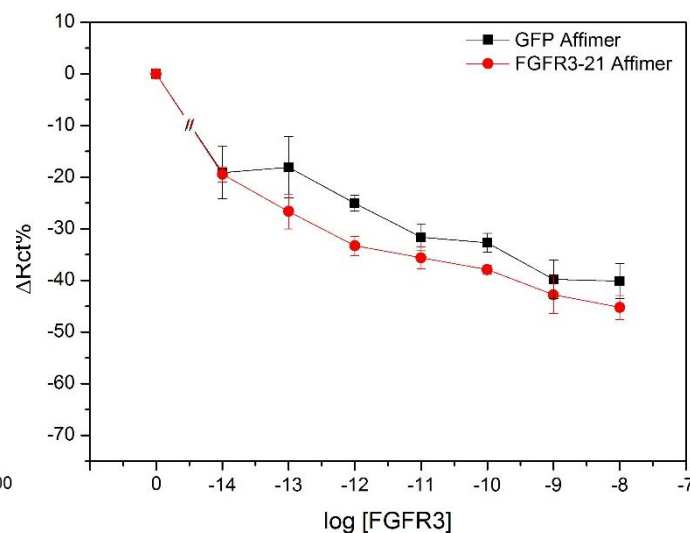
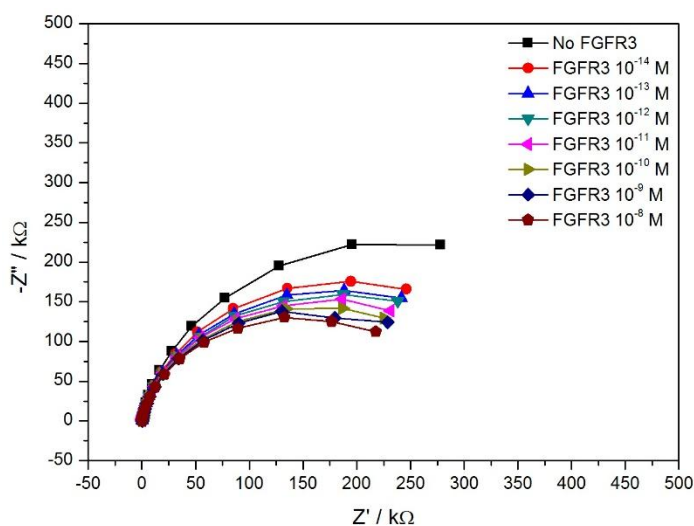
A 6.7 μM BSA**B** 2x casein blocking buffer

Figure 5.23 Effect of blocking agents on sensor performance subject to the modified protocol. The figures on the left panel are Nyquist plots of a FGFR3-21 Affimer sensor and the figures on the right panel are calibration curves of the biosensors for detecting FGFR3 in PBS buffer. The sensors were blocked with either 6.7 μM BSA, (A, $n = 3 \pm \text{SEM}$); 2x casein blocking buffer from Sigma-Aldrich, (B, $n = 3 \pm \text{SEM}$), or 0.2 mg/ml sodium caseinate, (C, $n = 3 \pm \text{SEM}$) prior to Affimer immobilisation. The sensors were exposed to FGFR3 concentrations ranging from 10^{-14} to 10^{-8} M. The EIS measurements were performed in the presence of 10 mM $\text{K}_3\text{Fe}(\text{CN})_6/\text{K}_4\text{Fe}(\text{CN})_6$ redox mediator. The response of the sensors was displayed as $\Delta\text{Rct}(\%)$.

C 0.2 mg/ml sodium caseinate

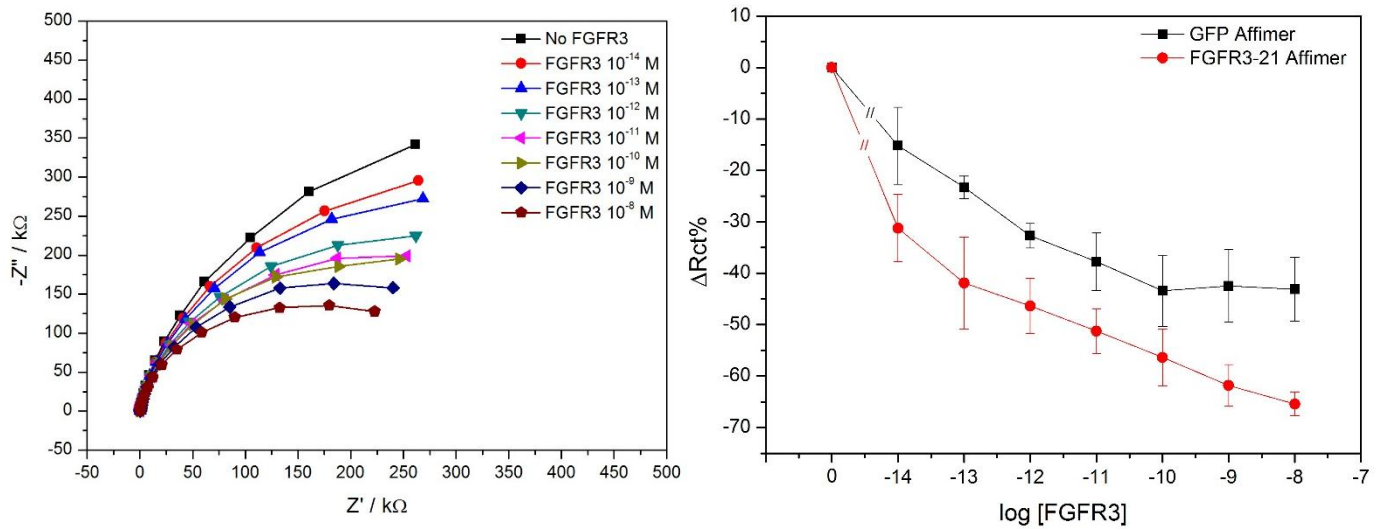


Figure 5.23 (continued) Effect of blocking agents on sensor performance subject to the modified protocol. The sensors were blocked with either 6.7 μM BSA, (A, $n = 3 \pm \text{SEM}$); 2x casein blocking buffer from Sigma-Aldrich, (B, $n = 3 \pm \text{SEM}$), or 0.2 mg/ml sodium caseinate, (C, $n = 3 \pm \text{SEM}$) prior to Affimer immobilisation.

5.3.4.3 Specificity of high BSA concentration blocked sensors to the analytes

To test whether the high BSA concentration blocked anti-FGFR3 Affimer sensors so that they only recognised FGFR3 protein, the sensors were challenged with FGFR3, β -2-microglobulin and antidigoxin IgG. The sensors were fabricated using the modified method in Section 5.3.4.1. The gold surface was deposited with polytyramine, following by functionalising with 3 μ M of NHS-biotin and 0.067 μ M of NeutrAvidin. The modified surface was then blocked with 6.7 μ M BSA prior to Affimer attachment. One μ M of GFP (control) or FGFR3-21 Affimer was immobilised onto the surface before the sensors were tested with different proteins.

The results presented in Figure 5.24 showed that even though the presence of FGFR3 can be detected by FGFR3-21 Affimer sensors with almost no change in R_{ct} response on control sensors (Figure 5.24A), non-specific binding was still a problem when testing the sensors with the other analytes. As shown in Figure 5.24B, non-specific binding of β -2-microglobulin could be found on both control and FGFR3-21 Affimer sensors, yet the response patterns were different. With the increasing of β -2-microglobulin concentrations, the shift of R_{ct} between 0 and 20% was detected on control sensors whereas a continuous decrease of R_{ct} from 0 to nearly -40% was displayed for FGFR3-21 Affimer sensors. In the same way, when testing the sensors with antidigoxin IgG, non-specific binding can be seen (Figure 5.24C). Although the shift in R_{ct} could not be seen when GFP Affimer (control) sensors were exposed to antidigoxin IgG, a decrease in R_{ct} was observed on FGFR3-21 Affimer sensors, indicating the non-specific binding event. Specific response of the sensors is presented in Figure 5.24D. To calculate the specific response, $\Delta R_{ct}(\%)$ of FGFR3-21 Affimer sensors were subtracted with $\Delta R_{ct}(\%)$ of anti-GFP Affimer sensors and plotted against a range of FGFR3 concentrations. The subtracted response for the

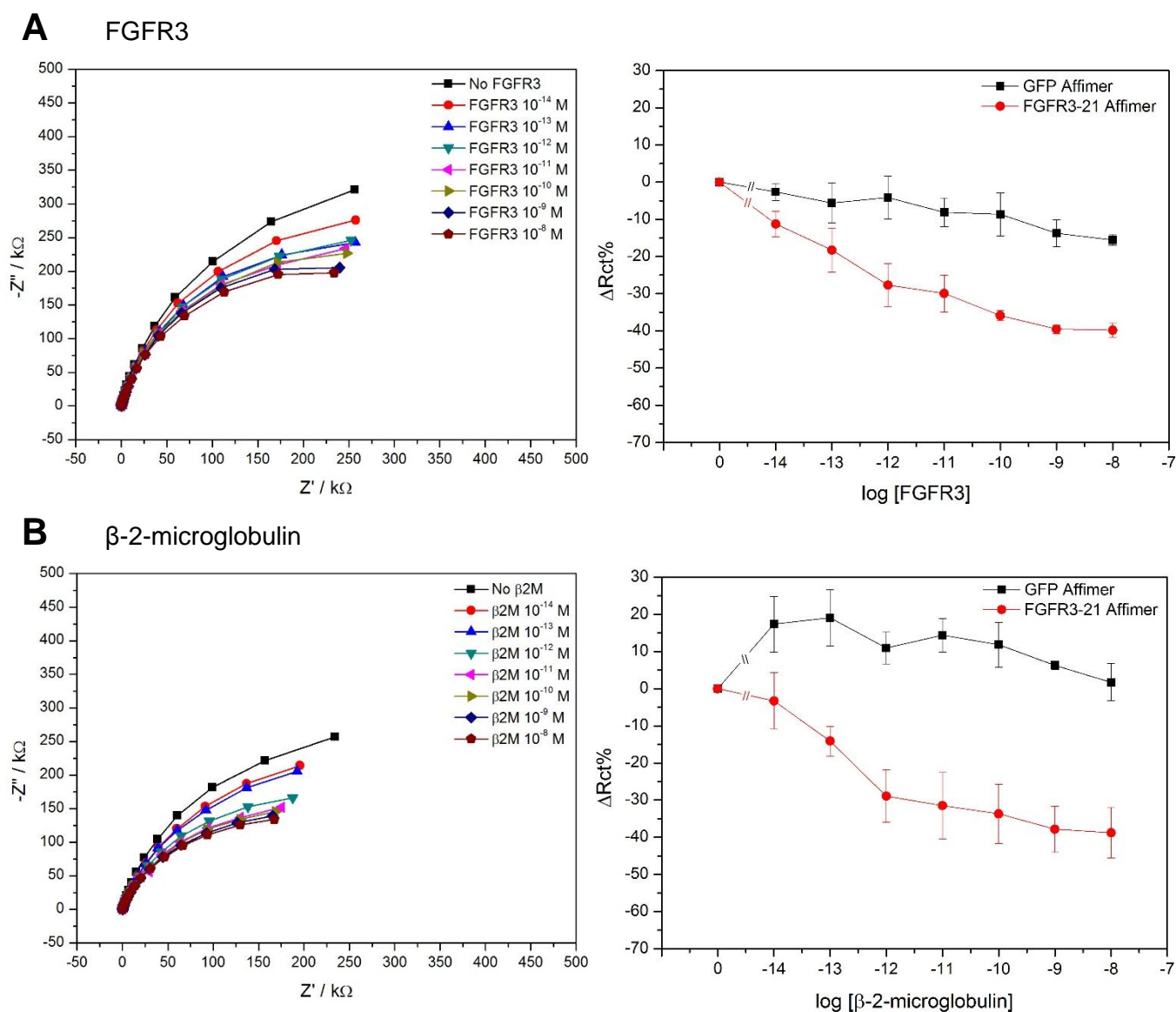
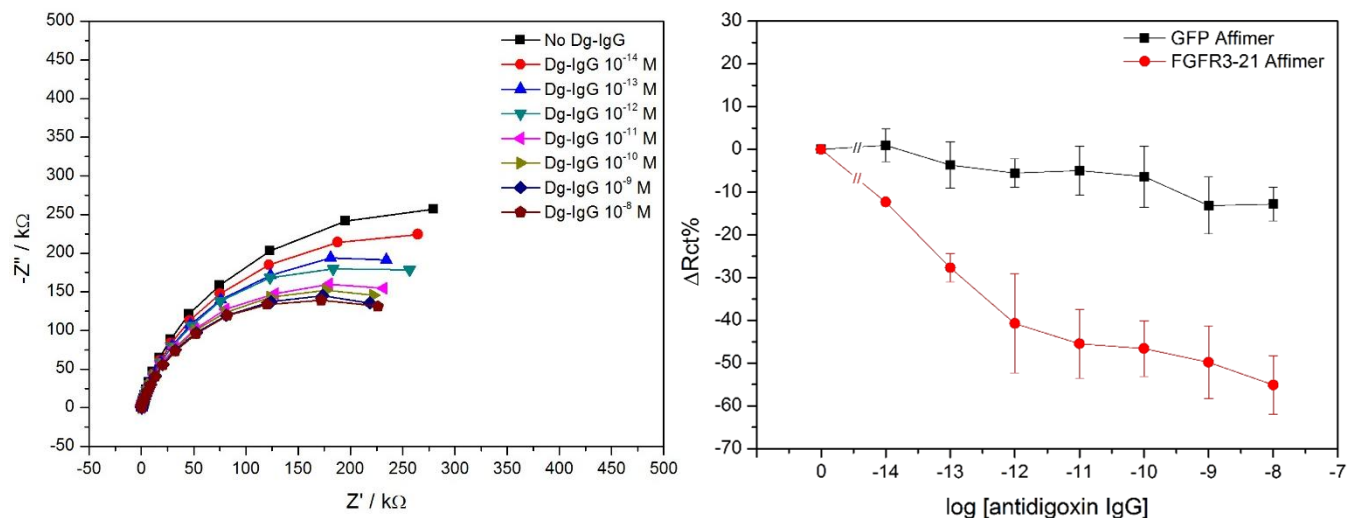


Figure 5.24 Specificity of biosensors to the analytes with data analysis subject the modified construction protocol. The figures on the left panel are Nyquist plots of a FGFR3-21 Affimer sensor and the figures on the right panel are calibration curves of the biosensors for detecting FGFR3 in PBS buffer. The sensors were blocked with 6.7 μ M BSA prior to Affimer attachment. The sensors were challenged with cumulative concentrations of analytes ranging from 10^{-14} M to 10^{-8} M with PBS washes in between. The analytes tested were FGFR3, (A, $n = 3 \pm \text{SEM}$); β -2-microglobulin, (B, $n = 3 \pm \text{SEM}$), and antidigoxin IgG, (C, $n = 3 \pm \text{SEM}$). The EIS measurements were performed in the presence of 10 mM $\text{K}_3\text{Fe}(\text{CN})_6/\text{K}_4\text{Fe}(\text{CN})_6$ redox mediator. The response of the sensors was displayed as $\Delta\text{Rct}(\%)$. (D) is subtracted data ($\Delta\text{Rct}(\%)$ for FGFR3-21 Affimer - $\Delta\text{Rct}(\%)$ for GFP Affimer) to determine specific response of the sensors.

C antidigoxin IgG



D subtracted response of the sensors

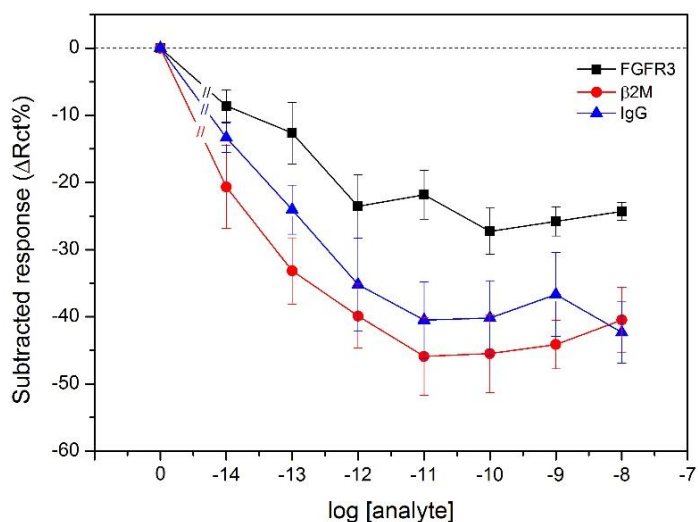


Figure 5.24 (continued) Specificity of biosensors to the analytes with data analysis subject the modified construction protocol. The sensors were challenged with cumulative concentrations of analytes ranging from 10^{-14} M to 10^{-8} M with PBS washes in between. The analytes tested were FGFR3, (A, $n = 3 \pm \text{SEM}$); β -2-microglobulin, (B, $n = 3 \pm \text{SEM}$), and antidigoxin IgG, (C, $n = 3 \pm \text{SEM}$). (D) is subtracted data ($\Delta Rct(\%)$ for FGFR3-21 Affimer - $\Delta Rct(\%)$ for GFP Affimer) to determine specific response of the sensors.

sensors tested with increasing FGFR3 was between 0% and -27% whilst the sensor responses for β -2-microglobulin and antidigoxin IgG were in the range of 0% - 45% and 0% - 43%, respectively (Figure 5.24D).

As well as FGFR3-21 Affimer, the FGFR3-14 Affimer was tested for its specificity for FGFR3 protein with anti-GFP Affimer as a control again. The sensor performance data are presented in Figure 5.25. As the sensors were tested with FGFR3 protein, a decrease in impedance (from 0% to -40%) over increasing concentrations of FGFR3 can be seen on FGFR3-14 Affimer sensors while a shift in impedance for control sensors was not observed (Figure 5.25A). However, when testing the sensors with β -2-microglobulin, a decrease in impedance (from 0% to approximately -30%) with increasing concentration of the analyte can be found on both FGFR3-14 and anti-GFP Affimer sensors (Figure 5.25B). Similarly, challenging the sensors with increasing concentrations of antidigoxin IgG showed a decrease in impedance (from 0% to -45%) on both FGFR3-14 and control sensors (Figure 5.25C). Subtracted $\Delta R_{ct}(\%)$ data to show specific response of the GFP/FGFR3-14 Affimer sensors are presented in Figure 5.25D. A continuous decrease of subtracted $\Delta R_{ct}(\%)$ from 0% to -40% can be seen when the sensors were tested with increasing concentration of FGFR3. On the other hand, the subtracted $\Delta R_{ct}(\%)$ data for the sensors exposed to β -2-microglobulin and antidigoxin IgG were almost constant with little shift between 15% and -10% as the concentration of analyte increased. This means that the effect of non-specific binding could be minimised by subtraction of its values in order to obtain only the response from specific interaction. However, as the non-specific Affimer (GFP Affimer) used for the data in Figure 5.24 and Figure 5.25 was identical, the sensor responses we anticipated to see should have been similar. Different responses of the sensors may be caused by any step of sensor assembly, leading to variation of sensor performance. Therefore, further optimisations are required in order to make sensors work consistently.

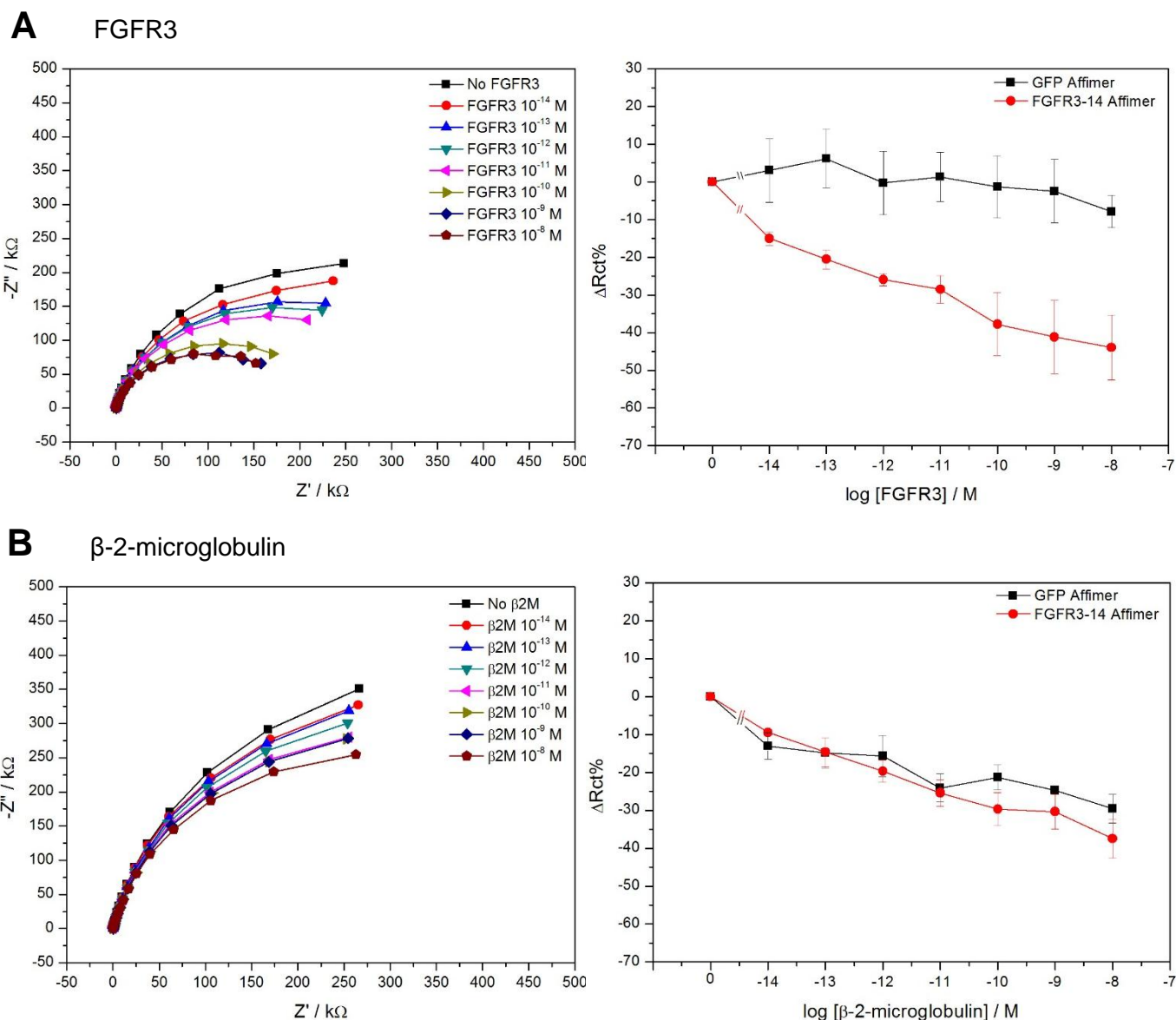


Figure 5.25 Specificity of biosensors to the analytes with data analysis subject the modified construction protocol. The figures on the left panel are Nyquist plots of a FGFR3-14 Affimer sensor and the figures on the right panel are calibration curves of the biosensors for detecting FGFR3 in PBS buffer. The sensors were blocked with 6.7 μ M BSA prior to Affimer attachment. The sensors were challenged with cumulative concentrations of analytes ranging from 10^{-14} M to 10^{-8} M with PBS washes in between. The analytes tested were FGFR3, (A, $n = 3 \pm \text{SEM}$); β -2-microglobulin, (B, $n = 3 \pm \text{SEM}$), and antidigoxin IgG, (C, $n = 3 \pm \text{SEM}$). The EIS measurements were performed in the presence of 10 mM $\text{K}_3\text{Fe}(\text{CN})_6/\text{K}_4\text{Fe}(\text{CN})_6$ redox mediator. The response of the sensors was displayed as $\Delta\text{Rct}(\%)$. (D) is subtracted data ($\Delta\text{Rct}(\%)$ for FGFR3-14 Affimer - $\Delta\text{Rct}(\%)$ for GFP Affimer) to determine specific response of the sensors.

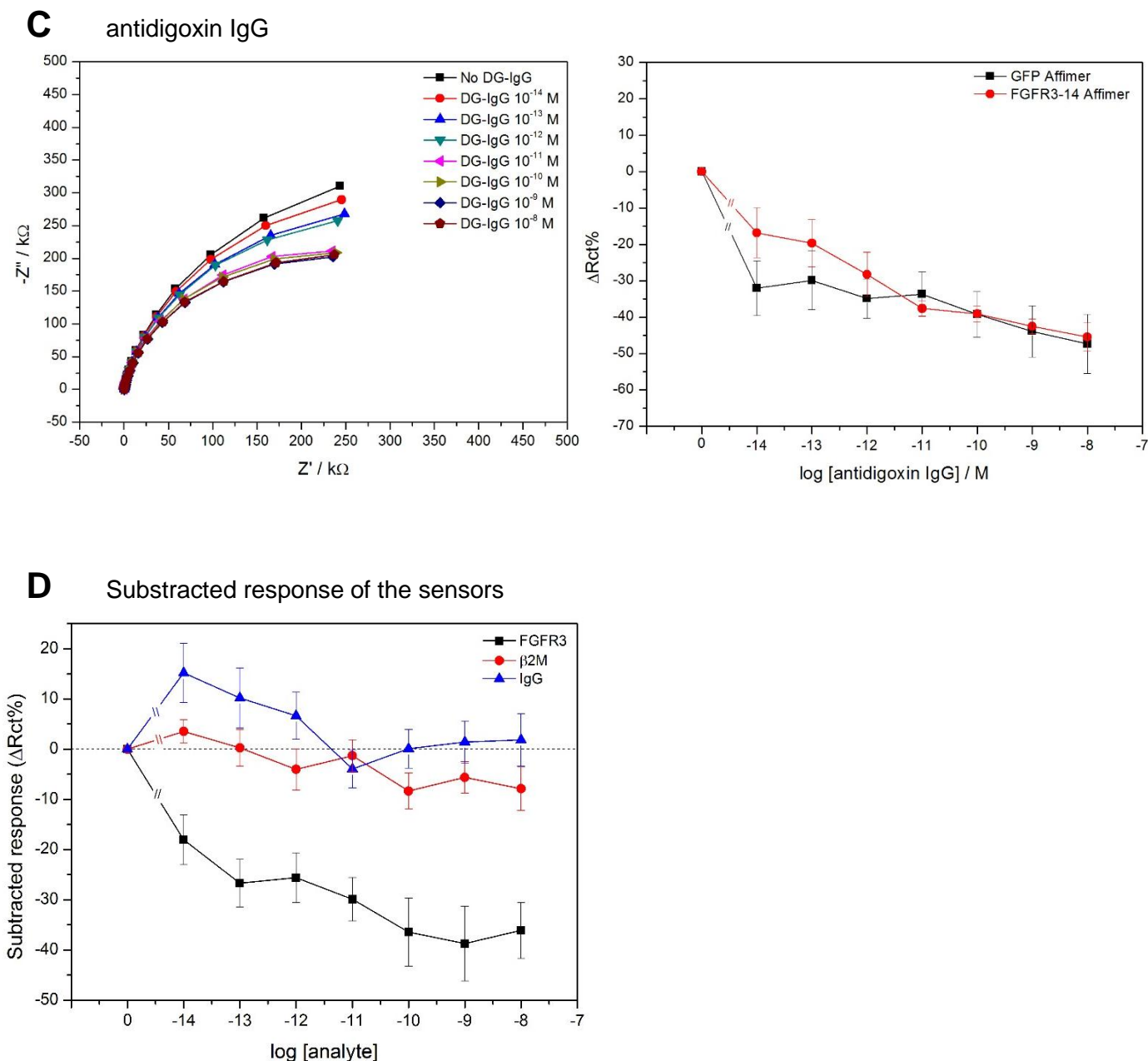


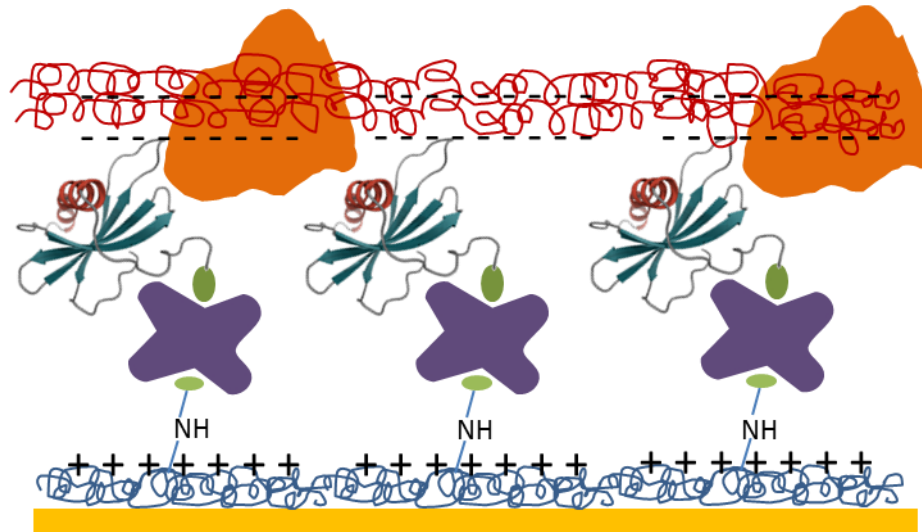
Figure 5.25 (continued) Specificity of biosensors to the analytes with data analysis subject the modified construction protocol. The sensors were challenged with cumulative concentrations of analytes ranging from 10^{-14} M to 10^{-8} M with PBS washes in between. The analytes tested were FGFR3, (A, $n = 3 \pm \text{SEM}$); β -2-microglobulin, (B, $n = 3 \pm \text{SEM}$), and antidigoxin IgG, (C, $n = 3 \pm \text{SEM}$). (D) is subtracted data ($\Delta Rct(\%)$ for FGFR3-14 Affimer - $\Delta Rct(\%)$ for GFP Affimer) to determine specific response of the sensors.

5.3.4.4 Effect of polystyrene sulfonate as a blocking agent on sensor performance

Charge on the transducer could be one source of non-specific interactions as it would allow oppositely charged molecules to bind. In this study, polytyramine was used as a supporting layer, providing amines as functional groups for chemical modification. However, at neutral pH when using PBS buffer, these amine groups are protonated. This means that the overall charge on the surface becomes positive. It was assumed that the positive charge surface can cause non-specific binding because the majority of the proteins have an isoelectric point (pI) below 7.0, making them negative. Therefore, changing the transducer surface charge to be negative may be the way of removing non-specific binding.

Polystyrene sulfonate is a polyanionic polymer. It was used in this study to modify the sensor surface as its charge may help minimise non-specific binding of most proteins in urine. In the normal way, electrode surface was sequentially deposited with polytyramine, 3 μM NHS-biotin, 0.067 μM NeutrAvidin and 1 μM biotin-tagged Affimer, and then polystyrene sulfonate at a concentration of 1 μM , 5 μM and 10 μM was tested for reduction of non-specific binding. The sensors were finally tested with a range of FGFR3 concentrations. Figure 5.26 shows a schematic of the sensor fabrication steps including the application of polystyrene sulfonate as a blocking agent.

At 1 μM polystyrene sulfonate (Figure 5.27A), the shifts of R_{ct} over the increasing concentrations of FGFR3 on control (GFP Affimer) and FGFR3-21 Affimer sensors were similar, indicating that 1 μM polystyrene sulfonate was unable to eliminate non-specific binding. Changing the concentration of polystyrene sulfonate to 5 μM reduced some non-specific binding of FGFR3 on control sensors (Figure 5.27B) with the decrease of R_{ct} with increasing FGFR3 concentrations on



6. Testing with FGFR3
5. Blocking with polystyrene sulfonate
4. Biotinylated Affimer immobilisation
3. NeutrAvidin attachment
2. Surface biotinylation
1. Tyramine polymerisation

Figure 5.26 Schematic representation of Affimer sensor construction. The sensor was blocked with polystyrene sulfonate after biotinylated Affimers were attached to the electrode. Polystyrene sulfonate presenting negative charge was used to neutralise positive charge on polytyramine surface.

FGFR3-21 sensors. However, a significant level of non-specific binding still remained. As the concentration of polystyrene sulfonate was increased to 10 μM , non-specific interaction on negative control sensors was not eliminated though the R_{ct} decrease for FGFR3-21 Affimer sensors was observed (Figure 5.27C). The results obtained from these experiments suggested that polystyrene sulfonate could not be employed as an effective blocking agent for this impedimetric biosensor platform. It is recommended that new antifouling agents should be tested for their blocking properties or searching for a proper washing buffer could be an alternative of minimising the non-specific binding events.

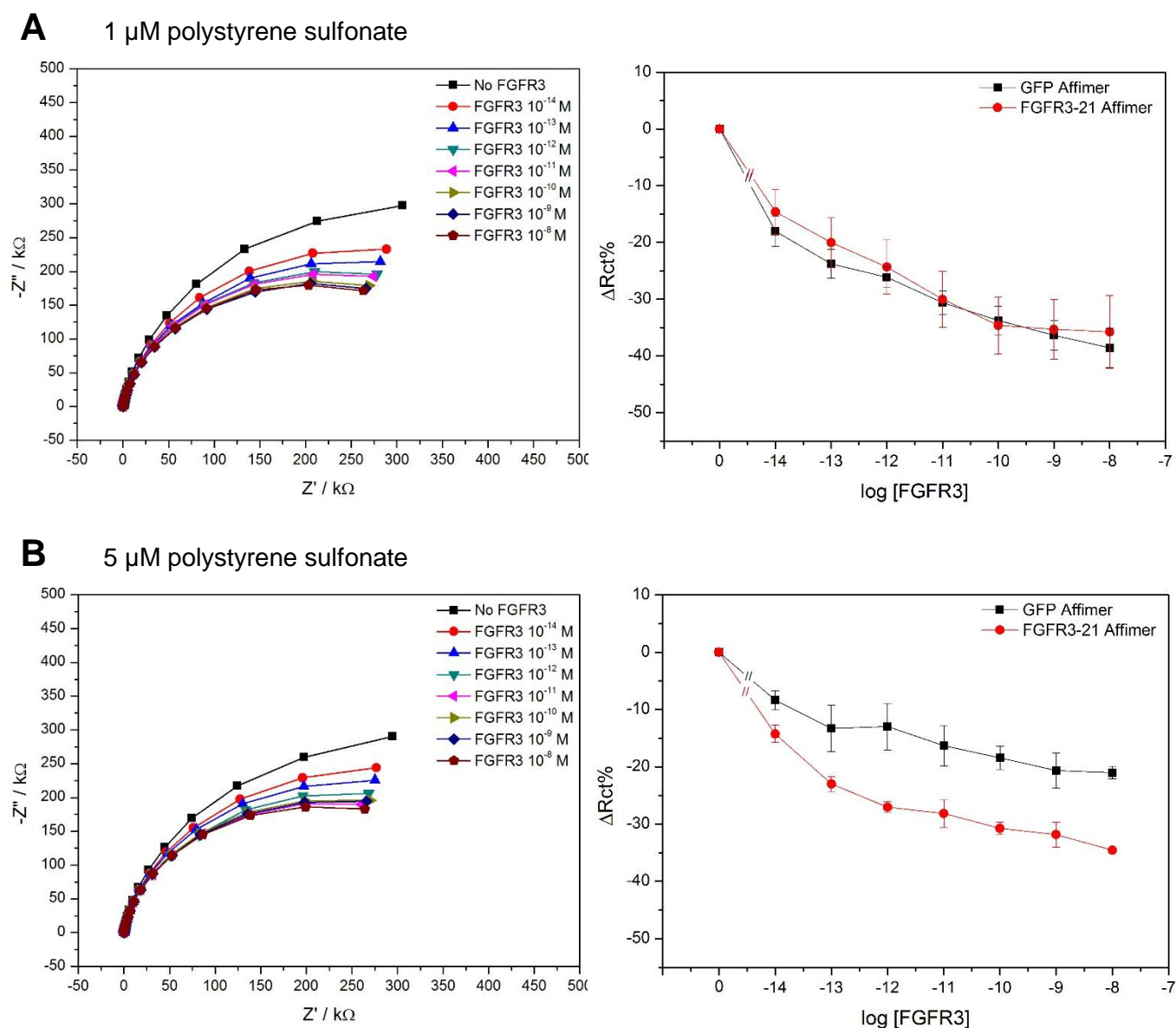


Figure 5.27 Effect of polystyrene sulfonate as a blocking agent on sensor performance. The figures on the left panel are Nyquist plots of a FGFR3-21 Affimer sensor and the figures on the right panel are calibration curves of the biosensors for detecting FGFR3 in PBS buffer. The sensors were blocked with different concentrations of polystyrene sulfonate, which were 1 μM , (A, $n = 4 \pm \text{SEM}$); 5 μM , (B, $n = 3 \pm \text{SEM}$), and 10 μM , ($n = 3 \pm \text{SEM}$). The sensors were challenged with cumulative concentrations of FGFR3 ranging from 10^{-14} M to 10^{-8} M with PBS washes in between. The EIS measurements were performed in the presence of 10 mM $\text{K}_3\text{Fe}(\text{CN})_6/\text{K}_4\text{Fe}(\text{CN})_6$ redox mediator. The response of the sensors was displayed as $\Delta\text{Rct}(\%)$.

C 10 μM polystyrene sulfonate

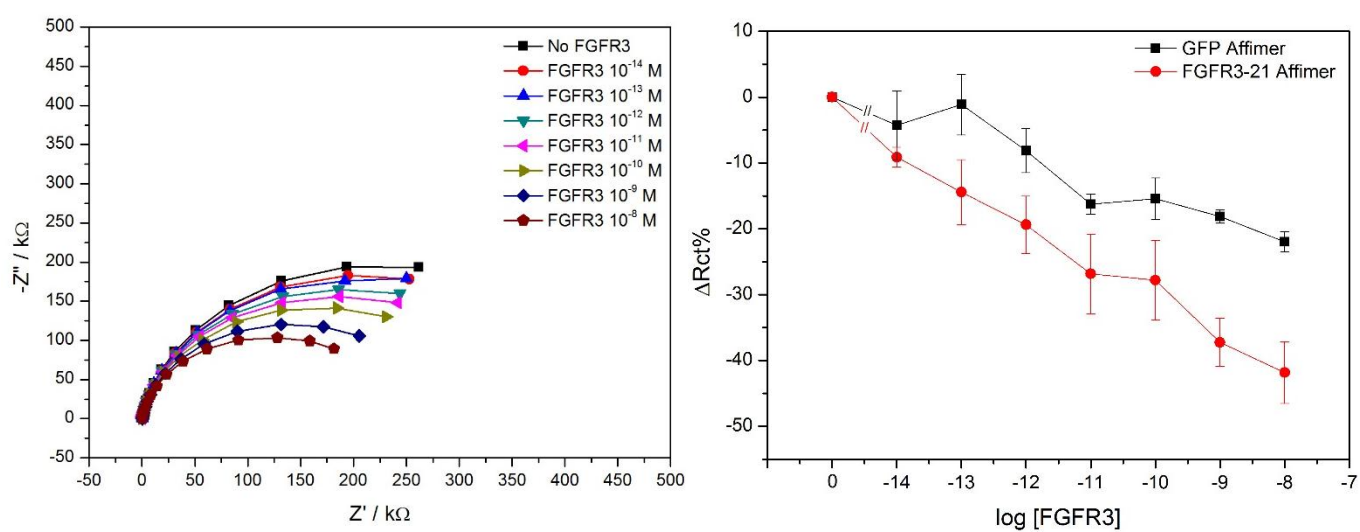


Figure 5.27 (continued) Effect of polystyrene sulfonate as a blocking agent on sensor performance. The sensors were blocked with different concentrations of polystyrene sulfonate, which were 1 μM , (A, $n = 4 \pm \text{SEM}$); 5 μM , (B, $n = 3 \pm \text{SEM}$), and 10 μM , ($n = 3 \pm \text{SEM}$).

5.4 Discussion

Impedimetric biosensors have been proved as a valuable tool to investigate the binding events between biorecognition elements and their target analytes (Rushworth et al., 2014, Ohno et al., 2013, Goode et al., 2016). In addition to bioreceptors, the method of sensor construction is one of the most important factors for sensor efficiency. Several approaches including adsorption, entrapment, covalent bonding via cross-linkers and bioaffinity can be used to immobilise bioreceptors to the transducer electrodes (Liebana and Drago, 2016).

In this chapter, two methods were used to attach Affimers to the sensor surface. The first one was ELISHA “gluing method”, which depended on covalent bonding via a cross-linker. It was expected that the cross-linker connecting between the polymer layer and Affimers could help control correct orientation of the Affimers, allowing the analyte to access the binding site of the Affimers. However, non-specific binding on sensors was observed (Figure 5.3B). As mentioned in the methodology section 2.2.7.1, a mixture of Affimer, linker and monomer was simultaneously deposited on a working electrode via cyclic voltammetry. Some molecules of Affimer may be placed on the polymer surface in the upright position, which allowed them to bind the target analytes. However the rest of the Affimer molecules could be trapped between the polymer layers, hampering access to the analytes. Moreover, neutral pH buffer such as PBS, amine functional groups on the polymer surface are protonated. As the majority of bodily proteins have an isoelectric point (pI) below 7.0, the overall charge on the proteins is negative. At this stage, the proteins can bind to the polymer surface via electrostatic forces, causing non-specific binding events that can be seen by a shift in charge transfer resistance (R_{ct}). Thus, an alternative method for sensor fabrication was introduced.

The other method relied on a non-covalent bonding for surface modification, NeutrAvidin-biotin interaction. This interaction is extremely strong with the dissociation constant (K_D) down to 10^{-15} M (Liebana and Drago, 2016, Sassolas et al., 2012). Using this type of linkage, correct orientation of bioceptors can be controlled. The Affimer-based impedimetric biosensor construction was successful as seen from the increase in impedance signal during each step of construction. After testing the sensors with the analyte (FGFR3 protein), a decrease in impedance values was observed. In general, the increase in impedance as the concentration of analyte increases is a common event (Billah et al., 2010, Esseghaier et al., 2008, Ohno et al., 2013). This is because more deposited materials on the sensor surface can cause the sensor more resistive and capacitive (Rushworth et al., 2013). However, in some circumstances when the binding between two molecules causes changes in the physical or chemical properties of the surface, a decrease in impedance can also be detected (Rushworth et al., 2013). The decrease in impedance is often seen when synthetic binding peptides are used as a biorecognition element and the difference of size between receptors and targets is significantly large (Rushworth et al., 2014, Goode et al., 2016). It was proposed that 'pinholing effect' from the binding of a small receptor and a large analyte lets the charge components transfer through the multiple layers of polymer and contact with transducer surface underneath (Goode, 2015). This effect results in the decrease in impedance that can be detected as exemplified in this work.

In this work, the performance of the sensors was determined using four different analytical approaches to the electrochemical data. Similar to the majority of previous publications (Ahmed et al., 2013, Barton et al., 2008, Caygill et al., 2012, Johnson et al., 2012), the change in R_{ct} was initially used to monitor the change upon the interaction of the Affimers and FGFR3 protein. Despite the large shift observed, fitting the impedance data with the Randle's equivalent circuit model may cause an

erroneous calculation of the R_{ct} since only half of a complete Nyquist plot was obtained from the measurement (Figure 5.9 in Section 5.3.2). Other alternatives were applied and compared to changes seen in the R_{ct} data. The percent change in capacitance values was successfully used to detect mRNA as a biomarker of tumours on the non-faradaic impedance biosensor platform (Jolly et al., 2016). However, applying this approach to our biosensor platform was not effective since the capacitance values of the sensors when detecting FGFR3 barely changed. Our results were similar to the previous publication (Weiss et al., 2005). In the study, the binding of avidin, following by biotinylated anti-haemoglobin IgG, to biotinylated SAM surface did not show any shift in capacitance values. However, a large change could be detected beyond the semicircular region of a Cole-Cole plot, indicating binding events happening outside of the thick layers on electrode surface. This situation also occurred in another study which reported the development of the impedemetric biosensor using the Affimers to detect C-reactive protein (CRP) (Johnson et al., 2012). The researchers found that the binding of the Affimers to CRP almost unaffected capacitance but the changes were dominated by charge-transfer resistance (R_{ct}). The shifts of phase angle (Sharma et al., 2016, Raina et al., 2015) and the changes of absolute values of impedance (Dapra et al., 2013, Park et al., 2018) have also been used to monitor sensor performance. However, both techniques were not able to distinguish the response of specific interaction from non-specific binding (Section 5.3.3.1). Comparing the results from all four analyses, the percentage change in R_{ct} is the most appropriate option for monitoring the binding of the Affimers and FGFR3 for the biosensor platform in this work.

The concentrations of Affimers and NeutrAvidin were also studied to improve the performance of the sensors when exposing to the analyte. At the optimal concentrations of both Affimers and NeutrAvidin, the effects of steric hindrance from both molecules could be minimised and the specific binding of the Affimer to its target

analyte could be detected. However, non-specific binding was a major problem. A wide range of blocking agents from small molecules such as pyromellitic dianhydride (MW = 218) to a large protein such as bovine serum albumin (BSA, MW = 66,500). The results from the sensor performance showed that mPEG-biotin and BSA seemed to be the best blocking agents for Affimer-based sensors using the NeutrAvidin-biotin based sensor construction method. Even though both mPEG-biotin and BSA could be used to minimise non-specific binding problem of FGFR3 to the sensors with the range of detection in picomolar, non-specific interactions of other non-related protein analytes to the modified surface are still problematic. For mPEG-biotin, even though polyethylene glycol (PEG) has been proven for its resistance to the adsorption of proteins to solid surfaces (Liu et al., 2013, Ostuni et al., 2001, Furuya et al., 2006), it was proposed that PEG can interact with proteins via physical adsorption to the hydrophobic regions on the protein (Rawat et al., 2010). There was evidence showing that PEG can bind to proteins such as BSA and human immunoglobulin G (Rawat et al., 2010, Ogi et al., 2009), and also promote the binding of bacteria to the modified surface (Riquelme et al., 2016). This may be an explanation for non-specific binding when using mPEG-biotin to block the surface. In the case of BSA, even though it has been widely used as a blocking agent in many immunoassays such as ELISA and western blotting, non-specific binding may occur because of the hydrophobic parts of BSA. With this property, albumin is able to bind fatty acids and steroid hormones (Spector et al., 1969, Weisiger et al., 2008) and is used as a protein carrier in serum. As an abundant soluble protein in plasma, albumin can also interact with other molecules including drugs, toxins, metal ions, amino acids (tryptophan and cysteine), and proteins (Weisiger et al., 2008, Borgstrom and Erlanson, 1978, Nygren et al., 1990, Schnitzer et al., 1992). This makes it possible for BSA to form hydrophobic interactions with some proteins, leading to non-specific binding detected by sensitive sensors. In a previous study by (Riquelme et al., 2016), bovine serum

albumin (BSA) and chicken serum albumin (CSA) were investigated for their ability of removing non-specific binding of bacteria to gold surface. The researchers found that BSA or CSA alone were not effective when used to block the surface from bacteria. However, BSA or CSA in combination with Tween 20 could significantly reduce non-specific binding from bacteria to the surface (Riquelme et al., 2016). Tween 20 is a surfactant that is normally added to the buffer used for the ELISA and western blotting in order to remove any unwanted components. This leads to the idea that if Tween 20 at low concentrations is introduced into the wash buffer used during biosensor measurement, non-specific binding formed by weak interactions between proteins and modified surface might be removed. However, because Affimers as bioreceptors are proteins, it is necessary to ensure that in the presence of a surfactant like Tween 20, the structure of the Affimers is still intact and can function properly.

Chapter 6

General discussion

6.1 General discussion

During the past decades, an increasing number of biosensor reports have emerged. This indicates a popular trend of biosensors becoming an analytical tool for point-of-care diagnosis and environmental monitoring. However, few biosensors have become commercialised because most of them cannot meet standard requirements for commercial production. To achieve this aim, optimising fundamental factors for sensor fabrication is the first step in the process.

The overall objective of this project was to develop and optimise the method to fabricate impedimetric biosensors employing Affimers, a type of synthetic non-antibody binding protein scaffolds, as a biorecognition element to detect a target analyte of interest. The tasks were divided into three parts, starting from Affimer selection from a phage display library, followed by Affimer characterisation using different approaches to characterise selected Affimers, and ending with the use of Affimers for biosensor construction. In this chapter, key and interesting technical observations, considerations and recommendations will be pointed out together with future work.

6.2 The challenge of Affimer selection against small molecules

Affimers are synthetic non-antibody binding proteins recently developed (Tiede et al., 2014, Tiede et al., 2017). As with many synthetic binding proteins, the selection of Affimers against a specific target can be conducted by biopanning a phage display library. In this thesis, dichlorodiphenyltrichloroethane (DDT), a small molecule insecticide, was selected as target for Affimer selection. Even though the originally established method from BSTG selected a number of Affimer clones from the Affimer population, none of the selected Affimers showed binding to the original form of DDT. During three biopanning cycles, biotinylated DDT was employed to pull out the phage displaying Affimers. Biotinylated DDT contains biotin, a short spacer and the DDT moiety. The data in Chapter 4 (Section 4.2) showed that most likely the selected Affimers recognised the biotin-spacer plus DDT construct used for selection but not DDT alone.

The selection of Affimers specific for small molecules is challenging. This is because the size of the target is much smaller as compared to bacteria and large biomolecules such as proteins. Proteins normally present multiple epitopes which facilitate the binding of Affimers to them. However, this is not the case for small molecules. Recently, an established protocol for selecting Affimers against small molecules was reported (Tiede et al., 2017). Counter selection was used to extract Affimers against 2,4,6-trinitrotoluene (TNT), a small organic compound. A TNT analogue, 2,4,6-trinitrobenzene sulfonic acid (TNBS) was conjugated with ovalbumin and IgG, resulting in TNBS-ovalbumin and TNBS-IgG conjugates. Two different conjugates were successfully used to perform the counter selection and Affimers showing specificities to TNT were obtained. This leads to the idea of protocol modification for selecting Affimers specific to DDT. The task will be more challenging

than the case of TNT because of the hydrophobic nature of DDT and extra steps to conjugate DDT to carrier proteins may be needed. However, conjugation of a DDT-protein carrier has been published elsewhere (Abad et al., 1997, Hong et al., 2002). It was also noticeable that when performing ELISA to check the specificity of selected Affimers to TNT, the detectable range fell in the μM range (Tiede et al., 2017). However, DDT is a hydrophobic molecule, making it poorly soluble in water (nM range). It is recommended that any assays to determine the binding of Affimers and DDT need to be carefully optimised.

6.3 Production and characterisation of Affimers for FGFR3 detection

The second analyte to be detected in this thesis was fibroblast growth factor receptor 3 (FGFR3). FGFR3 is a tyrosine kinase membrane protein in the FGFR family and is involved in many biological processes including cell proliferation, survival, migration and differentiation (Wesche et al., 2011). As overexpression and mutation of this protein are commonly found in bladder cancer cells, FGFR3 seems to be a promising biomarker for bladder cancer surveillance (Tomlinson et al., 2007). This means monitoring the risk of bladder cancer development could become possible with FGFR3 detection. Several Affimers against FGFR3 protein were selected from a phage display library via biopanning and subcloned into a pET11a expression vector for protein production in *E.coli*. Although producing Affimers using the bacterial system is well-known and convenient to operate compared to antibody production, because of the unique properties of each Affimer, some factors needed to be adjusted in order to obtain Affimers of high quality and yield.

The structure of Affimers has been claimed for its high thermal stability (Tiede et al., 2014). The melting temperature (T_m) can be up to 101 °C. However, this is not routine. In this work, even though GFP and FGFR3-21 Affimers provided high yields when the originally established expression protocol by BSTG (Raina et al., 2015, Tiede et al., 2014, Tiede et al., 2017) was applied, the expression yields for FGFR3-8 and FGFR3-14 Affimers were low and insufficient. By skipping the 50 °C heating step in the original protocol, the yields for FGFR3-8 and FGFR3-14 Affimers were significantly improved (Section 3.5.3). This indicates the unique properties of each Affimer, governed by 18 random amino acid sequences split over two variable peptide regions; this represents a significant proportion, around 20%, of the whole Affimer molecule.

In this thesis, a single cysteine residue was introduced at the C-terminus of an Affimer (Section 3.3). The Affimers do not contain Cys in the scaffold or loops and the additional cysteine can be used as a specific site for conjugation. This modification site allows users to control the orientation of Affimers when applying them in different biorecognition assays. In our work, as NeutrAvidin-biotin interaction was employed as a bridge and a maleimide reaction with biotin-maleimide was used to modify Affimers via the Cys-SH (Section 4.3.1). The successful conjugation of Affimers and biotin-maleimide was confirmed using ELISA and LC-MS (Figure 4.6, 4.7 and 4.8). This linkage permitted us to orient Affimers in the upright orientation in ELISA (Section 4.3.2), surface plasmon resonance (SPR) (Section 4.3.3), immunoprecipitation (pull-down) assay (Section 4.3.4). As a result, all three characterisation methods showed specific binding of some selected Affimers to FGFR3 proteins with no response by GFP Affimer as a negative control bioreceptor.

A common problem for Affimer users is aggregation (Raina et al., 2015, Mahatnirunkul, 2017). This event is often encountered when performing dialysis or during storage. In the original BSTG protocol, 20 - 40% (v/v) glycerol is generally

added into storage buffer in order to keep Affimers in their original conformation during storage. However, this is not optimum for impedimetric biosensor platforms since glycerol can interfere with sensor fabrication. The aggregation results from dimerisation of two Affimer molecules via disulfide linkage formation. In our cases, we found that diluting Affimer concentration to under 1 mg/ml could minimise aggregation and the problem disappeared when Affimers were biotinylated.

In addition to specific biorecognition properties like antibodies, Affimers are monoclonal and have a single, unmodified polypeptide. This means they can be expressed in prokaryotic systems such as *E.coli*. The problem of batch-to-batch variations is minimised and the cost of production reduced. With these advantages, a wide range of applications based on Affimers have emerged (Tiede et al., 2017, Kyle et al., 2015, Rawlings et al., 2015). In the area of biosensors, Affimers have been employed for the detection of C-reactive protein (Johnson et al., 2012), anti-myc tag antibody (Raina et al., 2015), human interleukin-8 (Sharma et al., 2016), and methylene blue (Koutsoumpeli et al., 2017). In this thesis, we have developed the first Affimer-based impedimetric sensors to detect FGFR3 protein.

6.4 Optimising fundamental parameters affecting impedimetric biosensor performance

To achieve the high sensitive and specific detection of any target of interest, several fundamental factors affecting sensor performance are basically taken into account when designing a method of sensor fabrication. In this thesis, some of the important parameters were considered and discussed in more detail as follows.

The choice of electrodes is one of the most important factors governing the achievement of the measurement. In this project, commercial gold screen-printed

electrode chips were employed for the whole experiments. The benefit of using this type of electrode is one chip contains two working electrodes, a reference electrode and a counter electrode. Therefore, the distances of internal electrodes can be fixed. However, the electrode surface is rough on the nano/microscales (Ahmed, 2015). This leads to the problem with sensor reproducibility. To minimise variation, using electrodes made from the same batch is recommended.

Regarding the surface roughness of the gold screen-printed electrodes, polytyramine, a non-conductive polymer, was utilised as a supporting layer for sensor fabrication. Polytyramine is known for its high stability, self-limiting insulating property, porosity and the presence of amine functional groups for modification (Ahmed et al., 2013, Losic et al., 2005). In the protocols published previously from the Millner group (Goode et al., 2016, Ahmed, 2015, Ahmed et al., 2013, Rushworth et al., 2014), tyramine was prepared in methanol with NaOH. However, it was observed that NaOH is not 100% soluble in MeOH and some NaOH left precipitated in solution. This leads to inconsistency of the solution concentration prepared at different times and causes problems with sensor reproducibility. Moreover, it was reported that tyramine is prone to precipitate rapidly during the polymerisation stage (Ahmed, 2015). In this study, tyramine was dissolved in Milli-Q water with NaOH. Tyramine dissolved completely in water and no precipitation was seen. When coating polytyramine on top of working electrodes, the surface was more resistive and capacitive than the surface deposited with polytyramine prepared in methanol (Figure 5.7), indicating a thicker supporting layer. Interestingly, sensor performance was more reproducible with the modified protocol.

Optimising concentration of bioreceptors (Affimers) was essential in order to achieve the maximum level of analyte binding. Owing to the roughness of the Dropsens electrode surface, coverage of the surface when immobilising bioreceptors was probably not homogeneous (Ahmed, 2015). Too high concentration of

bioreceptors can cause excessive packing density on the surface, leading to steric hindrance affecting the accessibility of Affimer binding sites to the analyte. This is supported by (Holford et al., 2013) and (Ahmed et al., 2013) who found that too concentrated bioreceptors led to lower impedance response when detecting the targets compared to bioreceptors at their optimal concentrations. The reason for this event is that at concentrations beyond the optimal point, further non-specific adsorption of bioreceptors to the primary, well-organised layer occurs, resulting in more disordered and thicker films (Holford et al., 2013). In the case of insufficient bioreceptors loading, it affects the signal generation during the measurements, but also non-specific binding from unwanted components to unblocked surface, often electrodes, can occur (Ahmed, 2015). Optimal concentration of NeutrAvidin was also investigated in this project. As a linker connecting between polymer-coated surface and bioreceptors (Affimers), the packing density of NeutrAvidin can also determine the optimal coating density of bioreceptors to the surface. Excess or insufficient NeutrAvidin could lead to suboptimal Affimer loading (Ahmed et al., 2013, Ahmed, 2015).

It should be noted here that the roughness of electrode surface is not the only source of sensor irreproducibility, but also each step of sensor assembly can be a source of variations. In this thesis, layer-by-layer sensor construction was done by manually pipetting. However, automated sensor fabrication could help minimise any errors caused by manual sensor assemblies. (Caygill et al., 2012) and (Holford et al., 2013) reported that an automated BioDot platform could significantly improve sensor reproducibility compared to sensors fabricated manually.

6.5 Effect of blocking agents on sensor response

It has been hypothesised that unoccupied transducer surface could be a source of non-specific binding. Blocking agents were applied to remove non-specific binding effects. In this thesis, although several blocking agents were tested for their antifouling abilities to protein analytes, two of them, mPEG-biotin and bovine serum albumin (BSA), seemed to be the best options for blocking unwanted interactions.

In the case of mPEG-biotin, its blocking ability worked well when the sensors were exposed to FGFR3 protein, but non-specific binding still remained when the sensors were tested with other non-FGFR3 proteins (Section 5.3.3.4). Polyethylene glycol (PEG) is widely used to passivate surfaces in biomedical uses (Liu et al., 2013, Ostuni et al., 2001, Furuya et al., 2006). However, the enhancement by PEG of protein and bacteria adsorption has also been reported (Rawat et al., 2010, Ogi et al., 2009, Riquelme et al., 2016). The interaction between PEG and proteins could be from physical adsorption between hydrophobic regions on proteins and PEG (Rawat et al., 2010).

BSA has been widely used as an effective blocking agent in many immunoassays. In this work, BSA was confirmed for its blocking properties to FGFR3 protein when used in the Affimer impedimetric sensor platform (Section 5.3.4.3). However, BSA failed to remove non-specific binding from non-FGFR3 protein analytes. Although BSA is hydrophilic, it has hydrophobic patches that can form hydrophobic interactions with other biomolecules. There are previous studies showing that BSA can interact with many analytes such as fatty acids, hormones, drugs, toxins, metal ions, amino acids and proteins (Weisiger et al., 2008, Borgstrom and Erlanson, 1978, Nygren et al., 1990, Schnitzer et al., 1992, Spector et al., 1969) and its natural biological role is to carry these molecules in the circulation. However, a previous study reported that BSA in combination with Tween 20 could apparently

resist non-specific binding from this strain of bacteria (Riquelme et al., 2016). Tween 20 is commonly added into wash buffers used in ELISA in order to minimise non-specific binding. This leads to the idea that introducing Tween 20 to wash buffer during sensor construction and measurements may help minimise non-specific binding from non-related analytes whereas specific binding from FGFR3 protein would still be retained.

6.6 Limitations in the field and possible opportunity of the sensors

Bladder cancer is one of the most frequently diagnosed cancers and cause of deaths worldwide. With an increasing number of patients every year, methods of cancer detection at early stages and regular follow-up of cancer recurrence after transurethral resection are highly advantageous. Nowadays, several approaches are employed (Budman et al., 2008, Proctor et al., 2010). Although cystoscopy and urine cytology are used as standard methods for monitoring bladder tumours, they show some disadvantages such as invasiveness, cost ineffectiveness and patient anxiety for cystoscopy, and insensitivity for cytology. Biomarker-based assays (as described in Section 1.6.2) are also commercially available, but poor specificity is still a problem, leading to false positives. Accordingly, there is still room for biosensor development.

Up until now, only one published work has been related to the use of biosensor to detect FGFR3 (Shin et al., 2013). The researchers developed a DNA sensing platform using the shift of resonance wavelength to detect mutational status of FGFR3 gene as a marker for bladder cancer. As no biosensors detecting FGFR3 protein have been reported yet, the work in this thesis is the first electrochemical biosensor that enables detection of FGFR3 protein. Even though more optimisations

to remove non-specific binding to the sensors and the real biological sample tests are still under investigation, the data until now present the idea of developing a more convenient, cheap, and label-free alternative to IHC and ELISA for the detection of FGFR3 protein as a promising marker for bladder tumour monitoring.

6.7 Future work

In this thesis, non-specific binding from non-FGFR3 proteins is a major concern that makes the developed sensors impractical in use. Attempts of optimising blocking conditions to eliminate non-specific interactions of proteins and non-related components to the sensor surface are still in progress. In the 'real world' applications, pure samples like serial dilutions of a specific protein do not truly exist. In fact, the biological samples collected from patients contain a plenty of biomolecules which can potentially cause noise background when the sensors perform the measurements. Therefore, it is imperative for sensors to discriminate the specific interaction between the bioreceptor and the target from any non-specific interactions to the surface. Other than blocking agents used to minimise non-specific binding effect, the choice of electrodes is one of the most important factors relating to reproducibility of the sensor performance. Electrodes with flatter gold surface may be a better alternative to the Dropsens screen-printed gold electrodes used in this study. Carbon electrodes are also commercially available and could be considered as an alternative for sensor fabrication. Biotin-avidin interaction was used in this work, but non-specific binding was problematic as presented in Chapter 5. Different bioconjugate chemistries should be considered for biosensor surface functionalisation (Section 1.4.2.3). As an Affimer possesses a thiol functional group, it can directly interact with a gold surface. This thiol-gold interaction was successfully used for the impedance biosensor to detect Her4 (Zhurauski et al., 2018). Heterobifunctional linkers such as sulfo-SMCC

were also used to link bioreceptors with a free thiol group to the functionalised surface, leading to correct orientation of bioreceptors when detecting their target analytes (Goode et al., 2016). EDC/NHS conjugation was employed to construct Affimer-based biosensors to detect various target analytes (Johnson et al., 2012, Raina et al., 2015, Sharma et al., 2016). With a collection of bioconjugation techniques, fabricating biosensors with repeatable output can be achievable.

Another weak point of this work is that even though there was the evidence showing the high expression level of FGFR3 in urine collected from bladder cancer patients (Blanca et al., 2016), no pathological level of FGFR3 in urine has been reported yet. We recommend here that ELISA be a standard method to determine the detectable level of FGFR3 in urine samples from normal people and bladder cancer patients and this range of detection should be used as a reference for biosensors to detect FGFR3 as a biomarker for bladder cancer monitoring.

Until the present, biosensing research has shifted towards label-free systems since they can offer cost effectiveness, simplicity and fewer reagents used. From a commercial perspective, precision and reproducibility are necessities for every sensor fabricated. Fundamental parameters need to be carefully optimised as every step of sensor assemblies leads to the success of sensor performance. It is also a requirement that the cost of sensor production should not be too high. Simplicity in use is also important when looking from a commercial view. Designing multitasking sensors by miniaturising input, measurement, signal generation and interpretation steps in one device could make the sensors easy to use in real situations. More importantly, those who work in this field should bear in mind that each target analyte has its unique properties. Therefore, a sensing platform designed for one target may not be suitable for others. On the other hand, it can be stated that every target requires its own optimisation. An optimised platform for a specific analyte like the work conducted in this thesis can only provide the way of assisting experimental

design for other targets. We hope that the Affimer-based impedimetric biosensor platform presented here may not only be an effective tool for bladder cancer surveillance, but also an initial platform to design methods of detecting other protein biomarkers of diseases.

References

- ABAD, A., MANCLUS, J. J., MOJARRAD, F., MERCADER, J. V., MIRANDA, M. A., PRIMO, J., GUARDIOLA, V. & MONTOYA, A. 1997. Hapten synthesis and production of monoclonal antibodies to DDT and related compounds. *Journal of Agricultural and Food Chemistry*, 45, 3694-3702.
- AHMED, A. 2015. *Fabrication of electrochemical biosensors for detection of microorganisms*. Doctor of Philosophy, University of Leeds.
- AHMED, A., RUSHWORTH, J. V., HIRST, N. A. & MILLNER, P. A. 2014. Biosensors for Whole-Cell Bacterial Detection. *Clinical Microbiology Reviews*, 27, 631-646.
- AHMED, A., RUSHWORTH, J. V., WRIGHT, J. D. & MILLNER, P. A. 2013. Novel Impedimetric Immunosensor for Detection of Pathogenic Bacteria *Streptococcus pyogenes* in Human Saliva. *Analytical Chemistry*, 85, 12118-12125.
- ALBERTS, B., JOHNSON, A., LEWIS, J., RAFF, M., ROBERTS, K. & WALTER, P. 2002. *Molecular Biology of the Cell*, New York, USA, Garland Science.
- ALGIERI, C., DRIOLI, E., GUZZO, L. & DONATO, L. 2014. Bio-Mimetic Sensors Based on Molecularly Imprinted Membranes. *Sensors*, 14, 13863-13912.
- ALIZADEH, T. & AKBARI, A. 2013. A capacitive biosensor for ultra-trace level urea determination based on nano-sized urea-imprinted polymer receptors coated on graphite electrode surface. *Biosensors & Bioelectronics*, 43, 321-327.
- ALON, R., BAYER, E. A. & WILCHEK, M. 1990. STREPTAVIDIN CONTAINS AN RYD SEQUENCE WHICH MIMICS THE RGD RECEPTOR DOMAIN OF FIBRONECTIN. *Biochemical and Biophysical Research Communications*, 170, 1236-1241.
- AMIZUKA, N., DAVIDSON, D., LIU, H. L., VALVERDE-FRANCO, G., CHAI, S., MAEDA, T., OZAWA, H., HAMMOND, V., ORNITZ, D. M., GOLTZMAN, D. & HENDERSON, J. E. 2004. Signalling by fibroblast growth factor receptor 3 and parathyroid hormone-related peptide coordinate cartilage and bone development. *Bone*, 34, 13-25.
- ANTONI, S., FERLAY, J., SOERJOMATARAM, I., ZNAOR, A., JEMAL, A. & BRAY, F. 2017. Bladder Cancer Incidence and Mortality: A Global Overview and Recent Trends. *European Urology*, 71, 96-108.

- ARNOUX, B., DUCRUIX, A. & PRANGE, T. 2002. Anisotropic behaviour of the C-terminal Kunitz-type domain of the alpha 3 chain of human type VI collagen at atomic resolution (0.9 angstrom). *Acta Crystallographica Section D-Biological Crystallography*, 58, 1252-1254.
- ARNTZ, Y., SEELIG, J. D., LANG, H. P., ZHANG, J., HUNZIKER, P., RAMSEYER, J. P., MEYER, E., HEGNER, M. & GERBER, C. 2003. Label-free protein assay based on a nanomechanical cantilever array. *Nanotechnology*, 14, 86-90.
- ARSHAK, K., VELUSAMY, V., KOROSTYNSKA, O., OLIWA-STASIAK, K. & ADLEY, C. 2009. Conducting Polymers and Their Applications to Biosensors: Emphasizing on Foodborne Pathogen Detection. *Ieee Sensors Journal*, 9, 1942-1951.
- ARYA, S. K., SOLANKI, P. R., DATTA, M. & MALHOTRA, B. D. 2009. Recent advances in self-assembled monolayers based biomolecular electronic devices. *Biosensors & Bioelectronics*, 24, 2810-2817.
- ARYA, S. K., SOLANKI, P. R., SINGH, R. P., PANDEY, M. K., DATTA, M. & MALHOTRA, B. D. 2006. Application of octadecanethiol self-assembled monolayer to cholesterol biosensor based on surface plasmon resonance technique. *Talanta*, 69, 918-926.
- ARYA, S. K., SOLANKI, P. R., SINGH, S. P., KANETO, K., PANDEY, M. K., DATTA, M. & MALHOTRA, B. D. 2007. Poly-(3-hexylthiophene) self-assembled monolayer based cholesterol biosensor using surface plasmon resonance technique. *Biosensors & Bioelectronics*, 22, 2516-2524.
- ATWELL, J. L., BREHENEY, K. A., LAWRENCE, L. J., MCCOY, A. J., KORTT, A. A. & HUDSON, P. J. 1999. scFv multimers of the anti-neuraminidase antibody NC10: length of the linker between V-H and V-L domains dictates precisely the transition between diabodies and triabodies. *Protein Engineering*, 12, 597-604.
- BACCAR, H., MEJRI, M. B., HAFIYEDH, I., KTARI, T., AOUNI, M. & ABDELGHANI, A. 2010. Surface plasmon resonance immunosensor for bacteria detection. *Talanta*, 82, 810-814.
- BAKER, M. 2015. BLAME IT ON THE ANTIBODIES. *Nature*, 521, 274-276.
- BANERJEE, P. & BHUNIA, A. K. 2009. Mammalian cell-based biosensors for pathogens and toxins. *Trends in Biotechnology*, 27, 179-188.
- BARBAS, C. F., BURTON, D. R., SCOTT, J. K. & SILVERMAN, G. J. 2001. *Phage display: a laboratory manual*, Cold Spring Harbour, New York,

USA, Cold Spring Harbour Laboratory Press.

- BARTLETT, P. N. & COOPER, J. M. 1993. A REVIEW OF THE IMMOBILIZATION OF ENZYMES IN ELECTROPOLYMERIZED FILMS. *Journal of Electroanalytical Chemistry*, 362, 1-12.
- BARTON, A. C., COLLYER, S. D., DAVIS, F., GARIFALLOU, G. Z., TSEKENIS, G., TULLY, E., O'KENNEDY, R., GIBSON, T., MILLNER, P. A. & HIGSON, S. P. J. 2009. Labelless AC impedimetric antibody-based sensors with pg ml⁻¹ sensitivities for point-of-care biomedical applications. *Biosensors & Bioelectronics*, 24, 1090-1095.
- BARTON, A. C., DAVIS, F. & HIGSON, S. P. J. 2008. Labelless immunosensor assay for prostate specific antigen with picogram per milliliter limits of detection based upon an ac impedance protocol. *Analytical Chemistry*, 80, 6198-6205.
- BEARD, J. & AUSTRALIAN RURAL HLTH RES, C. 2006. DDT and human health. *Science of the Total Environment*, 355, 78-89.
- BERGGREN, C., BJARNASON, B. & JOHANSSON, G. 2001. Capacitive biosensors. *Electroanalysis*, 13, 173-180.
- BERKENPAS, E., MILLARD, P. & DA CUNHA, M. P. 2006. Detection of Escherichia coli O157 : H7 with langasite pure shear horizontal surface acoustic wave sensors. *Biosensors & Bioelectronics*, 21, 2255-2262.
- BESTE, G., SCHMIDT, F. S., STIBORA, T. & SKERRA, A. 1999. Small antibody-like proteins with prescribed ligand specificities derived from the lipocalin fold. *Proceedings of the National Academy of Sciences of the United States of America*, 96, 1898-1903.
- BHARATHI, S., NOGAMI, M. & IKEDA, S. 2001. Novel electrochemical interfaces with a tunable kinetic barrier by self-assembling organically modified silica gel and gold nanoparticles. *Langmuir*, 17, 1-4.
- BILLAH, M. M., HODGES, C. S., HAYS, H. C. W. & MILLNER, P. A. 2010. Directed immobilization of reduced antibody fragments onto a novel SAM on gold for myoglobin impedance immunosensing. *Bioelectrochemistry*, 80, 49-54.
- BINNIG, G., QUATE, C. F. & GERBER, C. 1986. ATOMIC FORCE MICROSCOPE. *Physical Review Letters*, 56, 930-933.
- BINZ, H. K., AMSTUTZ, P. & PLUCKTHUN, A. 2005. Engineering novel binding proteins from nonimmunoglobulin domains. *Nature Biotechnology*, 23, 1257-1268.

- BISOFFI, M., HJELLE, B., BROWN, D. C., BRANCH, D. W., EDWARDS, T. L., BROZIK, S. M., BONDU-HAWKINS, V. S. & LARSON, R. S. 2008. Detection of viral bioagents using a shear horizontal surface acoustic wave biosensor. *Biosensors & Bioelectronics*, 23, 1397-1403.
- BLANCA, A., REQUENA, M. J., ALVAREZ, J., CHENG, L., MONTIRONI, R., RASPOLINI, M. R., REYMUNDO, C. & LOPEZ-BELTRAN, A. 2016. FGFR3 and Cyclin D3 as urine biomarkers of bladder cancer recurrence. *Biomarkers in Medicine*, 10, 243-253.
- BODOOR, K., GHABKARI, A., JARADAT, Z., ALKHATEEB, A., JARADAT, S., AL-GHAZO, M. A., MATAKA, I., MUSLEH, H. & HADDAD, Y. 2010. FGFR3 mutational status and protein expression in patients with bladder cancer in a Jordanian population. *Cancer Epidemiology*, 34, 724-732.
- BOLANDER, J., ROBERTS, S. J., EYCKMANS, J., GERIS, L. & LUYTEN, F. P. 2012. The Effect of Activating Fibroblast Growth Factor Receptor 3 Mutations on Osteogenic Differentiation and Ectopic Bone Formation by Human Periosteal Derived Cells. *Tissue Science & Engineering*, 8, 1-5.
- BORGSTROM, B. & ERLANSON, C. 1978. INTERACTIONS OF SERUM-ALBUMIN AND OTHER PROTEINS WITH PORCINE PANCREATIC LIPASE. *Gastroenterology*, 75, 382-386.
- BORMAN, S. 1987. OPTICAL AND PIEZOELECTRIC BIOSENSORS. *Analytical Chemistry*, 59, A1161-+.
- BOROLE, D. D., KAPADI, U. R., MAHULIKAR, P. P. & HUNDIWALE, D. G. 2006. Conducting polymers: an emerging field of biosensors. *Designed Monomers and Polymers*, 9, 1-11.
- BRADBURY, A. & PLUCKTHUN, A. 2015. Standardize antibodies used in research. *Nature*, 518, 27-29.
- BUDMAN, L. I., KASSOUF, W. & STEINBERG, J. R. 2008. Biomarkers for detection and surveillance of bladder cancer. *Canadian Urological Association Journal*, 2, 212-221.
- BUECHLER, K. F., MOI, S., NOAR, B., MCGRATH, D., VILLELA, J., CLANCY, M., SHENHAV, A., COLLEYMORE, A., VALKIRS, G., LEE, T., BRUNI, J. F., WALSH, M., HOFFMAN, R., AHMUTY, F., NOWAKOWSKI, M., BUECHLER, J., MITCHELL, M., BOYD, D., STISO, N. & ANDERSON, R. 1992. SIMULTANEOUS DETECTION OF 7 DRUGS OF ABUSE BY THE TRIAGE(TM) PANEL FOR DRUGS OF ABUSE. *Clinical Chemistry*, 38, 1678-1684.

- BYRNE, B., STACK, E., GILMARTIN, N. & O'KENNEDY, R. 2009. Antibody-Based Sensors: Principles, Problems and Potential for Detection of Pathogens and Associated Toxins. *Sensors*, 9, 4407-4445.
- CALLEJA, M., NORDSTROM, M., ALVAREZ, M., TAMAYO, J., LECHUGA, L. M. & BOISEN, A. 2005. Highly sensitive polymer-based cantilever-sensors for DNA detection. *Ultramicroscopy*, 105, 215-222.
- CAMPBELL, G. A. & MUTHARASAN, R. 2006. Piezoelectric-excited millimeter-sized cantilever (PEMC) sensors detect *Bacillus anthracis* at 300 spores/mL. *Biosensors & Bioelectronics*, 21, 1684-1692.
- CARTER, P. J. 2006. Potent antibody therapeutics by design. *Nature Reviews Immunology*, 6, 343-357.
- CAYGILL, R. L., HODGES, C. S., HOLMES, J. L., HIGSON, S. P. J., BLAIR, G. E. & MILLNER, P. A. 2012. Novel impedimetric immunosensor for the detection and quantitation of Adenovirus using reduced antibody fragments immobilized onto a conducting copolymer surface. *Biosensors & Bioelectronics*, 32, 104-110.
- CHAMES, P., VAN REGENMORTEL, M., WEISS, E. & BATY, D. 2009. Therapeutic antibodies: successes, limitations and hopes for the future. *British Journal of Pharmacology*, 157, 220-233.
- CHANG, B. Y. & PARK, S. M. 2010. Electrochemical Impedance Spectroscopy. *Annual Review of Analytical Chemistry*, 3, 207-229.
- CHAUHAN, N., NARANG, J., SUNNY & PUNDIR, C. S. 2013. Immobilization of lysine oxidase on a gold-platinum nanoparticles modified Au electrode for detection of lysine. *Enzyme and Microbial Technology*, 52, 265-271.
- CHEN, G. W., SONG, F. L., XIONG, X. Q. & PENG, X. J. 2013. Fluorescent Nanosensors Based on Fluorescence Resonance Energy Transfer (FRET). *Industrial & Engineering Chemistry Research*, 52, 11228-11245.
- CHEUNG, L. S. L., KANWAR, M., OSTERMEIER, M. & KONSTANTOPOULOS, K. 2012. A Hot-Spot Motif Characterizes the Interface between a Designed Ankyrin-Repeat Protein and Its Target Ligand. *Biophysical Journal*, 102, 407-416.
- CLARK, L. C. & LYONS, C. 1962. ELECTRODE SYSTEMS FOR CONTINUOUS MONITORING IN CARDIOVASCULAR SURGERY. *Annals of the New York Academy of Sciences*, 102, 29-&.
- CO, M. S. & QUEEN, C. 1991. HUMANIZED ANTIBODIES FOR THERAPY. *Nature*, 351, 501-502.

- COHN, B. A., CIRILLO, P. M., WOLFF, M. S., SCHWINGI, P. J., COHEN, R. D., SHOLTZ, R. I., FERRARA, A., CHRISTIANSON, R. E., VAN DEN BERG, B. J. & SIITERI, P. K. 2003. DDT and DDE exposure in mothers and time to pregnancy in daughters. *Lancet*, 361, 2205-2206.
- CONROY, D. J. R., MILLNER, P. A., STEWART, D. I. & POLLMANN, K. 2010. Biosensing for the Environment and Defence: Aqueous Uranyl Detection Using Bacterial Surface Layer Proteins. *Sensors*, 10, 4739-4755.
- CONROY, P. J., HEARTY, S., LEONARD, P. & O'KENNEDY, R. J. 2009. Antibody production, design and use for biosensor-based applications. *Seminars in Cell & Developmental Biology*, 20, 10-26.
- CONSTANTINIDES, P. P., TUSTIAN, A. & KESSLER, D. R. 2004. Tocol emulsions for drug solubilization and parenteral delivery. *Advanced Drug Delivery Reviews*, 56, 1243-1255.
- COOMBER, D. W. J., HAWKINS, N. J., CLARK, M. A. & WARD, R. L. 1999. Generation of anti-p53 Fab fragments from individuals with colorectal cancer using phage display. *Journal of Immunology*, 163, 2276-2283.
- CRIVIANU-GAITA, V. & THOMPSON, M. 2016. Aptamers, antibody scFv, and antibody Fab' fragments: An overview and comparison of three of the most versatile biosensor biorecognition elements. *Biosensors & Bioelectronics*, 85, 32-45.
- CUI, H. X., XIONG, X. L., GAO, B., CHEN, Z., LUO, Y. T., HE, F. J., DENG, S. X. & CHEN, L. C. 2016. A Novel Impedimetric Biosensor for Detection of Lead (II) with Low-cost Interdigitated Electrodes Made on PCB. *Electroanalysis*, 28, 2000-2006.
- DANIELS, J. S. & POURMAND, N. 2007. Label-free impedance biosensors: Opportunities and challenges. *Electroanalysis*, 19, 1239-1257.
- DANNENBERGER, O., WEISS, K., WOLL, C. & BUCK, M. 2000. Reactivity of self-assembled monolayers: formation of organized amino functionalities. *Physical Chemistry Chemical Physics*, 2, 1509-1514.
- DAPRA, J., LAURIDSEN, L. H., NIELSEN, A. T. & ROZLOSNIK, N. 2013. Comparative study on aptamers as recognition elements for antibiotics in a label-free all-polymer biosensor. *Biosensors & Bioelectronics*, 43, 315-320.
- DARMOSTUK, M., RIMPELOVA, S., GBELCOVA, H. & RUMIL, T. 2015. Current approaches in SELEX: An update to aptamer selection technology. *Biotechnology Advances*, 33, 1141-1161.

- DAVIES, T. G. E., FIELD, L. M., USHERWOOD, P. N. R. & WILLIAMSON, M. S. 2007. DDT, pyrethrins, pyrethroids and insect sodium channels. *Iubmb Life*, 59, 151-162.
- DE GROOT, M. T., EVERS, T. H., MERKX, M. & KOPER, M. T. M. 2007. Electron transfer and ligand binding to cytochrome c' immobilized on self-assembled monolayers. *Langmuir*, 23, 729-736.
- DEGNIN, C. R., LAEDERICH, M. B. & HORTON, W. A. 2011. Ligand activation leads to regulated intramembrane proteolysis of fibroblast growth factor receptor 3. *Molecular Biology of the Cell*, 22, 3861-3873.
- DI PIETRANTONIO, F., CANNATA, D., BENETTI, M., VERONA, E., VARRIALE, A., STAIANO, M. & D'AURIA, S. 2013. Detection of odorant molecules via surface acoustic wave biosensor array based on odorant-binding proteins. *Biosensors & Bioelectronics*, 41, 328-334.
- DICKERT, F. L. 2014. Biomimetic Receptors and Sensors. *Sensors*, 14, 22525-22531.
- DIMASHKIEH, H., WOLFF, D. J., SMITH, T. M., HOUSER, P. M., NIETERT, P. J. & YANG, J. 2013. Evaluation of UroVysion and Cytology for Bladder Cancer Detection. *Cancer Cytopathology*, 121, 591-597.
- DONG, S. J., WANG, B. X. & LIU, B. F. 1992. AMPEROMETRIC GLUCOSE SENSOR WITH FERROCENE AS AN ELECTRON-TRANSFER MEDIATOR. *Biosensors & Bioelectronics*, 7, 215-222.
- DU, Y. Z., NOMURA, Y., ZHOROV, B. S. & DONG, K. 2016. Evidence for Dual Binding Sites for 1,1,1-Trichloro-2,2-bis(p-chlorophenyl) ethane (DDT) in Insect Sodium Channels. *Journal of Biological Chemistry*, 291, 4638-4648.
- DURMUŞ, N. G., LIN, R. L., KOZBERG, M., DERMICI, D., KHADEMHOSEINI, A. & DEMIRCI, U. 2014. Acoustic-Based Biosensors. *Encyclopedia of Microfluidics and Nanofluidics*, 1-15.
- EBERSBACH, H., FIEDLER, E., SCHEUERMANN, T., FIEDLER, M., STUBBS, M. T., REIMANN, C., PROETZEL, G., RUDOLPH, R. & FIEDLER, U. 2007. Affilin-novel binding molecules based on human gamma-B-crystallin, an all 13-sheet protein. *Journal of Molecular Biology*, 372, 172-185.
- EKINCI, E., KARAGOZLER, A. A. & KARAGOZLER, A. E. 1996. The preparation and sensor application of poly(p-aminophenol). *Electroanalysis*, 8, 571-574.

- EKINCI, E., OGUNC, S. T. & KARAGOZLER, A. E. 1998. Electrochemical poly(1,3-phenylenediamine) synthesis as enzyme immobilization media. *Journal of Applied Polymer Science*, 68, 145-152.
- ELIASSON, M., OLSSON, A., PALMCRANTZ, E., WIBERG, K., INGANAS, M., GUSS, B., LINDBERG, M. & UHLEN, M. 1988. CHIMERIC IGG-BINDING RECEPTORS ENGINEERED FROM STAPHYLOCOCCAL PROTEIN-A AND STREPTOCOCCAL PROTEIN-G. *Journal of Biological Chemistry*, 263, 4323-4327.
- ERCOLE, C., DEL GALLO, M., MOSIELLO, L., BACCELLA, S. & LEPIDI, A. 2003. Escherichia coli detection in vegetable food by a potentiometric biosensor. *Sensors and Actuators B-Chemical*, 91, 163-168.
- ESSEGHAIER, C., HELALI, S., BEN FREDJ, H., TLILI, A. & ABDELGHANI, A. 2008. Polypyrrole-neutravidin layer for impedimetric biosensor. *Sensors and Actuators B-Chemical*, 131, 584-589.
- FAN, X. D., WHITE, I. M., SHOPOVA, S. I., ZHU, H. Y., SUTER, J. D. & SUN, Y. Z. 2008. Sensitive optical biosensors for unlabeled targets: A review. *Analytica Chimica Acta*, 620, 8-26.
- FANALI, G., DI MASI, A., TREZZA, V., MARINO, M., FASANO, M. & ASCENZI, P. 2012. Human serum albumin: From bench to bedside. *Molecular Aspects of Medicine*, 33, 209-290.
- FERNANDES, F. C. B., SANTOS, A., MARTINS, D. C., GOES, M. S. & BUENO, P. R. 2014. Comparing label free electrochemical impedimetric and capacitive biosensing architectures. *Biosensors & Bioelectronics*, 57, 96-102.
- FERRIGNO, P. K. 2016. Non-antibody protein-based biosensors. In: ESTRELA, P. (ed.) *Biosensor Technologies for Detection of Biomolecules*.
- FRITZ, J. 2008. Cantilever biosensors. *Analyst*, 133, 855-863.
- FURUYA, M., HARAMURA, M. & TANAKA, A. 2006. Reduction of nonspecific binding proteins to self-assembled monolayer on gold surface. *Bioorganic & Medicinal Chemistry*, 14, 537-543.
- GAO, W. M., KUICK, R., ORCHEKOWSKI, R. P., MISEK, D. E., QIU, J., GREENBERG, A. K., ROM, W. N., BRENNER, D. E., OMENN, G. S., HAAB, B. B. & HANASH, S. M. 2005. Distinctive serum protein profiles involving abundant proteins in lung cancer patients based upon antibody microarray analysis. *Bmc Cancer*, 5.

- GASPARYAN, V. K. & BAZUKYAN, I. L. 2013. Lectin sensitized anisotropic silver nanoparticles for detection of some bacteria. *Analytica Chimica Acta*, 766, 83-87.
- GERARD, M., CHAUBEY, A. & MALHOTRA, B. D. 2002. Application of conducting polymers to biosensors. *Biosensors & Bioelectronics*, 17, 345-359.
- GHAHROUDI, M. A., DESMYTER, A., WYNS, L., HAMERS, R. & MUYLDERMANS, S. 1997. Selection and identification of single domain antibody fragments from camel heavy-chain antibodies. *Febs Letters*, 414, 521-526.
- GILL, D. S. & DAMLE, N. K. 2006. Biopharmaceutical drug discovery using novel protein scaffolds. *Current Opinion in Biotechnology*, 17, 653-658.
- GOMEZ-ROMAN, J. J., SAENZ, P., GONZALEZ, J. C., ESCUREDO, K., CRUZ, S. S., JUNQUERA, C., SIMON, L., MARTINEZ, A., BANOS, J. L. G., LOPEZ-BREA, M., ESPARZA, C. & VAL-BERNAL, J. F. 2005. Fibroblast growth factor receptor 3 is overexpressed in urinary tract carcinomas and modulates the neoplastic cell growth. *Clinical Cancer Research*, 11, 459-465.
- GOODE, J., DILLON, G. & MILLNER, P. A. 2016. The development and optimisation of nanobody based electrochemical immunosensors for IgG. *Sensors and Actuators B-Chemical*, 234, 478-484.
- GOODE, J. A. 2015. *Development of biosensors using novel bioreceptors; Investigation and optimisation of fundamental parameters at the nanoscale*. PhD, University of Leeds.
- GREENE, K. L., BERRY, A. & KONETY, B. R. 2006. Diagnostic Utility of the ImmunoCyt/uCyt+ Test in Bladder Cancer. *Reviews in Urology*, 8, 190-197.
- GUANCIAL, E. A., WERNER, L., BELLMUNT, J., BAMIAS, A., CHOUETI, T. K., ROSS, R., SCHUTZ, F. A., PARK, R. S., O'BRIEN, R. J., HIRSCH, M. S., BARLETTA, J. A., BERMAN, D. M., LIS, R., LODA, M., STACK, E. C., GARRAWAY, L. A., RIESTER, M., MICHOR, F., KANTOFF, P. W. & ROSENBERG, J. E. 2014. FGFR3 expression in primary and metastatic urothelial carcinoma of the bladder. *Cancer Medicine*, 3, 835-844.
- HAMMERS, C. M. & STANLEY, J. R. 2014. Antibody Phage Display: Technique and Applications. *Journal of Investigative Dermatology*, 134.

- HANENBERG, M., MCAFOOSE, J., KULIC, L., WELT, T., WIRTH, F., PARIZEK, P., STROBEL, L., CATTEPOEL, S., SPANI, C., DERUNGS, R., MAIER, M., PLUCKTHUN, A. & NITSCH, R. M. 2014. Amyloid-beta Peptide-specific DARPins as a Novel Class of Potential Therapeutics for Alzheimer Disease. *Journal of Biological Chemistry*, 289, 27080-27089.
- HARMSSEN, M. M. & DE HAARD, H. J. 2007. Properties, production, and applications of camelid single-domain antibody fragments. *Applied Microbiology and Biotechnology*, 77, 13-22.
- HAURUM, J. S. 2006. Recombinant polyclonal antibodies: the next generation of antibody therapeutics? *Drug Discovery Today*, 11, 655-660.
- HE, H. G., HAN, C. H., HAO, L. & ZANG, G. H. 2016. ImmunoCyt test compared to cytology in the diagnosis of bladder cancer: A meta-analysis. *Oncology Letters*, 12, 83-88.
- HERMANSON, G. T. 2008. *Bioconjugate techniques*, Rockford, Illinois, USA, Academic Press.
- HERRINGTON-SYMES, A. P., FARYS, M., KHALILI, H. & BROCCINI, S. 2013. Antibody fragments: Prolonging circulation half-life special issue-antibody research. *Advances in Bioscience and Biotechnology*, 4, 689-698.
- HERZER, N., HOEPPENER, S. & SCHUBERT, U. S. 2010. Fabrication of patterned silane based self-assembled monolayers by photolithography and surface reactions on silicon-oxide substrates. *Chemical Communications*, 46, 5634-5652.
- HEY, T., FIEDLER, E., RUDOLPH, R. & FIEDLER, M. 2005. Artificial, non-antibody binding proteins for pharmaceutical and industrial applications. *Trends in Biotechnology*, 23, 514-522.
- HIGSON, S. P. 2012. *Biosensors for medical applications*, Cambridge, UK, Woodhead Publishing.
- HIRST, N. A. 2014. *Development of biosensors for early detection of anastomotic leak and sepsis*. PhD, University of Leeds.
- HIRST, N. A., HAZELWOOD, L. D., JAYNE, D. G. & MILLNER, P. A. 2013. An amperometric lactate biosensor using H₂O₂ reduction via a Prussian Blue impregnated poly(ethyleneimine) surface on screen printed carbon electrodes to detect anastomotic leak and sepsis. *Sensors and Actuators B-Chemical*, 186, 674-680.

- HOFFMANN, A., KOVERMANN, M., LILIE, H., FIEDLER, M., BALBACH, J., RUDOLPH, R. & PFEIFER, S. 2012. New Binding Mode to TNF-Alpha Revealed by Ubiquitin-Based Artificial Binding Protein. *Plos One*, 7.
- HOLFORD, T. R. J., HOLMES, J. L., COLLYER, S. D., DAVIS, F. & HIGSON, S. P. J. 2013. Label-free impedimetric immunosensors for psoriasis-Increased reproducibility and sensitivity using an automated dispensing system. *Biosensors & Bioelectronics*, 44, 198-203.
- HOLLIGER, P. & HUDSON, P. J. 2005. Engineered antibody fragments and the rise of single domains. *Nature Biotechnology*, 23, 1126-1136.
- HONG, J. Y., KIM, J. H. & CHOI, M. J. 2002. Hapten synthesis and influence of coating Ligands on enzyme-linked immunoreaction of DDT. *Bulletin of the Korean Chemical Society*, 23, 1413-1419.
- HOSSE, R. J., ROTHE, A. & POWER, B. E. 2006. A new generation of protein display scaffolds for molecular recognition. *Protein Science*, 15, 14-27.
- HOWARD, P. & MEYLAN, W. 1997. *Handbook of Physical Properties of Organic Chemicals*, Boca Raton, Florida, CRC Press, Lewis Publishers.
- HOWE, E. & HARDING, G. 2000. A comparison of protocols for the optimisation of detection of bacteria using a surface acoustic wave (SAW) biosensor. *Biosensors & Bioelectronics*, 15, 641-649.
- HU, Y. F., ZUO, P. & YE, B. C. 2013. Label-free electrochemical impedance spectroscopy biosensor for direct detection of cancer cells based on the interaction between carbohydrate and lectin. *Biosensors & Bioelectronics*, 43, 79-83.
- HUANG, Y., BELL, M. C. & SUNI, II 2008. Impedance Biosensor for Peanut Protein Ara h 1. *Analytical Chemistry*, 80, 9157-9161.
- HUDSON, P. J. & KORTT, A. A. 1999. High avidity scFv multimers; diabodies and triabodies. *Journal of Immunological Methods*, 231, 177-189.
- HUSSAIN, M., WACKERLIG, J. & LIEBERZEIT, P. A. 2013. Biomimetic Strategies for Sensing Biological Species. *Biosensors*, 3, 89-107.
- ISMAIL, F. & ADELOJU, S. B. 2010. Galvanostatic Entrapment of Penicillinase into Polytyramine Films and its Utilization for the Potentiometric Determination of Penicillin. *Sensors*, 10, 2851-2868.

- ISPAS, C. R., CRIVAT, G. & ANDREESCU, S. 2012. REVIEW: RECENT DEVELOPMENTS IN ENZYME-BASED BIOSENSORS FOR BIOMEDICAL ANALYSIS. *Analytical Letters*, 45, 168-186.
- JANATA, J. & JOSOWICZ, M. 2003. Conducting polymers in electronic chemical sensors. *Nature Materials*, 2, 19-24.
- JANSHOFF, A., GALLA, H. J. & STEINEM, C. 2000. Piezoelectric Mass-Sensing Devices as Biosensors-An Alternative to Optical Biosensors? *Angewandte Chemie (International ed. in English)*, 39, 4004-4032.
- JOHARI-AHAR, M., RASHIDI, M. R., BARAR, J., AGHAIE, M., MOHAMMADNEJAD, D., RAMAZANI, A., KARAMI, P., COUKOS, G. & OMIDI, Y. 2015. An ultra-sensitive impedimetric immunosensor for detection of the serum oncomarker CA-125 in ovarian cancer patients. *Nanoscale*, 7, 3768-3779.
- JOHNSON, A., SONG, Q. F., FERRIGNO, P. K., BUENO, P. R. & DAVIS, J. J. 2012. Sensitive Affimer and Antibody Based Impedimetric Label-Free Assays for C-Reactive Protein. *Analytical Chemistry*, 84, 6553-6560.
- JOHNSON, B. N. & MUTHARASAN, R. 2012. Sample Preparation-Free, Real-Time Detection of microRNA in Human Serum Using Piezoelectric Cantilever Biosensors at Attomole Level. *Analytical Chemistry*, 84, 10426-10436.
- JOLLY, P., BATISTUTI, M. R., MIODEK, A., ZHURAUWSKI, P., MULATO, M., LINDSAY, M. A. & ESTRELA, P. 2016. Highly sensitive dual mode electrochemical platform for microRNA detection. *Scientific Reports*, 6.
- JOLLY, P., FORMISANO, N., TKAC, J., KASAK, P., FROST, C. G. & ESTRELA, P. 2015. Label-free impedimetric aptasensor with antifouling surface chemistry: A prostate specific antigen case study. *Sensors and Actuators B-Chemical*, 209, 306-312.
- KADER, H. A., TCHERNEV, V. T., SATYARAJ, E., LEJNINE, S., KOTLER, G., KINGSMORE, S. F. & PATEL, D. D. 2005. Protein microarray analysis of disease activity in pediatric inflammatory bowel disease demonstrates elevated serum PLGF, IL-7, TGF-beta 1, and IL-12p40 levels in Crohn's disease and ulcerative colitis patients in remission versus active disease. *American Journal of Gastroenterology*, 100, 414-423.
- KAMADA, H., TAKI, S., NAGANO, K., INOUE, M., ANDO, D., MUKAI, Y., HIGASHISAKA, K., YOSHIOKA, Y., TSUTSUMI, Y. & TSUNODA, S. 2015. Generation and characterization of a bispecific diabody

targeting both EPH receptor A10 and CD3. *Biochemical and Biophysical Research Communications*, 456, 908-912.

- KAMBHAMPATI, D., NIELSEN, P. E. & KNOLL, W. 2001. Investigating the kinetics of DNA-DNA and PNA-DNA interactions using surface plasmon resonance-enhanced fluorescence spectroscopy. *Biosensors & Bioelectronics*, 16, 1109-1118.
- KAUFMAN, D. S., SHIPLEY, W. U. & FELDMAN, A. S. 2009. Bladder cancer. *Lancet*, 374, 239-249.
- KEUSGEN, M. 2002. Biosensors: new approaches in drug discovery. *Naturwissenschaften*, 89, 433-444.
- KHAN, R. & DHAYAL, M. 2009. Chitosan/polyaniline hybrid conducting biopolymer base impedimetric immunosensor to detect Ochratoxin-A. *Biosensors & Bioelectronics*, 24, 1700-1705.
- KIM, B. B., DIKOVA, E. B., SHELLER, U., DIKOV, M. M., GAVRILOVA, E. M. & EGOROV, A. M. 1990. EVALUATION OF DISSOCIATION-CONSTANTS OF ANTIGEN-ANTIBODY COMPLEXES BY ELISA. *Journal of Immunological Methods*, 131, 213-222.
- KIM, J. H., SONG, D. H., YOUN, S. J., KIM, J. W., CHO, G., KIM, S. C., LEE, H., JIN, M. S. & LEE, J. O. 2016. Crystal structures of mono- and bi-specific diabodies and reduction of their structural flexibility by introduction of disulfide bridges at the Fv interface. *Scientific Reports*, 6.
- KIM, T., KANG, J., LEE, J. H. & YOON, J. 2011. Influence of attached bacteria and biofilm on double-layer capacitance during biofilm monitoring by electrochemical impedance spectroscopy. *Water Research*, 45, 4615-4622.
- KNOWLES, M. A. & HURST, C. D. 2015. Molecular biology of bladder cancer: new insights into pathogenesis and clinical diversity. *Nature Reviews Cancer*, 15, 25-41.
- KOHLER, G. & MILSTEIN, C. 1975. CONTINUOUS CULTURES OF FUSED CELLS SECRETING ANTIBODY OF PREDEFINED SPECIFICITY. *Nature*, 256, 495-497.
- KOIDE, A., WOJCIK, J., GILBRETH, R. N., HOEY, R. J. & KOIDE, S. 2012. Teaching an Old Scaffold New Tricks: Monobodies Constructed Using Alternative Surfaces of the FN3 Scaffold. *Journal of Molecular Biology*, 415, 393-405.

- KOLAJA, G. J. & HINTON, D. E. 1977. EFFECTS OF DDT ON EGGSHELL QUALITY AND CALCIUM ADENOSINE-TRIPHOSPHATASE. *Journal of Toxicology and Environmental Health*, 3, 699-704.
- KONCKI, R. 2007. Recent developments in potentiometric biosensors for biomedical analysis. *Analytica Chimica Acta*, 599, 7-15.
- KONTERMANN, R. E., MARTINEAU, P., CUMMINGS, C. E., KARPAS, A., ALLEN, D., DERBYSHIRE, E. & WINTER, G. 1997. Enzyme immunoassays using bispecific diabodies. *Immunotechnology*, 3, 137-144.
- KORNDORFER, I. P., SCHLEHUBER, S. & SKERRA, A. 2003. Structural mechanism of specific ligand recognition by a lipocalin tailored for the complexation of digoxigenin. *Journal of Molecular Biology*, 330, 385-396.
- KOROTCENKOV, G. 2010. *Chemical Sensors: Volume 1 General Approaches*, Momentum Press.
- KOUTSOUMPELI, E., TIEDE, C., MURRAY, J., TANG, A., BON, R. S., TOMLINSON, D. C. & JOHNSON, S. 2017. Antibody Mimetics for the Detection of Small Organic Compounds Using a Quartz Crystal Microbalance. *Analytical Chemistry*, 89, 3051-3058.
- KRISHNAMOORTHY, S., ILIADIS, A. A., BEI, T. & CHROUSOS, G. P. 2008. An interleukin-6 ZnO/SiO₂/Si surface acoustic wave biosensor. *Biosensors & Bioelectronics*, 24, 313-318.
- KULYS, J. & VIDZIUNAITE, R. 2003. Amperometric biosensors based on recombinant laccases for phenols determination. *Biosensors & Bioelectronics*, 18, 319-325.
- KYLE, H. F., WICKSON, K. F., STOTT, J., BURSLEM, G. M., BREEZE, A. L., TIEDE, C., TOMLINSON, D. C., WARRINER, S. L., NELSON, A., WILSON, A. J. & EDWARDS, T. A. 2015. Exploration of the HIF-1 α /p300 interface using peptide and Adhiron phage display technologies. *Molecular Biosystems*, 11, 2738-2749.
- LABIB, M., ZAMAY, A. S., MUHAREMAGIC, D., CHECHIK, A. V., BELL, J. C. & BEREZOYSKI, M. V. 2012. Aptamer-Based Viability Impedimetric Sensor for Viruses. *Analytical Chemistry*, 84, 1813-1816.
- LACZKA, O., BALDRICH, E., MUNOZ, F. X. & DEL CAMPO, F. J. 2008. Detection of Escherichia coli and Salmonella typhimurium using interdigitated microelectrode capacitive immunosensors: The importance of transducer geometry. *Analytical Chemistry*, 80, 7239-7247.

- LAGARDE, F. & JAFFREZIC-RENAULT, N. 2011. Cell-based electrochemical biosensors for water quality assessment. *Analytical and Bioanalytical Chemistry*, 400, 947-964.
- LANDRY, J. P., KE, Y. H., YU, G. L. & ZHU, X. D. 2015. Measuring affinity constants of 1450 monoclonal antibodies to peptide targets with a microarray-based label-free assay platform. *Journal of Immunological Methods*, 417, 86-96.
- LAVRIK, N. V., SEPANIAK, M. J. & DATSKOS, P. G. 2004. Cantilever transducers as a platform for chemical and biological sensors. *Review of Scientific Instruments*, 75, 2229-2253.
- LEE, H. Y., JUNG, H. S., FUJIKAWA, K., PARK, J. W., KIM, J. M., YUKIMASA, T., SUGIHARA, H. & KAWAI, T. 2005. New antibody immobilization method via functional liposome layer for specific protein assays. *Biosensors & Bioelectronics*, 21, 833-838.
- LEE, J., CHOI, Y. S., LEE, Y., LEE, H. J., LEE, J. N., KIM, S. K., HAN, K. Y., CHO, E. C., PARK, J. C. & LEE, S. S. 2011. Sensitive and Simultaneous Detection of Cardiac Markers in Human Serum Using Surface Acoustic Wave Immunosensor. *Analytical Chemistry*, 83, 8629-8635.
- LEE, J. A., HWANG, S., KWAK, J., IL PARK, S., LEE, S. S. & LEE, K. C. 2008. An electrochemical impedance biosensor with aptamer-modified pyrolyzed carbon electrode for label-free protein detection. *Sensors and Actuators B-Chemical*, 129, 372-379.
- LEE, S. C., PARK, K., HAN, J., LEE, J. J., KIM, H. J., HONG, S., HEU, W., KIM, Y. J., HA, J. S., LEE, S. G., CHEONG, H. K., JEON, Y. H., KIM, D. & KIM, H. S. 2012. Design of a binding scaffold based on variable lymphocyte receptors of jawless vertebrates by module engineering. *Proceedings of the National Academy of Sciences of the United States of America*, 109, 3299-3304.
- LEHMANN, A. 2008. Ecallantide (DX-88), a plasma kallikrein inhibitor for the treatment of hereditary angioedema and the prevention of blood loss in on-pump cardiothoracic surgery. *Expert Opinion on Biological Therapy*, 8, 1187-1199.
- LESSEL, M., BAUMCHEN, O., KLOS, M., HAHN, H., FETZER, R., PAULUS, M., SEEMANN, R. & JACOBS, K. 2015. Self-assembled silane monolayers: an efficient step-by-step recipe for high-quality, low energy surfaces. *Surface and Interface Analysis*, 47, 557-564.
- LETASIOVA, S., MEDVED'OVA, A., SOVCIKOVA, A., DUSINSKA, M., VOLKOVOVA, K., MOSOIU, C. & BARTONOVA, A. 2012. Bladder

cancer, a review of the environmental risk factors. *Environmental Health*, 11.

- LI, K. Y., ZETTLITZ, K. A., LIPIANSKAYA, J., ZHOU, Y., MARKS, J. D., MALLICK, P., REITER, R. E. & WU, A. M. 2015. A fully human scFv phage display library for rapid antibody fragment reformatting. *Protein Engineering Design & Selection*, 28, 307-315.
- LIEBANA, S. & DRAGO, G. A. 2016. Bioconjugation and stabilisation of biomolecules in biosensors. In: ESTRELA, P. (ed.) *Biosensor Technologies for Detection of Biomolecules*.
- LIM, M. S., FENG, K., CHEN, X. Q., WU, N. Q., RAMAN, A., NIGHTINGALE, J., GAWALT, E. S., KORAKAKIS, D., HORNAK, L. A. & TIMPERMAN, A. T. 2007. Adsorption and desorption of stearic acid self-assembled monolayers on aluminum oxide. *Langmuir*, 23, 2444-2452.
- LIPOVSEK, D. 2011. Adnectins: engineered target-binding protein therapeutics. *Protein Engineering Design & Selection*, 24, 3-9.
- LITJEBLAD, J. F. D., TYRODE, E., THORMANN, E., DUBLANCHET, A. C., LUENGO, G., JOHNSON, C. M. & RUTLAND, M. W. 2014. Self-assembly of long chain fatty acids: effect of a methyl branch. *Physical Chemistry Chemical Physics*, 16, 17869-17882.
- LITTLE, M., KIPRIYANOV, S. M., LE GALL, F. & MOLDENHAUER, G. 2000. Of mice and men: hybridoma and recombinant antibodies. *Immunology Today*, 21, 364-370.
- LIU, B. W., HUANG, P. J. J., ZHANG, X., WANG, F., PAUTLER, R., IP, A. C. F. & LIU, J. W. 2013. Parts-per-Million of Polyethylene Glycol as a Non-Interfering Blocking Agent for Homogeneous Biosensor Development. *Analytical Chemistry*, 85, 10045-10050.
- LIU, Y. S. & YU, J. 2016. Oriented immobilization of proteins on solid supports for use in biosensors and biochips: a review. *Microchimica Acta*, 183, 1-19.
- LOFBLOM, J., FELDWISCH, J., TOLMACHEV, V., CARLSSON, J., STAHL, S. & FREJD, F. Y. 2010. Affibody molecules: Engineered proteins for therapeutic, diagnostic and biotechnological applications. *Febs Letters*, 584, 2670-2680.
- LOSIC, D., COLE, M., THISSEN, H. & VOELCKER, N. H. 2005. Ultrathin polytyramine films by electropolymerisation on highly doped p-type silicon electrodes. *Surface Science*, 584, 245-257.

- MAALOUF, R., FOURNIER-WIRTH, C., COSTE, J., CHEBIB, H., SAIKALI, Y., VITTORI, O., ERRACHID, A., CLOAREC, J. P., MARTELET, C. & JAFFREZIC-RENAULT, N. 2007. Label-free detection of bacteria by electrochemical impedance spectroscopy: Comparison to surface plasmon resonance. *Analytical Chemistry*, 79, 4879-4886.
- MAHATNIRUNKUL, T. 2017. *One-step gold nanoparticle size-shift assay using synthetic binding proteins and dynamic light scattering*. Doctor of Philosophy, University of Leeds.
- MAMLUK, R., CARVAJAL, I. M., MORSE, B. A., WONG, H., ABRAMOWITZ, J., ASLANIAN, S., LIM, A. C., GOKEMEIJER, J., STOREK, M. J., LEE, J., GOSSELIN, M., WRIGHT, M. C., CAMPHAUSEN, R. T., WANG, J., CHEN, Y., MILLER, K., SANDERS, K., SHORT, S., SPERINDE, J., PRASAD, G., WILLIAMS, S., KERBEL, R., EBOS, J., MUTSAERS, A., MENDLEIN, J. D., HARRIS, A. S. & FURFINE, E. S. 2010. Anti-tumor effect of CT-322 as an adnectin inhibitor of vascular endothelial growth factor receptor-2. *Mabs*, 2, 199-208.
- MAO, S. L., GAO, C. S., LO, C. H. L., WIRSCHING, P., WONG, C. H. & JANDA, K. D. 1999. Phage-display library selection of high-affinity human single-chain antibodies to tumor-associated carbohydrate antigens sialyl Lewis(x) and Lewis(x). *Proceedings of the National Academy of Sciences of the United States of America*, 96, 6953-6958.
- MATSUMOTO, M., OHTSUKI, Y., OCHI, K., SEIKE, Y., ISEDA, N., SASAKI, T., OKADA, Y., KURABAYASHI, A. & FURIHATA, M. 2004. Fibroblast growth factor receptor 3 protein expression in urothelial carcinoma of the urinary bladder, exhibiting no association with low-grade and/or non-invasive lesions. *Oncology Reports*, 12, 967-971.
- MAZOR, K. M., CALVI, J., COWAN, R., COSTANZA, M. E., HAN, P. K. J., GREENE, S. M., SACCOCCIO, L., COVE, E., ROBLIN, D. & WILLIAMS, A. 2010. Media Messages About Cancer: What Do People Understand? *Journal of Health Communication*, 15, 126-145.
- MCCAFFERTY, J., GRIFFITHS, A. D., WINTER, G. & CHISWELL, D. J. 1990. PHAGE ANTIBODIES - FILAMENTOUS PHAGE DISPLAYING ANTIBODY VARIABLE DOMAINS. *Nature*, 348, 552-554.
- MEHRPOUR, O., KARRARI, P., ZAMANI, N., TSATSAKIS, A. M. & ABDOLLAHI, M. 2014. Occupational exposure to pesticides and consequences on male semen and fertility: A review. *Toxicology Letters*, 230, 146-156.
- MEJRI, M. B., BACCAR, H., BALDRICH, E., DEL CAMPO, F. J., HELALI, S., KTARI, T., SIMONIAN, A., AOUNI, M. & ABDELGHANI, A. 2010. Impedance biosensing using phages for bacteria detection:

Generation of dual signals as the clue for in-chip assay confirmation. *Biosensors & Bioelectronics*, 26, 1261-1267.

- MERZ, T., WETZEL, S. K., FIRBANK, S., PLUCKTHUN, A., GRUTTER, M. G. & MITTL, P. R. E. 2008. Stabilizing ionic interactions in a full-consensus ankyrin repeat protein. *Journal of Molecular Biology*, 376, 232-240.
- MHAWRECH-FAUCEGLIA, P., CHENEY, R. T., FISCHER, G., BEEK, A. & HERRMANN, F. R. 2006. FGFR3 and p53 protein expressions in patients with pTa and pT1 urothelial bladder cancer. *Ejso*, 32, 231-237.
- MIAO, Y. Q., CHEN, J. R. & WU, X. H. 2004. Using electropolymerized non-conducting polymers to develop enzyme amperometric biosensors. *Trends in Biotechnology*, 22, 227-231.
- MICHEL, M. A., SWATEK, K. N., HOSPENTHAL, M. K. & KOMANDER, D. 2017. Ubiquitin Linkage-Specific Affimers Reveal Insights into K6-Linked Ubiquitin Signaling. *Molecular Cell*, 68, 233-+.
- MILLNER, P. A., CAYGILL, R. L., CONROY, D. J. R. & SHAHIDAN, M. A. 2012. Impedance interrogated affinity biosensors for medical applications: novel targets and mechanistic studies. *Biosensors for Medical Applications*. Woodhead Publishing.
- MILLNER, P. A., HAYS, H. C. W., VAKUROV, A., PCHELINTSEV, N. A., BILLAH, M. M. & RODGERS, M. A. 2009. Nanostructured transducer surfaces for electrochemical biosensor construction-Interfacing the sensing component with the electrode. *Seminars in Cell & Developmental Biology*, 20, 34-40.
- MIRECKA, E. A., HEY, T., FIEDLER, U., RUDOLPH, R. & HATZFELD, M. 2009. Affilin Molecules Selected against the Human Papillomavirus E7 Protein Inhibit the Proliferation of Target Cells. *Journal of Molecular Biology*, 390, 710-721.
- MITCHELL, A. M., BROWN, M., MENOWN, I. B. A. & KLINE, J. A. 2005. Novel protein markers of acute coronary syndrome complications in low-risk outpatients: A systematic review of potential use in the emergency department. *Clinical Chemistry*, 51, 2005-2012.
- MIYATA, T., JADOUL, M., KUROKAWA, K. & DE STRIHOU, C. V. 1998. beta-2 microglobulin in renal disease. *Journal of the American Society of Nephrology*, 9, 1723-1735.
- MOHAMAD, N. R., MARZUKI, N. H. C., BUANG, N. A., HUYOP, F. & WAHAB, R. A. 2015. An overview of technologies for immobilization

of enzymes and surface analysis techniques for immobilized enzymes. *Biotechnology & Biotechnological Equipment*, 29, 205-220.

- MONDON, P., DUBREUIL, O., BOUAYADI, K. & KHARRAT, H. 2008. Human antibody libraries: A race to engineer and explore a larger diversity. *Frontiers in Bioscience-Landmark*, 13, 1117-1129.
- MOR, G., VISINTIN, I., LAI, Y., ZHAO, H., SCHWARTZ, P., RUTHERFORD, T., YUE, L., BRAY-WARD, P. & WARD, D. C. 2005. Serum protein markers for early detection of ovarian cancer. *Proceedings of the National Academy of Sciences of the United States of America*, 102, 7677-7682.
- MURPHY, K. 2012. *Janeway's immunobiology*, New York, USA, Garland Science.
- NAM, Y. S., PARK, K. W., LEE, W. H. & CHOI, J. W. 2004. Fabrication and electrical characteristics of ferredoxin adsorbed poly-L-lysine/11-MUA hetero-self-assembly layer. *Materials Science & Engineering C-Biomimetic and Supramolecular Systems*, 24, 95-98.
- NAMBIAR, S. & YEOW, J. T. W. 2011. Conductive polymer-based sensors for biomedical applications. *Biosensors & Bioelectronics*, 26, 1825-1832.
- NELLIS, D. F., GIARDINA, S. L., JANINI, G. M., SHENOY, S. R., MARKS, J. D., TSAI, R., DRUMMOND, D. C., HONG, K., PARK, J. W., OUELLETTE, T. F., PERKINS, S. C. & KIRPOTIN, D. B. 2005. Preclinical manufacture of anti-HER2 liposome-inserting, scFv-PEG-Lipid conjugate. 2. Conjugate micelle identity, purity, stability, and potency analysis. *Biotechnology Progress*, 21, 221-232.
- NYGREN, P. A., LJUNGQUIST, C., TROMBORG, H., NUSTAD, K. & UHLEN, M. 1990. SPECIES-DEPENDENT BINDING OF SERUM ALBUMINS TO THE STREPTOCOCCAL RECEPTOR PROTEIN-G. *European Journal of Biochemistry*, 193, 143-148.
- NYGREN, P. A. & SKERRA, A. 2004. Binding proteins from alternative scaffolds. *Journal of Immunological Methods*, 290, 3-28.
- O'REILLY, A. O., KHAMBAY, B. P. S., WILLIAMSON, M. S., FIELD, L. M., WALLACE, B. A. & DAVIES, T. G. E. 2006. Modelling insecticide-binding sites in the voltage-gated sodium channel. *Biochemical Journal*, 396, 255-263.
- OGI, H., FUKUNISHI, Y., NAGAI, H., OKAMOTO, K., HIRAO, M. & NISHIYAMA, M. 2009. Nonspecific-adsorption behavior of polyethyleneglycol and bovine serum albumin studied by 55-MHz

- wireless-electrodeless quartz crystal microbalance. *Biosensors & Bioelectronics*, 24, 3148-3152.
- OHNO, R., OHNUKI, H., WANG, H. H., YOKOYAMA, T., ENDO, H., TSUYA, D. & IZUMI, M. 2013. Electrochemical impedance spectroscopy biosensor with interdigitated electrode for detection of human immunoglobulin A. *Biosensors & Bioelectronics*, 40, 422-426.
- OSTUNI, E., CHAPMAN, R. G., HOLMLIN, R. E., TAKAYAMA, S. & WHITESIDES, G. M. 2001. A survey of structure-property relationships of surfaces that resist the adsorption of protein. *Langmuir*, 17, 5605-5620.
- OWEN, V. 1997. Real-time optical immunosensors - A commercial reality. *Biosensors & Bioelectronics*, 12, R1-R2.
- PANCRAZIO, J. J., WHELAN, J. P., BORKHOLDER, D. A., MA, W. & STENGER, D. A. 1999. Development and application of cell-based biosensors. *Annals of Biomedical Engineering*, 27, 697-711.
- PAPARIEL, G. J., MUKHERJI, A. K. & SHEARER, C. M. 1973. Penicillin Selective Enzyme Electrode. *Analytical Chemistry*, 45, 790-792.
- PARK, J. S., KIM, H. J., LEE, J. H., PARK, J. H., KIM, J., HWANG, K. S. & LEE, B. C. 2018. Amyloid Beta Detection by Faradaic Electrochemical Impedance Spectroscopy Using Interdigitated Microelectrodes. *Sensors*, 18.
- PEETERS, M. 2015. Molecularly Imprinted Polymers (Mips) for Bioanalytical Sensors: Strategies for Incorporation of Mips into Sensing Platforms. *Austin Journal of Biosensors & Bioelectronics*, 1, 1-5.
- PEH, A. E. K. & LI, S. F. Y. 2013. Dengue virus detection using impedance measured across nanoporous alumina membrane. *Biosensors & Bioelectronics*, 42, 391-396.
- PENG, H., ZHANG, L. J., SOELLER, C. & TRAVAS-SEJDIC, J. 2009. Conducting polymers for electrochemical DNA sensing. *Biomaterials*, 30, 2132-2148.
- PEPE, M. S., ETZIONI, R., FENG, Z. D., POTTER, J. D., THOMPSON, M. L., THORNQUIST, M., WINGET, M. & YASUI, Y. 2001. Phases of biomarker development for early detection of cancer. *Journal of the National Cancer Institute*, 93, 1054-1061.
- PEREZ, E. A. 2001. Doxorubicin and paclitaxel in the treatment of advanced breast cancer: Efficacy and cardiac considerations. *Cancer Investigation*, 19, 155-164.

- PILEHVAR, S., MEHTA, J., DARDENNE, F., ROBBENS, J., BLUST, R. & DE WAEL, K. 2012. Aptasensing of Chloramphenicol in the Presence of Its Analogues: Reaching the Maximum Residue Limit. *Analytical Chemistry*, 84, 6753-6758.
- PONSEL, D., NEUGEBAUER, J., LADEZKI-BAEHS, K. & TISSOT, K. 2011. High Affinity, Developability and Functional Size: The Holy Grail of Combinatorial Antibody Library Generation. *Molecules*, 16, 3675-3700.
- POURNARAS, A. V., KORAKI, T. & PRODRMIDIS, M. I. 2008. Development of an impedimetric immunosensor based on electropolymerized polytyramine films for the direct detection of *Salmonella typhimurium* in pure cultures of type strains and inoculated real samples. *Analytica Chimica Acta*, 624, 301-307.
- PROCTOR, I., STOEBER, K. & WILLIAMS, G. H. 2010. Biomarkers in bladder cancer. *Histopathology*, 57, 1-13.
- QIU, J. D., ZHOU, W. M., GUO, J., WANG, R. & LIANG, R. P. 2009. Amperometric sensor based on ferrocene-modified multiwalled carbon nanotube nanocomposites as electron mediator for the determination of glucose. *Analytical Biochemistry*, 385, 264-269.
- RADI, A. E., MUNOZ-BERBEL, X., LATES, V. & MARTY, J. L. 2009. Label-free impedimetric immunosensor for sensitive detection of ochratoxin A. *Biosensors & Bioelectronics*, 24, 1888-1892.
- RAINA, M. 2013. *Development of An Impedimetric Biosensor Using A Non-antibody Based Biological Recognition Molecule*. Doctor of Philosophy, University of Leeds.
- RAINA, M., SHARMA, R., DEACON, S. E., TIEDE, C., TOMLINSON, D., DAVIES, A. G., MCPHERSON, M. J. & WALTI, C. 2015. Antibody mimetic receptor proteins for label-free biosensors. *Analyst*, 140, 803-810.
- RAMAMURTHY, V., KRISTEK, S. R., BUSH, A., WEI, A. Z., EMANUEL, S. L., DAS GUPTA, R., JANJUA, A., CHENG, L., MURDOCK, M., ABRAMCZYK, B., COHEN, D., LIN, Z., MORIN, P., DAVIS, J. H., DABRITZ, M., MCLAUGHLIN, D. C., RUSSO, K. A., CHAO, G., WRIGHT, M. C., JENNY, V. A., ENGLE, L. J., FURFINE, E. & SHERIFF, S. 2012. Structures of Adnectin/Protein Complexes Reveal an Expanded Binding Footprint. *Structure*, 20, 259-269.
- RANGLES, J. E. B. 1947. KINETICS OF RAPID ELECTRODE REACTIONS. *Discussions of the Faraday Society*, 1, 11-19.

- RAVALLI, A., DOS SANTOS, G. P., FERRONI, M., FAGLIA, G., YAMANAKA, H. & MARRAZZA, G. 2013. New label free CA125 detection based on gold nanostructured screen-printed electrode. *Sensors and Actuators B-Chemical*, 179, 194-200.
- RAWAT, S., SURI, C. R. & SAHOO, D. K. 2010. Molecular mechanism of polyethylene glycol mediated stabilization of protein. *Biochemical and Biophysical Research Communications*, 392, 561-566.
- RAWLINGS, A. E., BRAMBLE, J. P., TANG, A. A. S., SOMNER, L. A., MONNINGTON, A. E., COOKE, D. J., MCPHERSON, M. J., TOMLINSON, D. C. & STANILAND, S. S. 2015. Phage display selected magnetite interacting Adhirons for shape controlled nanoparticle synthesis. *Chemical Science*, 6, 5586-5594.
- REUBSAET, A., VAN OSCH, L., DE VRIES, H., DE COUL, M. R. O. & LECHNER, L. 2009. Some signals cannot wait: Effects of a national campaign on early detection of cancer among Dutch adults (> 55 years). *Cancer Epidemiology*, 33, 194-200.
- REYNOLDS, M. A., KIRCHICK, H. J., DAHLEN, J. R., ANDERBERG, J. M., MCPHERSON, P. H., NAKAMURA, K. K., LASKOWITZ, D. T., VALKIRS, G. E. & BUECHLER, K. F. 2003. Early biomarkers of stroke. *Clinical Chemistry*, 49, 1733-1739.
- RICHARDS, D. A., MARUANI, A. & CHUDASAMA, V. 2017. Antibody fragments as nanoparticle targeting ligands: a step in the right direction. *Chemical Science*, 8, 63-77.
- RICHTER, A., EGGENSTEIN, E. & SKERRA, A. 2014. Anticalins: Exploiting a non-Ig scaffold with hypervariable loops for the engineering of binding proteins. *Febs Letters*, 588, 213-218.
- RIQUELME, M. V., ZHAO, H., SRINIVASARAGHAVAN, V., PRUDEN, A., VIKESLAND, P. & AGAH, M. 2016. Optimizing blocking of nonspecific bacterial attachment to impedimetric biosensors. *Sensing and Bio-Sensing Research*, 8, 47-54.
- ROCCHITTA, G., SPANU, A., BABUDIERI, S., LATTE, G., MADEDDU, G., GALLERI, G., NUVOLI, S., BAGELLA, P., DEMARTIS, M. I., FIORE, V., MANETTI, R. & SERRA, P. A. 2016. Enzyme Biosensors for Biomedical Applications: Strategies for Safeguarding Analytical Performances in Biological Fluids. *Sensors*, 16.
- ROCHA-GASO, M. I., MARCH-IBORRA, C., MONTOYA-BAIDES, A. & ARNAU-VIVES, A. 2009. Surface Generated Acoustic Wave Biosensors for the Detection of Pathogens: A Review. *Sensors*, 9, 5740-5769.

- RODGERS, M. A., FINDLAY, J. B. C. & MILLNER, P. A. 2010. Lipocalin based biosensors for low mass hydrophobic analytes; development of a novel SAM for polyhistidine tagged proteins. *Sensors and Actuators B-Chemical*, 150, 12-18.
- ROGAN, W. J. & CHEN, A. M. 2005. Health risks and benefits of bis(4-chlorophenyl)-1,1,1-trichloroethane (DDT). *Lancet*, 366, 763-773.
- RONKAINEN, N. J., HALSALL, H. B. & HEINEMAN, W. R. 2010. Electrochemical biosensors. *Chemical Society Reviews*, 39, 1747-1763.
- ROTARIU, L., BALA, C. & MAGEARU, V. 2004. New potentiometric microbial biosensor for ethanol determination in alcoholic beverages. *Analytica Chimica Acta*, 513, 119-123.
- RUIGROK, V. J. B., LEVISSON, M., EPPINK, M. H. M., SMIDT, H. & VAN DER OOST, J. 2011. Alternative affinity tools: more attractive than antibodies? *Biochemical Journal*, 436, 1-13.
- RUSHWORTH, J. V., AHMED, A., GRIFFITHS, H. H., POLLOCK, N. M., HOOPER, N. M. & MILLNER, P. A. 2014. A label-free electrical impedimetric biosensor for the specific detection of Alzheimer's amyloid-beta oligomers. *Biosensors & Bioelectronics*, 56, 83-90.
- RUSHWORTH, J. V., HIRST, N. A., GOODE, J. A., PIKE, D. J., AHMED, A. & MILLNER, P. A. 2013. *Impedimetric biosensors for medical applications: current progress and challenges*, New York, USA, ASME Press.
- RUSMINI, F., ZHONG, Z. Y. & FEIJEN, J. 2007. Protein immobilization strategies for protein biochips. *Biomacromolecules*, 8, 1775-1789.
- SASSOLAS, A., BLUM, L. J. & LECA-BOUVIER, B. D. 2012. Immobilization strategies to develop enzymatic biosensors. *Biotechnology Advances*, 30, 489-511.
- SATJAPIPAT, M., SANEDRIN, R. & ZHOU, F. M. 2001. Selective desorption of alkanethiols in mixed self-assembled monolayers for subsequent oligonucleotide attachment and DNA hybridization. *Langmuir*, 17, 7637-7644.
- SCHILLING, J., SCHOPPE, J. & PLUCKTHUN, A. 2014. From DARPins to LoopDARPins: Novel LoopDARPin Design Allows the Selection of Low Picomolar Binders in a Single Round of Ribosome Display. *Journal of Molecular Biology*, 426, 691-721.

- SCHLEHUBER, S. & SKERRA, A. 2001. Duocalins: Engineered ligand-binding proteins with dual specificity derived from the lipocalin fold. *Biological Chemistry*, 382, 1335-1342.
- SCHLEHUBER, S. & SKERRA, A. 2005. Lipocalins in drug discovery: from natural ligand-binding proteins to 'anticalins'. *Drug Discovery Today*, 10, 23-33.
- SCHMITZ, U., VERSMOLD, A., KAUFMANN, P. & FRANK, H. G. 2000. Phage display: A molecular tool for the generation of antibodies - A review. *Placenta*, 21, S106-S112.
- SCHNITZER, J. E., SUNG, A., HORVAT, R. & BRAVO, J. 1992. PREFERENTIAL INTERACTION OF ALBUMIN-BINDING PROTEINS, GP30 AND GP18, WITH CONFORMATIONALLY MODIFIED ALBUMINS - PRESENCE IN MANY CELLS AND TISSUES WITH A POSSIBLE ROLE IN CATABOLISM. *Journal of Biological Chemistry*, 267, 24544-24553.
- SCHRAMA, D., REISFELD, R. A. & BECKER, J. C. 2006. Antibody targeted drugs as cancer therapeutics. *Nature Reviews Drug Discovery*, 5, 147-159.
- SCOUTEN, W. H., LUONG, J. H. T. & BROWN, R. S. 1995. ENZYME OR PROTEIN IMMOBILIZATION TECHNIQUES FOR APPLICATIONS IN BIOSENSOR DESIGN. *Trends in Biotechnology*, 13, 178-185.
- SEKAR, N. & RAMASAMY, R. P. 2013. Electrochemical Impedance Spectroscopy for Microbial Fuel Cell Characterization. *Microbial & Biochemical Technology*, S6, 1-14.
- SEXTON, W. J., WIEGAND, L. R., CORREA, J. J., POLITIS, C., DICKINSON, S. I. & KANG, L. C. 2010. Bladder Cancer: A Review of Non-Muscle Invasive Disease. *Cancer Control*, 17, 256-268.
- SHARMA, R., DEACON, S. E., NOWAK, D., GEORGE, S. E., SZYMONIK, M. P., TANG, A. A. S., TOMLINSON, D. C., DAVIES, A. G., MCPHERSON, M. J. & WALTI, C. 2016. Label-free electrochemical impedance biosensor to detect human interleukin-8 in serum with sub-pg/ml sensitivity. *Biosensors & Bioelectronics*, 80, 607-613.
- SHEN, S., FORERO, A., LOBUGLIO, A. F., BREITZ, H., KHAZAELI, M. B., FISHER, D. R., WANG, W. Q. & MEREDITH, R. F. 2005. Patient-specific dosimetry of pretargeted radioimmunotherapy using CC49 fusion protein in patients with gastrointestinal malignancies. *Journal of Nuclear Medicine*, 46, 642-651.

- SHEN, Y. M., YANG, X. C., DONG, N. Z., XIE, X. F., BAI, X. & SHI, Y. Z. 2007. Generation and selection of immunized Fab phage display library against human B cell lymphoma. *Cell Research*, 17, 650-660.
- SHI, J., CHAN, C., PANG, Y., YE, W., TIAN, F., LYU, J., ZHANG, Y. & YANG, M. 2015a. A fluorescence resonance energy transfer (FRET) biosensor based on graphene quantum dots (GQDs) and gold nanoparticles (AuNPs) for the detection of mecA gene sequence of *Staphylococcus aureus*. *Biosens Bioelectron*, 67, 595-600.
- SHI, J. Y., TIAN, F., LYU, J. & YANG, M. 2015b. Nanoparticle based fluorescence resonance energy transfer (FRET) for biosensing applications. *Journal of Materials Chemistry B*, 3, 6989-7005.
- SHIN, Y., PERERA, A. P. & PARK, M. K. 2013. Label-free DNA sensor for detection of bladder cancer biomarkers in urine. *Sensors and Actuators B-Chemical*, 178, 200-206.
- SILACCI, M., BAENZIGER-TOBLER, N., LEMBKE, W., ZHA, W. J., BATEY, S., BERTSCHINGER, J. & GRABULOVSKI, D. 2014. Linker Length Matters, Fynomer-Fc Fusion with an Optimized Linker Displaying Picomolar IL-17A Inhibition Potency. *Journal of Biological Chemistry*, 289, 14392-14398.
- SJOBRING, U., BJORCK, L. & KASTERN, W. 1989. PROTEIN-G GENES - STRUCTURE AND DISTRIBUTION OF IGG-BINDING AND ALBUMIN-BINDING DOMAINS. *Molecular Microbiology*, 3, 319-327.
- SKERRA, A. 2007. Alternative non-antibody scaffolds for molecular recognition. *Current Opinion in Biotechnology*, 18, 295-304.
- SKERRA, A. 2008. Alternative binding proteins: Anticalins - harnessing the structural plasticity of the lipocalin ligand pocket to engineer novel binding activities. *Febs Journal*, 275, 2677-2683.
- SMITH, G. P. 1985. FILAMENTOUS FUSION PHAGE - NOVEL EXPRESSION VECTORS THAT DISPLAY CLONED ANTIGENS ON THE VIRION SURFACE. *Science*, 228, 1315-1317.
- SONG, K. M., LEE, S. & BAN, C. 2012. Aptamers and Their Biological Applications. *Sensors*, 12, 612-631.
- SOSNOWSKA, M., PIETA, P., SHARMA, P. S., CHITTA, R., KC, C. B., BANDI, V., D'SOUZA, F. & KUTNER, W. 2013. Piezomicrogravimetric and Impedimetric Oligonucleotide Biosensors Using Conducting Polymers of Biotinylated Bis(2,2'-bithien-5-yl)methane as Recognition Units. *Analytical Chemistry*, 85, 7541-7561.

- SPECTOR, A. A., JOHN, K. & FLETCHER, J. E. 1969. BINDING OF LONG-CHAIN FATTY ACIDS TO BOVINE SERUM ALBUMIN. *Journal of Lipid Research*, 10, 56-&.
- SPEICH, S. M., CALAMBOKIDAS, J., SHEA, D. W., PEARD, J., WITTER, M. & FRY, D. M. 1992. EGG SHELL THINNING AND ORGANOCHLORINE CONTAMINANTS IN WESTERN WASHINGTON WATERBIRDS. *Colonial Waterbirds*, 15, 103-112.
- STADLER, L. K., HOFFMANN, T., TOMLINSON, D. C., SONG, Q., LEE, T., BUSBY, M., NYATHI, Y., GENDRA, E., TIEDE, C., FLANAGAN, K., COCKELL, S. J., WIPAT, A., HARWOOD, C., WAGNER, S. D., KNOWLES, M. A., DAVIS, J. J., KEEGAN, N. & FERRIGNO, P. K. 2011. Structure-function studies of an engineered scaffold protein derived from Stefin A. II: Development and applications of the SQT variant. *Protein Engineering Design & Selection*, 24, 751-763.
- STUMPP, M. T., BINZ, H. K. & AMSTUTZ, P. 2008. DARPins: A new generation of protein therapeutics. *Drug Discovery Today*, 13, 695-701.
- SUNG, J. Y., SUN, J. M., JEONG, B. C., SEO, S. I., JEON, S. S., LEE, H. M., CHOI, H. Y., KANG, S. Y., CHOI, Y. L. & KWON, G. Y. 2014. FGFR3 overexpression is prognostic of adverse outcome for muscle-invasive bladder carcinoma treated with adjuvant chemotherapy. *Urologic Oncology-Seminars and Original Investigations*, 32.
- TAWIL, N., SACHER, E., MANDEVILLE, R. & MEUNIER, M. 2012. Surface plasmon resonance detection of E. coli and methicillin-resistant S. aureus using bacteriophages. *Biosensors & Bioelectronics*, 37, 24-29.
- TEH, H. F., PEH, W. Y. X., SU, X. D. & THOMSEN, J. S. 2007. Characterization of protein-DNA interactions using surface plasmon resonance spectroscopy with various assay schemes. *Biochemistry*, 46, 2127-2135.
- THEURILLAT, J. P., DREIER, B., NAGY-DAVIDESCU, G., SEIFERT, B., BEHNKE, S., ZURRER-HARDI, U., INGOLD, F., PLUCKTHUN, A. & MOCH, H. 2010. Designed ankyrin repeat proteins: a novel tool for testing epidermal growth factor receptor 2 expression in breast cancer. *Modern Pathology*, 23, 1289-1297.
- TIEDE, C., BEDFORD, R., HESELTINE, S. J., SMITH, G., WIJETUNGA, I., ROSS, R., AL QALLAF, D., ROBERTS, A. P. E., BALLS, A., CURD, A., HUGHES, R. E., MARTIN, H., NEEDHAM, S. R., ZANETTI-DOMINGUES, L. C., SADIGH, Y., PEACOCK, T. P., TANG, A. A., GIBSON, N., KYLE, H., PLATT, G. W., INGRAM, N., TAYLOR, T., COLETTA, L. P., MANFIELD, I., KNOWLES, M., BELL, S., ESTEVES, F., MAQBOOL, A., PRASAD, R. K., DRINKHILL, M.,

- BON, R. S., PATEL, V., GOODCHILD, S. A., FERNANDEZ, M. M., OWENS, R. J., NETTLESHIP, J. E., WEBB, M. E., HARRISON, M., LIPPIAT, J. D., PONNAMBALAM, S., PECKHAM, M., SMITH, A., FERRIGNO, P. K., JOHNSON, M., MCPHERSON, M. J. & TOMLINSON, D. C. 2017. Affimers proteins are versatile and renewable affinity reagents. *Elife*, 6.
- TIEDE, C., TANG, A. A. S., DEACON, S. E., MANDAL, U., NETTLESHIP, J. E., OWEN, R. L., GEORGE, S. E., HARRISON, D. J., OWENS, R. J., TOMLINSON, D. C. & MCPHERSON, M. J. 2014. Adhiron: a stable and versatile peptide display scaffold for molecular recognition applications. *Protein Engineering Design & Selection*, 27, 145-155.
- TOMLINSON, D. C., BALDO, O., HAMDEN, P. & KNOWLES, M. A. 2007. FGFR3 protein expression and its relationship to mutation status and prognostic variables in bladder cancer. *Journal of Pathology*, 213, 91-98.
- TOMLINSON, D. C., L'HOTE, C. G., KENNEDY, W., PITT, E. & KNOWLES, M. A. 2005. Alternative splicing of fibroblast growth factor receptor 3 produces a secreted isoform that inhibits fibroblast growth factor-induced proliferation and is repressed in urothelial carcinoma cell lines. *Cancer Research*, 65, 10441-10449.
- TORCHILIN, V. P. 2005. Recent advances with liposomes as pharmaceutical carriers. *Nature Reviews Drug Discovery*, 4, 145-160.
- TRIPATHI, S. M., BOCK, W. J., MIKULIC, P., CHINNAPPAN, R., NG, A., TOLBA, M. & ZOUROB, M. 2012. Long period grating based biosensor for the detection of Escherichia coli bacteria. *Biosensors & Bioelectronics*, 35, 308-312.
- TRIVEDI, U. B., LAKSHMINARAYANA, D., KOTHARI, I. L., PATEL, N. G., KAPSE, H. N., MAKHIJA, K. K., PATEL, R. B. & PANCHAL, C. J. 2009. Potentiometric biosensor for urea determination in milk. *Sensors and Actuators B-Chemical*, 140, 260-266.
- TSEKENIS, G., GARIFALLOU, G. Z., DAVIS, F., MILLNER, P. A., PINACHO, D. G., SANCHEZ-BAEZA, F., MARCO, M. P., GIBSON, T. D. & HIGSON, S. P. J. 2008. Detection of Fluoroquinolone Antibiotics in Milk via a Labelless Immunoassay Based upon an Alternating Current Impedance Protocol. *Analytical Chemistry*, 80, 9233-9239.
- TSURUSHITA, N., HINTON, P. R. & KUMAR, S. 2005. Design of humanized antibodies: From anti-Tac to Zenapax. *Methods*, 36, 69-83.
- TURNER, N. & GROSE, R. 2010. Fibroblast growth factor signalling: from development to cancer. *Nature Reviews Cancer*, 10, 116-129.

- TURUSOV, V., RAKITSKY, V. & TOMATIS, L. 2002. Dichlorodiphenyltrichloroethane (DDT): Ubiquity, persistence, and risks. *Environmental Health Perspectives*, 110, 125-128.
- TZEN, T. R. J., CHENG, Y. Y. R., SAEIDPOURAZAR, R., APHALE, S. S. & JALILI, N. 2011. Adhesin-Specific Nanomechanical Cantilever Biosensors for Detection of Microorganisms. *Journal of Heat Transfer-Transactions of the Asme*, 133.
- URUSHIBATA, Y., ITOH, K., OHSHIMA, M. & SETO, Y. 2010. Generation of Fab Fragment-Like Molecular Recognition Proteins against Staphylococcal Enterotoxin B by Phage Display Technology. *Clinical and Vaccine Immunology*, 17, 1708-1717.
- VAIDYA, V. S., FERGUSON, M. A. & BONVENTRE, J. V. 2008. Biomarkers of acute kidney injury. *Annual Review of Pharmacology and Toxicology*.
- VALERIO, E., ABRANTES, L. M. & VIANA, A. S. 2008. 4-Aminothiophenol Self-Assembled Monolayer for the Development of a DNA Biosensor Aiming the Detection of *Cylindrospermopsis* Producing Cyanobacteria. *Electroanalysis*, 20, 2467-2474.
- VIDAL, J. C., GARCIA-RUIZ, E. & CASTILLO, J. R. 2003. Recent advances in electropolymerized conducting polymers in amperometric biosensors. *Microchimica Acta*, 143, 93-111.
- VLAOVIC, P. & JEWETT, M. A. 1999. Cyclophosphamide-induced bladder cancer. *The Canadian Journal of Urology*, 6, 745-748.
- WANG, J. 2001. Glucose biosensors: 40 years of advances and challenges. *Electroanalysis*, 13, 983-988.
- WANG, Y., KNOLL, W. & DOSTALEK, J. 2012. Bacterial Pathogen Surface Plasmon Resonance Biosensor Advanced by Long Range Surface Plasmons and Magnetic Nanoparticle Assays. *Analytical Chemistry*, 84, 8345-8350.
- WANG, Y. X., YE, Z. Z., SI, C. Y. & YING, Y. B. 2013. Monitoring of *Escherichia coli* O157:H7 in food samples using lectin based surface plasmon resonance biosensor. *Food Chemistry*, 136, 1303-1308.
- WEIDLE, U. H., AUER, J., BRINKMANN, U., GEORGES, G. & TIEFENTHALER, G. 2013. The Emerging Role of New Protein Scaffold-based Agents for Treatment of Cancer. *Cancer Genomics & Proteomics*, 10, 155-168.
- WEISIGER, R. A., DESANCHO, M. T., PASTORES, S. M. & WELLS, R. G. 2008. Synthetic Function. In: RODÉS, J., BENHAMOU, J. P., BLEI, A.

T., REICHEN, J. & RIZZETTO, M. (eds.) *Textbook of Hepatology: From Basic Science to Clinical Practice*. Oxford, UK: Blackwell Publishing Ltd.

- WEISS, S., MILLNER, P. & NELSON, A. 2005. Monitoring protein binding to phospholipid monolayers using electrochemical impedance spectroscopy. *Electrochimica Acta*, 50, 4248-4256.
- WESCHE, J., HAGLUND, K. & HAUGSTEN, E. M. 2011. Fibroblast growth factors and their receptors in cancer. *Biochemical Journal*, 437, 199-213.
- WHORTON, D., KRAUSS, R. M., MARSHALL, S. & MILBY, T. H. 1977. INFERTILITY IN MALE PESTICIDE WORKERS. *Lancet*, 2, 1259-1261.
- WILLIAMS, A. & BAIRD, L. G. 2003. DX-88 and HAE: a developmental perspective. *Transfusion and Apheresis Science*, 29, 255-258.
- WU, A. H. B., SMITH, A., CHRISTENSON, R. H., MURAKAMI, M. M. & APPLE, F. S. 2004. Evaluation of a point-of-care assay for cardiac markers for patients suspected of acute myocardial infarction. *Clinica Chimica Acta*, 346, 211-219.
- WU, G. H., DATAR, R. H., HANSEN, K. M., THUNDAT, T., COTE, R. J. & MAJUMDAR, A. 2001. Bioassay of prostate-specific antigen (PSA) using microcantilevers. *Nature Biotechnology*, 19, 856-860.
- WU, Y. X. & KWON, Y. J. 2016. Aptamers: The "evolution" of SELEX. *Methods*, 106, 21-28.
- WU, Z. S., LI, J. S., DENG, T., LUO, M. H., SHEN, G. L. & YU, R. Q. 2005. A sensitive immunoassay based on electropolymerized films by capacitance measurements for direct detection of immunospecies. *Analytical Biochemistry*, 337, 308-315.
- XI, J., CHEN, J. Y., GARCIA, M. P. & PENN, L. S. 2013. Quartz crystal microbalance in cell biology studies. *Biochips & Tissue Chips*, S5, 1-9.
- XU, D. K., XU, D. W., YU, X. B., LIU, Z. H., HE, W. & MA, Z. Q. 2005. Label-free electrochemical detection for aptamer-based array electrodes. *Analytical Chemistry*, 77, 5107-5113.
- XU, F. 1997. Effects of redox potential and hydroxide inhibition on the pH activity profile of fungal laccases. *Journal of Biological Chemistry*, 272, 924-928.

- XU, S. & MUTHARASAN, R. 2010. Rapid and Sensitive Detection of Giardia lamblia Using a Piezoelectric Cantilever Biosensor in Finished and Source Waters. *Environmental Science & Technology*, 44, 1736-1741.
- YANG, T., ZHOU, N., LI, Q. H., GUAN, Q., ZHANG, W. & JIAO, K. 2012. Highly sensitive electrochemical impedance sensing of PEP gene based on integrated Au-Pt alloy nanoparticles and polytyramine. *Colloids and Surfaces B-Biointerfaces*, 97, 150-154.
- ZAYATS, M., HUANG, Y., GILL, R., MA, C. A. & WILLNER, I. 2006. Label-free and reagentless aptamer-based sensors for small molecules. *Journal of the American Chemical Society*, 128, 13666-13667.
- ZELADA-GUILLEN, G. A., TWEED-KENT, A., NIEMANN, M., GORINGER, H. U., RIU, J. & RIUS, F. X. 2013. Ultrasensitive and real-time detection of proteins in blood using a potentiometric carbon-nanotube aptasensor. *Biosensors & Bioelectronics*, 41, 366-371.
- ZHURAIUSKI, P., ARYA, S. K., JOLLY, P., TIEDE, C., TOMLINSON, D. C., FERRIGNO, P. K. & ESTRELA, P. 2018. Sensitive and selective Affimer-functionalised interdigitated electrode-based capacitive biosensor for Her4 protein tumour biomarker detection. *Biosensors & Bioelectronics*, 108, 1-8.
- ZIEGLER, C. 2000. Cell-based biosensors. *Fresenius Journal of Analytical Chemistry*, 366, 552-559.